QUARTERLY PROGRESS REPORT

April 1 to June 30, 2016

Florida International University's Continued Research Support for the Department of Energy's Office of Environmental Management

Principal Investigator:

Leonel E. Lagos, Ph.D., PMP®

Prepared for:

U.S. Department of Energy
Office of Environmental Management
Under Cooperative Agreement No. DE-EM0000598

FIU | Applied Research Center
FLORIDA INTERNATIONAL UNIVERSITY

Introduction

The Applied Research Center (ARC) at Florida International University (FIU) executed work on four major projects that represent FIU-ARC's continued support to the Department of Energy's Office of Environmental Management (DOE-EM). The projects are important to EM's mission of accelerated risk reduction and cleanup of the environmental legacy of the nation's nuclear weapons program. The information in this document provides a summary of the FIU-ARC's activities under the DOE Cooperative Agreement (Contract # DE-EM0000598) for the period of April 1 to June 30, 2016.

The period of performance for FIU Performance Year 6 under the Cooperative Agreement will be August 29, 2015 to August 28, 2016. The projects have been reorganized for FIU Performance Year 6. Projects 2 and 3 from FIU Performance Year 5 have been combined into a single project (Project 2) focused on soil and groundwater remediation research. The D&D and Workforce Development projects were subsequently renumbered as Projects 3 (D&D) and 4 (Workforce Development). Project 1 (high level waste/waste processing) remains unchanged.

Executive highlights during this reporting period include:

Program-wide:

- A program review via VTC was conducted between DOE EM and FIU ARC on April 5 to April 7, 2016, as part of the DOE Cooperative Agreement. A total of five (5) technical presentations were conducted over the 3-day period. The DOE-FIU program review included participation from colleagues at DOE Headquarters (DC and Maryland Office), DOE national laboratories (Savannah River National Lab, Pacific Northwest National Lab, and Los Alamos National Lab) and DOE contractors (Washington River Protection Solutions and Savannah River Nuclear Solutions).

  The topics of the presentations included high-level waste/waste processing applied research, soil and groundwater applied research, D&D and IT for Environmental Management applied research, and workforce development and training of FIU STEM students (DOE Fellows Program). DOE Fellows presented during the workforce development presentations to highlight the applied research they are performing for DOE EM as part of this Cooperative Agreement. A final presentation was given on Thursday to highlight the major applied research accomplishments during the current year and to present the proposed research tasks for the new performance cycle, currently scheduled to start on August 29, 2016. All presentations are available for downloading on FIU's DOE Research webpage at http://doeresearch.fiu.edu.

- FIU completed the development of the Continuation Application for FIU Performance Year 7 of the DOE-FIU Cooperative Agreement that will begin on August 29, 2016 at the conclusion of the current FIU Performance Year 6 on August 28, 2016. The three-volume continuation application package was submitted to DOE three months prior to the end of the current performance year, on May 27, 2016.

***Project 1*: High level waste (HLW)/waste processing**

FIU is assisting DOE EM to meet the challenges of an aging HLW infrastructure through: 1) the development of robotic inspection tools and the evaluation of sensors that can assist in assessing the integrity of the DSTs and the waste transfer components; and 2) the testing of non-metallic materials that have been exposed to multiple stressors.

1. FIU is developing two distinct technologies for the inspection of primary double-shell tanks (DST) for HLW. Designing and prototyping have been completed for both technologies and bench-scale testing of both technologies has been performed.
    a. A miniaturized crawler that navigates through the refractory pad air channels under the primary liners of the DST's at Hanford while providing live video feedback, and
    b. A peristaltic crawler that crawls through the air supply pipe that leads to the central plenum of the primary tank of the DSTs and provides video feedback.
2. To aid in the evaluation of the HLW systems, FIU is developing a sectional full-scale mock-up of the DST tanks. This will include portions of the air supply line, central plenum, refractory pad, tank floor and tank wall. Recently, FIU has completed a structural analysis of the floor section of the tank mock up to determine if the support structure can handle the weight of the tank sections. Initial stresses were determined with ¼ inch carbon steel plates, with the stresses being well below the yield stress of the material. Additional analysis showed that the system could also take the loads created by 7/8 inch plates if needed, without having to make significant modifications to the design.
3. FIU has developed a test loop that is capable of exposing EPDM hose-in-hose transfer lines, gaskets and O-rings to a combination of elevated temperatures, exposure to caustic material and elevated pressures, simultaneously, for various lengths of time. Recently, FIU has completed the test loop and added necessary sensors to monitor the temperatures, flow rates and pressures within the test loop. Data acquisition software has been developed so that the sensor data can be stored and monitored in real time. This data will be continuously stored for up to a year. During the next month, the aging of the materials will commence. After six months and one year, specimens will be removed and the residual strength and changes in the material properties will be determined.

***Project 2:* Environmental remediation (ER)**

FIU is assisting DOE EM to meet the challenges of managing the environmental restoration of subsurface contamination in soil and groundwater. FIU is investigating: 1) the long-term behavior of contaminants in groundwater to reduce the potential for contaminant mobility or toxicity to develop the technical justification for implementation of enhanced attenuation strategies; 2) a surface water model to simulate flow and contaminant transport in Tims Branch at SRS; and 3) the influence and corresponding electrical geophysical response of microbial activity on uranium sequestration.

1. FIU helped to develop the scientific and technical justification to support implementation of an enhanced attenuation strategy using carbohydrate substrate (molasses) injection to create anaerobic reactive zones for metal and radionuclide remediation via the enhanced anaerobic reductive precipitation process. The experiments used samples from a field demonstration

performed at the SRS F-Area in 2010. FIU investigated the transitions between anaerobic to aerobic to evaluate the longevity of contaminant immobilization to baseline conditions. FIU is developing a peer-reviewed journal publication on the results of the application of this technology under the SRS environmental conditions.

2. FIU is applying geographical information systems (GIS) and stream/ecosystem modeling tools to the Tims Branch system at SRS to examine its response to historical discharges and environmental management remediation actions. Development of the surface water model has included: a) defining the model domain/boundary conditions which incorporates the entire Tims Branch watershed; b) input of configuration parameters into the MIKE SHE model to simulate overland flow, evapotranspiration and unsaturated flow; and c) preliminary delineation of the Tims Branch stream network to model stream flow using MIKE 11.
3. FIU is performing research to support the investigation of spectral induced polarization (SIP) as a geophysical technique to track the influence of microbial activity on the subsurface uranium sequestration process at Hanford. FIU, with the support of PNNL researchers, set up an experimental system that is equipped with an SIP apparatus and six (6) columns filled with Hanford soil mixed with uranium in the form of autunite. FIU has completed set up of the system including calibration of a pump and procurement of the ORP, pH and conductivity probes to measure changes in the column porewater geochemical parameters.

Project 3: **Deactivation and decommissioning (D&D)**

FIU is assisting DOE EM to meet high priority D&D needs and technical challenges across the DOE complex through: 1) technology development, demonstration and evaluation; 2) managing the vast amount of waste forecast information for planned treatment and disposal across the DOE complex; and 3) preserving and transferring D&D knowledge and information to assist future D&D projects and the future workforce.

1. FIU is investigating the layering or combining of an intumescent coating (IC) with a fixative product as a way to mitigate the release of radioisotopes during fire and/or extreme heat conditions that can potentially occur at a DOE contaminated facility/building. Testing shows that most fixatives significantly degrade between 200-400ºF resulting in the potential release radioactive contamination. FIU is completing the baseline testing of commercially available ICs. The initial results from the proof-of-concept experiments have been very promising which have led the SRS 235-F site personnel to request the research be expedited in order to support a potential "hot demo" onsite. FIU will begin planning for a full-scale cold demonstration for applying the final down-selected IC under the same operational and safety constraints encountered in a SRS 235-F hot cell. While the research is currently focused on defining and meeting the operational, safety, and regulatory requirements for deploying an IC as a fire resilient fixative in support of the SRS 235-F hot cells, the research has a high probability for broader applications of the IC technology to satisfy other problem sets and challenge areas related to fire / extreme heat conditions across the DOE complex.
2. FIU is providing a web-based tool to receive, organize, and report DOE waste forecast data from across the complex via a common application which provides efficiency to waste disposition decision making. FIU received a new set of waste stream forecast and transportation forecast data from DOE, completed the data import into the Waste

Management Information System (WIMS), and deployed the new data onto the test server for DOE testing and review. FIU received and incorporated feedback from the data review, and deployed the new data on the public server. The 2016 waste data set replaces the existing waste data and is now fully viewable and operational in WIMS.

3. FIU is maintaining and preserving the D&D knowledge base by developing tools to enhance communication, share and distribute information, and promote collaboration within the D&D community of practice. FIU has launched a D&D Fixative Module on the D&D Knowledge Management Information Tool (www.dndkm.org/fixativemodule/) to assist in the selection of commercially available fixatives, strippable coatings, and decontamination gels for application during D&D activities. The module includes a comprehensive database of commercially available fixatives and other contamination control products and is capable of filtering and sorting the available products according to the criteria entered by the user. The D&D Fixative Module allows users to browse and search through the commercially available contamination control products. FIU has also developed and deployed a light version of the D&D Fixative Module for use on mobile devices (m.dndkm.org/FixativeModule.aspx).

Project 4: **STEM workforce development**

FIU created the DOE Fellows Program in 2007 to assist DOE EM to address the problem of an aging federal workforce. The program provides training, mentorship, and professional development opportunities to FIU STEM students. The DOE Fellows provide critical support to the DOE EM research being conducted on high impact/high priority research being conducted at FIU.

1. In March 2016, DOE Fellow Christine Wipfli began a one year internship at the International Atomic Energy Agency (IAEA) Headquarters in Vienna, Austria. Christine is interning in the Waste Technology Section, Division of Nuclear Fuel Cycle & Waste Technology under the mentorship of Mr. Horst Monken-Fernandes. DOE EM included a write up on Christine's achievement, titled "IAEA Awards DOE Fellow Internship," in the Volume 8, Issue 5, of the EM Update newsletter dated March 16, 2016 (https://content.govdelivery.com/accounts/USDOEOEM/bulletins/13c48e1#link_1457990261444).
2. DOE Fellow Alejandro Garcia completed a 10-week spring 2016 internship at PNNL and summer internship arrangements were finalized for 11 DOE Fellows at LANL, SRNL, PNNL, WRPS, NETL, and DOE-HQ (Maryland). The 10-week internships will be conducted from June 6 to August 12, 2016 and each DOE Fellow will develop a summer internship technical report once they return to ARC based on the research they performed over the summer.
3. Seven (7) FIU STEM students joined the workforce development program as DOE Fellows Class of 2016 and were assigned to ARC mentors based on their field of study.

Project deliverables and milestones during this reporting period include:

***Project 1*: High level waste (HLW)/waste processing**

- Milestone 2015-P1-M19.2.2, complete the baseline testing on the nonmetallic materials, was completed in March and its corresponding deliverable was submitted to DOE HQ on April 8, 2016.
- Milestone 2015-P1-M17.1.2, complete the validation of impingement correlations for PJMs, was completed in May and its corresponding deliverable was submitted to DOE HQ on May 6, 2016.

***Project 2:* Environmental remediation (ER)**

- The deliverable for Task 2 (Subtask 2.1), progress report on batch experiments on sodium silicate application in multi-contaminant systems, was submitted to DOE and site contacts on April 4, 2016.
- The deliverable for Task 2 (Subtask 2.4), progress report on the synergy between colloidal Si and HA on the removal of U(VI), was submitted to DOE and site contacts on April 21, 2016.
- Milestone 2015-P2-M4, complete input of MIKE SHE model configuration parameters for simulation of unsaturated flow (Subtask 3.1), was completed by the date of April 29, 2016.
- The deliverable for Task 3 (Subtask 3.2), progress report on the application of GIS technologies for hydrological modeling support, was submitted to collaborators at SRNL, SREL and DOE HQ on May 25, 2016.
- The deliverable for Task 1 (Subtask 1.3.1), progress report on the effect of ammonia on uranium partitioning and kaolinite mineral dissolution, was submitted to DOE and Hanford Site contacts on June 22, 2016.
- The deliverable for Task 2 (Subtask 2.5), a progress report on the column experiments to investigate uranium mobility in the presence of humic acid, was submitted to DOE and SRS contacts on June 30, 2016.
- The deliverable for Task 3 (Subtask 3.1), progress report for modeling of surface water and sediment transport in the Tims Branch ecosystem, was submitted to DOE and SRS contacts on June 28, 2016.

***Project 3:* Deactivation and decommissioning (D&D)**

- FIU completed milestone 2015-P3-M3.4, the integration of D&D information into 4 Wikipedia articles, and sent a summary report sent to DOE on April 15, 2016.
- FIU completed milestone 2015-P3-M1.1, importing the 2016 data set for waste forecast and transportation data into WIMS, on May 13, 2016, and sent to DOE for review and testing.
- FIU completed milestone 2015-P3-M3.5, deployment of a pilot mobile application for the D&D Fixative Module on D&D KM-IT on May 20, 2016, and sent to DOE for review and testing.

- FIU completed a deliverable for a decision brief to Andrew Szilagyi and John De Gregory with DOE EM-13 on recommended technologies to test for FIU Performance Year 7 on May 11, 2016, as part of a larger briefing on FIU's current and future D&D research activities.
- A deliverable for a summary report on robotic technologies applicable to the SRS 235-F Facility has been reforecast to August 12, 2016. The circumstances and end path forward, including the new reforecasted date for this deliverable, have been closely coordinated with the stakeholders at Savannah River and DOE HQ. FIU discussed the issue with the SRNL collaborators and confirmed the agreement the deliverable date with an email sent to SRS on May 24, 2016 and DOE HQ contacts on May 27, 2016.
- FIU completed milestone 2015-P3-M2.3 by participating in the ASTM International's Executive Steering Committee Meeting from June 27 to June 29, 2016, and leading a ASTM International E10.03 Subcommittee meeting to develop standardized testing protocols and performance metrics for D&D technologies.
- FIU completed a deliverable for a technical progress report on the research to improve the operational effectiveness of fixative technologies in the critical area of fire resistance to better address the unique D&D challenges being faced by the SRS 235-F Project and other high priority efforts across the DOE complex, submitted on June 29, 2016.

Project 4: **STEM workforce development**

No milestones or deliverables were due in April, May, or June 2016.

The program-wide milestones and deliverables that apply to all projects (Projects 1 through 4) for FIU Performance Year 6 are shown on the following table:

Task	Milestone/ Deliverable	Description	Due Date	Status	OSTI
Program-wide (All Projects)	Deliverable	Draft Project Technical Plan	10/16/15	Complete	
	Deliverable	Monthly Progress Reports	Monthly	On Target	
	Deliverable	Quarterly Progress Reports	Quarterly	On Target	
	Deliverable	Draft Year End Report	10/14/16	On Target	OSTI
	Deliverable	Presentation overview to DOE HQ/Site POCs of the project progress and accomplishments (Mid-Year Review)	02/29/16*	Complete on 04/07/16	
	Deliverable	Presentation overview to DOE HQ/Site POCs of the project progress and accomplishments (Year End Review)	08/31/16*	On Target	

**Completion of this deliverable depends on availability of DOE-HQ official(s).*

Project 1
Chemical Process Alternatives for Radioactive Waste

Project Manager: Dr. Dwayne McDaniel

Project Description

Florida International University has been conducting research on several promising alternative processes and technologies that can be applied to address several technology gaps in the current high-level waste processing retrieval and conditioning strategy. The implementation of advanced technologies to address challenges faced with baseline methods is of great interest to the Hanford Site and can be applied to other sites with similar challenges, such as the Savannah River Site. Specifically, FIU has been involved in: analysis and development of alternative pipeline unplugging technologies to address potential plugging events; modeling and analysis of multiphase flows pertaining to waste feed mixing processes, evaluation of alternative HLW instrumentation for in-tank applications and the development of technologies to assist in the inspection of tank bottoms at Hanford. The use of field or *in situ* technologies, as well as advanced computational methods, can improve several facets of the retrieval and transport processes of HLW. FIU has worked with site personnel to identify technology and process improvement needs that can benefit from FIU's core expertise in HLW. The following tasks are included in FIU Performance Year 6:

Task No	Task
Task 17: Advanced Topics for Mixing Processes	
Subtask 17.1	Computational Fluid Dynamics Modeling of HLW Processes in Waste Tanks
Task 18: Technology Development and Instrumentation Evaluation	
Subtask 18.1	Evaluation of FIU's Solid-Liquid Interface Monitor for Estimating the Onset of Deep Sludge Gas Release Events
Subtask 18.2	Development of Inspection Tools for DST Primary Tanks
Subtask 18.3	Investigation Using an Infrared Temperature Sensor to Determine the Inside Wall Temperature of DSTs
Task 19: Pipeline Integrity and Analysis	
Subtask 19.1	Pipeline Corrosion and Erosion Evaluation
Subtask 19.2	Evaluation of Nonmetallic Components in the Waste Transfer System

Task 17: Advanced Topics for HLW Mixing and Processing

Task 17 Overview

The objective of this task is to investigate advanced topics in HLW processing that could significantly improve nuclear waste handling activities in the coming years. These topics have been identified by the Hanford Site technology development group, or by national labs and academia, as future methods to simulate and/or process waste streams. The task will focus on

long-term, high-yield/high-risk technologies and computer codes that show promise in improving the HLW processing mission at the Hanford Site.

More specifically, this task will use the knowledge acquired at FIU on multiphase flow modeling to build a CFD computer program in order to obtain simulations at the engineering-scale with appropriate physics captured for the analysis and optimization of PJM mixing performance. Focus will be given to turbulent fluid flow in nuclear waste tanks that exhibit non-Newtonian fluid characteristics. The results will provide the sites with mathematical modeling, validation, and testing of computer programs to support critical issues related to HLW retrieval and processing.

Task 17 Quarterly Progress

Subtask 17.1: Computational Fluid Dynamics Modeling of HLW Processes in Waste Tanks

In this reporting period, FIU developed and implemented a code for calculation of the turbulent dissipation rate (TDR) for the Bingham fluids using STAR-CCM+. The code was implemented in 2-D RANS simulations for evaluation purposes and small differences were observed between the TDR obtained from the solution of the related partial differential equation (PDE) and the resolved TDR. The code was later implemented in the direct numerical simulations (DNS) with extremely fine computational grids containing 8 million grid points.

The developed field functions in STAR-CCM+ was intended to obtain the resolved TDR according to Eqn.1 (Taylor, 1953 and Baldi et al., 2003).

$$\varepsilon = \nu \left\{ \begin{array}{l} 2\left(\overline{\left(\frac{\partial u_i}{\partial x_i}\right)^2} + \overline{\left(\frac{\partial u_j}{\partial x_j}\right)^2} + \overline{\left(\frac{\partial u_k}{\partial x_k}\right)^2} \right) + \\ + \overline{\left(\frac{\partial u_i}{\partial x_j}\right)^2} + \overline{\left(\frac{\partial u_j}{\partial x_i}\right)^2} + \overline{\left(\frac{\partial u_i}{\partial x_k}\right)^2} + \overline{\left(\frac{\partial u_k}{\partial x_i}\right)^2} + \overline{\left(\frac{\partial u_j}{\partial x_k}\right)^2} + \overline{\left(\frac{\partial u_k}{\partial x_j}\right)^2} + \\ + 2\left(\overline{\frac{\partial u_i}{\partial x_j} \cdot \frac{\partial u_j}{\partial x_i}} + \overline{\frac{\partial u_i}{\partial x_k} \cdot \frac{\partial u_k}{\partial x_i}} + \overline{\frac{\partial u_j}{\partial x_k} \cdot \frac{\partial u_k}{\partial x_j}} \right) \end{array} \right\} \qquad (1)$$

In this framework, a combination of 16 field monitors and first-order gradients were used for the terms in the above equation. Figure 1-1 shows the difference between the quantity obtained from the solution to the PDE equation of the TDR and the resolved TDR both obtained in a RANS simulation. The slight difference could be associated with the order of gradient and approximations used in the modeling of the eddy viscosity.

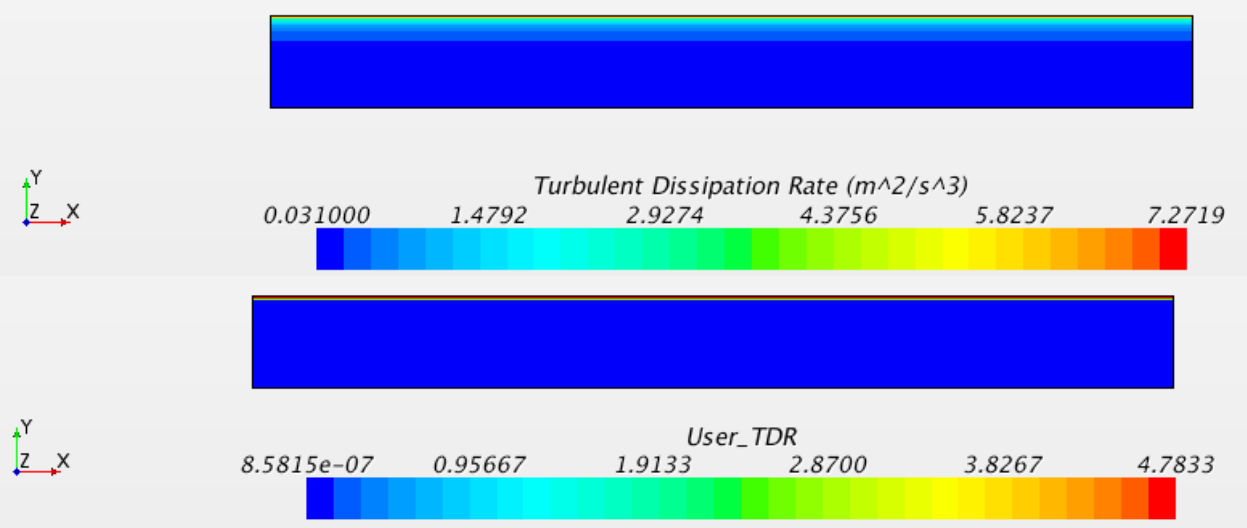

Figure 1-1. Comparison between the TDR from PDE (up) and the resolved TDR (bottom).

An attempt was made to calculate higher order (4th order) gradients in the application according to Eqn. 2 and Eqn. 3. Simple evaluations showed that using the cell index could create serious problems with the direction of the gradient calculation, as shown in Figure 1-2, where two consecutive cells are shown in blue. A better criterion will be pursued to access cell values in the axial direction (left and right sides of any computational cell) and in the span wise direction (up and down sides of any computational cell) for correct calculations.

$$\acute{u}_x = \frac{-\acute{u}_{i+2}+8\acute{u}_{i+1}-8\acute{u}_{i-1}+\acute{u}_{i-2}}{12\,h_x} \qquad (2)$$

$$\acute{u}_y = \frac{-\acute{u}_{j+2}+8\acute{u}_{j+1}-8\acute{u}_{j-1}+\acute{u}_{j-2}}{12\,h_x} \qquad (3)$$

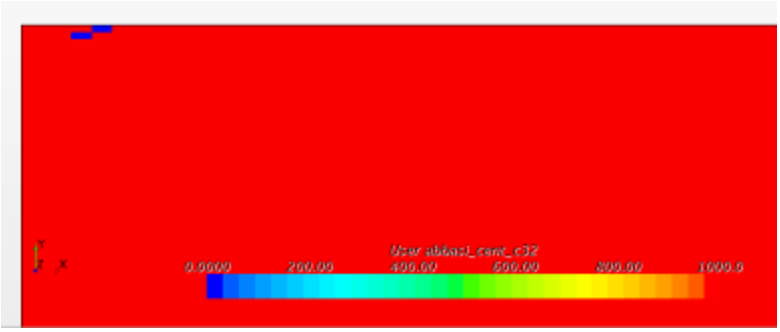

Figure 1-2. Contour of the scalar set to 1000 for all cells except for the cell # 10 and the cell # 11.

Furthermore, three grids with 8, 16, and 64 million points were created in the application. Eight million grid points satisfy the grid spacing requirement indicated by Eggless et al., 1993, i.e.,

$Re_\tau^{\frac{9}{4}} \approx 6.8 \times 106$; however, the intention for creating finer grids was to investigate the effect of grid spacing as indicated by Gageik et al. (2014).

The initial applications of the method in the 8m grid with a small time step size $\Delta T = 1 \times 10\text{-}5s$, resulted in the courant number of 0.2, and y+ = 0.01 for the first cell at the solid boundary. The definition of the courant number is $CFL = \frac{\text{Max(vel.mag)} \times \text{Timestep}}{\text{Min(cell.size)}}$, where $\text{cell.size} = \frac{1}{(\text{cell.volume})^{1/3}}$.

Figure 1-3 shows the resolved TDR for the 8m grid points which is significantly different from the 2-D results shown earlier in Figure 1-1. Additional simulations are in progress to eliminate the regions of extremely high shear in the center of the pipe. These regions show the transient effects caused by the one-step refinement of the grid.

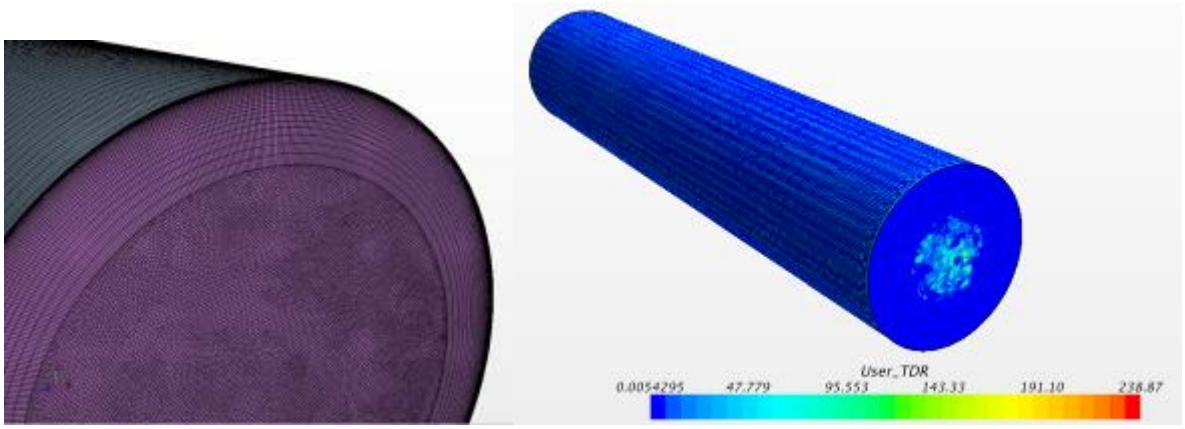

Figure 1-3. Computational mesh used for the DNS simulations and the resolved TDR in DNS simulation with 8m grid points.

Further, a comparison analysis was conducted between the results of the pipe flow simulation mentioned above and results obtained previously from the Reynold-averaged Navier-Stokes (RANS) simulations. FIU used the results of the RANS-alpha method as the validation tool since this method predicted the velocity profile accurately for the turbulent regime (The results of the alpha method have been submitted for publication in a journal). In this benchmark validation for the QDNS results, critical parameters such as the shear rate, velocity, and turbulent dissipation rate (TDR) were compared between RANS and QDNS simulations in order to investigate the differences. In addition, The courant number (CFL) as well as other turbulent quantities, such as Y+ on the wall, $\Delta r+$, $\Delta\theta+$, and $\Delta z+$ were monitored to insure that results comply with typical profiles in wall-bounded turbulent flows. Once the results were obtained, FIU compared the profile of the TDR, axial velocity, and shear rate between three methods, QDNS-HB, RANS-alpha, and RANS-HB. For this purpose, FIU used the user defined functions as mentioned above to compute the TDR in the QDNS simulations.

The QDNS results obtained indicated that turbulent quantities were similar to the values obtained by Shams et al. (2011) in their pipe flow simulation of fully turbulent flow. Table 1-1 shows that except for the $\Delta z+max$, smaller values were obtained for the turbulent quantities. These quantities suggest that mesh requirements were suitable for capturing the flow structures. In addition, the CFL number of the flow was kept as small as 0.2 to ensure that all pertinent structures were captured in the simulation.

Table 1-1. Mesh-Dependent Turbulent Quantities of the Flow

Turbulent quantity	Shams et al.,2011	This work
Δr^{+}_{max}	11	7.3
$\Delta \theta^{+}_{max}$	5	2.2
Δz^{+}_{max}	8	15.5
Y^{+}	-	0.1

Figure 1-4 shows the profiles of the TDR for RANS and QDSN simulations. It was observed that the peak of the TDR profile occurred in the middle range for the QDNS-HB approach. This was similar to the RANS-HB modeling where a peak was observed in the core flow. The magnitude for the maximum TDR was similar between the QDNS-HB and the RANS-alpha methods; however, the location of the maximum TDR was completely different between these approaches. FIU observed a maximum value at the location near the wall for the RANS-alpha methods.

For a qualitative comparison, FIU compared observations against typical profiles of energy for turbulent pipe flows published in the literature. Normalized quantities show peaks of the TDR profile occurred in low Y+ for the QDNS-HB and RANS-alpha methods. Similarly, Eggels et al. (1994) reported a TDR profile marked by a maximum in low Y+. Thus, results show an incorrect TDR profile for the RANS-HB method.

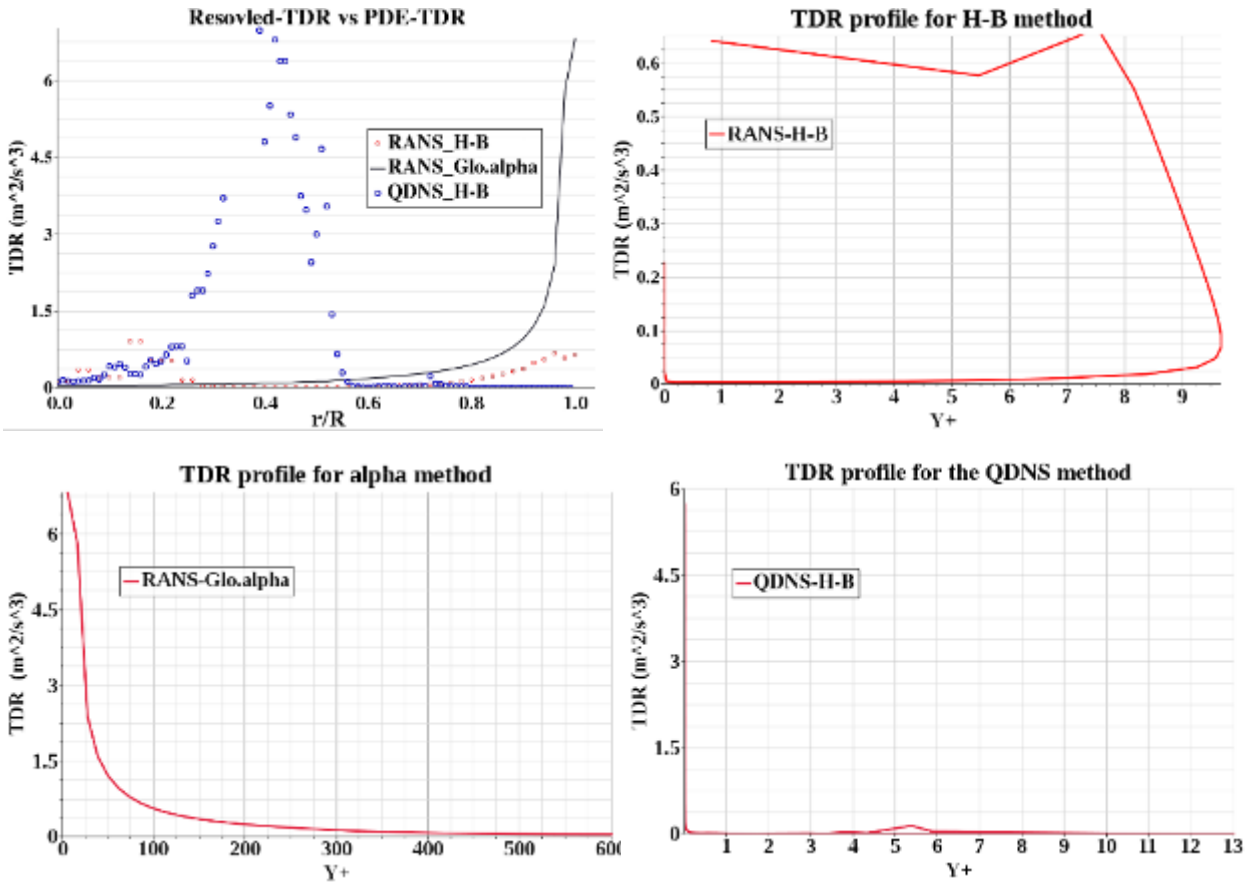

Figure 1-4. Profile of turbulent dissipation rate for RANS and QDSN simulations.

FIU also compared the shear rate (SR) between four methods. It was observed that the QDNS reported the maximum shear rate in the most of the core flow. Conversely, the RANS-alpha method reported the minimum of the shear rate in the most of the core flow except on the axis (r/R =0). The correlation used in the SRC method (Eqn. 4) must be corrected with a negative sign, since the correlation helps to increase the shear rate from the H-B profile which is the opposite effect.

$$|\Upsilon|^2_{SRC} = 2\,S_{ij}S_{ij} + \langle 2\,\acute{S}_{ij}\acute{S}_{ij}\rangle = 2\,S_{ij}S_{ij} + \frac{\varepsilon^{*}\rho}{(\mu_{H\text{-}B})_{SRC}} \qquad (4)$$

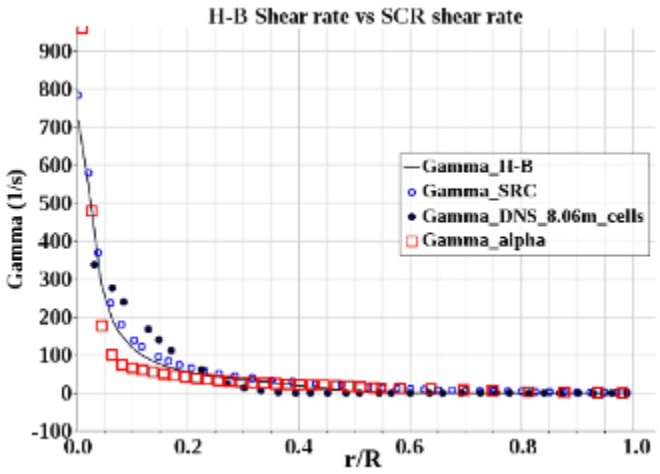

Figure 1-5. Profile of shear rate for RANS and QDSN simulations.

In addition, FIU compared the velocity profiles obtained from the RANS and QDNS simulations against the experimental data available in the literature. It was observed that inaccuracies associated with the QDNS method were in accord with the highest amount of shear rate reported earlier. Again, for a qualitative comparison, FIU compared the results against typical profiles of normalized velocity for turbulent pipe flows published in the literature. Here, only the RANS-alpha method could produce a realistic normalized velocity profile that was qualitatively similar to the data published by Eggels et al. (1994).

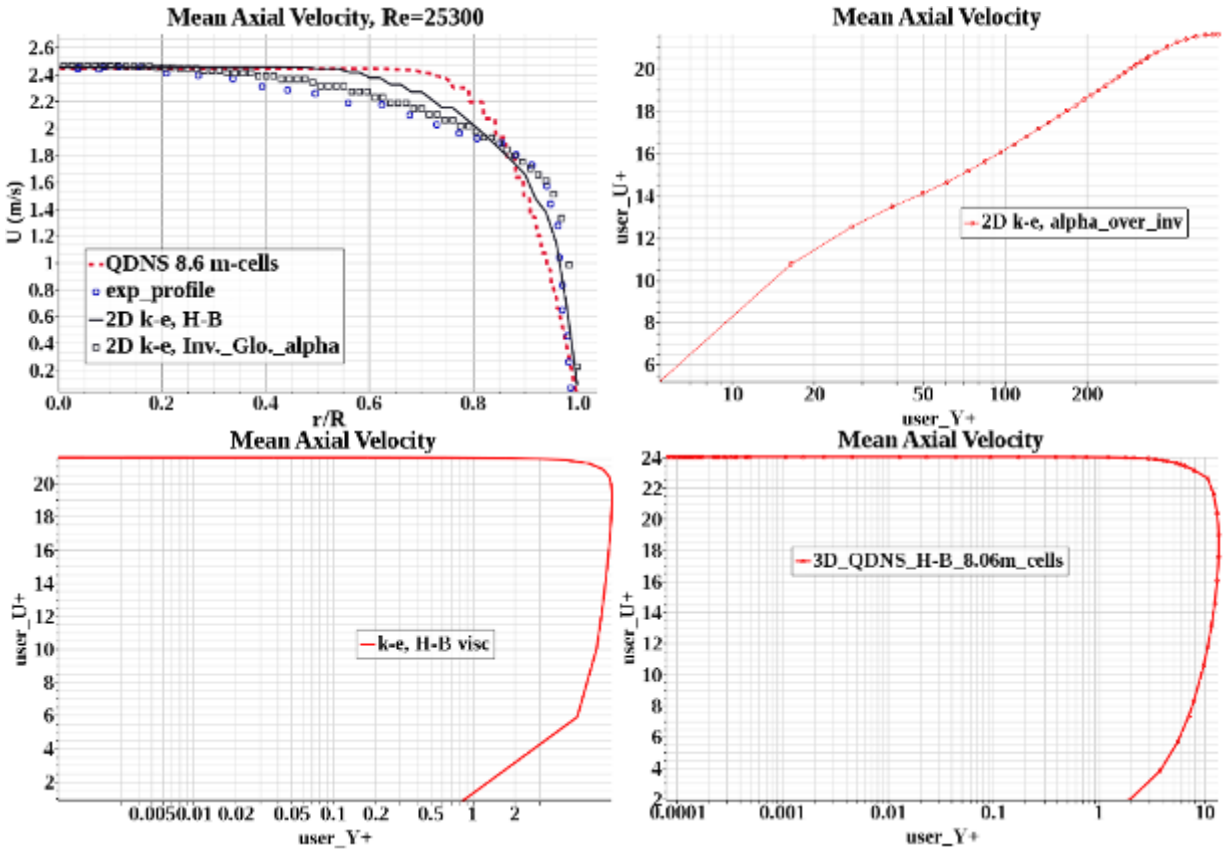

Figure 1-6. Profile of velocity for RANS and QDSN simulations.

In summary, results of the QDNS-HB method were obtained and compared against RANS methods. All mesh-dependent turbulent quantities were in acceptable range, as well as the CFL number of the flow. The TDR profile produced by the QDNS-HB method compared well with typical profiles of TDR for turbulent pipe flow; however, no such similarity was obtained between the profiles of dimensionless velocity. FIU encountered excessively increasing memory and space demands when switching from 8 million to 16 and 64 million cell grids which seemed unnecessary by reviewing the similar work of Shams et al. (2012) and Moin and Mahesh (1998). Fast and accurate results in QDNS could be obtained through the use of shorter computational domains, induced turbulence parameters at the boundaries, and use of smaller Reynolds numbers.

Further, FIU pursued an effort to discover an expression for shear correction in dissipative scales of turbulence using the accurate results of the RANS simulations. The general form of this expression relates the velocity and length scales of the Kolmogorov and Taylor eddies. For this purpose, the simulation results of the RANS modeling (the alpha method) was analyzed for two purposes: 1) To ensure that the turbulence quantities comply with the typical distribution profiles in wall-bounded turbulent flows, and 2) To obtain correlations to be used for future modification.

The initial study was conducted to observe the performance of method on fine and course meshes. For this purpose, two domains with 2117 cells and 7328 cells were considered and velocity profile and turbulent kinetic energy (TKE) of the flow was compared. As shown in Figure 1-7, even though the velocity profile perfectly matched the fine and mesh domains, TKE profiles were significantly different. A qualitative validation was obtained for the domain with 7328 cells by comparing these results with the typical profile reported by Becthel-CDadapco in 2015.

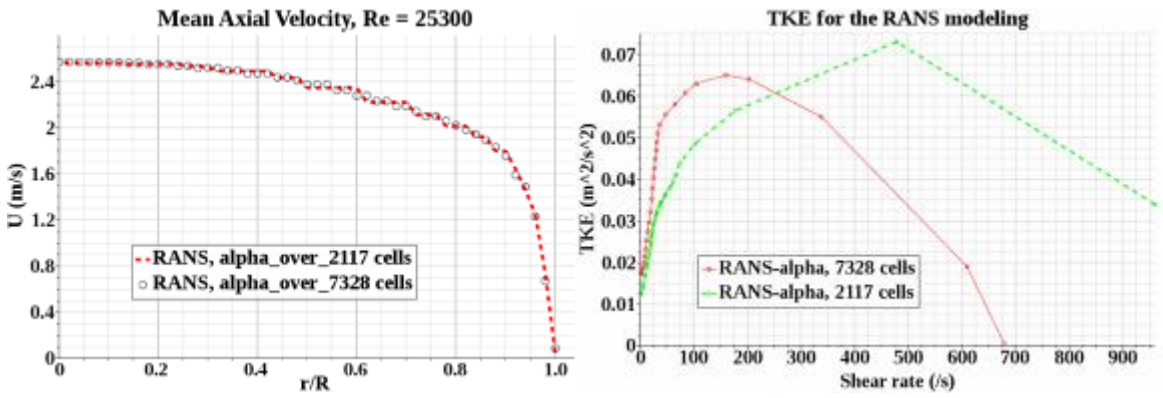

Figure 1-7. Comparison between results produced by 2117 and 7328 grid cells.

The evaluation was expanded to other turbulence quantities, such as TKE-versus-wall distance, and U+-versus-Y+ to ensure the acceptability of the results. Figure 1-8 shows that qualitative similarities exists between the reported results and the typical turbulent profiles of a pipe flow in the literature. Further, Figure 1-8 shows similarities between the profiles of TKE-r/R and U+-Y+, respectively, as generated by FIU and Eggeles (1994).

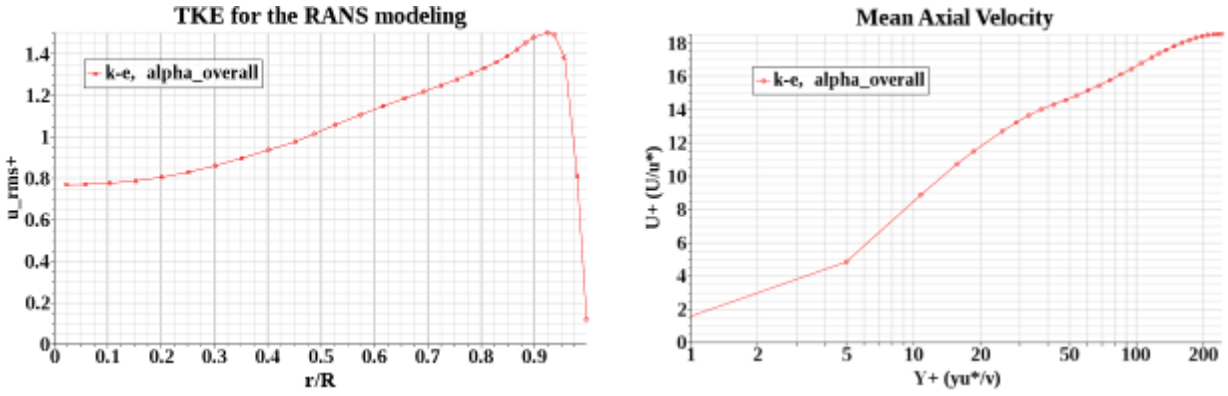

(a) **(b)**

Figure 1-8. Turbulent profiles obtained from the RANS modeling with 7328 cells.

After the validations obtained above, FIU focused on the expressions reported by Becthel-CDadapco and Tennekes (1968) which link the velocity and length scales to the shear rate in dissipative scales. The shear rate was plotted against the inverse length scale and linear segments were observed. FIU used the well-known expression for the Kolmogorov length scales as shown by Eqn.(5) and implemented this code in the STARCCM+ application.

$$\eta = \left(\frac{\nu^3}{\epsilon}\right)^{1/4} \qquad (5)$$

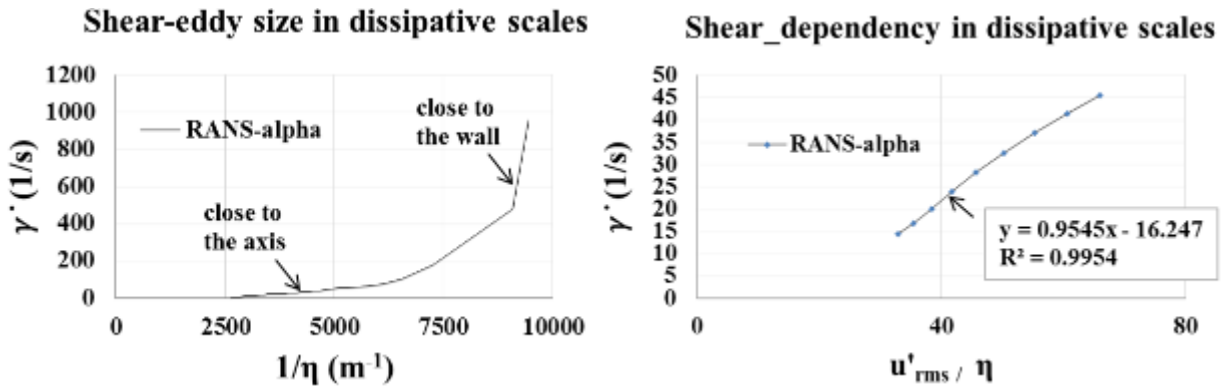

Figure 1-9. Profile of shear against inverse Kolmogorov scales size.

Based on the results obtained above, the following equation for the shear rate in small scales is proposed:

$$|\dot{\gamma}| = 0.96(\acute{u}/\eta) - 16.25 \qquad (6)$$

Similar attempts using various Reynolds numbers in RANS and QDNS simulations are needed to ensure about authenticity of this expression. In addition, an investigation on any possible linkage between filed variables and the intercept on the y-axis is needed.

Later, FIU assessed the capability of the STARCCM+ in generating power spectrum of TKE in a DNS simulation. The expressions for TKE and power spectral energy of the velocity fluctuations are shown by (7) and (8). To obtain a quick assessment, a pipe with reduced length, diameter,

and inlet velocity (L = 2.5 D and D= 0.01, Vavg@inlet = 0.3 m/s) was considered. Figure 1-10 (a) shows the distribution of the axial velocity on a cross sectional plane and along the computational domain.

$$TKE = R_{ii}(0) = \int_{-\infty}^{\infty} PSD(\omega)\, d\omega \quad (7)$$

$$PSD(\omega) = \frac{1}{2\pi}\int_{-\infty}^{\infty} e^{-i\omega\tau} R_{ii}(\tau)\, d\tau \quad (8)$$

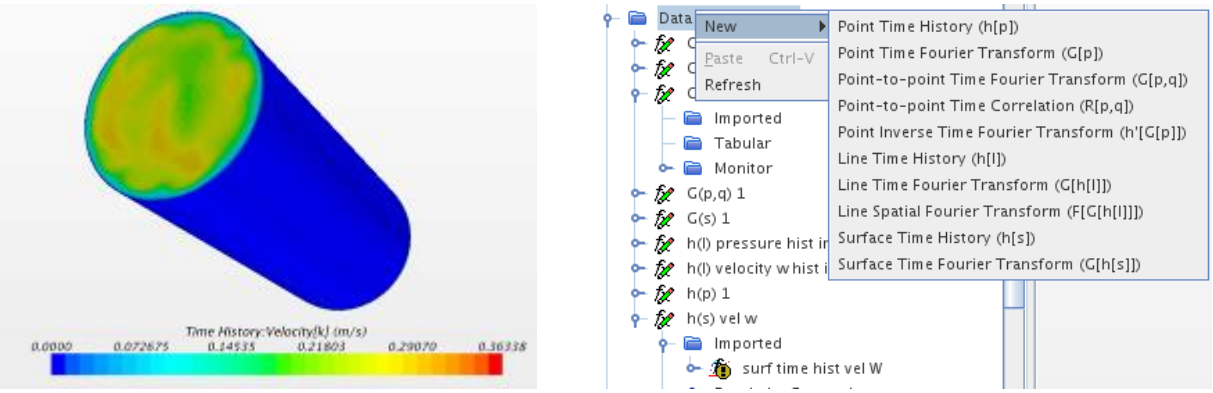

(a) **(b)**

Figure 1-10. Assessing Spectral density calculation in STARCCM+, a) contour of axial velocity from DNS simulation in statistically steady regime, b) FFT modules in STARCCM+.

Initially, a recorded time history of the velocity filed was created in the STARCCM+. Next, a review on 10 modules that create the spectral analysis of the variable in the application (Figure 1-10(b)) was performed. The Data Set Function feature of STARCCM+ was used to create fast Fourier transforms (FFT) of the velocity fluctuations from the results. Figure 1-11 shows the results of applying the FFT on a time history of the simulation results. The FFT of the axial velocity at 500 Hz is shown on the left and spectral density is shown on the right.

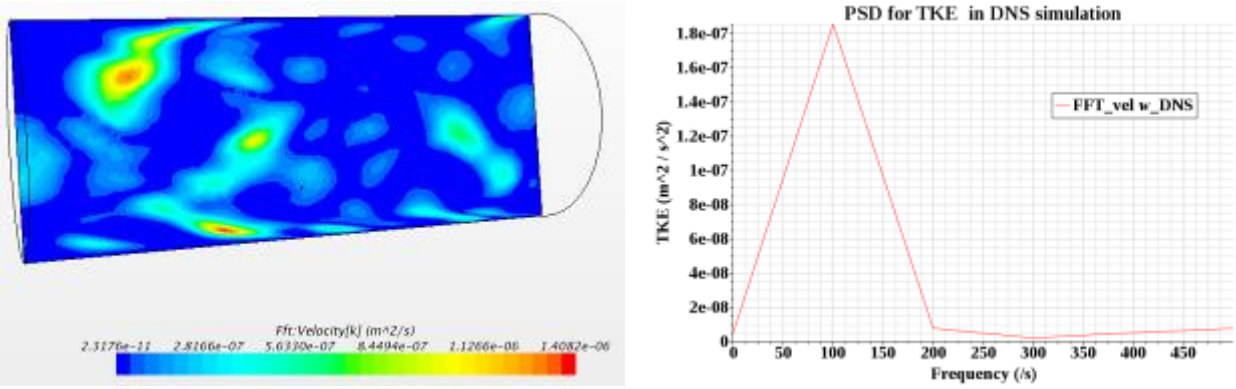

(a) **(b)**

Figure 1-11. Contour of axial velocity from DNS simulation in statistically steady regime.

Further investigations revealed that the current license for STARCCM+ does not allow for access to wavenumber space. To assist on this problem, a series of communications with the

software vendor is in progress to activate the module in the program and install the latest version of the application on the FIU-HPC.

References:

A. Shams, F. Roelofs, E.M.J. Komen, E. Baglietto, 2012, Optimization of a pebble bed configuration for quasi-direct numerical simulation, Nuclear Engineering and Design, Volume 242, Page 331– 340.

J.G.M.Eggels, F. Unger, M. H. Weiss, J.Westerweel, R.Adrian, R. Friedrich, F. T. M. Nieuwstadt, 1994, Fully Developed Turbulent Pipe Flow: A Comparison between Direct Numerical Simulation and Experiment, Journal of Fluid Mechanics, vol. 268, pp. 175-209.

J.G.M. Eggels, J. Westerweel, ET.M. Nieuwstadt, 1993, Direct Numerical Simulation of Turbulent Pipe Flow Journal of Fluid Mech. Volume 268, pp175-209.

M.A. Gageik, I. Klioutchnikov, H Olivier, 2014, Shock Wave Laboratory, RWTH Aachen University, Mesh Study For A Direct Numerical Simulation Of The Transonic Flow At Rec=500,000 Around A Naca 0012 Airfoil, Deutscher Luft- und Raumfahrt congress, Document ID: 340028.

P. Moin, K. Mahesh, 1998, Direct Numerical Simulation: A Tool In Turbulence Research, Journal of Annual Review Fluid Mechanics, Volume 30, pp 539-578

Peltier J, Andri R, Rosendall, Inkson N., Lo S., 2015, Evaluation of RANS Modeling of Non-Newtonian Bingham Fluids in the Turbulence Regime Using STAR-CCM+®, Advanced Simulation & Analysis, BecthelNuclear, Security & Environmental, Cd-adapcoTM , Conference: STAR Global Conference 2015.

S. Baldi, D. Hann and M. Yianneskis, 2003, On the measurement of turbulence energy dissipation in stirred vessels with PIV techniques, I&EC journal, Volume 42, Issue 26, pp 7006–7016.

Y. Kaneda, T. Ishihara, M. Yokokawa, K. Itakura, 2003, A. Uno, Energy dissipation rate and energy spectrum in high resolution direct numerical simulations of turbulence in a periodic box, Physics of Fluids 15, L21; doi: 10.1063/1.153985.

A second task in 17.1 is the investigation of radial wall jet correlations using STAR-CCM+. During this reporting period, all data was gathered and organized in a manner that will facilitate the formatting of a paper for publication. The final results suggested that Poreh's correlation for maximum velocity can predict the radial wall jets Um at different radial locations with reasonable accuracy. The trend shows an increasing error, with a maximum of 40%. The radial wall jet thickness also shows reasonable agreement with Poreh's correlation, with a maximum error of 30%. After an r/b of 5, the PJMs radial wall jets collide with each other, creating a region in which different physics apply and, therefore, was not explored. Studies of the effect of turbulence modeling were studied in previous efforts. For this research, a study showing the difference between a standard k-epsilon 2-layer modeling with high a low Y+ was also conducted.

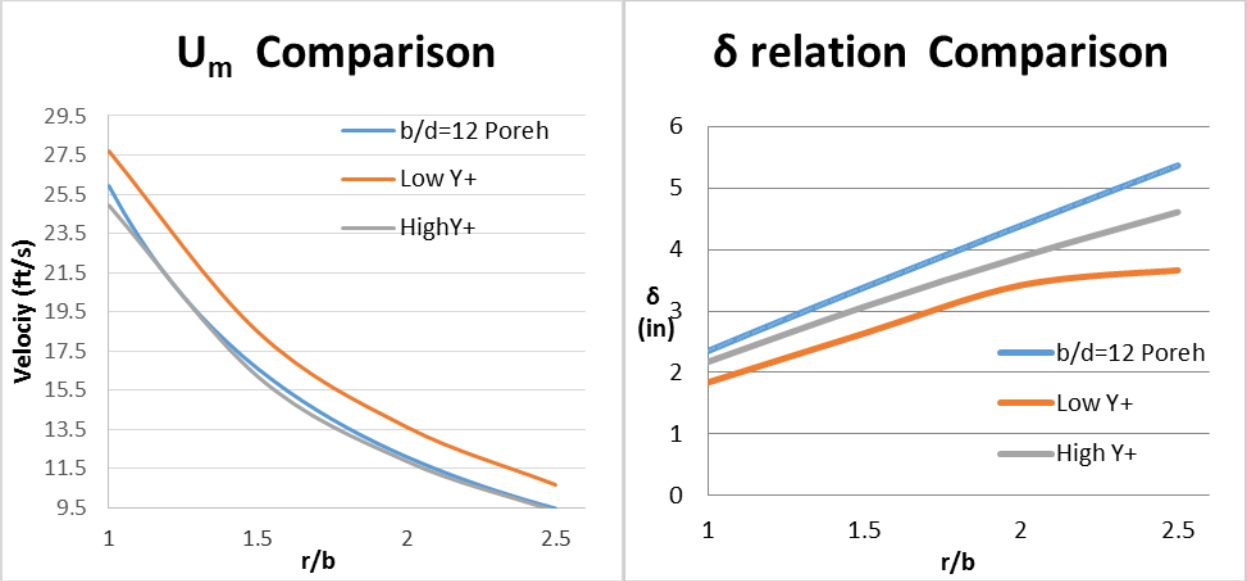

Figure 1-12. Correlation comparison between high and low Y+ using SKE-2 layer turbulence modeling.

It was concluded that the standard k-epsilon two-layer with a coarse mesh (pertaining to a high Y+) provided the best results. In both correlations, FIU noted an improved performance and, therefore, this is the selected mesh for the turbulence model under consideration. All simulations were re-run in order to obtain the final error and results.

Task 18: Technology Development and Instrumentation Evaluation

Task 18 Overview

The objective of this task is to assist site engineers in developing tools and evaluating existing technologies that can solve challenges associated with the high level waste tanks and transfer systems. Specifically, FIU is assisting in the evaluation of using a sonar (SLIM) developed at FIU for detecting residual waste in HLW tanks during pulse jet mixing (PJM). This effort would provide engineers with valuable information regarding the effectiveness of the mixing processes in the HLW tanks. Additionally, the Hanford Site has identified a need for developing inspection tools that provide feedback on the integrity of the primary tank bottom in DSTs. Recently, waste was found to be leaking from the bottom of the primary tank in AY-102. FIU will assist in the development of a technology to provide visual feedback of the tank bottom after traversing through the refractory pad underneath the primary tank.

Task 18 Quarterly Progress

Subtask 18.1: Evaluation of FIU's SLIM for Estimating the Onset of Deep Sludge Gas Release Events

The objective of this task is to assist DOE site scientists and engineers in developing tools and evaluating existing technologies that can solve challenges associated with the high-level waste (HLW) tanks and transfer systems. Specifically, FIU is assisting in the evaluation of using a 3D profiling sonar as part of its Solid-Liquid Interface Monitor (SLIM). SLIM was developed at FIU for imaging the settled solids layer in million gallon HLW tanks and for quantifying the residual

waste volume on the floor of HLW conditioning tanks during pulse jet mixing (PJM) operations. This effort would provide engineers with valuable information regarding the effectiveness of the mixing processes in the HLW tanks. In summer 2015, the focus of research was changed to address a new Hanford need to investigate the ability of the 3D sonar to image small increases in HLW volume as an early indication of possible deep sludge gas release events (DSGREs).

Additionally, the Hanford Site has identified a need for developing inspection tools that provide feedback on the integrity of the primary tank bottom in DSTs. Recently, waste was found to be leaking from the bottom of the primary tank in AY-102. FIU will assist in the development of a technology to provide visual feedback of the tank bottom after traversing through the refractory pad underneath the primary tank.

Task 18 Quarterly Progress

Subtask 18.1: Evaluation of FIU's SLIM for Estimating the Onset of Deep Sludge Gas Release Events

During April, FIU prepared to take measurements for the test matrix. Initial measurements were of lower quality than earlier this year and much worse than results for baseline cases taken in 2015. The instrument manufacturer was contacted and troubleshooting was initiated. A loose connection in the main sonar cable was discovered and the quality of the data was greatly improved to that of earlier this year. In addition, the zero offset was optimized which resulted in much better matching of the sonar's image from swath 1 (first swath) and swath 200 (last swath, same swath but from the opposite direction). The manufacturer also recommended that the targets being imaged should be at least 33 cm (13 inches) away from the sonar.

Measurements were taken of sand over a deflated bladder for the initial measurements. This flat but slightly angled disc of sand was measured for 6 heights (45, 45.184, 45.368, 45.552 45.736, and 45.92 cm). In Figure 1-13, the sonar in the tank and the disc of sand are clearly visible. In Figure 1-14, a 2D swath, a top view, and a 3D sonar image of this disc of sand are displayed.

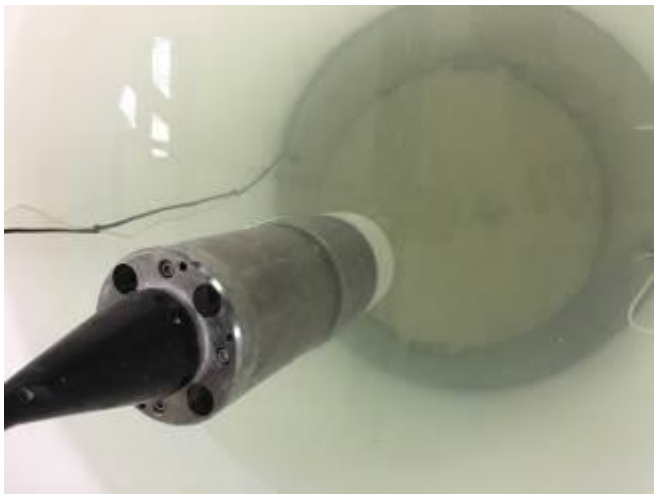

Figure 1-13. Sonar in the test tank and the target circular disc of sand.

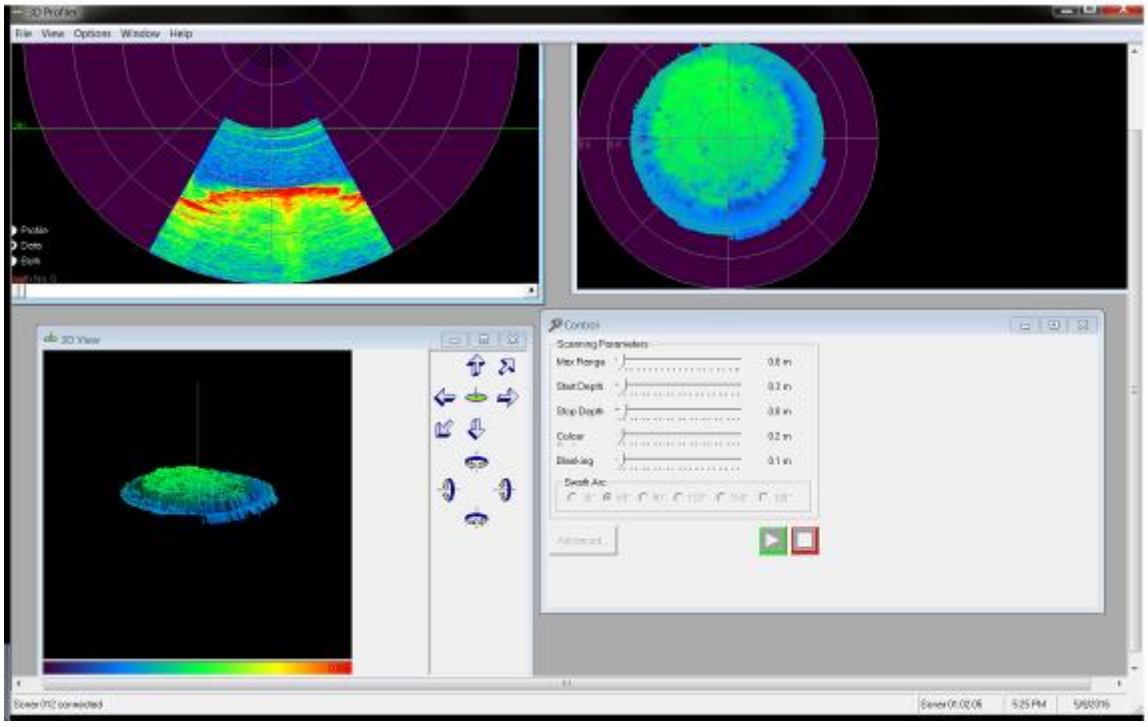

Figure 1-14. 2D, top view and 3D views of sonar imaging circular disc of sand at a distance of 45.92 cm.

In May, the 3D sonar test plan entitled, "Experimental Test Plan to Assess the Utility of 3D Sonars for Monitoring High-Level Radioactive Waste Settled Solids Surfaces for Indicators of Developing Deep Sludge Gas Release Events," was completed. This testing included sonar measurements on an air bladder under sand and a modified circular test pattern to determine the resolution and capability of the sonar for detecting small changes in the volume of settled solids in the field of view as a measure of possible gas retention in deep sludge layers.

Experimental Setup

The experimental setup included the 3-D sonar mounted inside a plastic tank that is 28 inches in height and 23.5 inches in diameter (ID) with a floor that slopes downward in the center to allow liquid to be drained from the bottom. A 23-inch diameter circular aluminum plate was inserted in the bottom of the tank to create a flat floor surface in the tank. The tank with the plate inside and the sonar inserted and with sand covering a bladder was used for Part I of this test plan. For Part II of this testing, the bladder was removed and a test object was inserted and imaged from multiple heights since accuracy of the sonar is limited to +/- 1% of the distance from the sonar to the object imaged.

FIU mounted an air bladder to a 40-cm diameter plastic lid with a 33-mm high lip and then loaded paving sand onto the lid to a depth of 33 mm at the edge of the lid and 57 mm in the center (fully deflated bladder). Figure 1-15 contains a photograph of the bladder mounted inside the lid (left) and the same bladder and lid with wet sand mounded over the bladder (right). The lid filled with sand sitting on a large metal plate at the bottom of the test tank is shown in the photo in Figure 1-16.

Figure 1-15. Photographs of air bladder mounted inside plastic lid and with sand added covering the bladder.

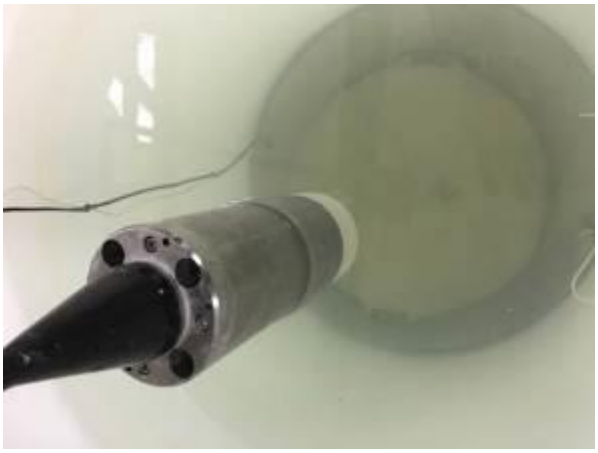

Figure 1-16. Photograph of sonar in the test tank with metal plate and plastic lid, bladder and sand.

From the test plan, it was important to measure the volume of the sand in the bottom of a tank from multiple heights. The accuracy of the sonar scales with the height from sonar head to the imaged target. While exact measurements of the highest sand surface over the bladder was measured with a measuring stick accurate to millimeters, the overall shape and volume of the sand for this experiment with the bladder was not well defined. In the final test matrix, the air bladder was either fully deflated, inflated 1 inch above fully deflated, or fully inflated (~1.5 inches higher than fully deflated). The sonar height was modified by adding 1, 2 or 3 metal spacers (4 cm thick) under the sonar platform.

Table 1-2. Test Matrix

Height of highest point of sand over bladder	Initial Sonar height above base plate
57 mm (deflated)	31.0 cm
57 mm (deflated)	35.0 cm
57 mm (deflated)	39.0 cm
57 mm (deflated)	43.0 cm
82 mm (1 increment of air)	31.0 cm
82 mm (1 increment of air)	35.0 cm
82 mm (1 increment of air)	39.0 cm
82 mm (1 increment of air)	43.0 cm
94 mm (2 increments of air)	31.0 cm
94 mm (2 increments of air)	35.0 cm
94 mm (2 increments of air)	39.0 cm
94 mm (2 increments of air)	43.0 cm

Initial sonar images from the test matrix are shown below. Some preliminary volume calculations have been done on the images and more refinement in the volume measurement is expected during June. The sand in the plastic lid with a deflated air bladder is shown from 2 sonar heights differing by 4 cm.

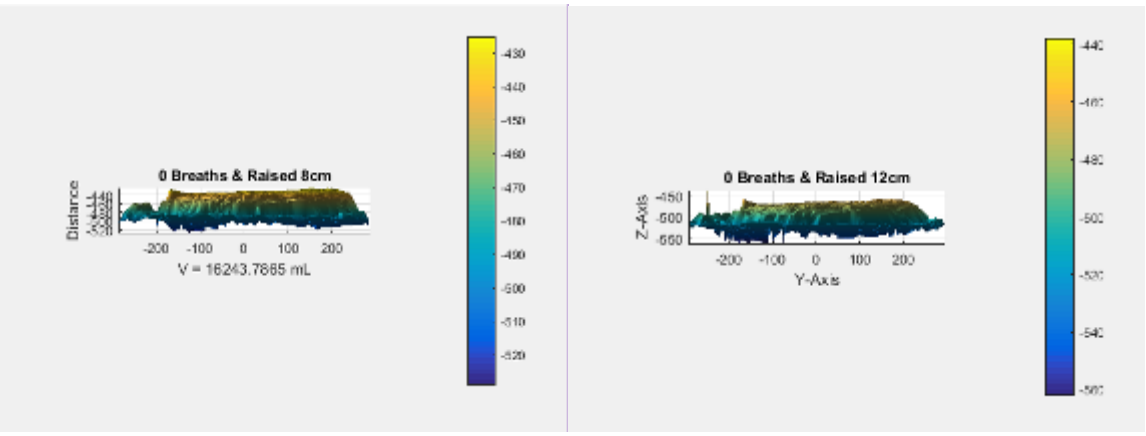

Figure 1-17. Images of same mound of sand with mounded sand atop but from 2 different sonar heights.

The sonar images below are taken from the same sonar position in the tank but the sand above the bladder (highest point) differs by ½ inch with the "2 breaths" being the fully inflated bladder.

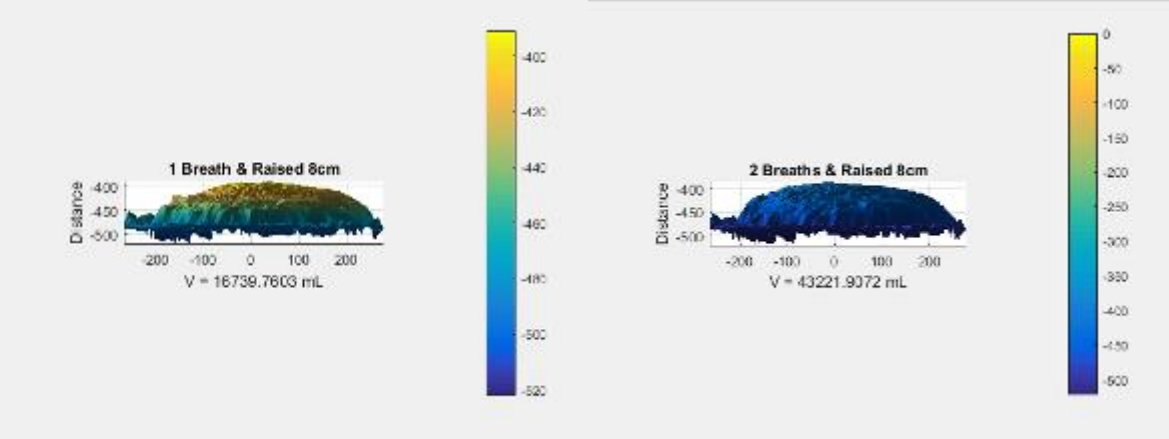

Figure 1-18. Images from same sonar height but with differing volumes in air bladder.

The second part of the test plan was to image a pattern in order to better determine the overall accuracy of the sonar for imaging settled solids volumes. The originally proposed linear test pattern was not effective since the radial scans of the sonar failed to hit the features with enough pings. A test pattern involving concentric circles was used and was very effective since each sonar swath hit the various sand heights found in the test pattern shown in Figure 1-19. The height and diameter of each ring of sand was measured accurately to the millimeter. Volume analysis of the sonar results will be completed in June.

Figure 1-19. Test object with circles of sand of varying heights and diameters measured to mm resolution.

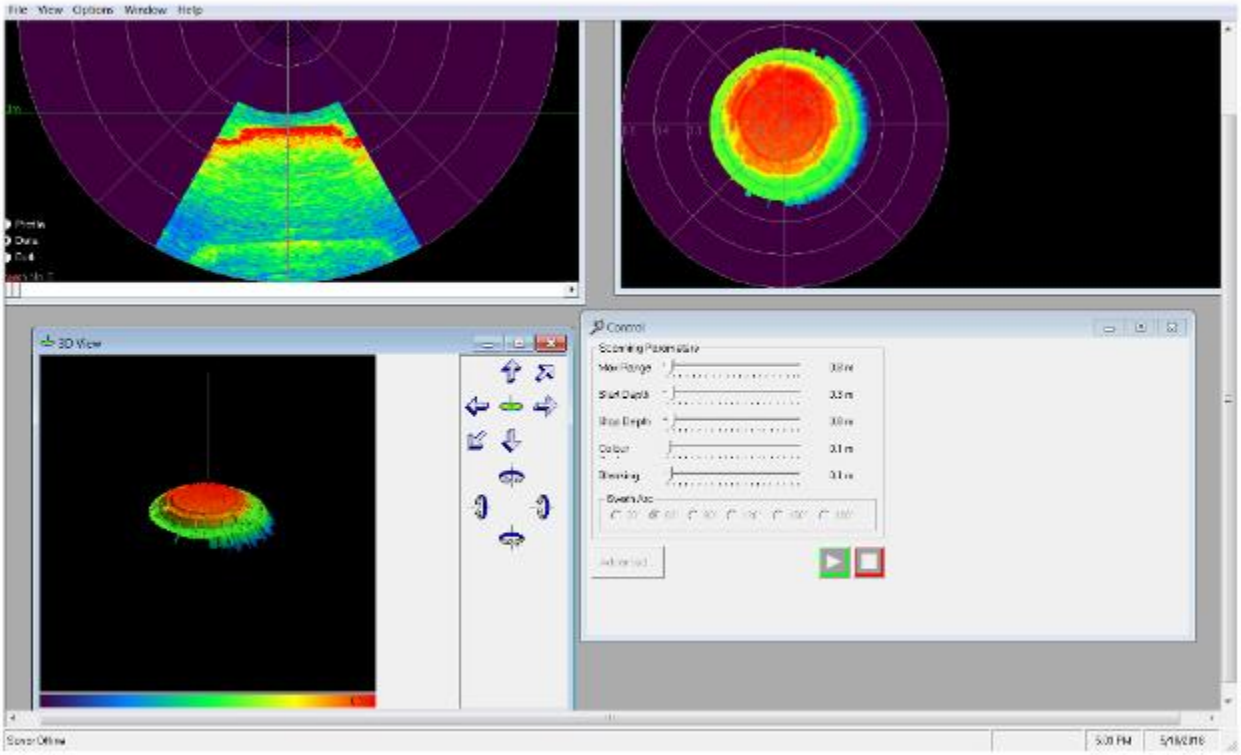

Figure 1-20. Sonar image of the circles of sand.

Development of software which approximates the volume of objects scanned has progressed to a point where a volume is very simply generated of the scanned surface. The algorithm in which the software processes the captured sonar data and displays it involves creating a triangular mesh between each and every point. Due to this meshing, a surface is created, in particular a convex hull, and, using the standard library functions provided by Matlab, the volume of the scanned surfaces is quantified and a differential volume is measured.

In June, analysis continued of the sonar images from the completed test plan entitled, "Experimental Test Plan to Assess the Utility of 3D Sonars for Monitoring High-Level Radioactive Waste Settled Solids Surfaces for Indicators of Developing Deep Sludge Gas Release Events."

The accuracy of the volume calculation (Matlab Code) was shown to vary from below 5% to over 500%. Measuring the volume of objects with known volumes allowed FIU to diagnose that there was a problem with the baseline (Z=0 plane) being calculated automatically in the Matlab code. For measuring the volume of HLW in tanks and monitoring the solids surface for changes over time, a calibration will be needed to ensure proper baselining.

The volume of settled solids in a HLW tank, $V_{t,}$ can be calculated by:

$$V_t = (h_L - z - d_{ave}) * \pi * R^2$$

where h_L is the height of the surface liquid level above the tank floor, z is the depth that the tip of the sonar head penetrated below the liquid surface, d_{ave} is the average depth (z-coordinate) of the solids surface below the sonar tip and R is the radius of the HLW tank.

The sonar images below from the test matrix show calculations of total volumes resulted in 14 to 50 liters of volume, which is much larger than the object being imaged (volume of the combined sand, air bladder and plastic lid of sand). The differential volume as shown below between 0 breaths and 1 breath is 0.496 cm^3 or ~1/2 liter (see Figure 1-21 and Figure 1-22). This volume is within 10% of the 448 cm^3 that was roughly measured for the irregular surface.

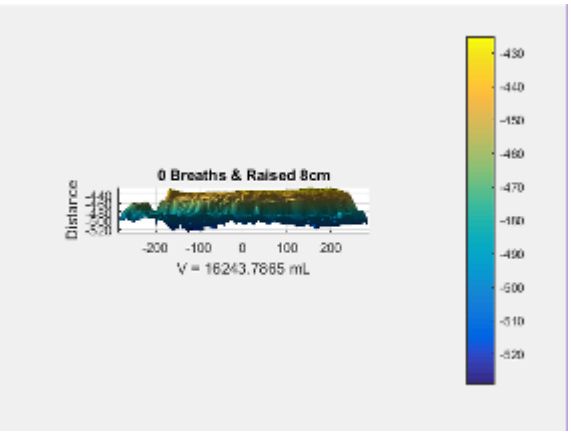

Figure 1-21. Images of mound of sand over deflated bladder a particular height.

The difference in volume of the system with 2 breaths of air in the bladder versus 1 breath was 26.5 liters versus the half liter between 0 and 1 breath (see Figure 1-22). This confirms that the volume measurement and its associated baseline are incorrect and need correction.

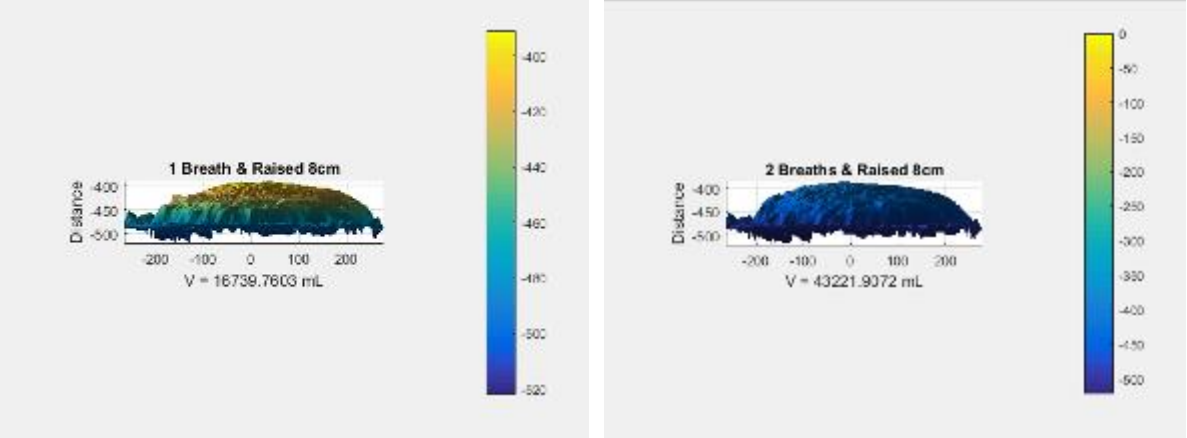

Figure 1-22. Images of mound of sand from same sonar height but with differing volumes in air bladder.

The second part of the test plan was to image a pattern in order to better determine the overall accuracy of the sonar for imaging settled solids volumes. The originally proposed linear test pattern was not effective since the radial scans of the sonar failed to hit the features with enough pings. A new test pattern was used with concentric circles of sand and metal strap for the circles (see Figure 1-23). With the sonar image from the commercial sonar imaging package, FIU was able to distinguish the height of the sand and the outer two circles (see Figure 1-24). The innermost circle is not visible in the image. Post-processing the sonar data with the FIU imaging algorithm allowed FIU to distinguish the 3 circles and the annulus around the innermost and middle circles. An estimation of the maximum error due to the resolution of the 3D sonar will be made from this image.

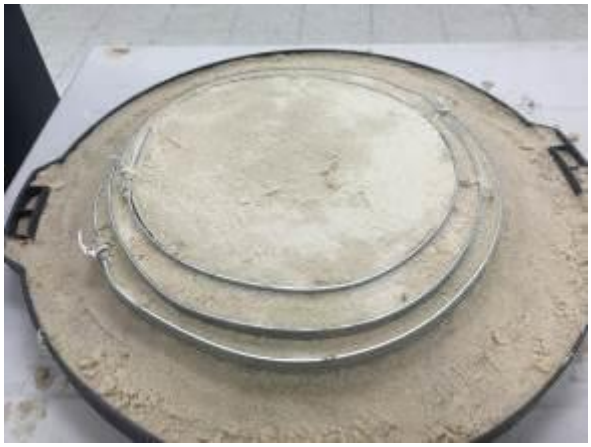

Figure 1-23. Test object with circles of sand of varying heights and diameters measured to mm resolution.

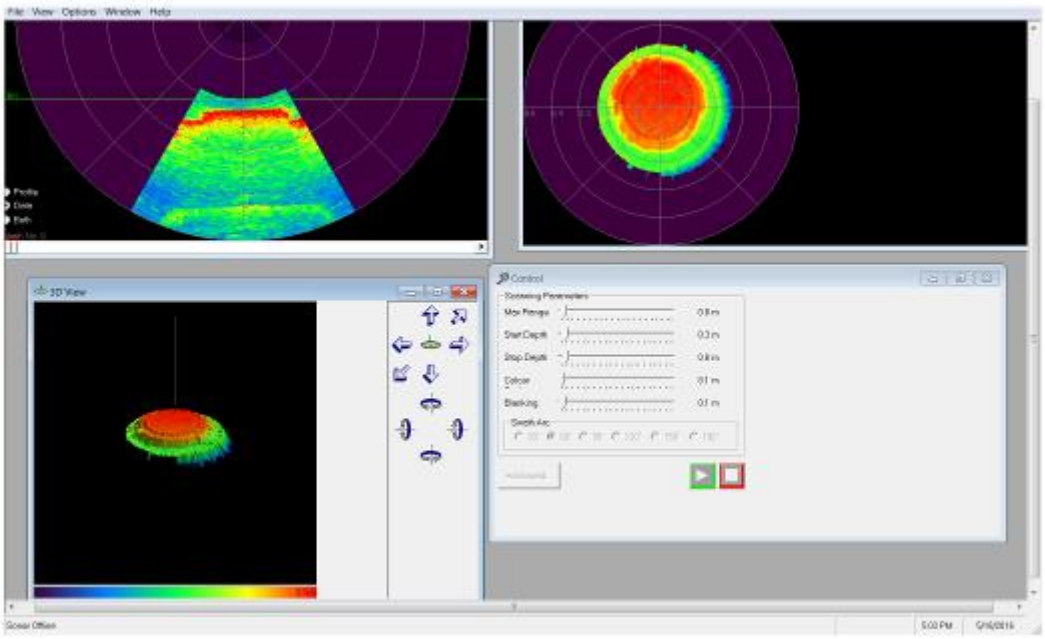

Figure 1-24. Sonar image of the circles of sand.

In order to better understand and then correct the volume measurement, FIU has imaged several objects with specific volumes. The first object was a plaster mold created in a glass dish and was used to test the volume algorithm. The object has the shape of a frustum of a right circular cone, or sometimes labeled as a truncated cone.

The volume of truncated cone, $V_{tc} = \pi \times h \times (R^2+r^2+R\times r)/3$

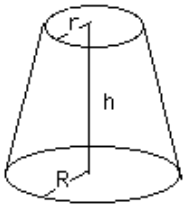

The dimensions measured are: h=7cm; R=6.9 cm; r=6.4 cm yielding V_{tc} = 973 cm^3. This compares well with the volume of the dish measured by liquid which yielded 946 cm^3. See the photograph of the plaster object below in Figure 1-25.

Figure 1-25

Figure 1-25. Plaster object used to test and correct volume calculation.

Figure 1-26 shows the image for the plaster object pictured above.

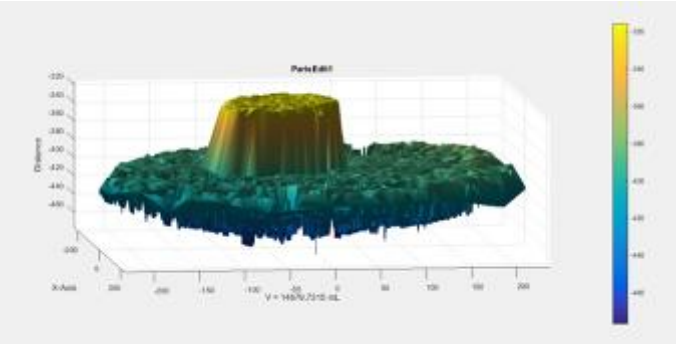

Figure 1-26. Sonar image of the plaster object used to help correct volume measurement.

Subtask 18.2: Development of Inspection Tools for DST Primary Tanks

Peristaltic Crawler

The main activities for the pneumatic crawler were focused on designing:

a) A full-scale sectional mockup of the DST;

b) A full-scale mockup of the ventilation riser of the DST; and

c) An instrumentation module.

The new mockups and the instrumentation module will be used to evaluate the performance of the robotics tool being developed at FIU, operating under similar conditions at the proposed inspection at Hanford. The design of new gripper for an electric version of the crawler was continued, as well.

Full-scale Sectional Mockup of the DST

A conceptual design has been developed (Figure 1-27) and the cost analysis for the construction is underway. In the mockup, the tank floor will be elevated, providing access not only to the top plates, but also to the bottom refractory pads. The setup will include the air supply line within the refractory which will also provide two of the outer refractory slots. The refractory pad will slide into the bottom frame and will be modular so that additional refractory configurations can be evaluated. Additional sections, including a vertical wall and central plenum, are being considered. The tank walls and knuckle will be built with 1/4" carbon steel plate; however, the sections will also be modular. If different plate thicknesses are needed, sections can be replaced with the appropriate size plates. The mockup dimensions are shown in Figure 1-28.

Figure 1-27. Full scale mockup testbed prototype.

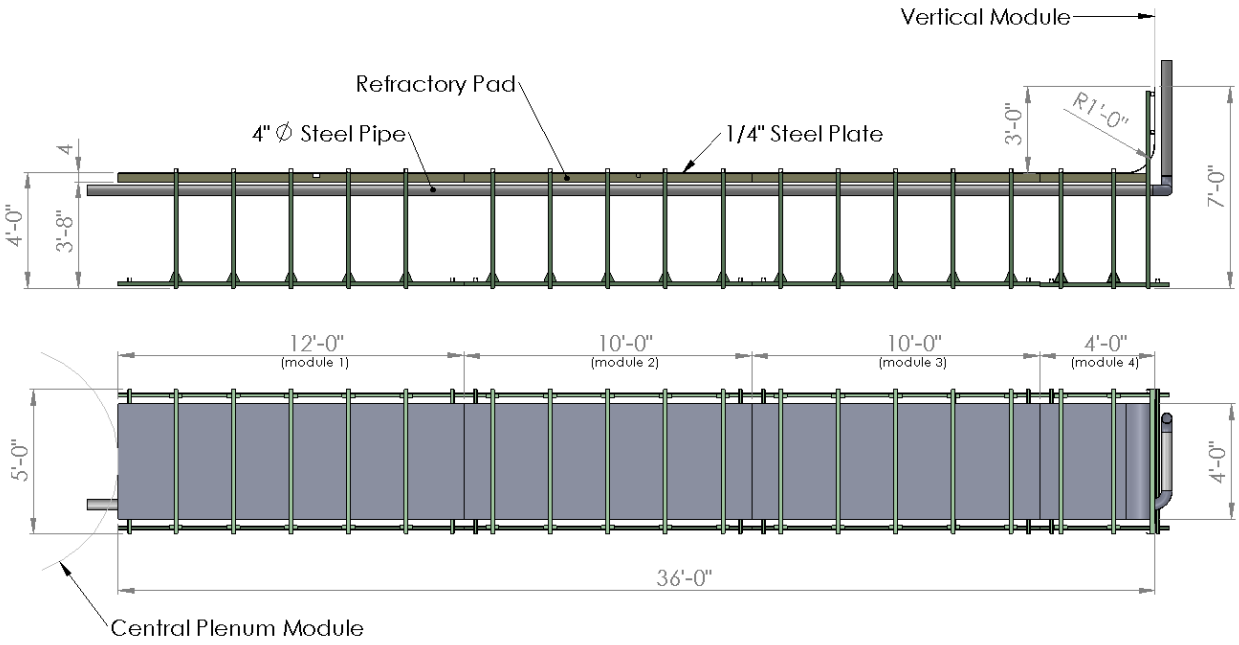

Figure 1-28. Mockup and module dimensions.

A structural analysis of mockup module 1 was perfromed using a finite element analysis. In the analysis, FIU investigated a possible future upgrade where plates with 7/8" thickness could be used, instead of the proposed thickness of 1/4". The total weight of the 1/4" plate is

approximately 500 lbs and for the 7/8” plate, 1720 lbs. The increase in weight of the plate is a concern, and may lead to excessive stresses acting on the structure.

The purpose of the analysis was to determine if a design overhaul would be necessary with thicker plates. Of particular concern are the plate hangers, clamps and threaded rods. Figure 1-29 below shows the stress distribution throughout the system is lower than the yield strength associated with 1023 carbon steel which is approximately 41 ksi.

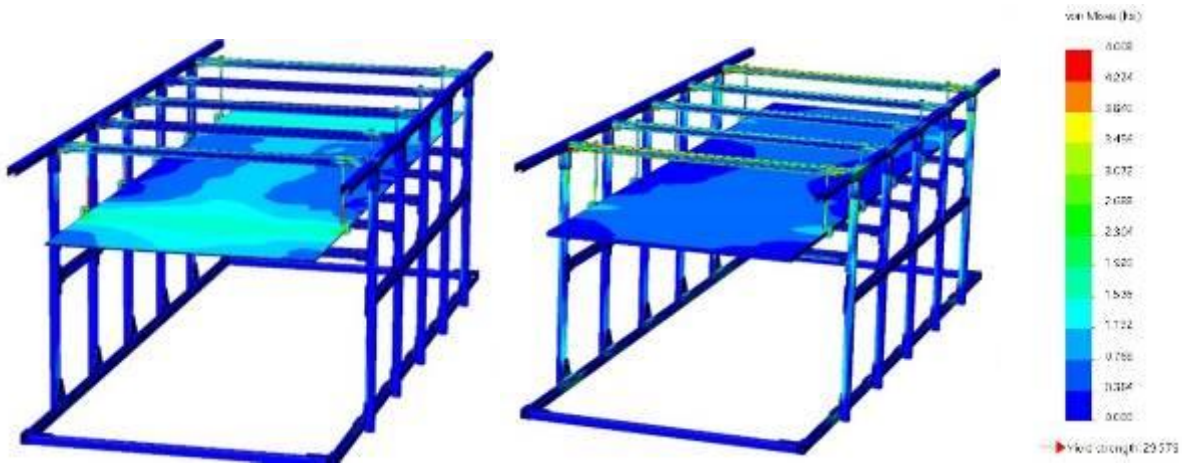

Figure 1-29. Stress distribution with 1/4” (left) and 7/8” (right) thick steel plate due static weight.

Figure 1-30 shows the displacement profile of module 1. The largest deflections are located in the horizontal areas near the center of the structure, width wise. This shows that even with the increase in plate size and weight, the deformation is negligible. This also implies that the structure itself will not need to be redesigned for the thicker plates.

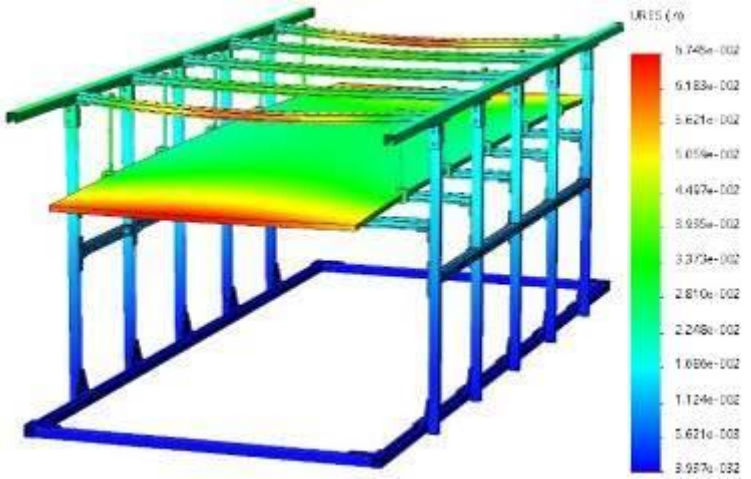

Figure 1-30. Exaggerated structure displacement of 7/8” steel plate due static weight.

The structural elements experiencing high stress values are the threaded rods and the clamps that connect the plate to the structure. Figure 1-31 shows their stress distribution and Table 1-3 shows the max load associated with the rod with a radius of 1/2”.

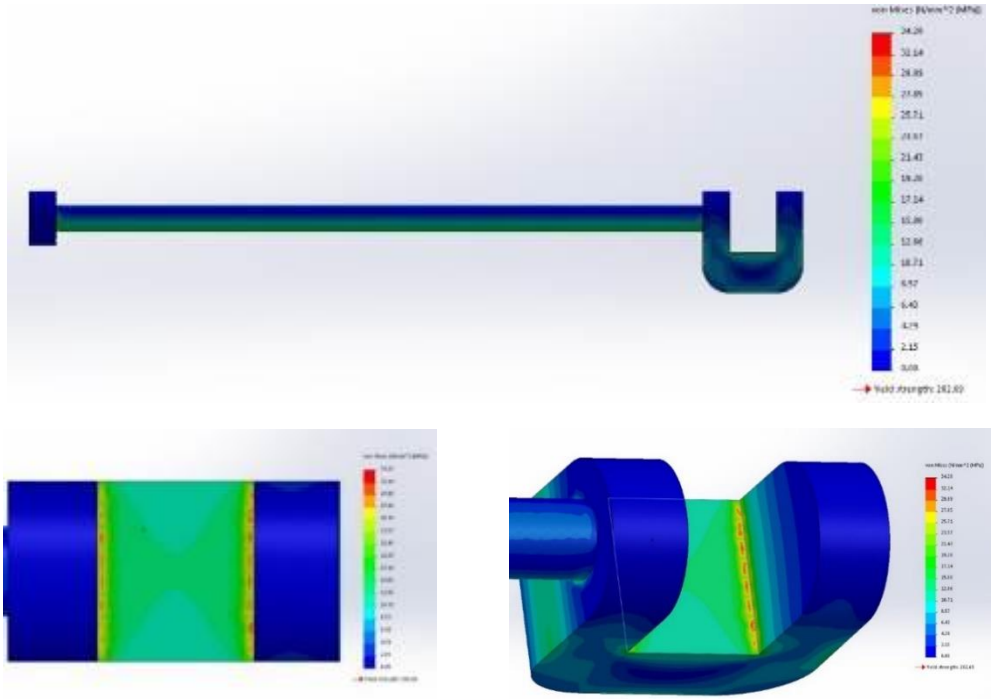

Figure 1-31. Stress distribution on threaded rods and clamps.

Table 1-3. Rod Dimensions and Their Associated Max Load

Rod Size (in)	Threads per Inch	Max Load (lbs)	Weight (lbs/ft)
1/4	20	240	0.12
3/8	16	730	0.30
1/2	13	1350	0.53
5/8	11	2160	0.84

Thus, the structure is structurally sound and will be able to handle the load introduced by the heavier 7/8" steel plate. With the exception of using wider c-clamps, further redesign will not be needed.

A full-scale mockup of the ventilation riser of the DST

The new mockup of the ventilation riser will be used to evaluate the performance of the peristaltic crawler, operating under similar conditions at the proposed inspection at Hanford. The main concern is the crawler's ability to manage the tether and to overcome the increasing dragging force during the inspection. The path dimensions of the proposed inspection are shown in Figure 1-32.

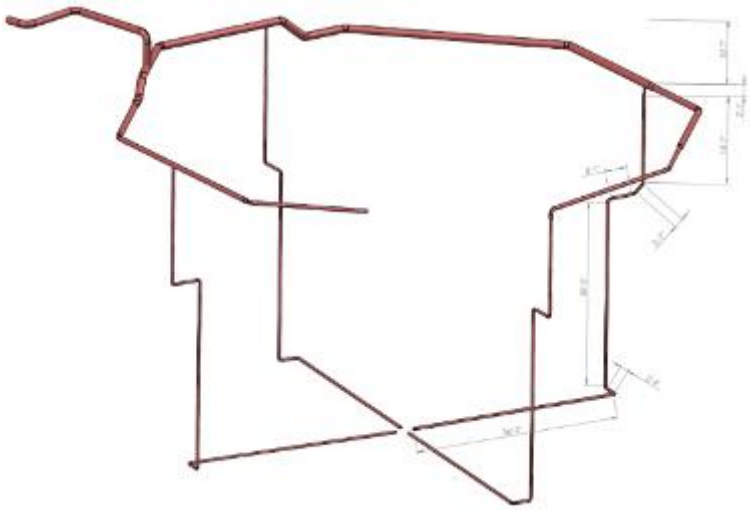

Figure 1-32. AY-102 ventilation riser.

The designed mockup, shown in Figure 1-33 below, has a layout equivalent to one of the AY-102 ventilation risers. However, in the design, the initial vertical section runs horizontally, which is structurally cost effective, considering the approximately 60 feet of piping that need to be vertically supported. In addition, a horizontal configuration will be more challenging, considering that during the vertical section, the crawler would be almost gravity fed. Figure 1-34 details the layout of the mockup.

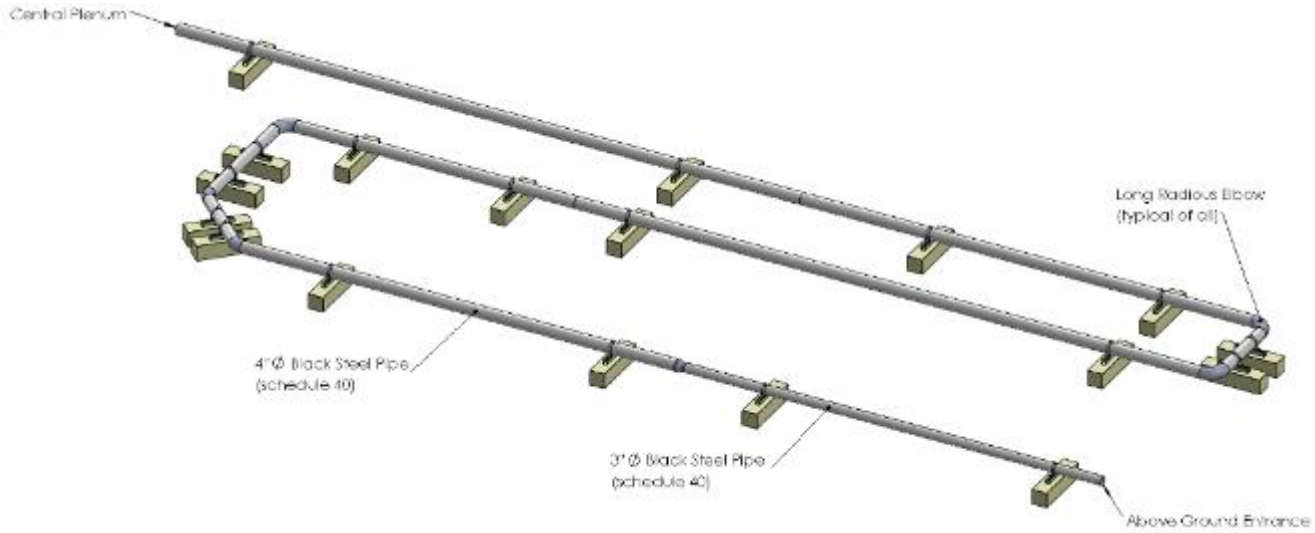

Figure 1-33. Ventilation riser mockup.

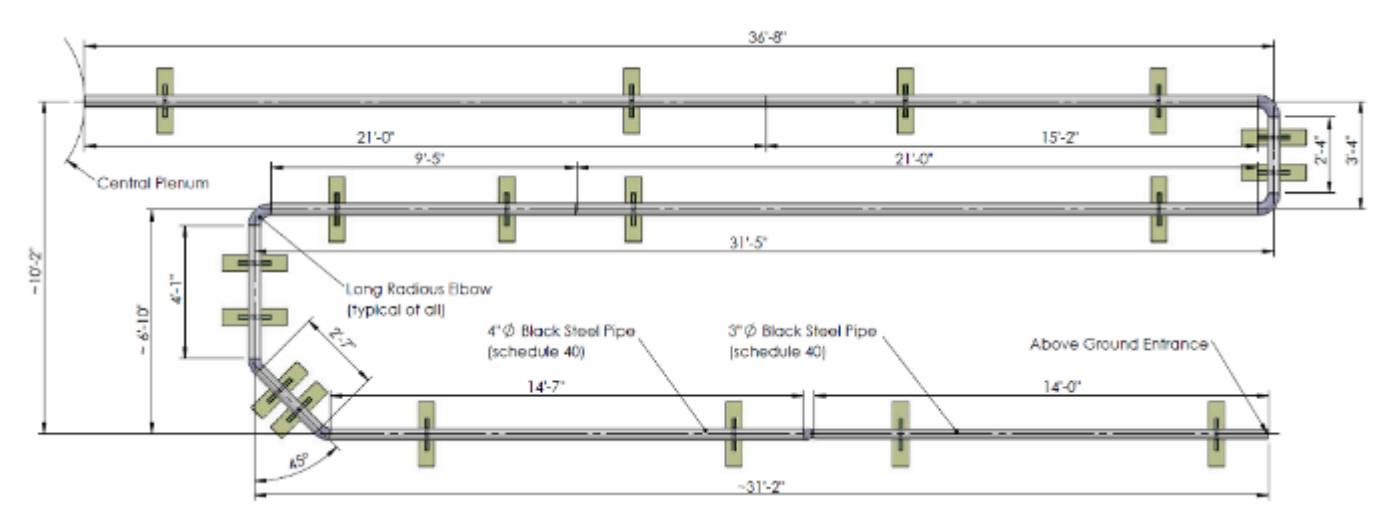

Figure 1-34. Layout of the ventilation riser mockup.

The construction of the mockup are almost complete; all parts were purchased, the pipelines were cut to length, and the assembling started.

Instrumentation Module

The conceptual design of the new instrumentation module has been almost finalized. However, FIU is still working on the software that will enable the module control and communication. In addition, the use of force sensitive resistors (FSR) were investigated. The sensors could be planted in the claw pads of the gripping mechanism, which would provide a means to measure the grip force. The FSR varies its resistance depending on how much pressure is being applied to the sensing area. The harder the force, the lower the resistance. Figure 1-35 shows an FSR with a round, 0.5" diameter sensing area that senses applied forces anywhere in the range of 100 g to 10 kg. The addition of FSR to the design would provide gripping and sliding feedback during the mockup tests and future inspections.

Figure 1-35. Force Sensitive Resistor (FSR).

The new module will be used to measure the performance of the current design under full-scale mockup tests, and it can be incorporated the tool enhancing its robustness.

Electric Gripper

Figure 1-36 shows a preliminary design of the electric grippers, which will be used as proof of concept. In the design, the gripping mechanism is actuated by a leadscrew driven by a micro DC gearmotor.

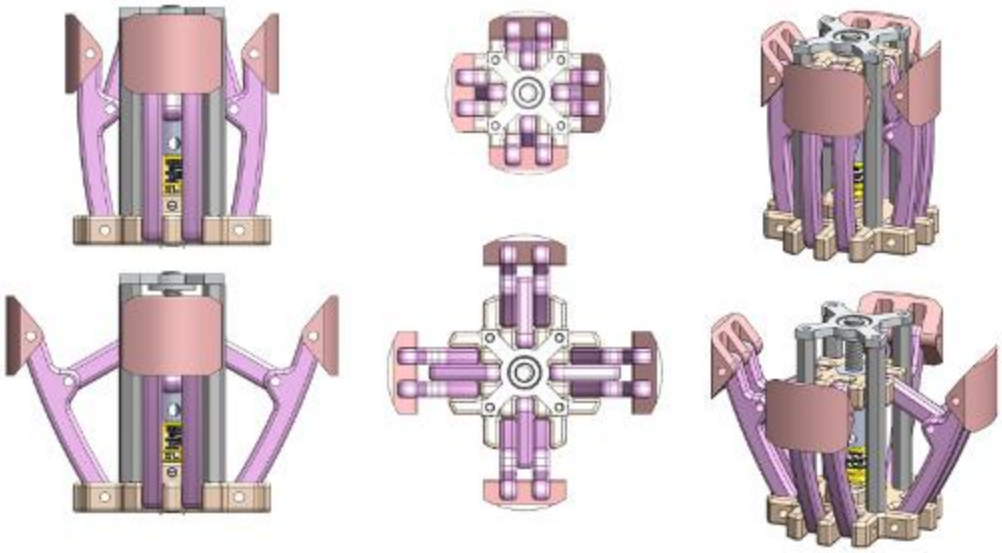

Figure 1-36. Electric gripper preliminary design.

An electric version of the crawler has the potential to develop stronger and smaller inspection tools. However, the output speed is a design concern.

The output torque of a leadscrew depends on a number of characteristics for the screw, including the sliding nut and the collar clamp. The theoretical output capability of the power screw is:

$$T_R = \frac{d_m \cdot W}{2}\left[\frac{\mu_s + \cos(\theta_n)\cdot\tan(\alpha)}{\cos(\theta_n) - \mu_s \cdot \tan(\alpha)}\right] + \frac{d_{mc}\cdot\mu_c\cdot W}{2}$$

Where:

- d_m = mean screw diameter
- d_{mc} = mean collar diameter
- W = desired force output (axial)
- θ = thread angle (radians)
- $\theta_n = tan^{-1}(cos\alpha \cdot tan\theta)$
- μ_s = coefficient of friction of the screw surfaces
- A = helix/lead angle (radians)
- μ_c = coefficient of friction of the screw/thrust collar surfaces

Figure 1-37 shows the output of a 1/4” stainless steel ACME threaded lead screw with a bronze sliding nut, and the following dimensions: d_m= 0.21875 in, d_{mc}= 1/2 in, θ= 29˚, μ_s= 0.15-0.23, α= 5.2˚, and μ_c = 0.09-0.15.

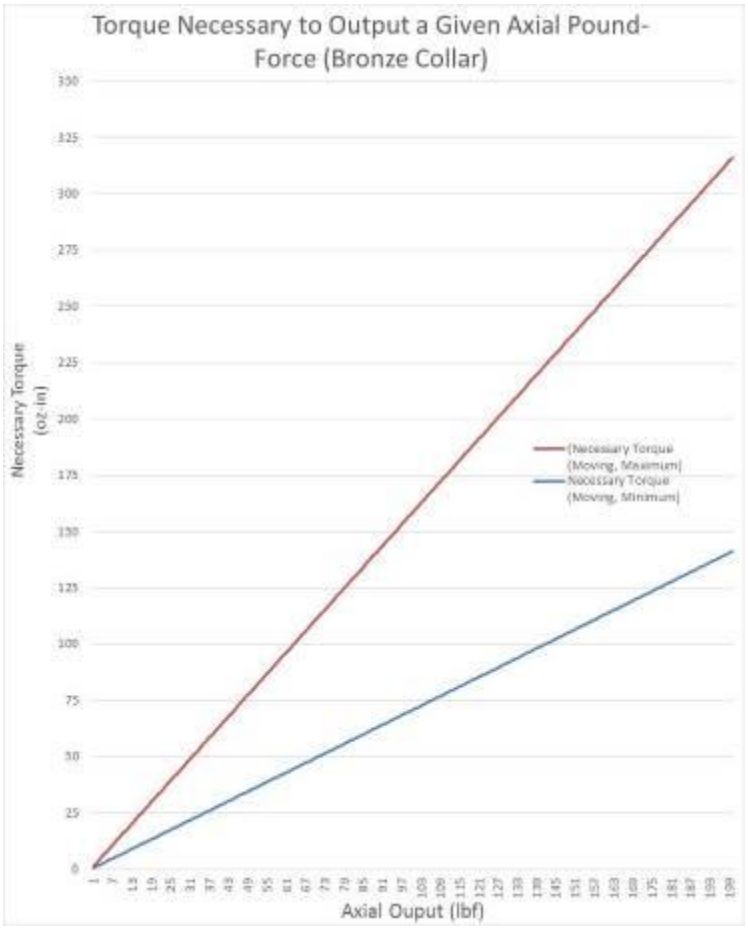

Figure 1-37. Power screw output.

Base this preliminary analysis, the micro gearmotor prototype has been selected, and it is being evaluated.

Miniature Magnetic Rover

For the miniature rover, testing and validations were conducted with the objective of verifying the navigation of the inspection tool on curved surfaces. To date, the navigation of the inspection tool has only been verified on flat surfaces. These tests demonstrate the potential of the rover to provide inspections in carbon steel pipes as well as refractory channels.

For the initial testing, a bench-scale set up was used which included 3-in and 4-in diameter pipes as shown in Figure 1-38.

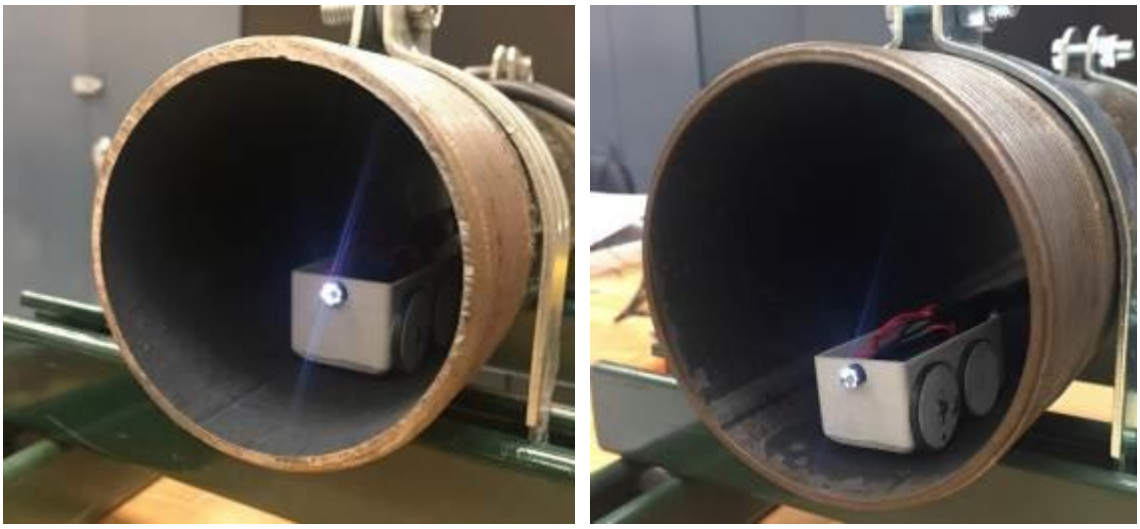

Figure 1-38. Inspection tool tested inside a (a) 3" and (b) 4" pipe bench-scale.

In previous updates, it was shown that the magnetic force drops significantly with the increase in space between the magnet array and the ferromagnetic surface. The inspection tool was able to navigate inside both 3-in and 4-in diameter sample pipes. However, during the deployment and detachment phase, there was a notable reduction in the magnetic force which is due to an increase in distance due to the curvature of the pipe. Similarly, there was a higher magnet force observed when deployed on the exterior or convex surface of the pipe. The quantification and formulization of the magnet force on curved surfaces is currently being evaluated. These initial tests demonstrate the potential of utilizing the rover on curved surfaces without any design modifications.

An experiment was conducted to evaluate the ability of the rover to navigate across gaps. Testing was conducted over two separate pieces of steel plate aligned using a clamp. A gap was created by separating the steel plates (Figure 1-39) with an initial gap of 1 mm. After each successful test, the gap was increased. The maximum gap the inspection tool was able to overcome was 28.02 mm, which is almost half of length of the inspection tool (62.98 mm).

Figure 1-39. Test set up for navigation over a gap.

The navigation of the tool in a corroded steel pipe was also evaluated. This test was conducted inside five steel pipes that were 20 feet in length and 3-in in diameter. The 5 pipes that were used for the testing are shown in Figure 1-40a. Similar to the initial bench-scale tests, the magnetic force and pulling capability of the inspection tool was significantly decreased. However, the tool was able to navigate through the 20-ft pipes. Significant debris did build up on the magnets (Figure 1-40b but this didn't impede the progression of the inspection tool. Another notable issue was the weight and drag from the tether which applied a torque on the body of the device, preventing the inspection tool from navigating in a straight path.

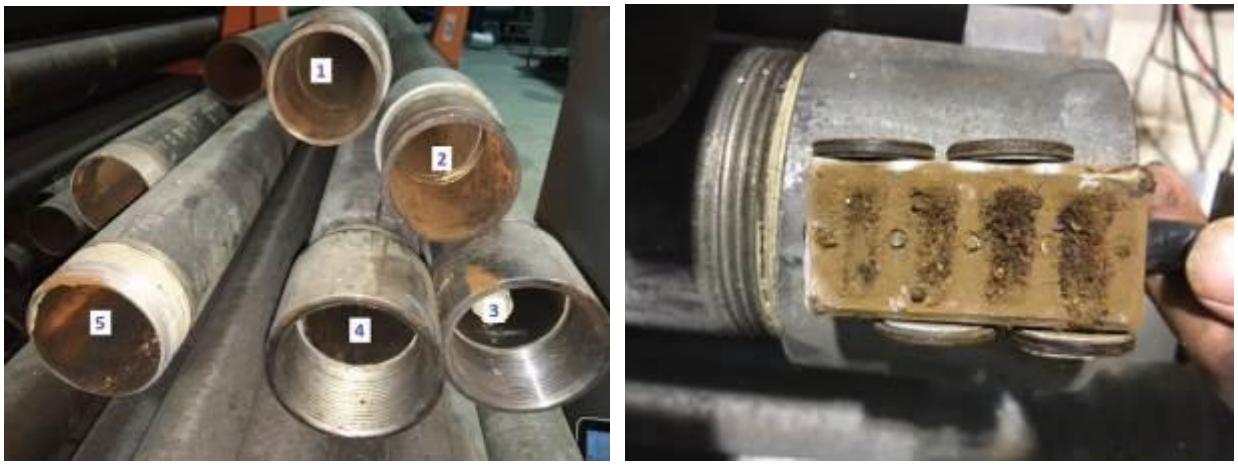

Figure 1-40. a) The corroded pipes used for navigation test and b) debris build up on the magnets after 100 feet of navigation.

During this period, magnet force measurement tests were also conducted to verify the accuracy of the theoretical approach. The gap between the magnet and the surface was increased from 0 mm to 2 mm with steps of 0.1 mm. The experimental set up is shown in Figures 1-41a and 1-41b. Figure 1-41c shows how well the experimental measurements correlate with the theoretical values.

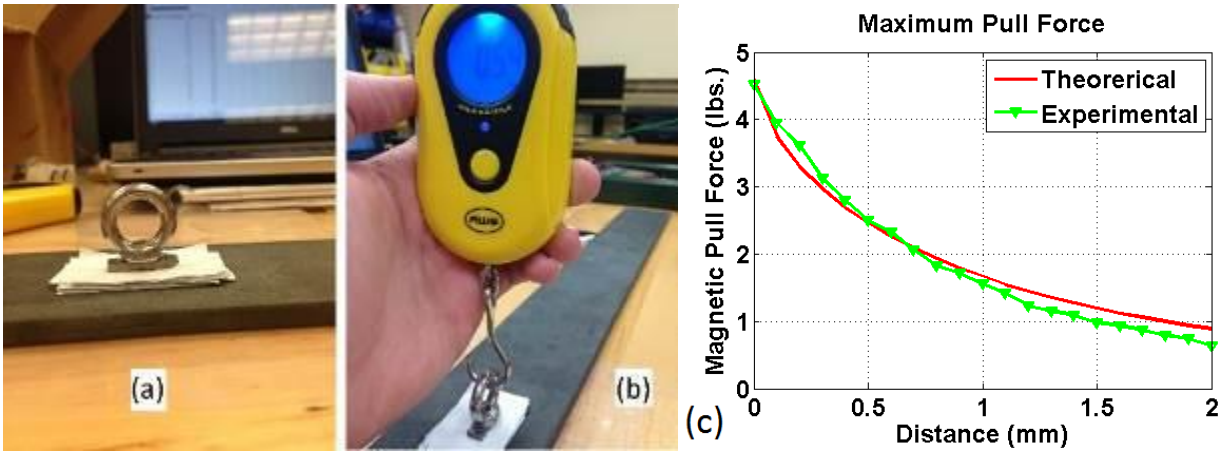

Figure 1-41. a) Using sheets to create air gap, (b) measuring air gap, (c) pull force theory vs. experimental.

Separate experimental tests were designed and conducted to identify the force of the magnet inside the pipes. The objective of the test was to measure the correlation between the size of the air gap and magnetic adhesion force inside the varying-diameter pipes. Additionally, FIU wanted

to identify the equivalent value of air gap when measured against the surface. Figure 1-42a is a schematic diagram that shows the maximum gap measured when the inspection tool was inserted inside a pipe with a diameter of 3 inches. Figure 1-42b shows a similar measurement with a diameter of 4 inches.

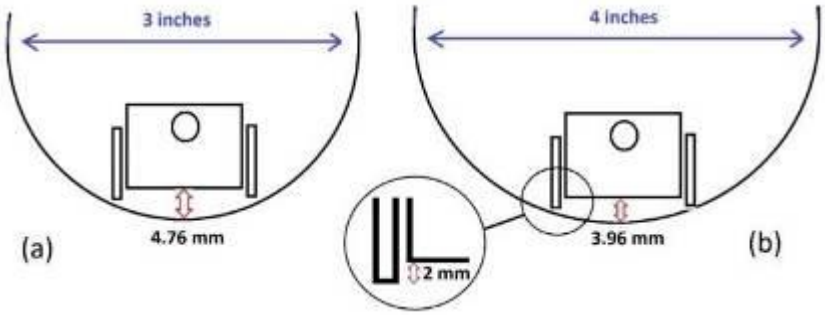

Figure 1-42. Schematic diagram of inspection tool inside a 3-in diameter pipe (a) and 4-in diameter pipe (b).

In order to measure the maximum pull force inside a pipe, a slightly modified inspection tool was needed. A flexible wire rope was passed through the holes on the inspection tool (originally intended for the inspection camera). As shown in Figure 1-43, the wire was passed through both ends of the pipe to reach the measurement scale. The tension inside the wire was considered to be uniform and, due to use of a pulley at the edges of the pipes and equal length of wire rope inside and outside the pipes, the scale was used to measure the detaching force of the magnet.

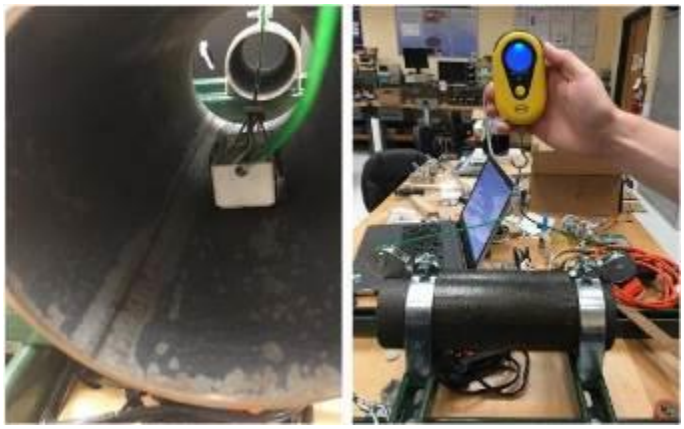

Figure 1-43. (a) Deployment inside pipe, (b) Magnetic force measurement set-up.

The result of the pull force test in the 4-inch pipe was 1.44 lb. This means that there was an individual pull force of 0.36 lb for each of the four magnets. This value is equivalent to pull force on the flat surface with an air gap of 3.75 mm. In the case of the 3-inch diameter pipe, an overall value of 1.06 lb was measured. This correlates to 0.26 lb equivalent to the pull force on the flat surface with an air gap of 4.45 mm. Navigating in the concave internal surface of the pipes increases the air gap and reduces the magnetic adhesion. For the 3-inch diameter pipe, 88% of the adhesion force is lost due to the increase in the gap compared to flat surfaces. For the 4-inch diameter pipe, 59% of the adhesion force is lost.

FIU also developed a new test set-up that can measure the pull force of the tether with more realistic materials and coefficients of friction. The design included 17 feet of the 1.5 in. by 1.5 in.

channels and two turns: one 90 degree turn at the end of the channel and another turn 8 inches away. Figure 1-44 shows the test bed which was constructed using brick pavers to provide more realistic friction forces.

Figure 1-44. Laboratory scale test bed created for determining the pull force created by tether.

Measurements of the current tether pull force provided a range from 2.8 to 4.4 lbs. When a smoother Ethernet cable was utilized, the average pull force was about 1.2 lbs. Since the geometry of the current inspection tool does not allow for 90 degree turns (the initial goal is to make it through the first 17 ft of straight section), the tool was manually placed after the first turn and on average was able to navigate 4 inches after the first turn. Several standardized protocols allow electrical power to be transmitted along with data over Ethernet cabling. Depending on the standard of cabling, a maximum power of 25.5 watts would be available using Power over Ethernet (PoE). Figure 1-45 compares the pull force using the existing tether and the Ethernet cable.

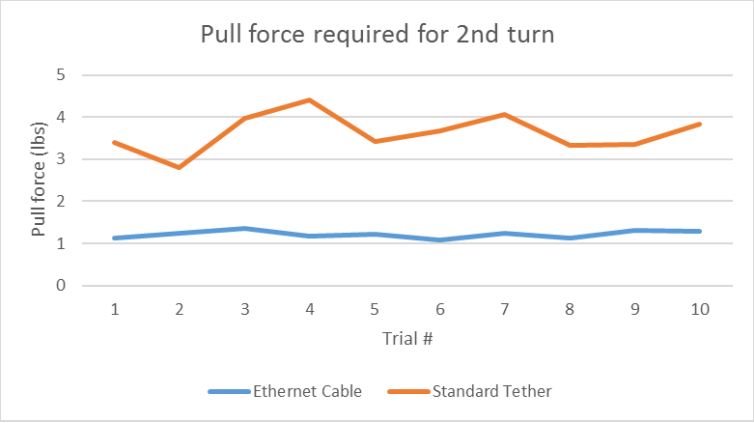

Figure 1-45. Comparison of the tether pull-force inside the test bed.

A tether management system was also designed and assembled during this period of performance. This system is necessary to provide a tangle free means of storing/supplying the tether for the inspection tool. A first prototype of the tether management system was developed

with a step motor as the primary driving force. A timing belt was used to coil the tether around its base and can adjust the gear ratio of the system (Figure 1-46).

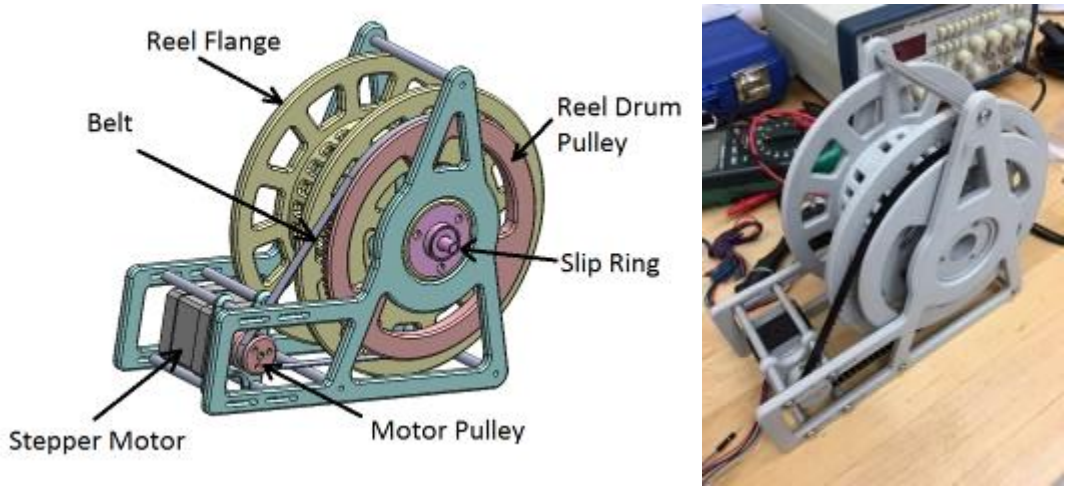

Figure 1-46. Tether management system for inspection tool.

A DRV8825 micro-stepping bipolar stepper motor driver was calibrated using current to drive the stepper motor. Control of the stepper motor and inspection tool were synced so as the rover moves, the tether system rotates in the proper direction to feed/collect the tether.

Subtask 18.3: Investigation Using an Infrared Temperature Sensor to Determine the Inside Wall Temperature of DSTs

FIU completed emissivity calibration for a carbon steel tank and conducted bench-scale testing of the Raytek MI3 infrared (IR) sensor. The Raytek IR sensor is calibrated for emissivity based on the test material. A carbon steel drum (tank) has been used to represent the double-shell tank (DST) material. The tank has a capacity of 10 gallons and is 0.0375" thick (20 gauge). Its outer diameter is 14 5/8" and height is 18 7/8". The test included filling the tank with to a certain height and heating it using an electric immersion coil heater (120 V/ 1350 watts) that can heat up to 212ºF. The test set up is as shown in Figure 1-47a and the heating coil is as shown in Figure 1-47b. The Raytek sensor was used to measure the temperature on the outer surface of the tank with an emissivity setting of 0.9 (as an initial estimate). A thermocouple was also placed at that location to take the temperature readings as shown in Figure 1-47c. The emissivity of the Raytek sensor was adjusted until both readings matched. The final emissivity was chosen as 0.79 which is in agreement with the literature value of the emissivity range of carbon steel.

Figure 1-47. a) Bench scale test set up, b) immersion coil, and c) thermocouple and Raytek sensor head.

Once the emissivity had been adjusted, bench-scale tests were conducted based on the previously defined test matrix with varying parameters including temperature, sensor distance from the tank and height. In this case, the temperature of the water was measured using the Raytek sensor and thermocouples on the outer surface, while a thermometer was used to measure the temperature close to the wall (inner surface). The three pieces of equipment used for temperature measurement are as shown in Figure 1-48a. Sample experimental results at different time intervals are tabulated in Table 1-4. Roller surface K-type thermocouples along with the universal thermocouple connectors (UTC-USB) were used to acquire the temperature data as shown in Figure 1-48b.

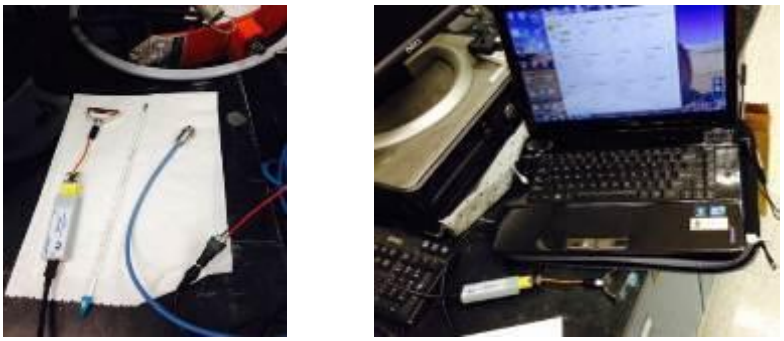

Figure 1-48. a) Equipment for temperature readings, b) data acquisition using the UTC-USB connector.

It was observed that the readings obtained from the Raytek sensor and the thermocouples showed an uncertainty of 2-8%. This could be due to the adjustment required for the sensor ambient background temperature compensation which is currently being investigated. Also, it is observed that the horizontal distance of the sensor from the surface did not significantly influence temperature readings as long as the range was between 2” and 6”.

Table 1-4. Comparison of Temperatures Readings

Height (inch)	Thermometer Reading (°F)	Thermocouple Reading (°F)	Raytek IR Sensor Reading (°F)
9	128	129	131
11	130	130	132
9	144	141	150
11	144	145	154
9	155	153	157
11	155	151	160
9	168	166	171
11	167	166	170

FIU researched all of the equipment necessary for engineering-scale testing of the infrared (IR) sensor, obtained quotations for the materials needed, completed procurement, built the experimental set-up, and conducted baseline experiments.

A schematic of the engineering-scale system is shown in Figure 1-49 and photographs are shown in Figure 1-50. It consists of a stainless steel tank with dimensions 2x4x3 ft., filled with water to about half the tank height. A 1300 watt precision coil heater is being used to increase the temperature. A carbon steel plate (7/8th in thickness) is suspended on the surface of the water using bars and C-clamps. At various intervals of time, temperature measurements are recorded using the IR sensor, thermocouple, laser gun and a thermometer. The IR sensor is scanned along the length of the plate (x-direction) and also at various heights (y-direction).

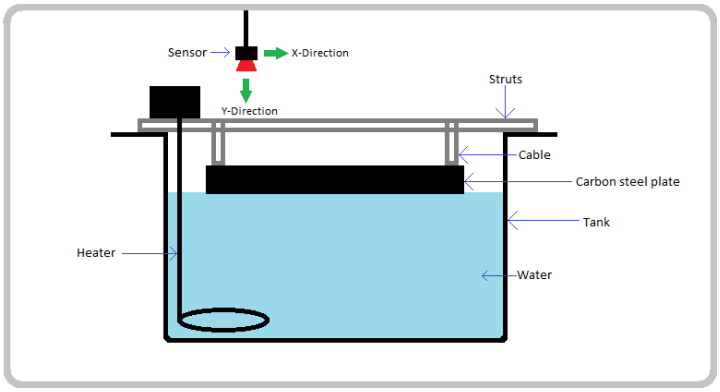

Figure 1-49. Engineering scale test set up.

Figure 1-50. (a) Engineering scale test set up. (b) Measurements using the thermocouple.

To conduct the baseline experiments, a test matrix has been established based on the experimental set up and considering the following parameters:

- Temperature of water inside the tank – The temperature of the water bath in the tank is varied from 90ºF to 130ºF in intervals of 10ºF.
- Measurement along the length of the test piece (x-direction) – These set points for temperatures represent the vertical height of the tank and are specified in intervals of 6 inches starting from one end to the other.
- Distance of the IR sensor from the test piece (y-direction) – The annulus of DSTs is approximately 3 ft wide, so the IR sensor is configured and physically placed to capture readings at distances of 2 in, 6 in, 12 in and 24 in.

Temperature measurements using a thermocouple (Figure 1-51b) are taken as the standard and are matched with those obtained by Raytek MI3 IR sensor. As described in the test matrix, height and length based measurements are taken. Sample test results are given in Table 1-5. It is evident from the table that the Raytek IR sensor is prone to sensitivity as the temperature measurements vary about 3-6%. This could be due to the variation in the ambient temperatures during the experiments.

Table 1-5. Sample Temperature Results Using IR Sensor and Thermocouple

Distance(in)	Y=2	Y=6	Y=12	Y=18	Y=24	TC
X = 0.1	102	102	102	102	102	102
X = 6	110	110	110	110	109	100
X = 12	108	108	108	107	107	100
X = 18	108	108	107	106	105	101
X = 24	104	102	102	102	102	100
X = 30	104	102	101	101	102	100
X = 36	103	103	102	102	101	100
X = 42	103	104	104	104	103	99

TC - Thermocouple

In order to study the variations, a regression analysis has been performed on different sets of sample data obtained from the Raytek IR sensor. Results are as shown in Figure 1-51 (a). The

data scatter shows the sensitivity of the Raytek sensor. To obtain an overview of the temperature distribution, a thermal camera has also been used and a typical sample image (temperatures between 85ºF and 95ºF) is shown in Figure 1-51 (b).

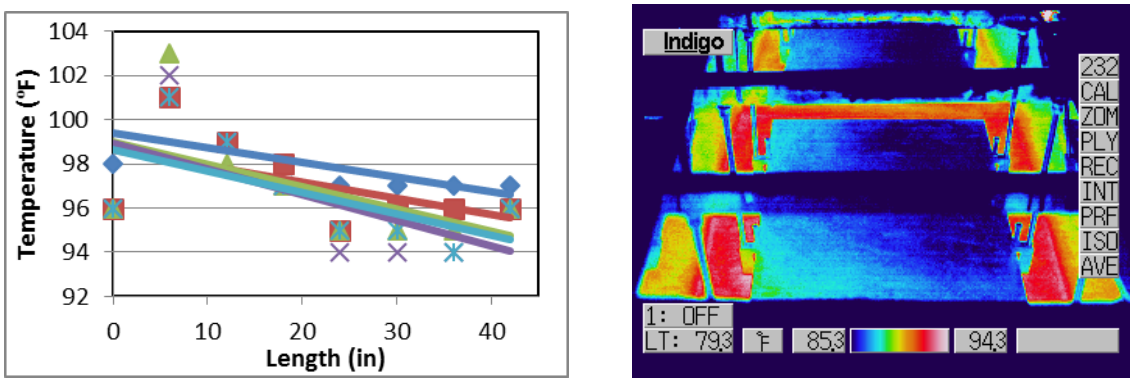

Figure 1-51. (a) Temperature variations along the length (b) Temperature contours using thermal camera.

Currently, FIU is in the process of analyzing the baseline experimental data to further redefine the test matrix and continue conducting the new experiments. Also, simulation based thermal analysis will be conducted for validation and verification.

Task 19: Pipeline Integrity and Analysis

Task 19 Overview

The objective of this task is to support the DOE and site contractors at Hanford in their effort to evaluate the integrity of waste transfer system components. This includes primary piping, encasements, and jumpers. It has been recommended that at least 5% of the buried carbon steel DSTs waste transfer line encasements be inspected. Data has been collected for a number of these system components and analyzed. Currently, different ultrasonic transducer systems are being investigated for thickness data measurement to determine the actual erosion/corrosion rates so that a reliable life expectancy of these components can be obtained. An additional objective of this task is to provide the Hanford Site with data obtained from experimental testing of the hose-in-hose transfer lines, Teflon® gaskets, EPDM O-rings, and other nonmetallic components used in their tank farm waste transfer system under simultaneous stressor exposures.

Task 19 Quarterly Progress

Subtask 19.1: Pipeline Corrosion and Erosion Evaluation

FIU received final quotations (for purchase and leasing) for the two potential ultrasonic transducers (UT) systems: the Ultran mini sensors and the Permasense guided wave sensors. FIU communicated closely with the site engineers to finalize the decision to purchase of one of the systems; it was decided to procure the guided wave sensors for pipeline erosion and corrosion testing of pipe sections (2”, 3” and 4”). The manufacturer chosen is Permasense and the sensors are the WT 210 series along with the corresponding data acquisition systems. FIU initiated procurement of the Permasense Guided Wave sensors. The manufacturer has supplied the quotation and FIU is awaiting purchasing to approve the request.

These sensors have proven applications in oil and gas industries and similar areas. As a recent example, erosion/corrosion monitoring using the permanent mount ultrasonic transducer (UT) systems (from Permasense) in European refineries has been successfully implemented [1]. Thinning of pipes was determined based on real-time continuous monitoring.

The sensor system consists of the 304 stainless steel wave guides, sensor head, antenna, battery and a stabilizer. In addition, there is a built-in thermocouple probe to monitor the pipe surface temperature which also allows the wall thickness measurement to be temperature compensated when required. The sensors communicate using the WirelessHART protocol, creating a self-forming and self-managing wireless mesh, which delivers continuous wall thickness measurements of the highest integrity and accuracy directly to the end user.

The sensors are capable of operating up to 600°C (1100°F). This is due to their patented waveguide technology that holds the sensor head (with ultrasonic transducers, electronics, and battery) away from the hot metal. The sensor's measurements are transmitted wirelessly back to a gateway (wireless access point) mounted near the main unit. Figure 1-52 show the Permasense WT 210 series UT sensor and a system schematic is shown in Figure 1-53.

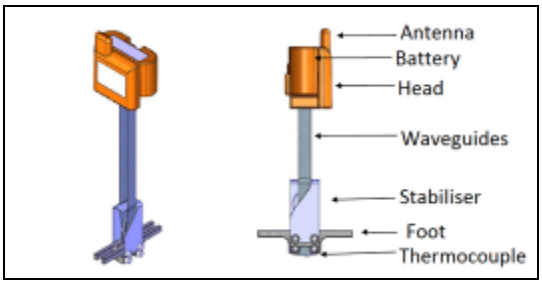

Figure 1-52. Permasense WT 210 series UT sensor.

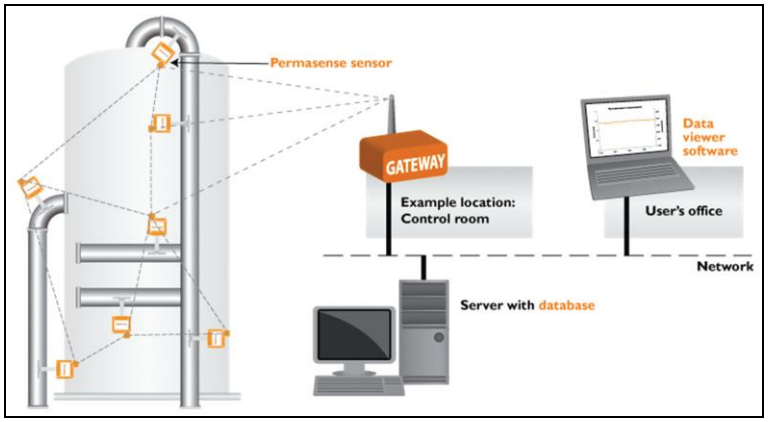

Figure 1-53. Permasense corrosion monitoring system [1].

Since there is no cost associated with measurement acquisition or measurement retrieval, the frequency of measurement can be configured to be as frequent as every 15 minutes. Connection of the gateway to the operator's existing information technology infrastructure allows the data to be viewed from personnel desks. Sensor battery life of up to 10 years allows continuous data delivery between turnarounds without access to a sensor's physical location.

After the purchase of the sensor system is complete, the unit will be utilized in the sectional tank test bed being developed.

References:

Philip T. and Jake D., "Monitoring and simulation resolves overhead corrosion – online corrosion monitoring in tandem with simulation modelling identified the root cause of corrosion in a crude unit overhead", www.eptq.com – PTQ Q1 2016.

Subtask 19.2: Evaluation of Nonmetallic Components in the Waste Transfer System

FIU has acquired and completed installation of the sensors that measure the flow parameters within each loop. On each of the three loops, a flow meter, pressure transducer and a thermocouple was installed, as per the recommendations of site personnel, to measure flow parameters including pressure, flow rate and temperature. Each loop has a transducer tree (Figure 1-54) where the pressure transducer, thermocouple and pressure gauge are mounted.

Figure 1-54. Transducer tree.

The pressure will be measured within each loop by means of a pressure transducer (Figure 1-55). Each of the three pressure transducers (Dwyer® Series 628CR) has a 0-30 psi range with ±1% of full scale accuracy. A ceramic sensor is housed within a NEMA 4X 316L stainless steel body. The output signal is an analog 4 – 20 mA.

Figure 1-55. Dwyer® Series 628CR pressure transducer.

The flow rate of each loop will be measured with a digital paddlewheel flow transmitter (Figure 1-56). Each of the three flow transmitters (Dwyer® Series DFMT) has an accuracy of ±1.5% of full scale. The sensor and impeller are made of polyvinylidene fluoride (PVDF) with a ceramic shaft and fluoroeastomer O-rings. The output signal is an analog 4 – 20 mA.

Figure 1-56. Dwyer® Series DFMT flow transmitter.

The flow's temperature will be measured by a thermocouple (Figure 1-57). Each of the three thermocouples (Omega® JQIN Series J-type) has an Inconel® sheath and a permanently molded male connector.

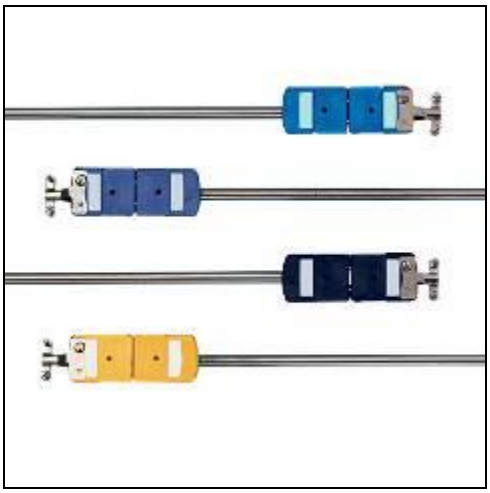

Figure 1-57. Omega® JQIN Series J-type thermocouples.

Signal measurements and processing will be conducted via National Instruments™ LabVIEW data acquisition software. The data acquisition code for signal measurements and processing using LabVIEW has been developed and validated.

All three loops were started in June and ran continuously. After being run for several days, loop #1 running at near 180°F started leaking from the lower 1" bulkhead fitting feeding the pump. As a result, the loop was shut down in order to determine the source of the leak. Upon examination of the fitting, it was determined to be cracked. The polyethylene fitting was replaced and the loop was restarted. After running for a week, the upper ¾" polyethylene fitting started leaking. Upon examination, it too was determined to be cracked (Figure 1-58).

Figure 1-58. Cracked 3/4" polyethylene bulkhead fitting.

Since both fittings were made of polyethylene, which has a max design operating temperature of 180°F, it was determined that the cracks were due to the fitting being operated at high temperatures near its upper limit of the design temperature envelope. FIU decided to stop all three loops and replace both polyethylene fittings with 316 stainless steel bulkhead fittings (Figure 1-59).

Figure 1-59. Stainless steel bulkhead fitting.

A 1” as well as a ¾” 316 stainless steel bulkhead fitting have been ordered and will be installed when they are received.

Milestones and Deliverables

The milestones and deliverables for Project 1 for FIU Performance Year 6 are shown on the following table. Milestone 2015-P1-M19.2.2, complete the baseline testing on the nonmetallic materials, was completed in March and its corresponding deliverable was submitted to DOE HQ on April 8, 2016. Milestone 2015-P1-M17.1.2, complete the validation of impingement correlations for PJMs was completed in May and its corresponding deliverable was submitted to DOE HQ on May 6, 2016.

FIU Performance Year 6 Milestones and Deliverables for Project 1

Task	Milestone/ Deliverable	Description	Due Date	Status	OSTI
Task 17: Advanced Topics for Mixing Processes	2015-P1-M17.1.2	Complete validation of impingement correlations	05/6/2016	Complete	
	Deliverable	Draft Summary Report for Subtask 17.1.1	08/28/2016	On Target	OSTI
	Deliverable	Draft Summary Report for Subtask 17.1.2	05/6/2016	Complete	OSTI
Task 18: Technology Development and Instrumentation Evaluation	2015-P1-M18.1.1	Complete test plan for evaluating SLIM's ability to detect a precursor of DSGREs	12/18/2015	Complete	
	Deliverable	Draft Test Plan for Subtask 18.1.1	12/18/2015	Complete	OSTI
	2015-P1-M18.3.1	Complete test plan for temperature measurements using IR sensors	12/18/2015	Complete	
	2015-P1-M18.2.1	Finalize the design and construction of the refractory pad inspection tool	02/26/2016	Complete	
	2015-P1-M18.2.2	Complete engineering scale mock-up testing	08/28/2016	On Target	
	Deliverable	Draft Summary Report for Subtask 18.2.1 and 18.2.2	08/28/2016	On Target	OSTI
	2015-P1-M18.2.3	Finalize the design and construction of the air supply line inspection tool	02/26/2016	Complete	
	Deliverable	Draft Summary Report for Subtask 18.2.3	02/26/2016	Complete	OSTI
	Deliverable	Draft Summary Report for Subtask 18.3.1	07/29/2016	On Target	OSTI
Task 19: Pipeline Integrity and Analysis	2015-P1-M19.2.1	Complete test loop set up	11/20/2015	Complete	
	2015-P1-M19.1.1	Evaluate and down select alternative UT systems for bench scale testing	03/11/2016	Complete	
	Deliverable	Draft Summary document for Subtask 19.1.1	03/11/2016	Complete	OSTI
	2015-P1-M19.2.2	Complete baseline experimental testing	03/25/2016	Complete	
	Deliverable	Draft Summary Report for Subtask 19.2.2	04/8/2016	Complete	OSTI

Work Plan for Next Quarter

Project-wide:

- Draft the Year End Report (YER) for FIU Performance Year 6 (August 2015 to August 2016).
- Draft the Project Technical Plan (PTP) for FIU Performance Year 7 (August 2016 to August 2017).

Task 17: Advanced Topics for Mixing Processes

- FIU will install the latest version of the STARCCM+ on the FIU-HPC and conduct simulations in 3D space. Fast Fourier analysis on the turbulent kinetic energy and the dissipation rate of the kinetic energy will be continued in the last version of the application. The investigation regarding the correlation for the shear correction will be extended to flows with lower Reynolds numbers in RANS-alpha and QDNS simulations. Once a general agreement was obtained about the form of the correlation for shear correction in dissipative scales, the correlation will be implemented in the RANS-HB modeling for different flow Reynolds numbers and comparisons with the experimental data will be conducted.

Task 18: Technology Development and Instrumentation Evaluation

- For the SLIM task, FIU will complete the volume calculations with a proper baseline and develop the year end (annual) report for this task, which will end the task. The Hanford Site engineers have stated that the technology is not needed until 2018 or 2019 and is not a high priority for 2017. The annual report will summarize the research results for the sonar work performed over multiple years but will focus primarily on the past year's progress. The volume estimation algorithm will be corrected to allow for monitoring for changes in the volume of the HLW in double-shelled tanks. This volume estimation will help Hanford measure the HLW in the tanks and to monitor the volume change over time.
- For the inspection tools, the designing and manufacturing of the full-scale sectional mockup of the DST will be finalized and extensively coordinated with WRPS.
- The peristaltic crawler will be tested under similar conditions as the proposed robotic inspection at Hanford, and improvements will continue to be incorporated to the design as needed. The manufacturing of the full-scale mockup of the ventilation riser will be finalized. The instrumentation module design will be completed and used in full-scale mockup tests. In addition a portable control box will be designed and manufactured for field deployment.
- For the miniature magnetic rover, FIU will continue to investigate design modifications to allow for sharper turns in the refractory channels and improve the unit's reliability. The tether management system will also be manufactured and tested. Modifications to the design and control of the tether management system will be made as needed. FIU will also evaluate preliminary concepts for incorporating the unit onto a deployment platform.
- For the IR sensor task, FIU will complete the engineering scale testing of the Raytek IR sensor. Plates with varying thicknesses will be evaluated for thermal performance and

variances in the material (inside the tanks) including fluids, slurry and solids will be tested. Also, sensitivity based studies for the IR sensor will be conducted. Further, simulation models will be developed for advanced heat transfer analysis.

Task 19: Pipeline Integrity and Analysis

- For the ultrasonic sensor task, FIU will procure the ultrasonic sensors, conduct initial bench scale tests to evaluate their performance and demonstrate their capabilities on the full scale sectional mock up being constructed at FIU-ARC.
- For the non-metallic materials task, efforts during the next quarter will include installing the stainless steel bulkhead fittings and resumption of the specimen aging tests. In order to prevent future failures of the CPVC and polypropylene parts on the high temperature loop, the loop will be run at a temperature slightly lower than 180°F.

Project 2
Environmental Remediation Science and Technology

Project Description

This project will be conducted in close collaboration between FIU, Hanford Site, Savannah River Site, and the Waste Isolation Pilot Plant (WIPP) scientists and engineers in order to plan and execute research that supports the resolution of critical science and engineering needs, leading to a better understanding of the long-term behavior of contaminants in the subsurface. Research involves novel analytical methods and microscopy techniques for characterization of various mineral and microbial samples. Tasks include studies which predict the behavior and fate of radionuclides that can potentially contaminate the groundwater system in the Hanford Site 200 Area; laboratory batch and column experiments, which provide relevant data for modeling of the migration and distribution of natural organic matter injected into subsurface systems in the SRS F/H Area; laboratory experiments investigating the behavior of the actinide elements in high ionic strength systems relevant to the Waste Isolation Pilot Plant; surface water modeling of Tims Branch at SRS supported by the application of GIS technology for storage and geoprocessing of spatial and temporal data;.

The following tasks are included in FIU Performance Year 6:

Task No	Task
Task 1: Remediation Research and Technical Support for the Hanford Site	
Subtask 1.1	Sequestering uranium at the Hanford 200 Area vadose zone by in situ subsurface pH manipulation using NH_3 gas
Subtask 1.2	Investigation of microbial-meta-autunite interactions - effect of bicarbonate and calcium ions
Subtask 1.3	Evaluation of ammonia fate and biological contributions during and after ammonia injection for uranium treatment
Task 2: Remediation Research and Technical Support for Savannah River Site	
Subtask 2.1	FIU's support for groundwater remediation at SRS F/H Area
Subtask 2.2	Monitoring of U(VI) bioreduction after ARCADIS demonstration at the SRS F-Area
Subtask 2.3	Humic acid batch sorption experiments into the SRS soil
Subtask 2.4	The synergetic effect of HA and Si on the removal of U(VI)
Subtask 2.5	Investigation of the migration and distribution of natural organic matter injected into subsurface systems
Task 3: Surface Water Modeling of Tims Branch	
Subtask.3.1	Modeling of surface water and sediment transport in the Tims Branch ecosystem
Subtask 3.2	Application of GIS technologies for hydrological modeling support
Subtask 3.3	Biota, biofilm, water and sediment sampling in Tims Branch

Task 4: Sustainability Plan for the A/M Area Groundwater Remediation System	
Subtask 4.1	Sustainable Remediation Analysis of the M1 Air Stripper
Subtask 4.2	Sustainable Remediation Support to DOE EM Student Challenge
Task 5: Remediation Research and Technical Support for WIPP	

Task 1: Remediation Research and Technical Support for the Hanford Site

Task 1 Overview

The radioactive contamination at the Hanford Site created plumes that threaten groundwater quality due to potential downward migration through the unsaturated vadose zone. FIU is supporting basic research into the sequestration of radionuclides such as uranium in the vadose zone, which is more cost effective than groundwater remediation. One technology under consideration to control U(VI) mobility in the Hanford vadose zone is a manipulation of sediment pH via ammonia gas injection to create alkaline conditions in the uranium-contaminated sediment. Another technology need for the ammonia remediation method is to investigate the potential biological and physical mechanisms associated with the fate of ammonia after injection into the unsaturated subsurface.

Task 1 Quarterly Progress

Subtask 1.1. Sequestering Uranium at the Hanford 200 Area Vadose Zone by In Situ Subsurface pH Manipulation Using NH_3 Gas

In the month of April, FIU initiated the sequential liquid extraction experiments to investigate the stability of precipitates created after ammonia gas injections. A total of 24 samples (duplicate filtered and unfiltered) were prepared and a dry weight was recorded for each sample.

The protocol for the extractions will follow Jim Szecsody's protocol (Szecsody et al., 2015) for future cross-referencing of the results. The solid/solution ratio for each step of the sequential extraction experiments will be in the range 1:15 to 1:40 to ensure that U measurements are within the detection limits of the KPA instrument. The solid/solution ratio may change based on the experimental observations and calculations on the volume of the extracting solutions. The first two phases in the sequential extraction target water soluble and adsorbed/exchangeable uranium phases. Carbonate extractions using the acetic acid at pH 2.3 are based on ensuring the pH stays at 2.3 as all the carbonate in the sample dissolves. The remaining two extractions define the harder to extract uranium minerals or coated surface phases. The extraction procedures consist of the following 6 steps (Szecsody et al., 2015):

Table 2-1. Extraction Procedure

Solution	Time (h)	Target Compounds
DIW	1	Aqueous U phases
0.0144 M $NaHCO_3$ + 0.028 M Na_2CO_3 (pH 9.3)	1	Adsorbed U phases
1 M Sodium-Acetate	1	Dissolved some U-carbonates
Acetic Acid (pH 2.3)	120	Dissolve most U-carbonates and hydrated U silicates
8 M Nitric Acid	2	Dissolve hard-to-extract U-phases
0.0144 M $NaHCO_3$ + 0.028 M Na_2CO_3	1000	To measure the U at long term

The initial sequential extraction experiments were initiated with six unfiltered samples, sample composition provided in Table 2-2, after sample centrifugation. The mass of the precipitate in each vial was determined by subtracting the mass of the empty vial from the mass of the vial containing the precipitate.

Table 2-2. Sample Composition and Dry Weight of the Precipitate

Sample composition	Precipitate dry weight, g
50 mM Si + 5 mM Al + 3 mM HCO_3 + 0 mM Ca + 2 ppm U	0.0130
50 mM Si + 5 mM Al + 3 mM HCO_3 + 5 mM Ca + 2 ppm U	0.0309
50 mM Si + 5 mM Al + 3 mM HCO_3 + 10 mM Ca + 2 ppm U	0.0533
50 mM Si + 5 mM Al + 50 mM HCO_3 + 0 mM Ca + 2 ppm U	0.0335
50 mM Si + 5 mM Al + 50 mM HCO_3 + 5 mM Ca + 2 ppm U	0.1251
50 mM Si + 5 mM Al + 50 mM HCO_3 + 10 mM Ca + 2 ppm U	0.2474

SEM/EDS analyses were conducted on selected samples using a backscattered mode (Figure 2-1).

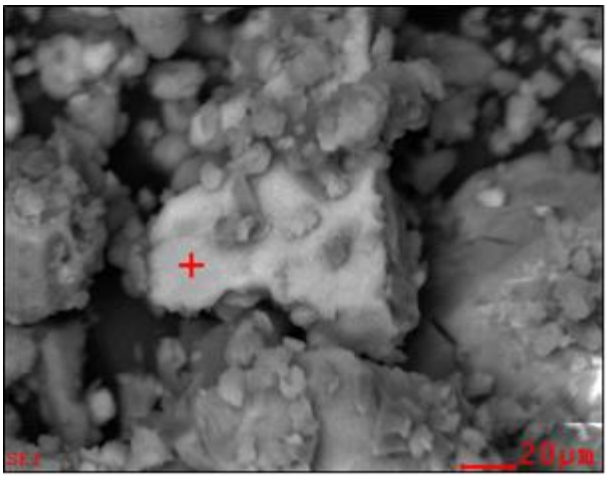

Element	*Wt%*	*At%*
CK	08.24	15.18
NK	04.13	06.53
OK	32.78	45.37
NaK	08.81	08.48
AlK	02.19	01.80
SiK	20.51	16.17
ClK	04.57	02.85
KK	01.53	00.87
CaK	02.46	01.36
UL	14.78	01.37
Matrix	Correction	ZAF

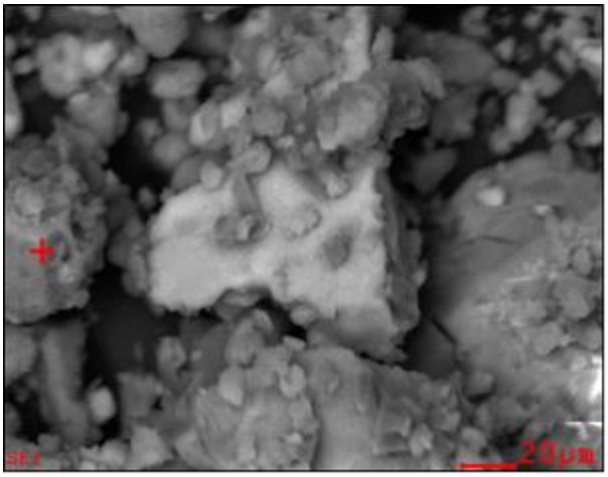

Element	Wt%	At%
CK	11.27	21.96
NK	05.18	08.66
OK	21.89	32.02
NaK	04.51	04.59
AlK	02.85	02.48
SiK	24.23	20.19
ClK	04.05	02.68
KK	03.27	01.96
CaK	06.63	03.87
UL	16.11	01.58
Matrix	Correction	ZAF

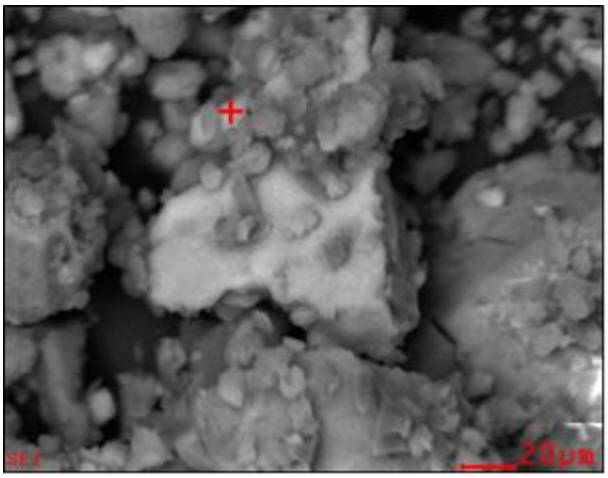

Element	Wt%	At%
CK	10.25	18.49
NK	05.51	08.52
OK	32.44	43.91
NaK	10.04	09.46
AlK	01.57	01.26
SiK	15.34	11.83
ClK	04.78	02.92
KK	01.38	00.77
CaK	02.55	01.38
UL	16.13	01.47
Matrix	Correction	ZAF

Figure 2-1. SEM/EDS analysis for samples composed of 50 mM Si + 5 mM Al + 50 mM HCO_3 + 10 mM Ca + 500 ppm of U(VI).

The analyses presented evidence that the "hot" spots are high in Si and U. No crystals were observed compared to previous non-filtered sample preparation.

FIU continued with solids characterization studies during April- June. Due to the formation of bubbles in the previous set of samples, new epoxy molds were prepared for solid phase analysis using a sample preparation method slightly modified to remove pockets of air prior to curing (Figure 2-2). After preparing the 100:45 (by weight) mix of resin and hardener, the mixture was immediately degassed in the antechamber of a glovebox in a 25-in-Hg vacuum over five minutes. The degassed epoxy was then added to the disposable molds and cured over 24 hours, after which a ¼-inch hole was drilled for the addition of a sample/epoxy mixture. Due to the analytical limitations, only 8 samples were selected for crushing and fixing in the epoxy (Table 2-3).

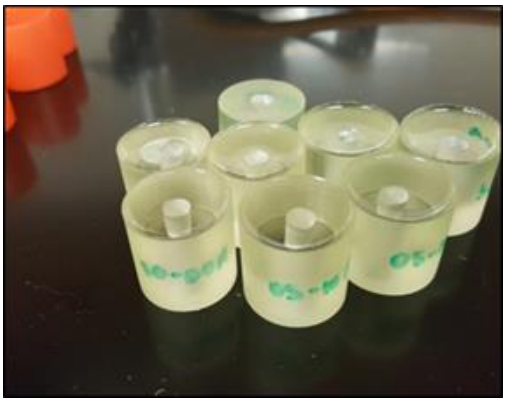

Figure 2-2. Labeled epoxy molds.

Table 2-3. Samples Elected for Epoxy Fixing and Analysis

Sample Labels		Key Variables
• 05-00A	• 05-00B	5 mM HCO_3^- and no Ca^{2+}
• 05-10A	• 05-10B	5 mM HCO_3^- and 10 mM Ca^{2+}
• 50-00A	• 50-00B	50 mM HCO_3^- and no Ca^{2+}
• 50-10A	• 50-10B	50 mM HCO_3^- and 10 mM Ca^{2+}

*Samples labeled "B" are duplicate precipitates which were rinsed with DIW

The mass of uranium precipitated will be estimated using the difference between the concentration of uranium initially added to the sample and that determined by KPA analysis of the supernatant phase. Prior to sending the samples to Pacific Northwest National Laboratory for final preparation and analysis, this concentration, paired with the mass of the sample added to the molds, will be used to estimate the mass of uranium fixed in the sample. Additionally, preparations for the digestion and KPA analysis of specimen from the precipitates will be made to try and achieve a more accurate estimate of uranium concentration. This method of determination will reduce the potential error caused by transfer-loss from the supernatant and precipitate sample phases.

In the month of May, FIU continued the sequential liquid extraction experiments to investigate the stability of precipitates created after ammonia gas injections. Twelve (12) sample duplicates (unfiltered) were processed via the extraction protocol. As many as six (6) different sequential liquid extractions have been used to characterize U in different mineral phases in the ammonia treated precipitates (Table 2-4). Before initiating sequential extraction experiments, the centrifuge tubes containing the previously prepared and set-to-dry precipitates for analysis, were weighed on different days to ensure the weights were stable and not changing. The sequential extraction procedures followed Jim Szecsody's protocol (Szecsody et al., 2015). The solid/solution ratio for each step of the sequential liquid extraction experiments was in the range 1:15 to 1:40 to ensure that U measurements are within the detection limits of the KPA instrument.

Table 2-4. Solutions for Sequential Extractions

Step	Solution	Time (h)	Target Compounds
1	Synthetic groundwater / Boiled deionized water	1	Aqueous U phases
2	0.0144 M $NaHCO_3$ + 0.028 M Na_2CO_3 (pH 9.3)	1	Adsorbed U phases
3	1 M Sodium-Acetate	1	Dissolved some U-Carbonates
4	Acetic Acid (pH 2.3)	120	Most U-Carbonates and hydrated boltwoodite
5	8 M Nitric Acid	2	Dissolved harder U phases
6	0.0144 M $NaHCO_3$ + 0.028 M Na_2CO_3	1000	Carbonate Solution

The experiment was performed with the following procedures that included a DIW washing solution step to prevent carryover of uranium to the next step. The general procedure for each step shown in Table 2-4 was as follows:

- The corresponding quantity calculated to meet the dilution factor was poured into each of the corresponding centrifuge tubes.
- The tubes were set on a shaker for the appropriate duration following the procedures.
- The samples were set to centrifuge for 30 minutes in order to completely separate liquid from the solid particles.
- The supernatant solution was removed and collected in labeled vials.
- For steps 2 through 6, a wash step was performed. This was accomplished by adding 2 mL of DIW to each sample, then placing the vials on the shaker for approximately 10 minutes (30 minutes after the centrifuging step). The supernatant was collected for further analysis.

The supernatant solutions collected after each sequential extraction step including wash solutions were analyzed for uranium via the KPA instrument. KPA analyses were conducted using different dilutions factors (1:10, 1:20 and 1:200). The highest dilution factor was needed for steps 5 and 6. The results from the uranium analysis were used for mass balance calculations in order to validate U mass measured in each step. The extractions suggested the highest percentage for steps 5 and 6.

The extraction procedures were repeated for the duplicate samples containing unfiltered uranium precipitates. This time, precipitates were crushed inside the vials before undergoing the sequential liquid extraction procedures to ensure that the solutes can diffuse from the solid to the liquid phase. In addition, the solid/solution ratio for each step was 1:40 and the extraction solution volumes for each sample varied based on the weight of precipitate. The procedure followed the same scheme and all the supernatant solutions collected after each sequential extraction step were analyzed using KPA. The results of the KPA and the subsequent mass balance calculated are presented in Figure 2-3.

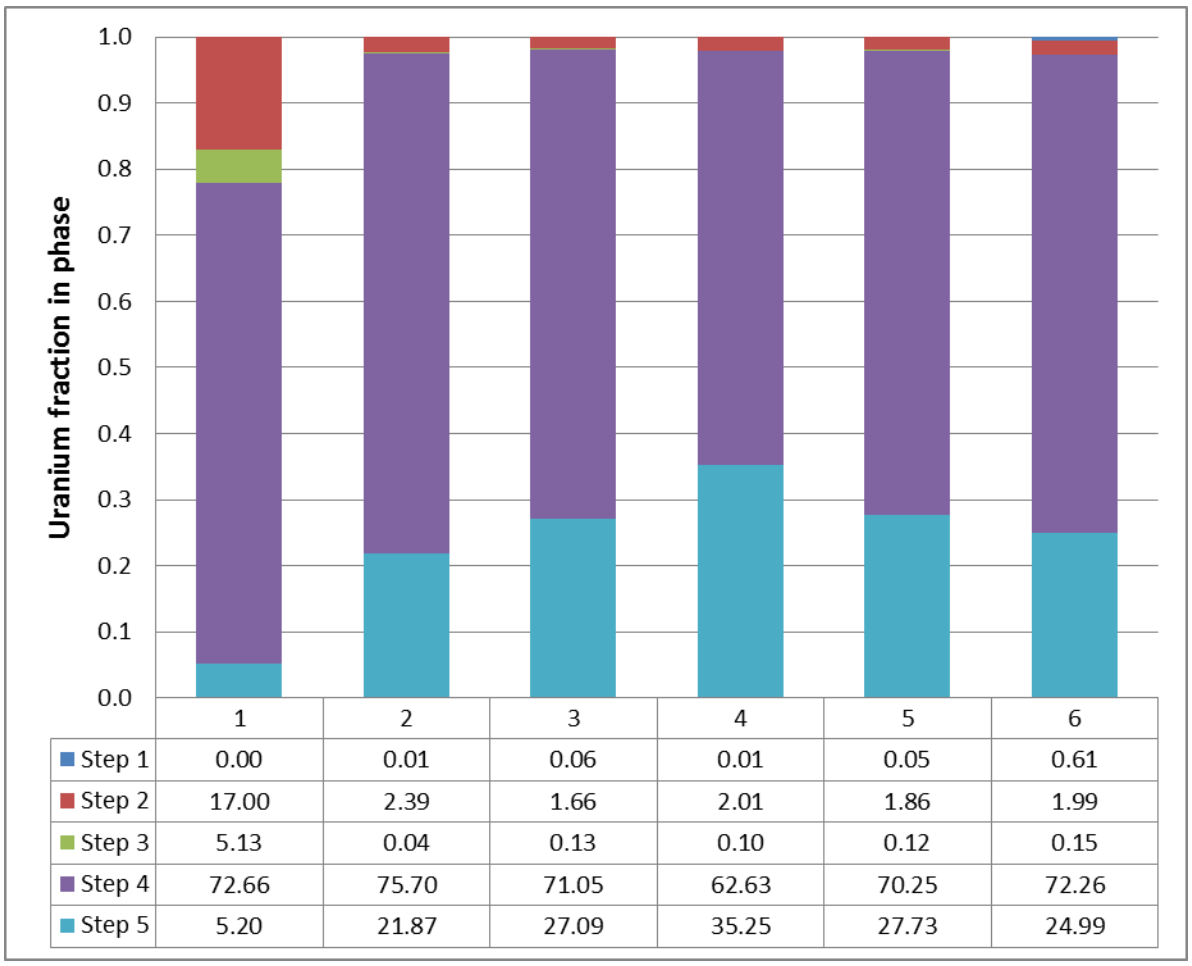

	1	2	3	4	5	6
Step 1	0.00	0.01	0.06	0.01	0.05	0.61
Step 2	17.00	2.39	1.66	2.01	1.86	1.99
Step 3	5.13	0.04	0.13	0.10	0.12	0.15
Step 4	72.66	75.70	71.05	62.63	70.25	72.26
Step 5	5.20	21.87	27.09	35.25	27.73	24.99

Figure 2-3. Sequential extractions for six unfiltered samples.

Comparing results for two experiments, it was concluded that sample crushing provided better diffusion of solutions and the results were more accurate for each sequential extraction step. The highest uranium extraction was noted for acetic acid (pH 2.3) and nitric acid.

In addition, during month of May, the extraction solutions were re-prepared to reflect more accurately the solution composition previously used in these experiments (Table 2-5) (Smith and Szecsody, 2011).

Table 2-5. Corrected Composition for Sequential Extractions

Solution	Time	Target Compounds
DIW	1 h	Aqueous U phases extractable with DIW
0.0144 M $NaHCO_3$ + 0.0028 M Na_2CO_3 (pH 9.3)	1 h	Adsorbed U species
1 M Sodium-Acetate +acetic acid (pH 5. 1)	1 h	Dissolved some U-carbonates and Na-boltwoodite
Acetic acid + calcium nitrate extractant (pH 2.3) (0.44 mol/L acetic acid, and 0.1mol/L $Ca(NO_3)_2$)	120 h	Dissolve predominantly Na-boltwoodite
8 M Nitric Acid	2 h	Dissolve hard-to-extract U-phases
0.0144 M $NaHCO_3$ + 0.0028 M Na_2CO_3	1000 h	To measure U at long term

In the month of May, FIU continued solid phase characterization of precipitates. The epoxy mounted samples were prepared and cured over 24 hours. A comparison of the initial mass of uranium added to the solutions and the mass retained in the supernatant after undergoing the ammonia injection procedure, as determined by KPA analysis, was used to assess how much uranium was removed into the precipitates. Using this information, the mass of uranium included in each epoxy mold was estimated based on the mass of sample added to the mold and the mass of uranium per mg of total sample (Table 2-6). The final samples were set aside while preparing for shipping to Pacific Northwest National Laboratory for grinding, polishing, and surface analysis by electron microprobe.

Table 2-6. Mass of Uranium in Epoxy

Sample Label	Supernatant [U] (ppm)	Mass U in Supernatant (mg)	Rinse Solution [U] (ppm)	Mass U in Rinse (mg)	Mass U in Precipitate (mg)	Mass U per mg sample (mg_U/mg_{Sample})	Mass Sample Loaded in Epoxy (mg)	Mass U in epoxy (mg)
05-00A	211.9874	2.119874	----	----	2.880	0.07956	14.1	1.122
05-10A	148.5517	1.485517	----	----	3.514	0.07951	16.8	1.336
50-00A	337.986	3.37986	----	----	1.620	0.03665	13.2	0.4838
50-10A	313.1001	3.131001	----	----	1.869	0.02111	20.3	0.4287
05-00B	284.128	2.84128	42.4492	0.2122	1.946	0.04325	16.8	0.7267
05-10B	148.4254	1.484254	15.5254	0.0776	3.438	0.07104	18.3	1.200
50-00B	370.9988	3.709988	52.679	0.2634	1.027	----	13.3	----
50-10B	322.7689	3.227689	56.3127	0.2816	1.491	0.02993	30.8	0.9220

The plan to digest and analyze the solid uranium samples by KPA was suspended. Alternatively, a sequential extraction study was done using a series of 5 solutions used to selectively extract different potential uranium phases in the sample. The solutions were prepared with the composition presented in Table 2-2 and extractions completed over the course of 7 days. Each extraction was followed by a 5-mL DIW rinse, the analyte contents of which would be added to the mass of the preceding extractant. The KPA analysis of the extraction solutions is ongoing.

In the month of June, FIU continued the sequential liquid extraction experiments to investigate the stability of precipitates created after ammonia gas injections. Twelve (12) duplicate filtered samples were processed via the extraction protocol. Precipitates crushing inside the vials before undergoing the sequential liquid extraction procedures to ensure that the solutes can diffuse from the solid to the liquid phase. The solid/solution ratio for each step was the same as in previous experiments, 1:40, and the extraction solution volumes for each sample varied based on the weight of precipitate (Table 2-5). All the supernatant solutions were collected after 30 min centrifugation following each sequential extraction step.

The experiment was performed following the same procedures outlined in the May report. Each extraction step was following a DIW washing solution step to prevent carryover of uranium to the next step. The supernatant solutions collected after each sequential extraction step including wash solutions were analyzed for uranium via the KPA instrument. KPA analyses were conducted using different dilutions factors (1:10, 1:20 and 1:100). The highest dilution factor

was needed for steps 3, 4 and 5. The results from the uranium analysis were used for mass balance calculations in order to validate U mass measured in each step. The extractions suggested the highest percentage of uranium extraction for steps 3, 4 and 5. As a general tendency these three steps accounted for more than 86% of the total uranium extracted in all the six samples.

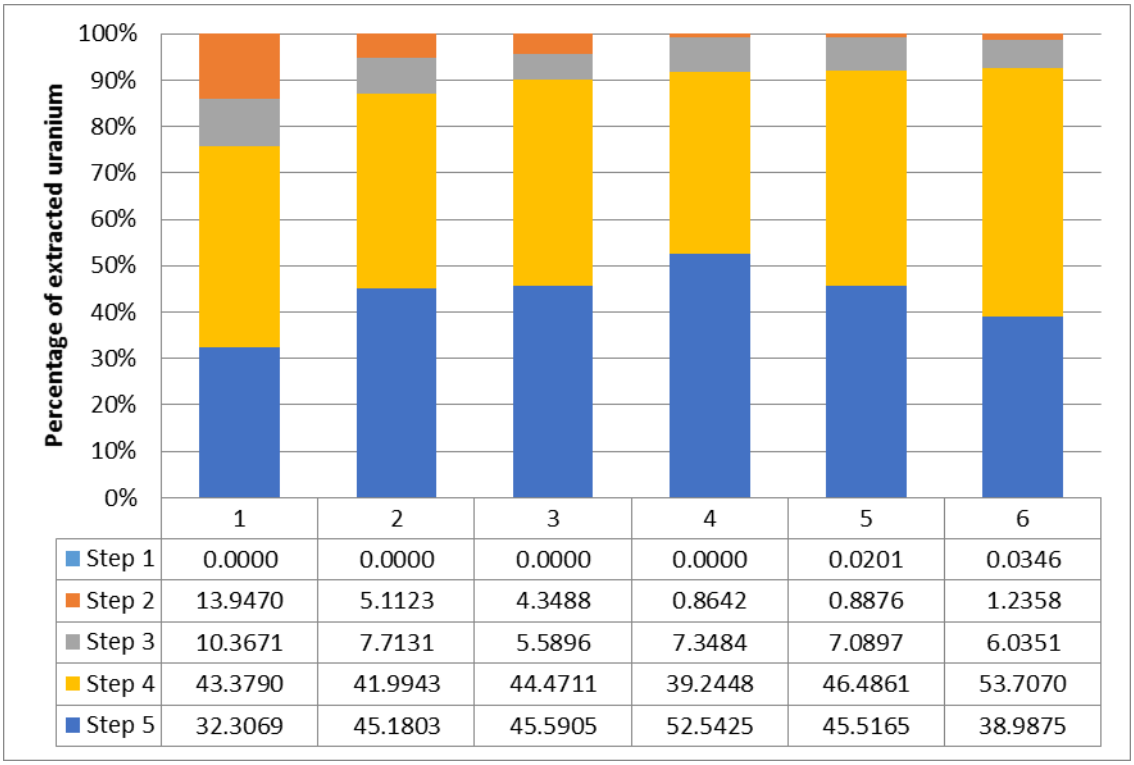

	1	2	3	4	5	6
Step 1	0.0000	0.0000	0.0000	0.0000	0.0201	0.0346
Step 2	13.9470	5.1123	4.3488	0.8642	0.8876	1.2358
Step 3	10.3671	7.7131	5.5896	7.3484	7.0897	6.0351
Step 4	43.3790	41.9943	44.4711	39.2448	46.4861	53.7070
Step 5	32.3069	45.1803	45.5905	52.5425	45.5165	38.9875

Figure 2-4. Percentage of extracted uranium accounted for in each sequential extraction step.

Uranium analyses for the duplicate filtered samples are still in progress and will be presented in the next monthly report.

FIU has continued conducting isopiestic measurements of U-bearing samples composed of silica-based precipitates mimicking those created after ammonia gas injection to the vadose zone. Measurements indicated that the humidity level in the isopiestic chamber reached 84%. The uptake of water by solids suggests the dependence of the water retention by the precipitates as a function of water activity. The shape of most of the water adsorption isotherms obtained in the isopiestic experiments is generally similar for all solid composition tested. They are characterized by an increase in water retention in a range of a_w up to 0.75 and then a steep upward swing due to vapor condensation starting at a_w = 0.78-0.84 (Figure 2-5). FIU also initiated desorption experiments by inserting in the chamber a crucible with concentrated sulfuric acid that adsorbs excessive water from solids.

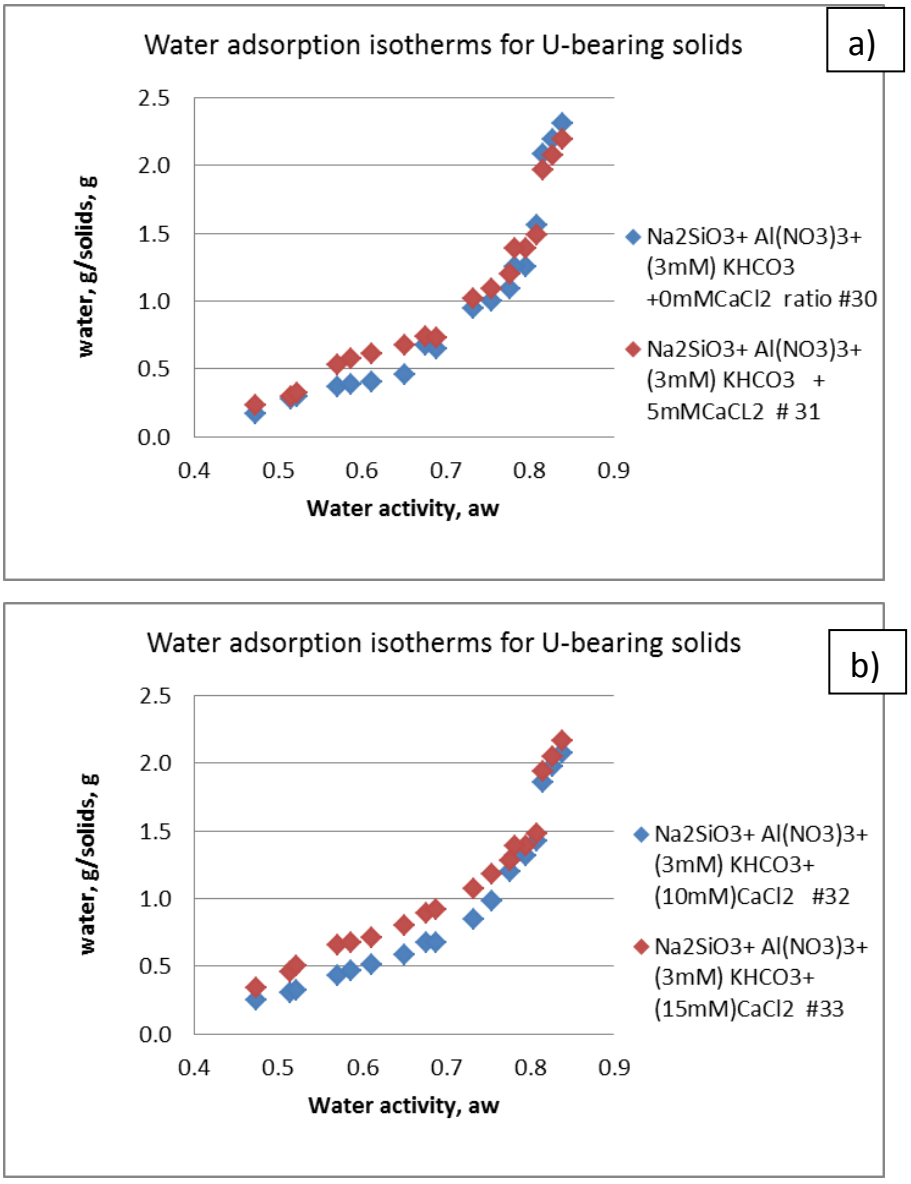

Figure 2-5. Water adsorption isotherms for U-bearing solids for the precipitates composed of 50mMSi, 3mMHCO3, 5mM Al and Ca. a) 0mMCa and 5mMCa, b) 10mMCa and 15mMCa.

FIU also continued solid phase characterization of the precipitates. The five solution sequential extraction of solid uranium precipitate samples was completed over the course of 7 days. After centrifuging, each extracting and rinse solution was isolated and stored for analysis. Based on the likely concentrations in each solvent, based on comparing the percentage removed in similar studies to the maximum possible concentration in solution, a three-step serial dilution was done to prepare three dilution factors (Table 2-7). This would allow maximum possible concentrations, estimated at 8500 ppm, to be diluted to 85 ppb, well within the upper limit of the 0.1-100 ppm range typically used for KPA analysis.

Table 2-7. Extractant Dilution Steps

Dilution Step	Total Solution Dilution
1:100	1:100
1:100	1:10000
1:10	1:100000

The dilution of samples was errantly completed using distilled deionized (DDI) water, rather than a nitric acid solution which is standard for KPA analysis, requiring the re-preparation of these samples. Before beginning this re-preparation, a preliminary KPA analysis of the 05-00B set of DDI water diluted extraction samples was used to get a general idea of the concentrations that would be found in the various solvents (Figure 2-6). This information would allow for the modification of the dilution factors used in the next samples to best ensure that future sample analysis fell within the range of the instrument calibration. The results were relatively consistent with expectations, with the majority of analyte being extracted in the lattermost extractions. Equipped with this new data, the preparations of new diluted solutions in nitric acid is currently underway.

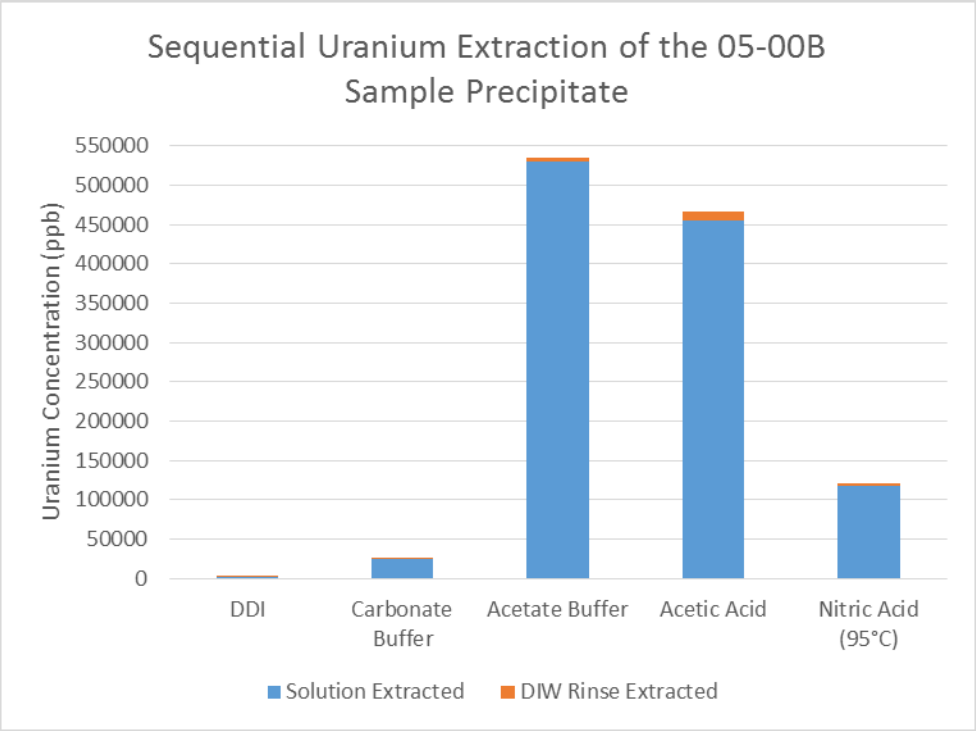

Figure 2-6. Sequential uranium extraction of the 05-00B sample precipitate.

The completed epoxy mounted samples were surveyed for activity before being packaged and shipped to Pacific Northwest National Laboratory for further sample preparation and analysis. While sample preparation, grinding and polishing, is underway, analysis of the sequential extraction data will be used to prioritize 2-4 samples for electron microprobe analysis.

References:

Smith, S., and J. Szecsody. 2011. Influence of contact time on the extraction on of 233-uranyl spike and contaminant uranium from Hanford Site sediment. Radiochim. Acta 99:693–704. doi:10.1524/ract.2011.1876

Subtask 1.2. Investigation on Microbial-Meta-Autunite Interactions – Effect of Bicarbonate and Calcium Ions

A graduate research assistant, Sandra Herrera, who was supporting this task graduated from FIU with an M.S. in environmental engineering. A new student (Sarah Solomon, B.S. in environmental engineering expected in 2018) was hired as a DOE Fellow to work on the project.

FIU completed preparations for the next experiment to monitor U-bacteria interactions in the presence of three different bicarbonate concentrations (0, 3 and 10 mM) in autunite-free samples. A bacterial culture for this experiment will be grown from *Shewanella Oneidensis* MR-1 stock kept at -80ºC in the freezer. The objective of this experiment is to test the hypothesis that there are potentially two antagonistic mechanisms with similar kinetic rates taking place: 1) the formation of secondary minerals and bioreduction which are removing U, Ca and P from the aqueous phase; and 2) autunite dissolution which is re-introducing those elements to the aqueous phase, resulting in an apparent equilibrium of those elements in the supernatant. In the proposed experiment, a decrease in the elemental concentration in the aqueous phase will signify the existence of the two antagonistic mechanisms (since there will be no autunite dissolution); whereas, if all concentrations remain the same, this will imply that the formation of secondary minerals takes place to a very limited degree and that the driving force behind the apparent equilibrium is the mineral dissolution.

All media solutions were prepared for the samples needed to initiate the batch experiment that will replicate the exact conditions (U, Ca and P concentrations along with three different bicarbonate concentrations) before inoculation with bacteria in the absence of autunite (mineral-free). The media was prepared in 1 L of DIW using 0.02 M Na-Hepes buffer (mass = 4.766 g) and 0.024 mol/L sodium lactate ($C_3H_5NaO_3$, 60% w/w) as an electron donor (mass = 2.6894 g) with pH adjusted to neutral conditions. The resulting solution was divided into 4 flasks that were previously sterilized by autoclaving. As the experiment is based on the U-bacteria interactions in the presence of different bicarbonate concentrations, the first bottle was kept bicarbonate-free in the anaerobic glove box, and the other two were amended with the calculated amount of $KHCO_3$ (3 and 10 mM) and filter-sterilized to other sterile bottles. The final solutions were introduced into the "Coy" glove box to ensure anaerobic conditions are maintained throughout the experiment. Fresh bacterial cultures will be prepared.

Based on the literature, uranyl acetate was chosen as a source for the uranyl ions and FIU obtained a two-percent (2%) uranyl acetate solution in water. FIU prepared a detailed proposal for the FIU Radiation Control Committee where all safety procedures for using uranyl acetate for the microbial research as well as sample collection and analyses were presented. The proposal also includes a description of the work area (anaerobic glove box), as well as procedures for waste management, storage and radiation surveys. The procedure was sent to the FIU Radiation Safety Officer and is currently under review.

FIU prepared 24 samples for each bicarbonate concentration (0, 3 and 10 mM) using 10 mL of bicarbonate amended media, 40 ppm of Ca and 500 ppm of P. These concentrations were chosen based on our previous experiments and the levels of these elements detected. In order to create

the desired concentrations, 20 µL were introduced in the vial from a stock $CaCl_2$ solution (20,000 ppm) and 160 µL from a NaH_2PO_4 stock solution (31,000 ppm). The final chloride concentration in each sample was calculated to be approximately 3 ppm, which is well below the chloride interference level for KPA (13 ppm); the samples will be further diluted later. Then the samples were spiked with the appropriate amount of uranyl-acetate stock solution: 178 µL and 356 µL from a solution of 11 ppm U(VI) in order to create a final U(VI) concentration of 200 ppb (for 0 mM HCO_3^-) and 400 ppb (for 3 mM HCO_3^-), respectively as well as 133 µL from a solution of 112 ppm U(VI) in order to create a final U(VI) concentration 1.5 ppm (for 10 mM HCO_3^-). Then the samples were spiked with the appropriate amount of cell suspension in order to create a final cell concentration of 10^6 cells/mL. For each bicarbonate concentration, abiotic controls were prepared (containing all elements and no bacteria) and controls containing only uranium in DI water as a reference of initial uranium concentration were also prepared. All preparations were completed inside the anaerobic glovebox under inert atmosphere (N_2) (Figure 2-7).

Figure 2-7. Samples in the anaerobic glovebox.

Subtask 1.3. Evaluation of Ammonia Fate and Biological Contributions During and After Ammonia Injection for Uranium Treatment

Subtask 1.3.1: Investigation of NH_3 partitioning in relevant Hanford minerals and synthetic porewater

During the months of April – June, the following experiments were completed: (1) sequential extractions for 25 g/L kaolinite and 500 ppb U in the presence of synthetic porewater or NaCl under neutral pH 7.5 or treated with either 2.5 M NH_4OH or 2.5 M NaCl + 0.025 M NaOH to pH 11.5, (2) batch experiments with 500 ppb U for quartz, illite and montmorillonite in the presence of NaCl and for Hanford sediments in the presence of synthetic porewater under the three conditions (pH 7.5 or pH 11.5 by 2.5 M NH_4OH or 2.5 M NaCl + 0.025 M NaOH). Moreover, data is currently being compiled for batch experiments with muscovite and calcite in the presence of synthetic porewater. Future experiments for montmorillonite, calcite and muscovite in the presence of NaCl will continue in August. In addition, BET surface area was analyzed for the minerals utilized in batch experiments and was used to normalize partitioning coefficients.

During the month of June, a technical progress report was submitted to DOE EM entitled, "Effects of Ammonia on Uranium Partitioning and Kaolinite Mineral Dissolution," and will be submitted to the *Journal of Environmental Radioactivity* during the month of July. Further, DOE Fellow Silvina Di Pietro traveled to Pacific Northwest National Laboratory (PNNL) for a ten-week summer internship under the mentorship of Dr. Jim Szecsody.

Sequential Extraction Preparation

Tables 2-8 and 2-9 describe the equilibrium pH of the triplicate samples and the extraction steps, respectively. Figures 2-8 and 2-9 represent the aqueous U concentration and fraction removed during each of the extraction steps, respectively. Figures 2-10 and 2-11 represent the aqueous Al and Si removed by the extraction steps, respectively. It is assumed that the first three fractions represent the *available* fraction or the potentially mobile fraction of U. This assumption is based on previous work on sediments at Savannah River Site (Serkiz, Johnson et al. 2007). However, because the Hanford vadose zone is not acidic, the fourth extraction is not included here, although Serkiz did include this fraction for the acidic plume at the Savannah River Site.

A significantly smaller fraction and aqueous concentration of the U is present in the 0.007 M NaCl versus synthetic porewater samples for the aqueous and exchangeable fractions (with the exception of the initial synthetic porewater). For the aqueous fraction, these differences are likely attributable to the presence of carbonate and calcium in the synthetic porewater which can form stable aqueous complexes with U. Further, it is possible that alkaline earth cations (Ca/Mg) present in the initial condition (pH ~7.5) synthetic porewater more strongly compete with U, leading to a smaller fraction/concentration in the exchangeable fraction. However, the mechanism leading to an increase in U in the exchangeable fraction for the treated samples with synthetic porewater is still under investigation. In addition, the carbonate extraction results are still being interpreted. It is interesting that a slightly higher concentration of U is present for 0.007 M NaCl versus synthetic porewater treatment as the NaCl did not have carbonate added to the initial solution. However, there is also a significantly greater removal of Al/Si in the second carbonate extraction. This result shows that the extractions are likely not as specific as is often claimed.

Table 2-8. Summary of Equilibrium pH for Batch Experiments at 20 g/L Kaolinite in the Presence of 500 ppb Uranium

Sample ID	pH
NaCl-NH_4OH	11.69±0.02
NaCl-NaOH	11.53±0.03
Synpore-NH_4OH	11.44±0.01
Synpore-NaOH	11.50±0.04
Synpore-Initial	7.47±0.08
NaCl-Initial	6.71±0.05

Table 2-9. Extraction Procedure

Operationally-Defined Fraction	Extraction Conditions
(1) Aqueous	Synthetic porewater
(2) Adsorbed/ Exchangeable	1 M $MgNO_3$ at pH 7 for 16 hours
(3) Some Carbonates	1 M Sodium Acetate adjusted to pH 5 with Acetic Acid for 1 hour
(4) Remaining Carbonates	1.45 M Acetic Acid at pH 2.3 for 5 days
(5) Residual	8 M HNO_3 @ 95°C for 2 hours

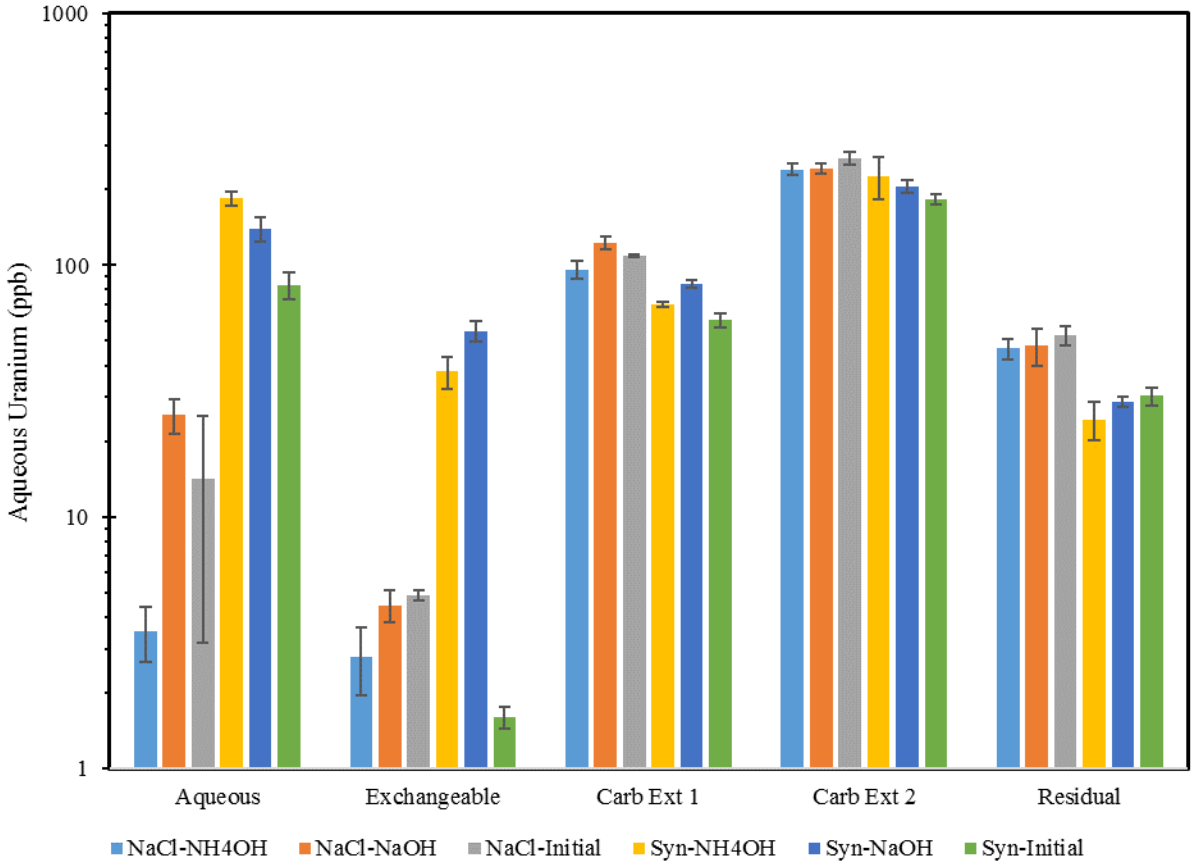

Figure 2-8. Aqueous concentration of U (ppb) removed during the operationally-defined extraction steps for 25 g/L kaolinite suspensions equilibrated for >30 days with 500 ppb U(VI) in either 0.007 M NaCl or synthetic porewater where initial samples represent neutral pH without base addition and treated samples have either 2.5 M NH_4OH or 2.5 M NaCl + 0.025 M NaOH added to pH ~11.5.

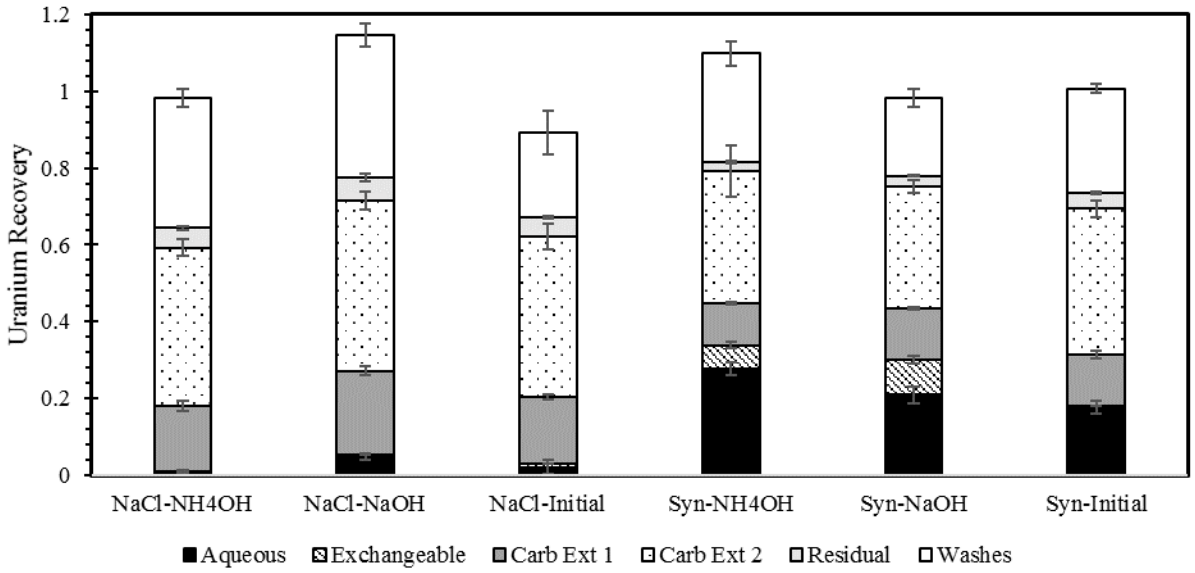

Figure 2-9. Fraction of U removed from the solid phase removed during the operationally-defined extraction steps for 25 g/L kaolinite suspensions equilibrated for >30 days with 500 ppb U(VI) in either 0.007 M NaCl or synthetic porewater where initial samples represent neutral pH without base addition and treated samples have either 2.5 M NH_4OH or 2.5 M NaCl + 0.025 M NaOH added to reach pH ~ 11.5.

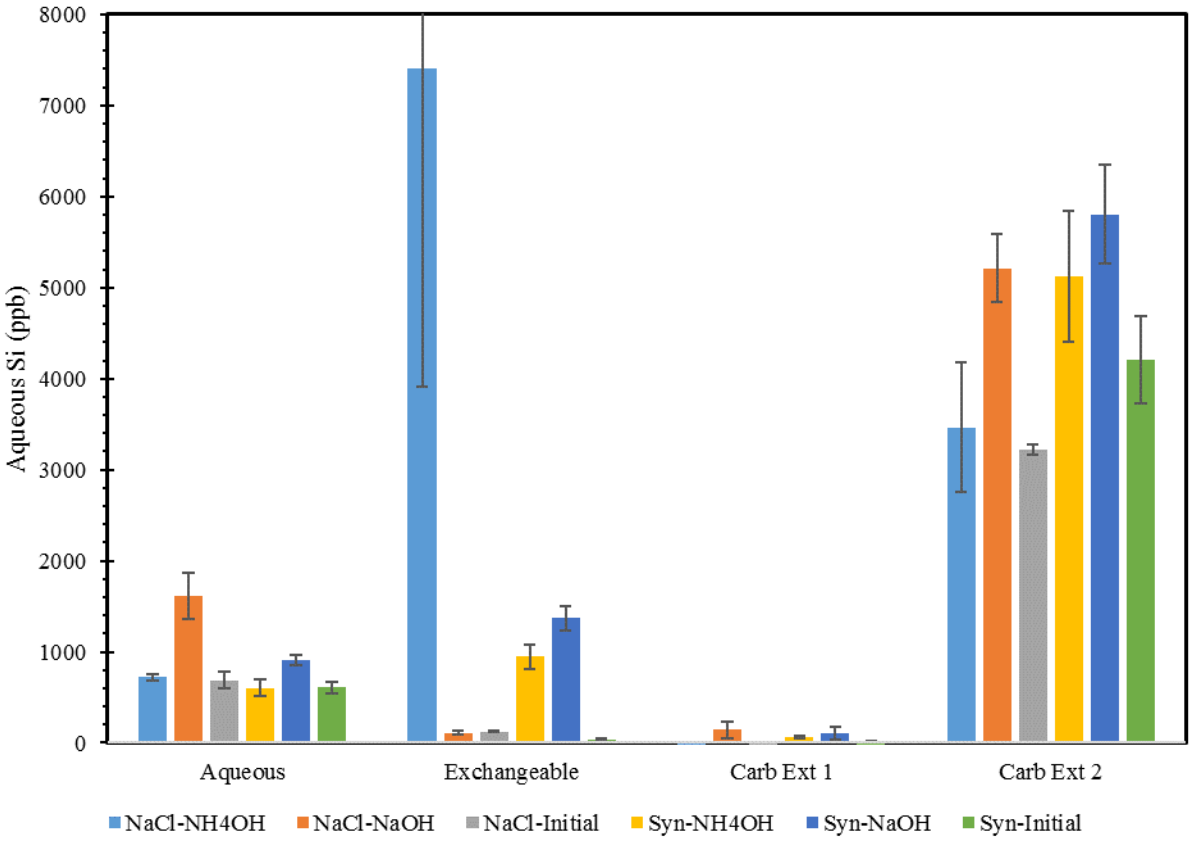

Figure 2-10. Dissolution of Si from the solid phase during the operationally-defined extraction steps for 25 g/L kaolinite suspensions equilibration for >30 days with 500 ppb U(VI) in either 0.007 M NaCl or synthetic porewater where initial samples represent netural pH without base addition and treated samples have either 2.5 M NH_4OH or 2.5 M NaCl + 0.025 M NaOH added to reach pH ~ 11.5.

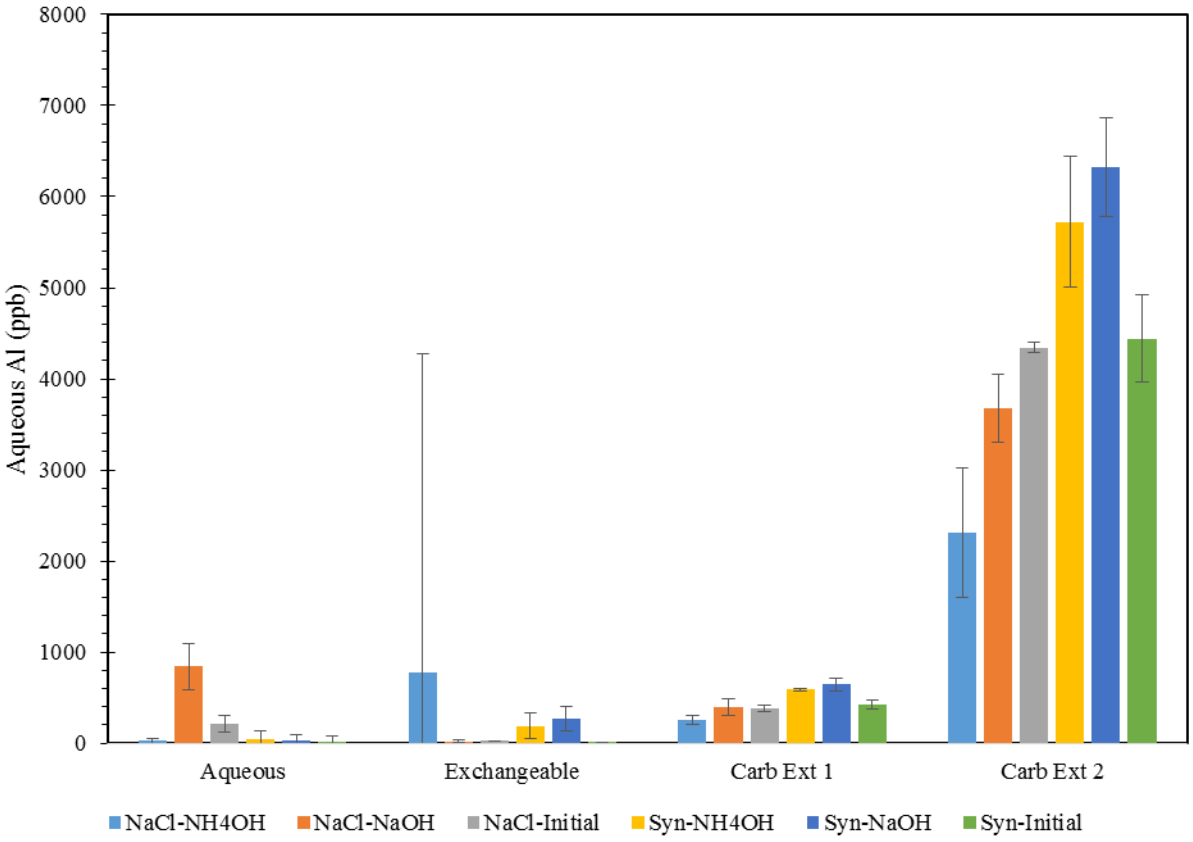

Figure 2-11. Dissolution of Al from the solid phase during the operationally-defined extraction steps for 25 g/L kaolinite suspensions equilibration for >30 days with 500 ppb U(VI) in either 0.007 M NaCl or synthetic porewater where initial samples represent netural pH without base addition and treated samples have either 2.5 M NH_4OH or 2.5 M NaCl + 0.025 M NaOH added to reach pH ~ 11.5.

Batch Experimental Results

Synthetic Porewater Experiments

Results are presented below for BET surface area of minerals and Hanford sediments (Table 2-10), equilibrium uranium partitioning (Figure 2-12) and mineral dissolution (Figure 2-13) for 500 ppb U in the presence of 25 g/L Hanford sediments in synthetic porewater, and control samples for U in synthetic porewater (without solids) (Figure 2-14). Finally, a comparison is drawn between U partitioning in the presence of variable minerals and Hanford sediments with respect to K_d in mL/g and mL/m^2 (Figures 2-15 and 2-16, respectively).

The apparent K_d's in mL/g follow the trends on the minerals for synthetic porewater with a significant increase in removal from the aqueous phase with the base treatment and slightly greater removal with NH_4OH treatment as compared to NaOH. However, the Si dissolution is different than kaolinite and illite but similar to that of montmorillonite. For kaolinite and illite, significantly greater aqueous Si and Al was observed for NH_4OH treatment versus NaOH treatment but similar aqueous Si and Al was observed for both for montmorillonite. Further, Al dissolution is slightly greater with NH_4OH treatment versus NaOH for Hanford sediments in the presence of synthetic porewater. Speciation modeling and activity correction calculations are

ongoing to better understand the differences in mineral dissolution with treatment. The surface area normalization shows that the sorption to quartz with respect to surface area is actually significantly greater than that of the clays and Hanford sediment.

The results for the control samples (without a solid phase) show that losses to the vial and pH adjustment for the initial conditions (pH~7.5) are minimal, 9±6%. However, when the pH is increased with either NH_4OH or NaOH treatments, significant losses occur, likely due to co-precipitation with other ions in solution (Figure 2-13). Further, these losses are greater than in the presence of the solid phase (Hanford sediments) with 1.2±0.2% vs. 41±6% for control and Hanford sediment with NH_4OH treatment and 9±6% vs. 79±1% for control and Hanford sediment with NaOH treatment. Further work is in progress to explain the greater removal in samples without a solid phase for the base treatments.

Table 2-10. BET Surface Area for Relevant Minerals and Hanford Sediment

Mineral ID	m^2/g
Quartz	0.046
Kaolinite	17.9
Illite	19.1
Montmorillonite	23.8
Hanford Sediment	17.4
Muscovite	0.096

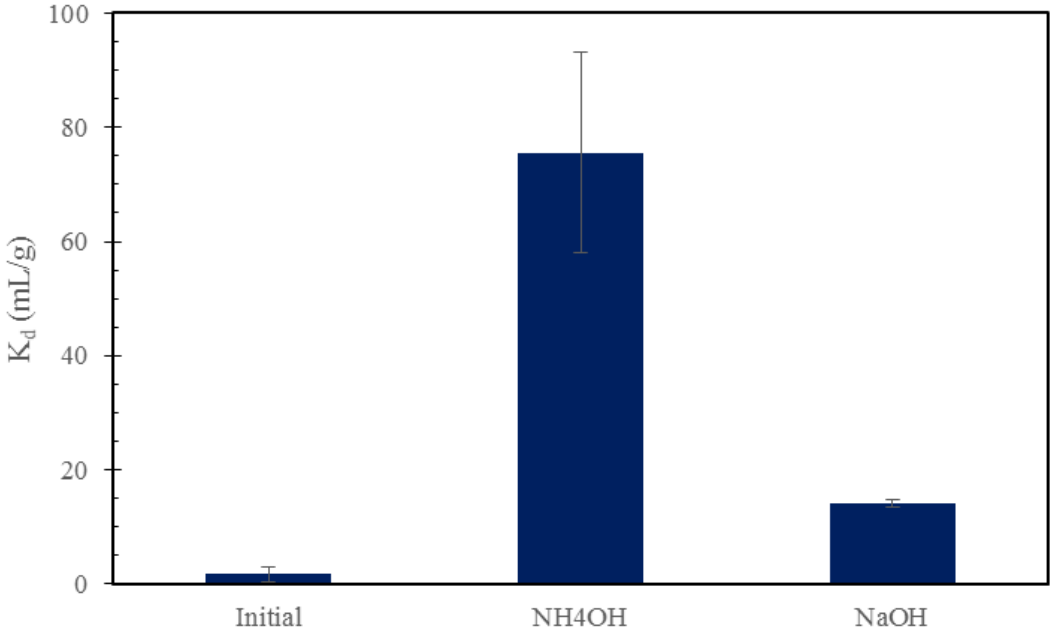

Figure 2-12. Apparent equilibrium K_d (mL/g) for U (500 ppb) removal in the presence of Hanford sediment (25 g/L) in synthetic porewater with pH at ~11.5 via adjustment with either NaOH (yellow) or NH_4OH (blue) or at ~7.5 to represent initial conditions prior to base. Treatment.

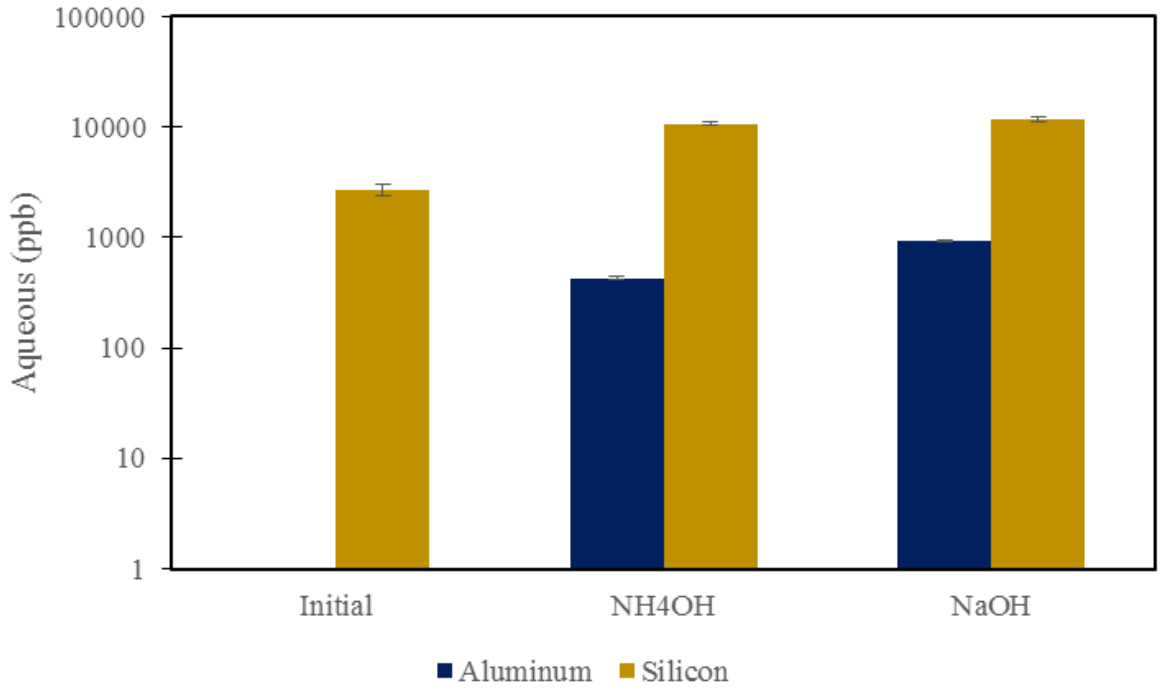

Figure 2-13. Aqueous Al and Si dissolved from Hanford sediment (25 g/L) in synthetic porewater with pH at ~11.5 via adjustment with either NaOH (yellow) or NH_4OH (blue) or at ~7.5 to represent initial conditions prior to base treatment, Note: Fe was also monitored but was below detection limits.

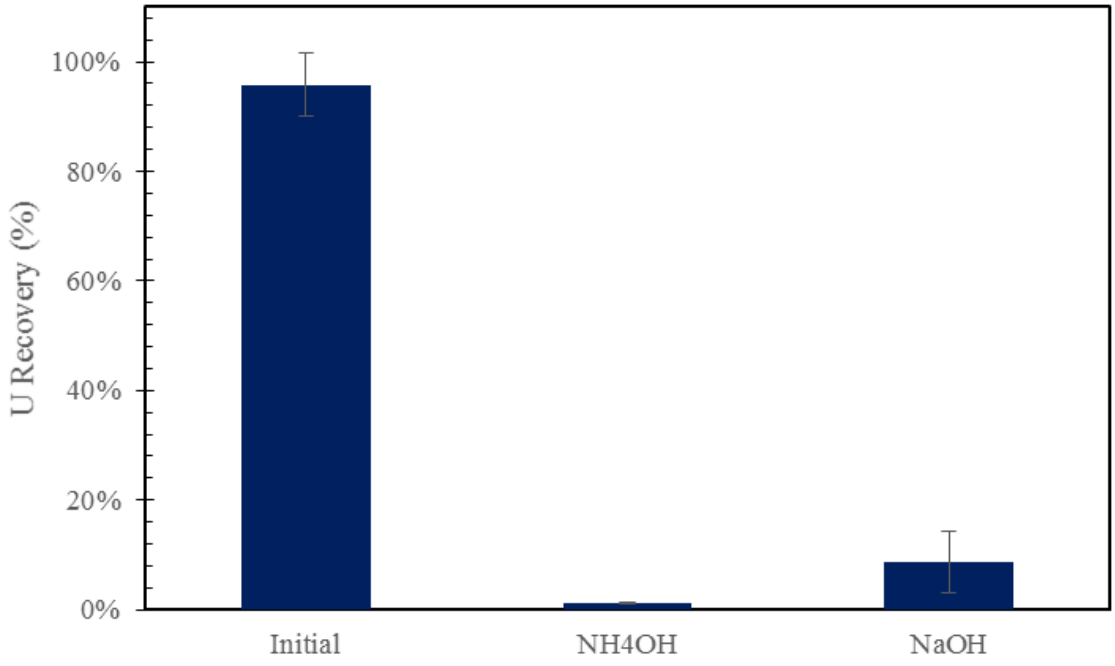

Figure 2-14. Recovery of U in the aqueous phase for triplicate control samples (no solids) for initial conditions (pH ~7.5) and following treatment to pH ~11.5 with either NH_4OH or NaOH.

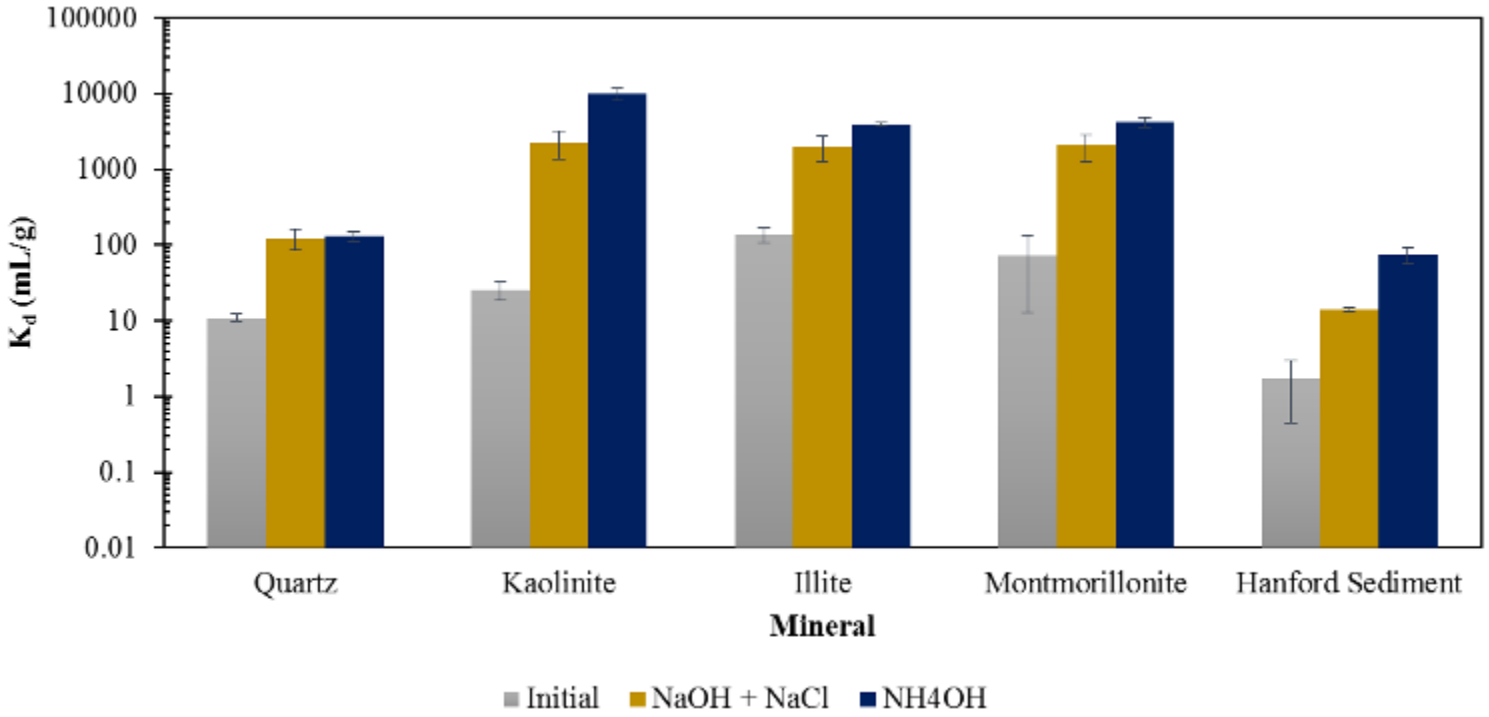

Figure 2-15. Apparent K_d (mL/g) for U (500 ppb) removal in the presence of kaolinite (5 g/L), quartz (100g/L), illite (5 g/L), montmorillonite (5 g/L) or Hanford sediment (25 g/L) in synthetic porewater with pH at ~11.5 via adjustment with either NaOH (yellow) or NH_4OH (blue) or at ~7.5 to represent initial conditions prior to base treatment.

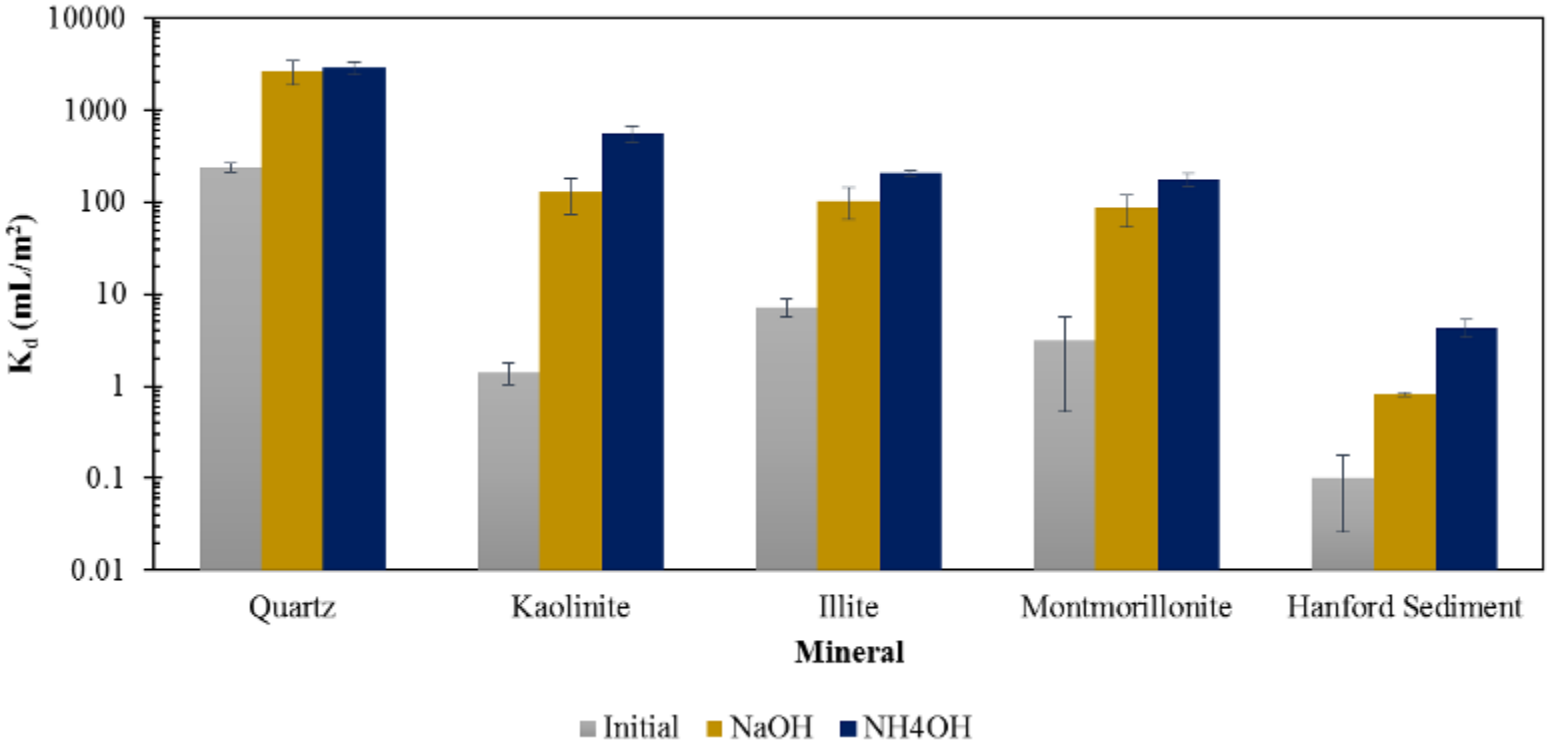

Figure 2-16. Apparent K_d (mL/m^2) for U (500 ppb) removal in the presence of kaolinite (5 g/L), quartz (100g/L), illite (5 g/L), montmorillonite (5 g/L) or Hanford sediment (25 g/L) in synthetic porewater with pH at ~11.5 via adjustment with either NaOH (yellow) or NH_4OH (blue) or at ~7.5 to represent initial conditions prior to base treatment.

3.2 mM NaCl Experiments

Triplicate samples were prepared with 5 g/L illite, 5 g/L montmorilloniteor 25 g/L quartz and 500 ppb U in 3.2 mM NaCl solution. This solution is used because it represents the simplest chemical system representative of Hanford's groundwater. Using the simplest solution at a similar ionic strength to the Hanford groundwater allows for a better understanding of the fate of U without the more complex cations present in the actual groundwater. Further, it is compared with the more complex synthetic porewater formula to understand the importance of these different ions. Samples were adjusted and equilibrated at pH ~7.5 for ~3 days. Then, samples were treated with either 2.5 M NH_4OH or 2.5 M NaCl + 0.025 M NaOH. Control samples (without solid mineral) were run alongside to represent conditions before treatment. Table 2-11 shows a summary of equilibrium pH readings.

Table 2-11. Equilibrium pH for Batch Experiment at 5 g/L Illite and Quartz 25 g/L of 500 ppb U

Treatment	Sample ID	Average
Initial	illite-1-6	7.41 ± 0.15
NaOH	illite-1-3	11.6 ± 0.10
NH_4OH	illite-4-6	11.9 ± 0.01
Initial	quartz 1-6	7.21 ± 0.16
NaOH	quartz-1-3	11.4 ± 0.03
NH_4OH	quartz-4-6	11.6 ± 0.02

Figure 2-17 compares K_d values for equivalent experiments having different minerals with NaCl solution at the same initial ionic strength based on BET surface area measurements in Table 2-12. The mobility of U in the presence NaCl are similar at the initial conditions. However, when pH is increased, treatment lowers apparent K_d (i.e. increases environmental mobility). This is likely due to the relative importance of carbonates in uranium complexation at elevated pH which is competing with sorption sites for uranium. Further, the uranyl carbonate complexes are less likely to sorb to the minerals due to their neutral or negative charge. However, should ammonia be used for treatment, it is expected that uranium would co-precipitate with Al and Si as the pH lowers back towards neutral as ammonia off-gases. This will be the subject of future experiments.

A increase is seen in both aqueous Al and Si in all samples at pH ~11.5 (Figure 2-18). It is important to note that there is a greater dissolution of the mineral with NaOH treated samples. This may be due to NH_4OH-treated samples having greater precipitation of alumino-silicates than NaOH-treated samples due to differences in the total activity as the total ionic strengths are similar but the NH_4OH-treated samples have a majority of molecular (uncharged) species while NaOH-treated samples are mostly ionic (charged) species. However, montmorillonite's Si content (20.46%) is twice that of Al (9.83%), thus contributing to more aqueous Si in the system for both treaments (Weinrich 2016). Further, Fe aqueous concentrations were also analyzed. However, all but NH_4OH were below background levels. A possible explanation as to why Fe was above background in the ammonia treated samples may be due to: 1) Fe presence in the ammonia stock, or 2) ammonium cation exchanging iron present in system better than the counter cation treatment with sodium. This is currently under investigation.

Table 2-12. BET Surface Area for Relevant Minerals

Mineral ID	m^2/g
Quartz	0.046
Kaolinite	17.9
Illite	19.1
Montmorillonite	23.8

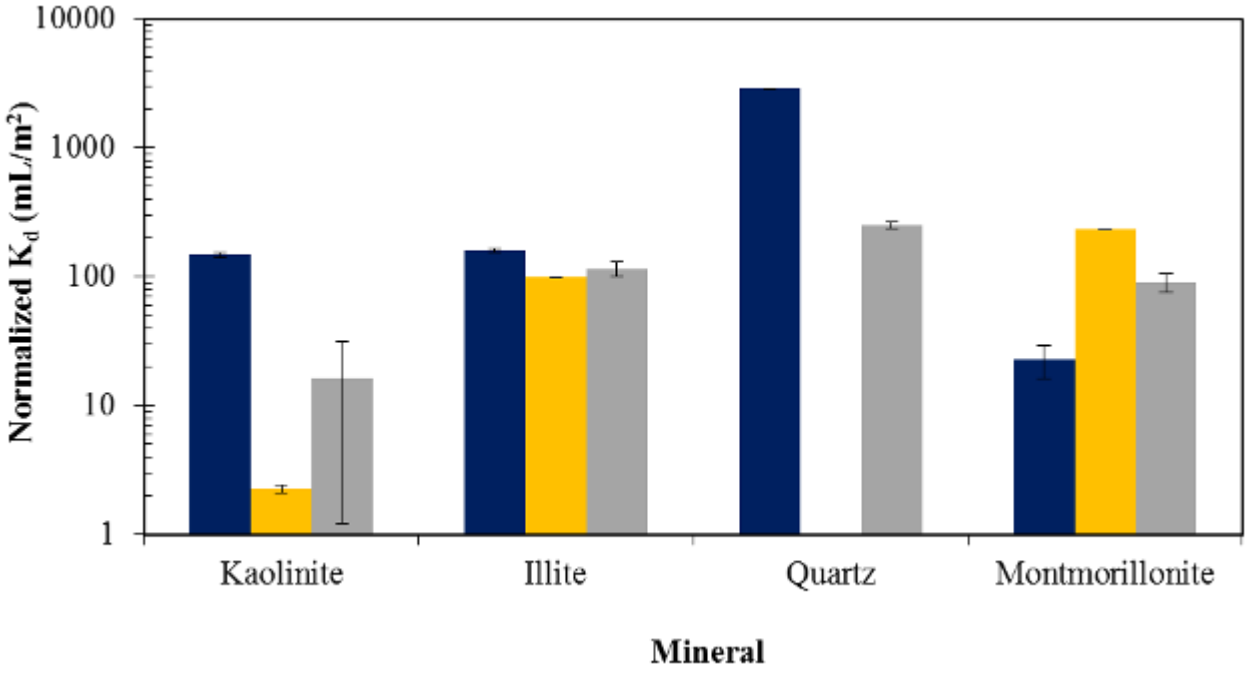

Figure 2-17. Normalized apparent Kd (mL/m^2) for U (500 ppb) removal in the presence of kaolinite (5 g/L), illite (5 g/L), quartz (100g/L) or montmorillonite (5 g/L) in 3.2 mM NaCl solution with pH at ~11.5 via adjustment with either NaOH (yellow) or NH4OH (gray) or at ~7.5 to represent initial conditions prior to base treatment (blue), Note: NaOH treatment for quartz is still being analyzed.

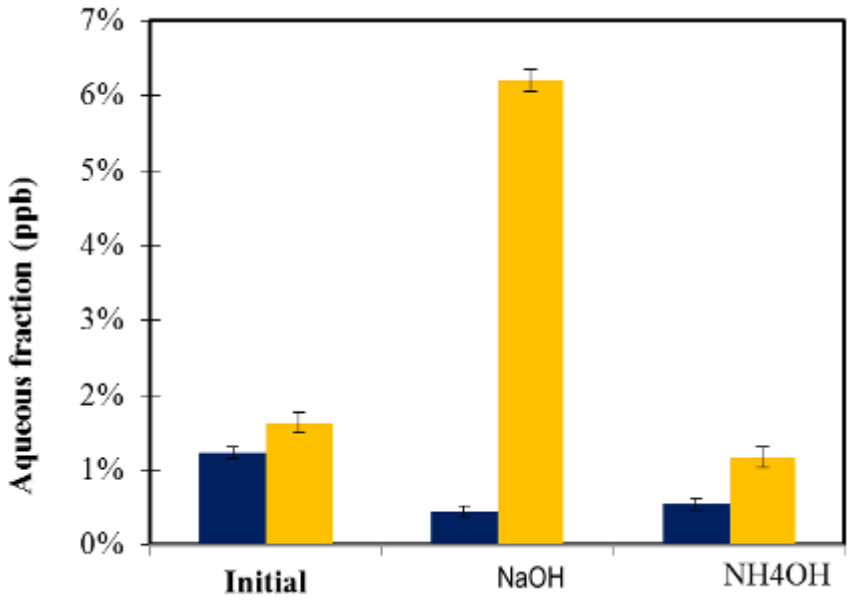

Figure 2-18. Aqueous Al (blue) and Si (yellow) dissolved from montmorillonite (5 g/L) in 3.2 mM NaCl at pH ~11.5 via adjustment with either NaOH or NH4OH or at pH ~7.5 to represent initial conditions prior to base treatment.

Aqueous Speciation Modeling

Geochemist Workbench Standard version 10.0.04 (GWB) was used to model the aqueous speciation of uranium within these systems. The Visual Minteq database was used for modeling with several additions to update uranium species based on new thermodynamic data. Specifically, several aqueous and solid species were updated based on two reviews (Guillamont, Fanghanel et al. 2003, Gorman-Lewis, Shvareva et al. 2009). However, it must be noted that thermodynamic data for aqueous and solid actinide species under alkaline and hyperalkaline conditions are still incomplete, especially with respect to ternary aqueous complexes and solid phases (Altmaier, Gaona et al. 2013).

The neutral calcium – uranyl – carbonate species [$Ca_2UO_2(CO_3)_3$] was modified based on previous work (Kalmykov and Choppin 2000, Bernhard, Geipel et al. 2001, Dong and Brooks 2006). This neutral species was first reported in literature by Bernhard (Bernhard, Geipel et al. 1996). Additional complexes for ternary uranyl carbonate complexes with alkaline earth metals were included based on previous work (Dong and Brooks 2006). Notably, the $MgUO_2(CO_3)_3^{-2}$ species was added based on Dong and Brookw (2006) as it was absent from the original database. It should be noted that the neutral calcium – uranyl – carbonate species measured by Kalmykov et al., Dong and Brooks, and Bernhard et al. are all within the experimental error of each other with the $Log\beta_{213}$ = 29.8±0.7, 30.7±0.05, and 30.55±0.25, respectively. In addition, several uranyl hydroxide and uranyl carbonate species were added based on the OECD NEA update (Guillamont, Fanghanel et al. 2003)

Although several researchers have previously investigated the thermodynamic properties of the becquerelite [$Ca(UO_2)_6O_4(OH)_6(H_2O)_8$] solid based on the review by Gorman-Lewis et al. (2009), there is still a significant error between measurements (> 6 log units for the K_{sp}).

Therefore, this species was not included in the final database. Metaschoepite was also not included in the database due to its similarity to the schoepite species from the OECD NEA update and the significant variability between researchers (Guillamont, Fanghanel et al. 2003, Gorman-Lewis, Shvareva et al. 2009).

The most recent thermodynamic data added to the database is for K-boltwoodite, uranophane and coffinite (Shvareva, Mazeina et al. 2011, Szenknect, Mesbah et al. 2016). Shvareva et al. (2011) also measured parameters for Na-boltwoodite which were within the error of the previous value reported in the updated OECD NEA database (Guillamont, Fanghanel et al. 2003). Therefore, these values are expected to be accurate measurements. The uranophane K_{sp} replaced the highly variable measurements previously summarized by Gorman-Lewis et al. (2009). Further, the coffinite K_{sp} value from Szenknect et al. (2016) is an important addition because it has been reported in many natural, low-temperature aquatic systems (Guo, Szenknect et al. 2015). Szenknect et al. (2016) reported a standard free energy of formation for coffinite of -1862.3 ± 7.8 kJ/mol which compares well with the previously measured values ranging from -1872 ± 6 to -1886 ± 6 kJ/mol (Langmuir 1978, Grenthe, Wanner et al. 1992, Guo, Szenknect et al. 2015). In addition, the size of the coffinite grains used in the study are considered representative of coffinite in nature and as an alteration product of spent nuclear fuel (Szenknect, Mesbah et al. 2016).

A comparison is shown in Figure 2-19 comparing the aqueous speciation in the synthetic porewater at pH 7.5 as predicted with the final updated database, the standard thermo.dat database, and the standard thermo_minteq.dat database. It must be noted that similar species were summed to allow for a simpler comparison (i.e., "U-Carb" represents a summation of all uranyl carbonate species). The major difference between the updated database in GWB is due to the formation of ternary calcium or magnesium uranyl carbonate species. Further, it is notable that the GWB software with the updated database and the predictions presented in the February monthly report using Visual Minteq with the thermo.vdb database are similar with the exception that a slightly greater fraction is predicted in the Ca/Mg-U-CO_3 species versus the U-OH-CO_3 species due to the latter species not being present in the database for Visual Minteq (Table 2-13).

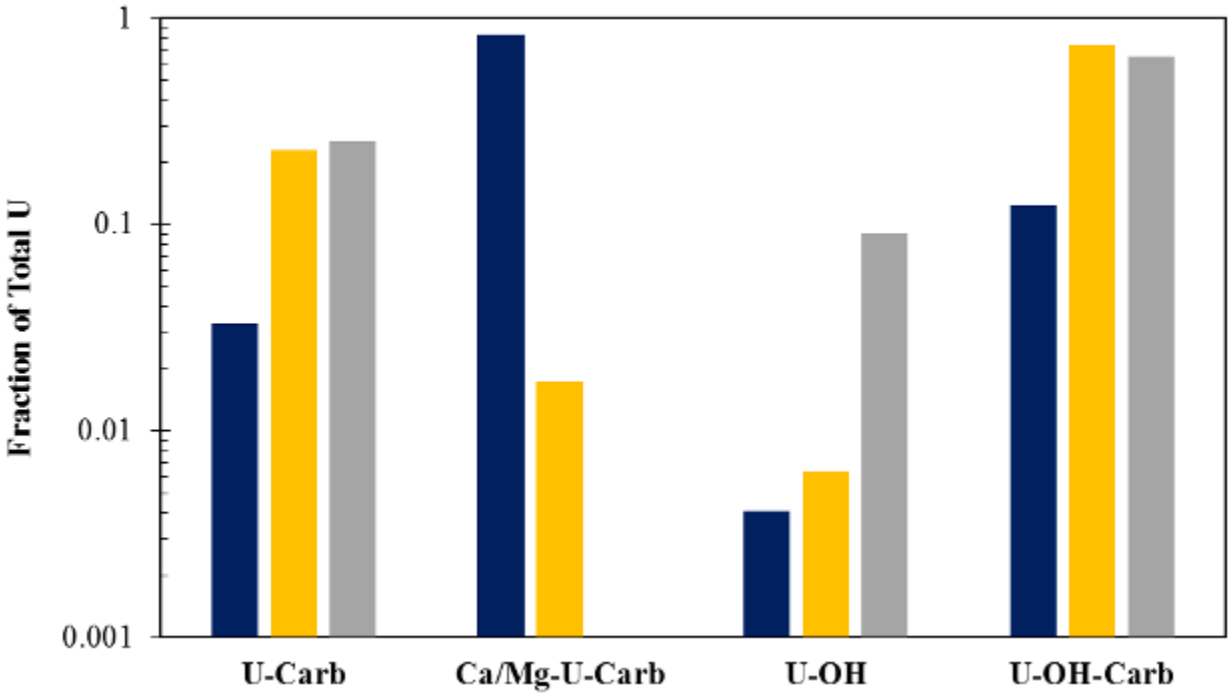

Figure 2-19. A comparison of predictions for types of aqueous species with different databases using Geochemist Workbench including the Updated database (blue), Visual Minteq database (yellow) and Thermo database (gray).

Table 2-13. Comparison of Predictions for Types of Aqueous Species Modeled with GWB using the Updated GWB Database or with Visual Minteq using the Standard Database

Species Type	Vis Minteq	Updated GWB
U-Carb	5.092%	3.301%
Ca/Mg-U-Carb	94.125%	83.819%
U-OH	0.782%	0.411%
U-OH-Carb	0%	12.469%

Future Experiments:

Ongoing Batch Experiments at FIU

Following the experiments with montmorillonite, kaolinite, illite and quartz in NaCl, equivalent batch experiments with muscovite, calcite and natural Hanford sediments will be completed for comparison. These will be completed upon DOE Fellow Silvina Di Pietro's return from her summer internship at PNNL. Data analysis for equilibrium batch sorption for synthetic porewater in the presence of calcite and muscovite is currently in progress. Statistical comparison through t-testing will be completed in the future to compare the NaOH and NH_4OH treatments. Speciation modeling will also be employed to better understand the partitioning of uranium and mineral dissolution.

Internship at PNNL

Silvina Di Pietro began a summer internship at PNNL this month. She is being mentored by the lead scientist at the PNNL environmental system group, Dr. Jim Szecsody. She has been learning about the geology and hydrology of the Hanford Site, including an introduction to lava flows and rock formation, Bowen series and different types of minerals.

In addition, she has been introduced to new laboratory techniques including: spectrophotometry (ferrozine colorimetric analysis method for Fe), use of hand-held pH meters with low maintenance electrodes, conductivity electrodes and operation basics for an anaerobic/vacuum chamber. She has also learned to work with syringe needles when extracting an aliquot from septum-closed anaerobic glass bottles. This is a common practice in many fields, yet requires skill, and it will be applied throughout her dissolution/kinetics experiments at PNNL.

The focus of this internship will be mineral dissolution experiments. Table 2-14 shows the minerals to be investigated and Table 2-15 represents the conditions. The dissolution of seven minerals in 3.1 M NH_4OH (equilibrium with 5% NH_3 gas) or 0.01 M NaOH solutions will be compared using either DIW or synthetic groundwater (SGW). Two minerals, muscovite and montmorillonite, will go through all conditions since they have previously been shown to readily dissolve at the target pH (Szecsody et al., 2012). Baseline samples will be run in an anaerobic environment in 3.1 M NH_4OH solution (labeled A-G). Four minerals (H-K) will also be investigated under aerobic conditions for comparison.

Table 2-14. Minerals to be used in Dissolution Experiments and Hanford Site Percent by Weight

Mineral	Formula	Hanford fm (% wt)
Quartz	SiO_2	38.4 ± 12.8
Microcline	$KAlSi_3O_8$	15.3 ± 4.4
Calcite	$CaCO_3$	1.91 ± 1.71
Illite	$(Al,Mg,Fe)_2(Si,Al)_4O_{10}[(OH)_2,(H_2O)]$	2.46 ± 3.74
Montmorillonite	$(Na,Ca)_{0.33}(Al,Mg)_2(Si_4O_{10})(OH)_2 \cdot nH_2O$	TBD
Muscovite	$KAl_2(Si_3AlO_{10})(OH)_2$	2.46 ± 3.74
Epidosite	$\{Ca_2\}\{Al_2Fe^{3+}\}[O\|OH\|SiO_4\|Si_2O_7]$	1.78 ± 3.75

Xue, Y., Murray, C., Last, G., R. Mackley. 2003. Mineralogical and bulk-rock geochemical signature of Ringold and Hanford formation sediments
Pacific Northwest National Laboratories, PNNL-14202.

Table 2-15. Dissolution Rate Experimental Conditions and Sampling Events for Seven Hanford Site Minerals
(note: letters represent the labels to be used for sample bottles)

Mineral	Anaerobic DIW + 5% NH_3	Aerobic DIW + 5% NH_3	Anaerobic SGW + U + 5% NH_3	Anaerobic SGW + U + 5% NH3 – 4 wk age then air strip to pH 8	Anaerobic DIW + 0.01 M NaOH
Muscovite	A	H	L	N	P
Montmorillonite	B	I	M	O	Q
Quartz	C				
Illite	D	J			R
Calcite	E				
Epidosite	F	K			S
Microcline	G				T

Four additional bottles will contain 1 ppm U (L-M and N-O). The difference between these two sets of experiments is that N and O bottles will go through an air-stripping technique with compressed gas after a four-week period prior to sampling. The goal of this condition is to investigate mineral dissolution after ammonia off-gases and reaches a neutral pH value. A test (without U) was performed with air-stripping with compressed air over a 6 hr period (Figure 2-20) at a flow rate of 5.4 mL/sec and reached a pH ~9.

During the month of June, preliminary experiments were begun and standards were prepared using $FeCl_2$ for colorimetric analysis. Figure 2-21 shows the fit for the concentration of the Fe^{2+} standards versus absorbance. Future work will focus on analyzing the aqueous phase of dissolution experiments for Fe(II) and total Fe mineral concentrations by ferrozine colorimetric method, U analysis by KPA and major cations by ICP-OES (at FIU), as well as other solid phase analysis techniques including XRD and FTIR.

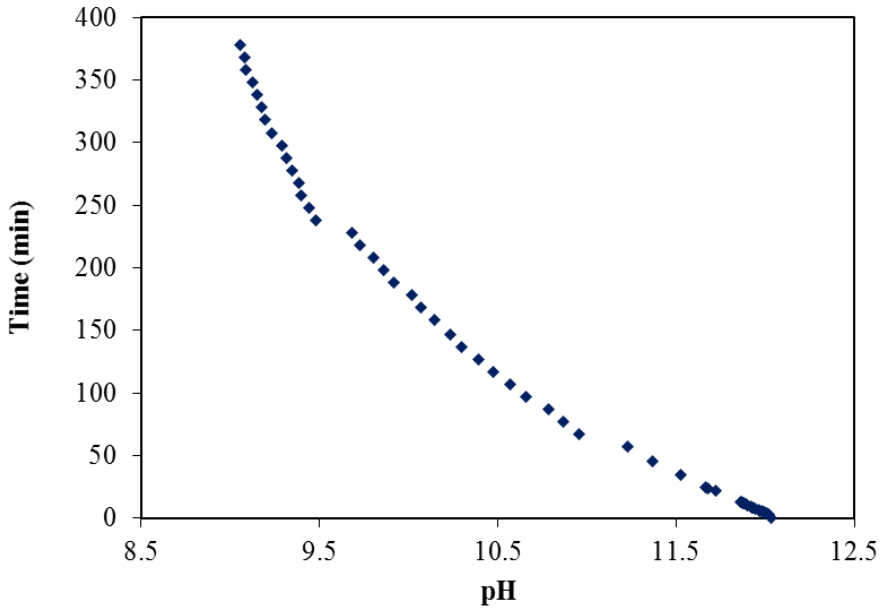

Figure 2-20. 3.1 M NH4OH solution air-stripped with compressed air test to pH neutralization versus time.

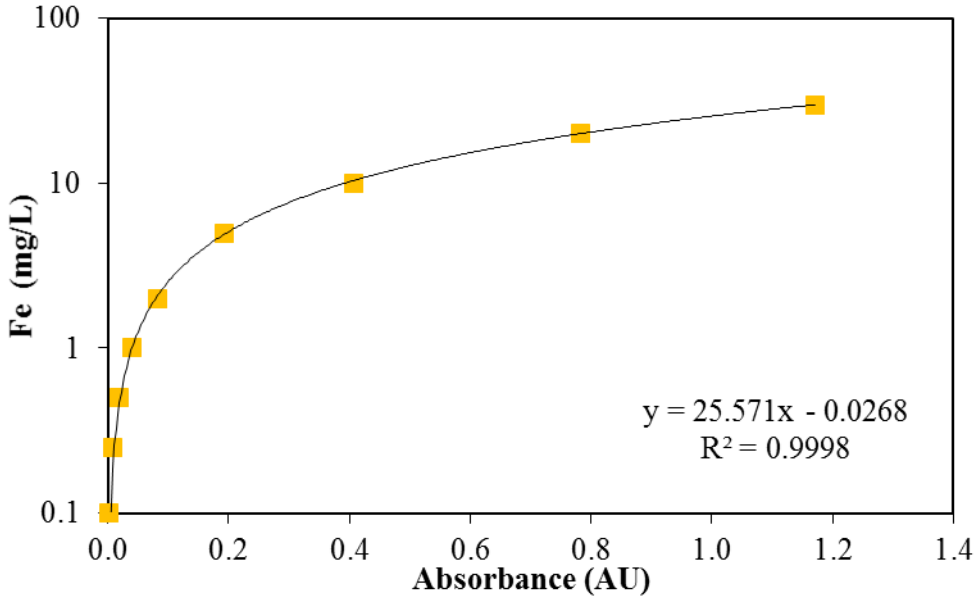

Figure 2-21. Ferrous iron calibration using the Ferrozine method.

References:

1. Altmaier, M., X. Gaona and T. Fanghanel (2013). "Recent advances in aqueous actinide chemistry and thermodynamics." Chem Rev **113**(2): 901-943.
2. Bernhard, G., G. Geipel, V. Brendler and H. Nitsche (1996). "Speciation of uranium in seepage waters of a mine tailing pile studied by time-resolved laser-induced fluorescence spectroscopy (TRLFS)." Radiochimica Acta **74**(s1): 87-92.
3. Bernhard, G., G. Geipel, T. Reich, V. Brendler, S. Amayri and H. Nitsche (2001). "Uranyl (VI) carbonate complex formation: Validation of the Ca2UO2 (CO3) 3 (aq.) species." Radiochimica Acta International journal for chemical aspects of nuclear science and technology **89**(8/2001): 511.
4. Dong, W. and S. C. Brooks (2006). "Determination of the formation constants of ternary complexes of uranyl and carbonate with alkaline earth metals (Mg2+, Ca2+, Sr2+, and Ba2+) using anion exchange method." Environmental science & technology **40**(15): 4689-4695.
5. Gorman-Lewis, D., T. Shvareva, K.-A. Kubatko, P. C. Burns, D. M. Wellman, B. McNamara, J. E. S. Szymanowski, A. Navrotsky and J. B. Fein (2009). "Thermodynamic Properties of Autunite, Uranyl Hydrogen Phosphate, and Uranyl Orthophosphate from Solubility and Calorimetric Measurements." Environmental Science & Technology **43**(19): 7416-7422.
6. Grenthe, I., H. Wanner and I. Forest (1992). "Chemical thermodynamics of uranium."
7. Guillamont, R., T. Fanghanel, I. Grenthe, V. Neck, D. Palmer and M. Rand (2003). Update on the Chemical Thermodynamics of Uranium, Neptunium, Plutonium, Americium and Technetium. Chemical Thermodynamics, OECD Nuclear Energy Agency. **5:** 959.
8. Guo, X., S. Szenknect, A. Mesbah, N. Clavier, C. Poinssot, S. V. Ushakov, H. Curtius, D. Bosbach, R. C. Ewing and P. C. Burns (2015). "Thermodynamics of formation of

coffinite, USiO4." Proceedings of the National Academy of Sciences **112**(21): 6551-6555.
9. Kalmykov, S. N. and G. R. Choppin (2000). "Mixed Ca2+/UO22+/CO32-complex formation at different ionic strengths." Radiochimica Acta International journal for chemical aspects of nuclear science and technology **88**(9-11/2000): 603.
10. Langmuir, D. (1978). "Uranium solution-mineral equilibria at low temperatures with applications to sedimentary ore deposits." Geochimica et Cosmochimica Acta **42**(6): 547-569.
11. Shvareva, T. Y., L. Mazeina, D. Gorman-Lewis, P. C. Burns, J. E. Szymanowski, J. B. Fein and A. Navrotsky (2011). "Thermodynamic characterization of boltwoodite and uranophane: Enthalpy of formation and aqueous solubility." Geochimica et Cosmochimica Acta **75**(18): 5269-5282.
12. Szenknect, S., A. Mesbah, T. Cordara, N. Clavier, H.-P. Brau, X. Le Goff, C. Poinssot, R. C. Ewing and N. Dacheux (2016). "First experimental determination of the solubility constant of coffinite." Geochimica et Cosmochimica Acta **181**: 36-53.
13. Weinrich, D. (2016). "Montmorillonite Mineral Data." Mineralogy Database Retrieved June 29, 2016, from http://webmineral.com/data/Montmorillonite.shtml#.V3wCuufh0Wr.

Subtask 1.3.3: The influence of microbial activity on the corresponding electrical geophysical response after ammonia injections in the vadose zone

DOE Fellow Alejandro Garcia completed a 10-week spring 2016 internship at PNNL and began preparations for the column experiments related to the spectral induced polarization (SIP) signatures of microbial activity designed to remediate uranium-contaminated vadose zone sediment. Space within an FIU laboratory involving radioactive materials has been designated for this research and FIU provided a computer for taking measurements. FIU ordered the necessary materials and electrodes in order to conduct the column research.

FIU prepared a detailed proposal for the FIU Radiation Control Committee where all safety procedures for packing columns with a mixture of Hanford soil and autunite particles as well as sample collection and analyses were presented. The proposal also includes a description of the work area, as well as procedures for waste management, storage and radiation surveys. The procedures were sent to the FIU Radiation Safety Officer and Radiation Control Committee and were approved.

Researchers from PNNL, Drs. Brady Lee and Jonathan Thomle, traveled to FIU to help in setting up the columns for the experiment. All columns and electrodes to take SIP measurements were fabricated at PNNL. The experimental set up includes six clear PVC columns and large opaque PVC end caps. Each column has a coiled Ag/AgCl current electrode on each end, 4 potential electrodes along the length, and 3 sampling ports, with one positioned between each potential electrode pair. The current electrodes are made from a coiled silver (Ag-AgCl) wire; the potential electrodes use a straight wire encased in agar gel that makes contact with the sediment in the column. FIU has begun connecting the pump and tubing which will deliver solution into the column. The tubing is hard Teflon as well as flexible silicone. Flow will be powered by a peristaltic pump with a target flow rate of 50 mL/d for each column. There will be four separate solutions which have to be sparged with nitrogen in order to remove any dissolved gas which may form bubbles within the column. Each bottle of solution is connected to a bag full of

nitrogen, which will prevent the solutions from equilibrating with carbon dioxide. Bacterial cultures will be shipped to FIU in a dry state in order to inoculate the columns.

The media solutions for bacteria culturing will be prepared in aerobic conditions within a standard laboratory hood designated for work with radioactive materials. These cultures will be shipped to FIU in a desiccated state.

Figure 2-22. Experimental set up with six columns. The set up allows for the collection of SIP measurements and enables correlation of the data with changes in the columns' porewater geochemical parameters.

Task 2: Remediation Research and Technical Support for Savannah River Site

Task 2 Overview

The acidic nature of the historic waste solutions received by the F/H Area seepage basins caused the mobilization of metals and radionuclides, resulting in contaminated groundwater plumes. FIU is performing basic research for the identification of alternative alkaline solutions that can amend the pH and not exhibit significant limitations, including a base solution of dissolved silica and the application of humic substances. Another line of research is focusing on the evaluation of microcosms mimicking the enhanced anaerobic reductive precipitation (EARP) remediation method previously tested at SRS F/H Area.

Task 2 Quarterly Progress

Subtask 2.1. FIU's Support for Groundwater Remediation at SRS F/H –Area

Sequential extraction experiments were designed to assess the remobilization of U(VI) under environmental conditions. Sequential extraction is a technique which is used to chemically leach metals out of soils, mimicking the remobilization of metals under different environmental

conditions. Theoretically, the most mobile metals are removed in the first fraction, continuing in order of decreasing of mobility (Zimmerman & Weindorf, 2010). In an attempt to provide an internationally accepted sequential extraction protocol, a modified BCR (Community Bureau of Reference or now the Standards, Measurements and Testing Program of the European Commission) sequential extraction procedure was developed (Rauret et al., 1999). This procedure is largely similar to that produced by Tessier (Tessier et al., 1979), with the chief difference being in the first fraction of the procedure. Instead of evaluating the exchangeable and carbonate bound separately, the BCR procedure combines both in the first fraction (Ure et al., 1993).

The sequential extraction experiments were conducted using approximately 0.8 g SRS background soil (180μm<d<2mm) which was brought into contact with 40 ml of synthetic SRS groundwater spiked with 500 ppb U (VI); sodium silicate was added (70 ppm) to adjust the pH to circumneutral conditions. The mixture was left for 24 hours to equilibrate; aliquots were taken and analyzed by means of KPA to determine residual U (VI) concentration. Subsequently, the supernatant was then removed. All experiments were conducted in triplicate. Sequential extraction experiments followed the BCR (Community Bureau of Reference) protocol. More specifically, after the initial sorption step, the metal-laden solid was suspended in 40 ml 0.11 M CH_3COOH and shaken at room temperature for 16 h at 120 rpm. The extract was separated from the solid residue by centrifugation for 10 min (5000 rpm) and decanted into a polyethylene container and stored in a refrigerator at 4ºC before analysis. The residue was washed with 10 ml of deionized water by shaking for 10 min, centrifuged, and the washings discarded. Step 1 aims to determine the exchangeable and acid soluble fraction of sorbed uranium. The second step involved the suspension of the solid in 40 mL of 0.5 M hydroxylamine hydrochloride ($H_2NO{\cdot}HCl$, Alfa Aesar), pH 1.5, acidified with HCl, and the extraction procedure was performed as described above. The goal of step 2 is the determination of uranium bound to Fe and Mn oxides. Subsequently, the solid was treated with 10 mL of H_2O_2 for 1h at room temperature, followed by 1 more hour of treatment in a 85ºC water bath, until the volume was reduced to less than 2 ml. Then, 50 mL of $NH_4CH_3CO_2$ 1M, pH adjusted with HNO_3 acid, were introduced. The suspension was shaken for 16 h at room temperature at 120 rpm and the extraction procedure was repeated, as described above. Step 3 provides information on the oxidisable fraction of sorbed uranium. The residual amount of retained uranium was calculated by subtracting the sum of the fractions mentioned above from the total mass of sorbed uranium (Rauret et al., 1999). The steps are summarized in Table 2-16.

Table 2-16. Procedure of BCR Sequential Extraction (He et al., 2013; Zemberyova et al., 2006)

Target phase	Reagents	Conditions
Exchangeable, water and acid-soluble	40 mL 0.11M CH_3COOH	16 h, room temperature
Reducible (Fe and Mn oxides)	40 mL 0.5M NH_2OH-HCl (pH 1.5)	16 h, room temperature
Oxidisable (Organic matter and sulfides)	10 mL 8.8M H_2O_2, 50 mL 1M $NH_4CH_3CO_2$ (pH2)	1 h, room temperature 1 h, 85°C
Residual	HNO_3-HCl digestion	

The results of BCR sequential extraction for U(VI) sorbed on SRS soil are presented at Table 2-17.

Table 2-17. Percentage of U(VI) Recovered in Each Stage of BCR Sequential Extraction Protocol

BCR target phase	U(VI) recovery %
Exchangeable, water and acid soluble	83 ± 7
Reducible form - bound to Fe and Mn oxides	10 ± 1
Oxidisable form – bound to organic matter and sulfides	2 ± 1
Residual	5 ± 4

The majority of the uranium that was retained by SRS soil was recovered in the first step of the process, indicating that the uranium that is uptaken by the soil is found mostly in acid soluble form. Nevertheless, the preliminary desorption experiments that involved uranium-loaded soil and deionized water (pH 6.5) as a desorbing agent revealed practically no recovery of uranium. These results suggest that the sorbed uranium on SRS soil may be re-mobilized only by acidic agents, such as 0.11 M CH_3COOH, that was used during step 1. Ten percent of the total uranium retained is associated with iron oxides, since the SRS background soil from the F/H area does not contain a significant amount of manganese oxides, as it can be seen in Table 2-18. The amount of uranium in oxidisable and residual form was found to be practically zero, given the experimental error. The background soil from the SRS F/H Area is a low organic, quartz dominated soil (Dong et al., 2012); hence, the experimental results were rather expected. Typically, metals of anthropogenic activity tend to accumulate in the first three phases and metals found in the residual fraction are metals of natural occurrence incorporated in the crystal lattice of the parent rock (Ratuzny et al., 2008; Tessier et al., 1979).

Table 2-18. Adaptation of Elemental Composition of SRS F/H Area Background Soil Obtained by Means of X-Ray Fluorescence, courtesy of Dr. Miles Denham

Mineral phase	SRS F/H area soil percentage (%)
Quartz	92 ± 4
Kaolinite	6 ± 2
Goethite	1.0 ± 0.5
MnO_2	<0.01

Specific surface area analysis was used to measure the specific surface area of the different SRS background soil fractions, namely d<63μm, 63μm <d<180μm, 180μm<d<2mm. The specific surface area was used to normalize results from previous sorption experiments of the different soil fractions. Furthermore, desorption experiments were designed to assess the remobilization of U (VI) under acidic environmental conditions. These experiments are a continuation of previous desorption experiment on the different SRS background soil fractions. The results are presented in Table 2-19.

Table 2-19. BET Specific Surface Area Results

SRS Soil Fraction	BET Surface Area
d <63μm	8.4 ± 0.12 m²/g
63μm <d<180μm	2.8 ± 0.1 m²/g
180μm<d<2mm	0.41 ± 0.01 m²/g

Experiments were conducted using approximately 0.2 g SRS background soil (d<63μm, 63μm <d<180μm, 180μm<d<2mm), which was brought in contact with 10 ml synthetic SRS groundwater spiked with 500 ppb U (VI). Sodium silicate was added (final concentration of sodium silicate was 70 ppm) in order to adjust the pH to circumneutral conditions. The mixture was left for 24 hours to equilibrate; aliquots were taken and analyzed by means of KPA to determine residual U (VI) concentration. Subsequently, the supernatant was then removed, and 10 ml of synthetic SRS groundwater were re-introduced. All experiments were conducted in triplicate. The mix was left for another 24 hours to equilibrate; aliquots were taken and analyzed by means of KPA to determine residual U (VI) concentration recovered from the soil. Summary of the results are shown in Table 2-20.

Table 2-20. Sorption and Desorption Results for the Different Fraction, Alongside the Fe Concentration

SRS Soil Fraction	[Fe] (mg/g)	Sorption		Desorption
		U(VI)% Removal	μg U(VI) Sorbed/ m² of soil	U(VI)% Recovered
d<63μm	89 ± 2	96 ± 0.4	3.1 ± 0.02	63 ± 3
63μm <d<180μm	70 ± 7	90 ± 2	8.7 ± 0.2	84 ± 4
180μm<d<2mm	40 ± 4	60±0.5	35 ± 0.4	61 ± 5

Understanding U (VI) sorption on the different SRS soil fractions gives greater insight on the mechanisms by which U (VI) sorbs to the soil surface. Results from Table 2-20 suggest a correlation between the mean particle diameter and U (VI) % removal. As the diameter decreases, the U (VI) % removal increases. Subsequently, these results were normalized using the specific surface area (μg of U (VI) sorption per m² of soil). Results suggest that as the surface area increases, U (VI) sorption per m² of soil decreases. However, Table 2-20 shows Fe concentrations from the different SRS soil fractions, which denotes a positive correlation between the Fe content of the soil and the U(VI) % removal. These results could suggest a greater involvement of Fe, in the form of goethite, in the mechanism of U(VI) sorption.

On the other hand, desorption is statistically the same for the fine (d<63 μm) and the coarse fraction (180 μm<d<2mm), but desorption seems to be higher for the intermediate fraction. The desorption experiment for the intermediate fraction will be repeated.

Another set of batch experiments was designed in order to investigate the influence of the Ca^{2+} and Mg^{2+} ions on the sorption of U(VI) on SRS sediment from the F/H Area under circumneutral conditions. The experiments were conducted, bringing in contact 400 mg of SRS sediment (average particle diameter 0.18<d<2mm) with 20 ml of SRS synthetic groundwater with pH 3.5 bearing 500 ppb of U(VI). 70 ppm of sodium silicate was added to achieve circumneutral conditions and then different quantities from stock solutions of $Ca(NO_3)_2$ and $Mg(NO_3)_2$ were

added in order to achieve the desired electrolyte concentrations. The concentrations of $Ca(NO_3)_2$ and $Mg(NO_3)_2$ were 0.0001, 0.001 and 0.01 M. Control samples (no addition of electrolyte) were also studied, which already contained a concentration of Ca^{2+} $2.5 \cdot 10^{-5}$ M and Mg^{2+} $1.5 \cdot 10^{-5}$ M. After 24h, aliquots were isolated from the supernatant and the residual concentration of U(VI) in the supernatant was determined by means of KPA. All experiments were performed in triplicate and the results are presented in Table 2-21.

Table 2-21. U(VI) Retention by SRS Soil under Circumneutral Conditions as a Function of Ca^{2+} and Mg^{2+}Concentration in the Aqueous Phase

Cation concentration	% U(VI) retention by SRS soil
Ca^{2+}	
0.000025	63 ± 5
0.0001	54 ± 6
0.001	60 ± 2
0.01	45 ± 3
Mg^{2+}	
0.000015	63 ± 5
0.0001	64 ± 5
0.001	52 ± 9
0.01	50 ± 6

U(VI) retention seems to be unaffected by the presence of Ca in the range $2.5 \cdot 10^{-5}$-0.001 M, whereas at higher concentrations (0.01M), it seems to decrease slightly. Magnesium concentration does not seem to play major role in U(VI) retention for the range of concentrations studied. The experimental findings imply that calcium and magnesium may bind in different sites than the ones that uranium is bound to. Nevertheless, calcium uptake by goethite has been reported in literature, based on the following scheme $=SO\text{-}Ca^{+}$, where S stands for the solid surface and O is the oxygen atom. Goethite may constitute only a small fraction of SRS soil; nevertheless, it is very reactive towards metal cations in the solution.

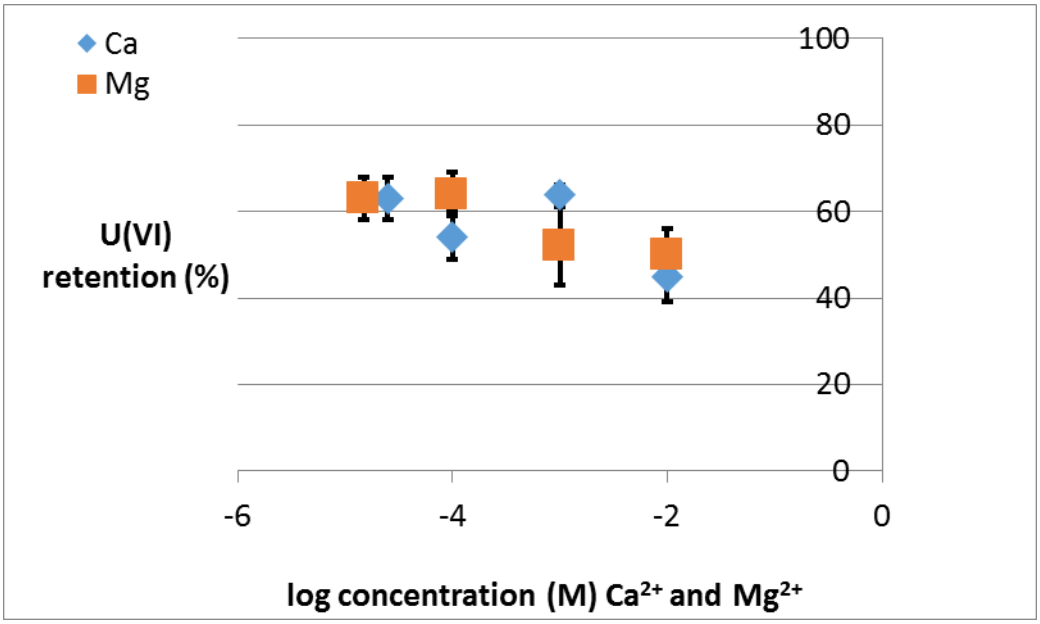

Figure 2-23. Percentage of U(VI) as a function of Ca2+ and Mg2+ concentration by SRS sediments under circumneutral conditions.

Finally, if the presence of divalent cations such as calcium and magnesium interferes with uranium sorption, this may be taking place in quite high concentrations of those metals (>0.01M), which were not in the scope of the present experimental work.

References

Dong, W., Tokunaga, T.K., Davis, J.A., Wan, J. 2012. Uranium(VI) adsorption and surface complexation modeling onto background sediments from the F-Area Savannah River Site. *Environ Sci Technol*, **46**(3), 1565-71.

Ratuzny, T., Gong, Z., Wilke, B.-M. 2008. Total concentrations and speciation of heavy metals in soils of the Shenyang Zhangshi Irrigation Area, China. *Environmental Monitoring and Assessment*, **156**(1), 171-180.

Rauret, G., F. Lopez-Sanchez, J., Sahuquillo, A., Rubio, R., Davidson, C., Ure, A., Quevauviller, P. 1999. Improvement of the BCR three step sequential extraction procedure prior to the certification of new sediment and soil reference materials. *Journal of Environmental Monitoring*, **1**(1), 57-61.

Tessier, A., Campbell, P.G.C., Bisson, M. 1979. Sequential extraction procedure for the speciation of particulate trace metals *Analytical Chemistry* **51**(7), 844-851.

Ure, A.M., Quevauviller, P., Muntau, H., Griepink, B. 1993. Speciation of Heavy Metals in Soils and Sediments. An Account of the Improvement and Harmonization of Extraction Techniques Undertaken Under the Auspices of the BCR of the Commission of the European Communities. *International Journal of Environmental Analytical Chemistry*, **51**(1-4), 135-151.

Zimmerman, A.J., Weindorf, D.C. 2010. Heavy Metal and Trace Metal Analysis in Soil by Sequential Extraction: A Review of Procedures. *International Journal of Analytical Chemistry*, **2010**.

Subtask 2.2. Monitoring of U(VI) Bioreduction after ARCADIS Demonstration at F-Area

This task is finished. FIU is working on a draft summary of the results on the application of this technology for the SRS environmental conditions.

Subtask 2.3: Sorption Properties of Humate Injected into the Subsurface System

FIU worked on the data analysis for the results on the effect of pH on Huma-K sorption onto SRS sediments. The results were compared with the literature data. FIU also started an experiment to study the removal percentage of different concentrations of Huma-K at pH 4 in soil-free samples. In the set-up, a fresh Huma-K stock solution of 1000 mg L^{-1} was prepared by dissolving 1000 mg of Huma-K in 1 L of deionized. Also, fresh stock solutions of 0.1M of HCl and NaOH were prepared for the pH adjustment.

FIU initiated the soil-free equilibrium study experiment using Huma-K concentrations ranging between 10 and 500 mg L^{-1} at pH 4. The equilibrium experiments were conducted for a period of five days. The purpose of this experiment was to subtract the amount of Huma-K precipitated at pH 4 without the contribution of SRS soil from the total removal of Huma-K + SRS soil to calculate the amount of Huma-K sorbed onto SRS soil.

For the experiment, Huma-K concentrations ranging between 10 and 500 mg L^{-1} were pipetted in centrifuge tubes and DI water was added up to a total volume of 19 mL to leave 1 mL of volume for the pH adjustment. The pH was adjusted to 4 for all the samples by using either 0.1 M HCL or 0.1 M NaOH. DI water was added to end up with a final volume of 20 mL in each tube. All the samples were vortex mixed and placed in a shaker table at 100 RPM for five days. After the equilibration time, samples were centrifuged at 2700 RPM. Then, the supernatant was analyzed using a Thermo Scientific Genesys 10S UV-Vis spectrophotometer at 254nm. The analysis involved transferring 3 mL of a liquid sample to a quartz cuvette and placing the quartz cuvette in the spectrophotometer to measure the concentration of Huma-K solution that was not precipitated after the solution equilibration at pH 4. All samples were done in triplicate.

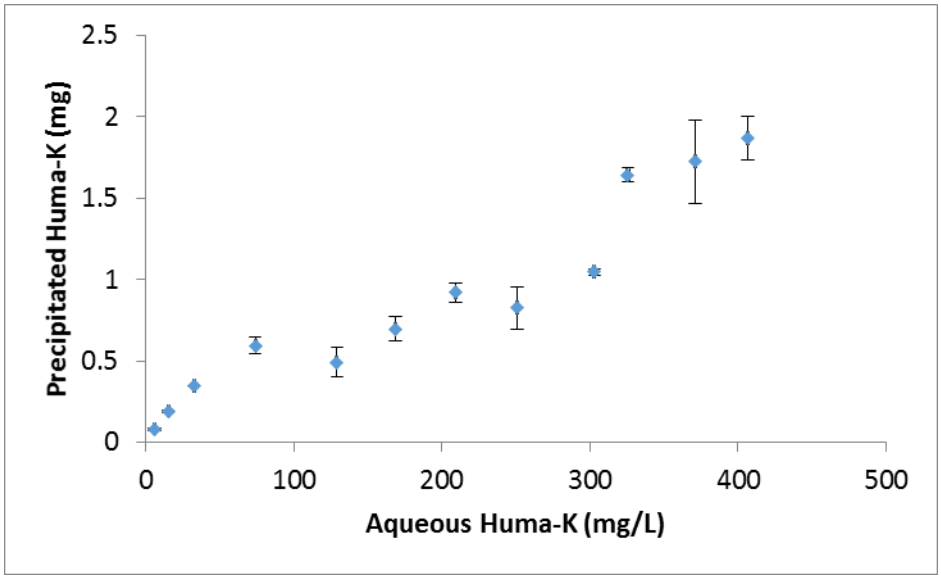

Figure 2-24. Precipitation of Huma-K at pH 4.

The results show that the precipitation of Huma-K at pH 4 increases with the concentration. It can be explained by the protonation of the functional groups in Huma-K such as carboxyl and phenol groups making possible agglomeration of humic molecules through hydrophobic interactions.

DOE Fellow, Hansell Gonzalez, started a 10-week internship at Savannah River Site under the mentorship of Dr. Miles Denham. The objective of the internship is to study the removal of metals with oxidation state (+1, +2, and +3) such as silver (Ag^{+}), zinc (Zn^{2+}), and cerium (Ce^{3+}) using sediments that were previously coated with Huma-K. The experiments are being performed at two different pH values: 4.5 and 6.5. The purpose of doing the experiments at pH 6.5 is to test if soil amended with Huma-K can be used for the removal of metals at conditions different from acidic environments. Hansell completed all required safety training to be able to work in the lab and conducted a literature review to have a better understanding of the experimental design. He also prepared the Job Hazard Analysis form which summarizes all the steps that are going to be performed during the experiment, the possible hazards of the experiments, and the required safety protection procedures.

Experiments to study the removal of Ag, Zn, and Ce, using sediments amended with Huma-K at pH 4.5 and 6.5 will be initiated next. Experiments for the removal of metals will also be initiated with an isotherm experiment to determine how much Huma-K is sorbed to the sediments. Once the amount it takes to reach the saturation point is determined, that concentration will be used to study the removal of the three metals.

Subtask 2.4. The Synergistic Effect of HA and Si on the Removal of U(VI)

FIU submitted a progress report summarizing accomplishments under this task in April. Preparation of samples for analysis via KPA and ICP to measure the concentration of uranium and silica were continued. Samples for the pH 3 and pH 4 batches were centrifuged at 2700 rpm for 30 minutes to allow the separation of the solids from the solution. After being centrifuged, the filtered samples were diluted using 1% HNO_3 by a dilution factor of 10, filtered using a 0.45 μm syringe filter, and 4 mL were placed in each KPA vial. The unfiltered samples were diluted

using 1% HNO_3 by a dilution factor of 10 and 4 mL were placed in another KPA vial. Each filtered and unfiltered sample was then prepared for analysis via KPA to measure the concentration of uranium. The data for the ICP analysis is in progress and will be used to determine the concentration of suspended colloidal silica. The KPA analysis data for the pH 3 and pH 4 samples was collected and recorded; data analysis is in progress.

FIU continued the synergy experiments with sets of triplicate batch samples with pH 5 and 6, prepared with 30 ppm of humic acid (HA), 3.5 mM of silica (Si), 400 mg of sediment and 0.5 ppm uranium. Uranium was added prior to the pH adjustment and care was taken when adding deionized water to allow for addition of acid/base so the final volume was approximately 20 ml. The pH of the samples was adjusted with a stock solution of 0.01M HCl and 0.1M NaOH to pH 5 and 6, measured and readjusted daily if there was as a change in pH, and placed on a platform shaker at the end of each daily pH adjustment. The following tables display the total volume of constituents, acid and base and final pH values at the end of each day for the samples. The samples will be centrifuged at 2700 rpm for 30 minutes to allow the separation of the solids from the solution and diluted with and without filtration for final analysis.

Table 2-22. Sample Matrix of pH 5 Batch Samples

pH 5 Adjusted Set		Constituents							
		SiO2	Humic Acid (HA)	Sediments	Uranium, U (VI)	Volume of acid/ base	DIW, H2O	pH	
		mL	mL	mg	mL	mL	mL	Initial	Final
Batch No. 2	2.1	2.1	6	0	0.01	0.235	11.25	4.35	5.04
	2.2					0.072	11.25	4.26	5.07
	2.3					0.045	11.25	4.52	5.13
Batch No. 3	3.1	0	6	0	0.01	0.075	13.25	4.66	5.11
	3.2					0.053	13.25	4.7	5.05
	3.3					0.06	13.25	5.18	5.12
Batch No. 5	5.1	2.1	6	400	0.01	0.066	11.25	3.8	5.04
	5.2					0.125	11.25	4.06	5.07
	5.3					0.045	11.25	4.54	5.1
Batch No. 6	6.1	0	6	400	0.01	0.22	13.25	4.04	5.08
	6.2					0.33	13.25	3.91	5.15
	6.3					0.13	13.25	4.03	5.21

Table 2-23. Daily pH Adjustments of Samples

Sample #		pH						
		Day 1	Day 2	Day 3	Day 4	Day 5	Day 6	Day 7
Batch No. 2	2.1	4.97	4.97	4.99	4.91	5.07	5.04	5.04
	2.2	4.91	5.07	4.99	5.03	5.08	5.07	5.07
	2.3	4.94	5.01	5.06	5.03	5.09	5.13	5.13
Batch No. 3	3.1	5.24	5.05	5.05	5.10	5.04	5.11	5.11
	3.2	4.98	5.01	4.99	5.04	4.97	5.05	5.05
	3.3	5.18	5.05	5.09	4.99	5.02	5.12	5.12
Batch No. 5	5.1	4.98	5.04	4.88	4.93	4.99	5.07	5.04
	5.2	5.36	5.01	5.00	5.05	5.07	5.11	5.07
	5.3	4.94	4.99	5.03	5.04	5.08	5.02	5.10
Batch No. 6	6.1	5.11	5.11	4.98	5.02	5.06	4.99	5.08
	6.2	5.16	5.10	5.09	4.86	5.01	5.05	5.15
	6.3	5.66	5.00	5.10	4.95	5.09	5.06	5.21

Table 2-24. Sample Matrix for pH 6 Batch Samples

pH 6 Adjusted Set		Constituents							
		SiO2	Humic Acid (HA)	Sediments	Uranium, U (VI)	Volume of acid/ base	DIW, H2O	pH	
		ml	ml	mg	ml	ml	ml	Initial	Final
Batch No. 2	2.1	2.1	6	0	0.01	0.185	11.25	4.01	6.03
	2.2					0.115	11.25	4.64	6.04
	2.3					0.197	11.25	4.65	6.02
Batch No. 3	3.1	0	6	0	0.01	0.142	13.25	4.12	5.95
	3.2					0.240	13.25	4.53	6.05
	3.3					0.105	13.25	4.53	6.03
Batch No. 5	5.1	2.1	6	400	0.01	0.059	11.25	4.77	6.00
	5.2					0.069	11.25	4.73	6.04
	5.3					0.079	11.25	4.70	6.03
Batch No. 6	6.1	0	6	400	0.01	0.272	13.25	4.04	6.04
	6.2					0.242	13.25	4.12	6.01
	6.3					0.139	13.25	3.73	6.05

Table 2-25. Daily pH Adjustments of Samples

Sample #		pH						
		Day 1	Day 2	Day 3	Day 4	Day 5	Day 6	Day 7
Batch No. 2	2.1	6.20	6.07	5.96	6.09	6.08	6.02	6.03
	2.2	5.97	6.06	5.94	6.06	6.06	6.05	6.04
	2.3	5.92	6.09	5.97	6.03	6.03	6.01	6.02
Batch No. 3	3.1	5.98	6.03	6.01	5.93	5.96	6.04	5.95
	3.2	6.05	6.09	6.03	6.07	6.06	6.02	6.05
	3.3	6.02	6.09	6.10	5.98	5.99	6.00	6.03
Batch No. 5	5.1	6.07	6.04	5.90	5.90	6.01	6.01	6.00
	5.2	6.00	6.00	6.05	6.01	6.03	6.00	6.04
	5.3	5.92	6.05	6.07	6.07	6.08	6.04	6.03
Batch No. 6	6.1	6.02	6.05	6.085	6.01	6.09	6.03	6.04
	6.2	6.07	6.01	6.00	6.05	6.06	6.02	6.01
	6.3	5.99	6.03	5.99	6.00	6.08	6.06	6.05

Subtask 2.5. Investigation of the Migration and Distribution of Natural Organic Matter Injected into Subsurface Systems

The work completed for this task will assemble, integrate, and develop a practical and implementable approach to quantify and simulate potential natural organic matter (NOM, such as humic and fulvic acids, humate, etc.) deployment scenarios over the range of conditions at DOE sites. Initial laboratory experiments and an initial set of simplified models have been developed at SRNL. Under this task, additional batch and column studies and testing will be conducted at FIU to provide the transport parameters for an extension of the current model scenarios. The following was accomplished during this reporting period:

- DOE Fellows Sarah Bird and Alexis Smoot who have been supporting this task are participating in a 10-week summer 2016 internship at DOE-HQ under the mentorship of Carol Eddy-Dilek and Skip Chamberlain.
- Total organic carbon (TOC) analysis on sediments from previous experiments was completed. Data was received from the TOC analysis for the columns previously exposed to Huma-K and the average carbon percentage was found to be 0.03 and 0.02 for columns with pH 3.5 and 5.0, respectively.
- Preparations (such as calibrating sensors, pump etc.) were completed in order to run additional column experiments. The pumps were tested in order to initiate column experiments with 0.5 pore volumes (PV) Huma-K sorption/desorption followed by uranium injection to study the effect of sorbed Huma-K on uranium mobility.
- The column experiments are being carried out in FIU-ARC's Soil & Groundwater Laboratory. Since this work includes the use of uranium, a proposal was prepared and submitted to FIU's Radiation Committee for approval.

- Soil samples were dried in order to fill the column. Packing the columns was completed.
- The bromide electrode was refurbished for use during this experiment to conduct tracer tests. An issue with the bromide sensor was discovered while attempting to run the tracer tests. The issue has been resolved and the tests were completed.
- An artificial groundwater (AGW) solution with pH 3.5 was injected into the column to saturate the column. The pH of the column reached 3.55 after approximately 1.5 L of AGW solution.
- A 10,000 ppm humic acid solution with pH 9.0 was injected into the column. Effluent samples were collected at regular intervals and the pH and concentration of humic acid were measured immediately.
- An AGW solution with pH 3.5 was injected until the concentration of humic acid reached 2% of the initial concentration. A 100 ppb uranium solution with pH 3.5 was then injected into the column to study the mobility of uranium through the humate-sorbed sediment.
- A series of AGW solutions that were pH adjusted to 3.5, 4.5 and 5.5 were injected into the column to observe uranium and humic acid release from the sediment.
- A progress report on the results obtained based on the experiment was drafted and submitted to DOE HQ and SRS contacts on June 30, 2016.

Task 3: Surface Water Modeling of Tims Branch

Task 3 Overview

This task will perform modeling of surface water, and solute/sediment transport specifically for mercury and tin in Tims Branch at the Savannah River Site (SRS). This site has been impacted by 60 years of anthropogenic events associated with discharges from process and laboratory facilities. Tims Branch provides a unique opportunity to study complex systems science in a full-scale ecosystem that has experienced controlled step changes in boundary conditions. The task effort includes developing and testing a full ecosystem model for a relatively well defined system in which all of the local mercury inputs were effectively eliminated via two remediation actions (2000 and 2007). Further, discharge of inorganic tin (as small micro-particles and nanoparticles) was initiated in 2007 as a step function with high quality records on the quantity and timing of the release. The principal objectives are to apply geographical information systems and stream/ecosystem modeling tools to the Tims Branch system to examine the response of the system to historical discharges and environmental management remediation actions.

Task 3 Quarterly Progress

Subtask 3.1. Modeling of Surface Water and Sediment Transport in the Tims Branch Ecosystem

- Milestone 2015-P2-M3 was completed and submitted by the due date of April 29, 2016. This involved completing the input of the MIKE SHE model configuration parameters for simulation of unsaturated flow. An email was sent to SRNL and DOE HQ personnel to mark the completion of this milestone and a brief update was provided on the progress of

the model development. The following provides the accomplishments in setting up the unsaturated zone module:

- The UZ module was developed using two methods: Two Layer Unsaturated Zone (Figures 2-25 to 2-28) and Richards Equation (Figures 2-29 & 2-30).
- Richards equation is set to be used for the preliminary simulation setup.

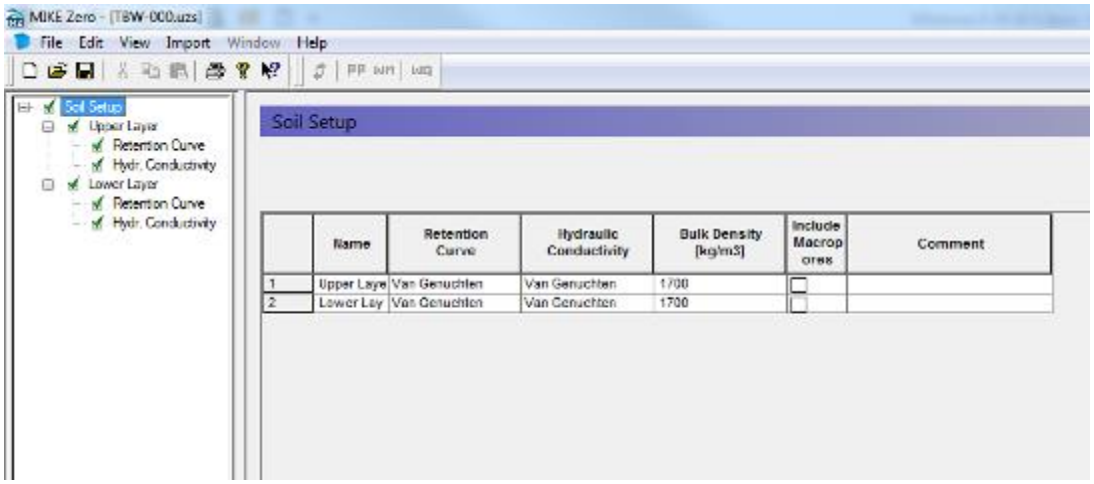

Figure 2-25. Two Layer UZ setup in MIKE SHE. For each layer, retention curve and hydraulic conductivity has been defined.

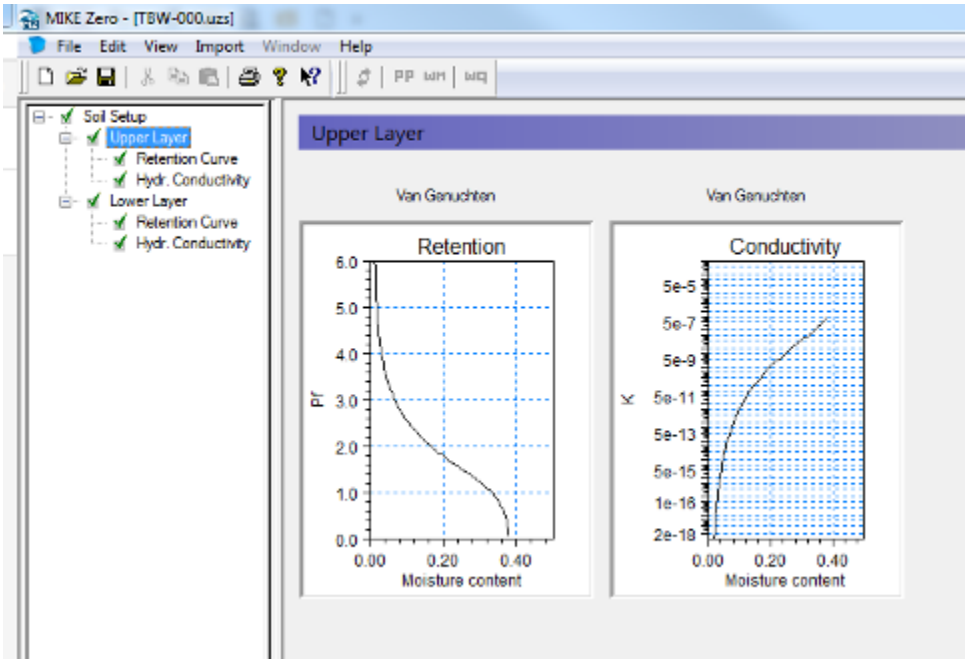

Figure 2-26. Two-Layer UZ retention curve and hydraulic conductivity. These parameters have been set up for each layer separately.

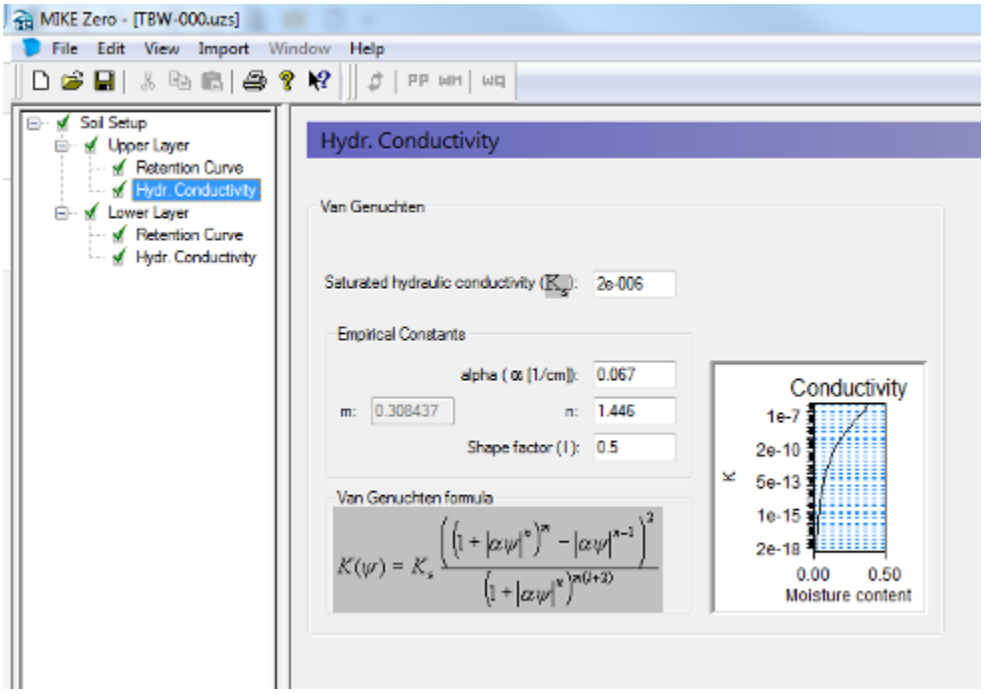

Figure 2-27. MIKE SHE default parameters for UZ module using two-layer set up.

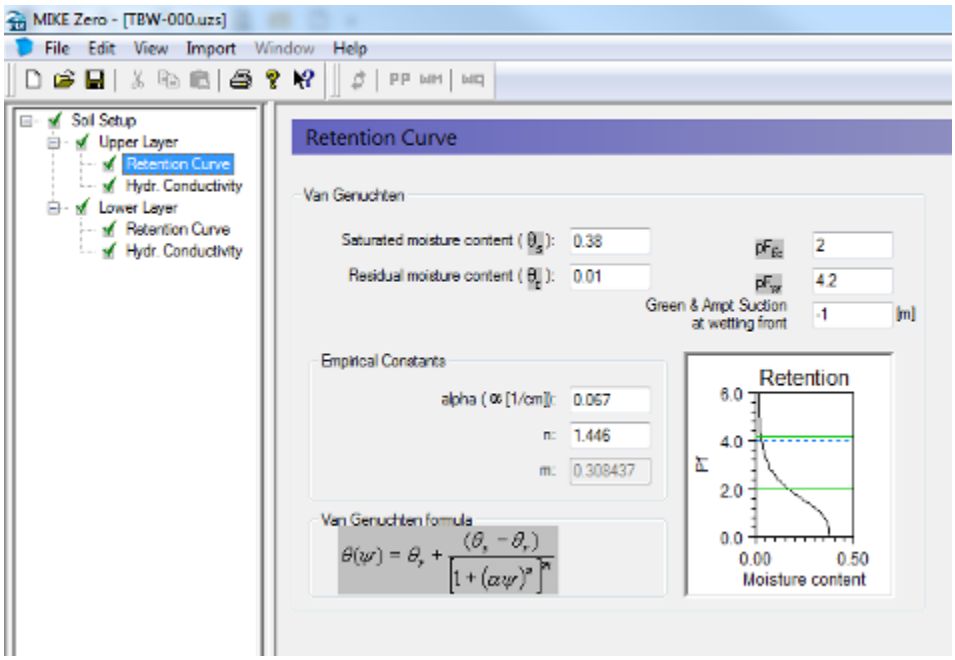

Figure 2-28. MIKE SHE default is being used for preliminary simulation in UZ set up.

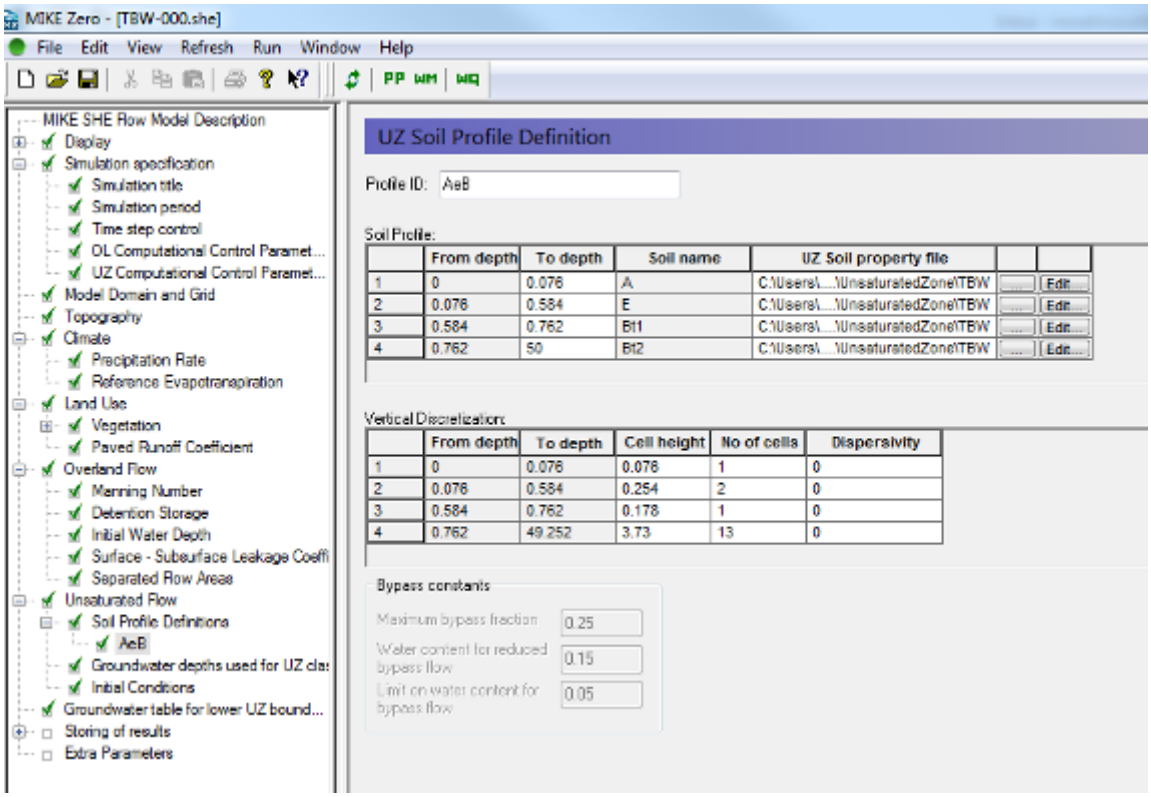

Figure 2-29. UZ set up module using Richards equation. A uniform soil type of AeB (Ailey sand, 2 to 6 percent slopes, wet substratum) has been used. This soil consists of four horizons.

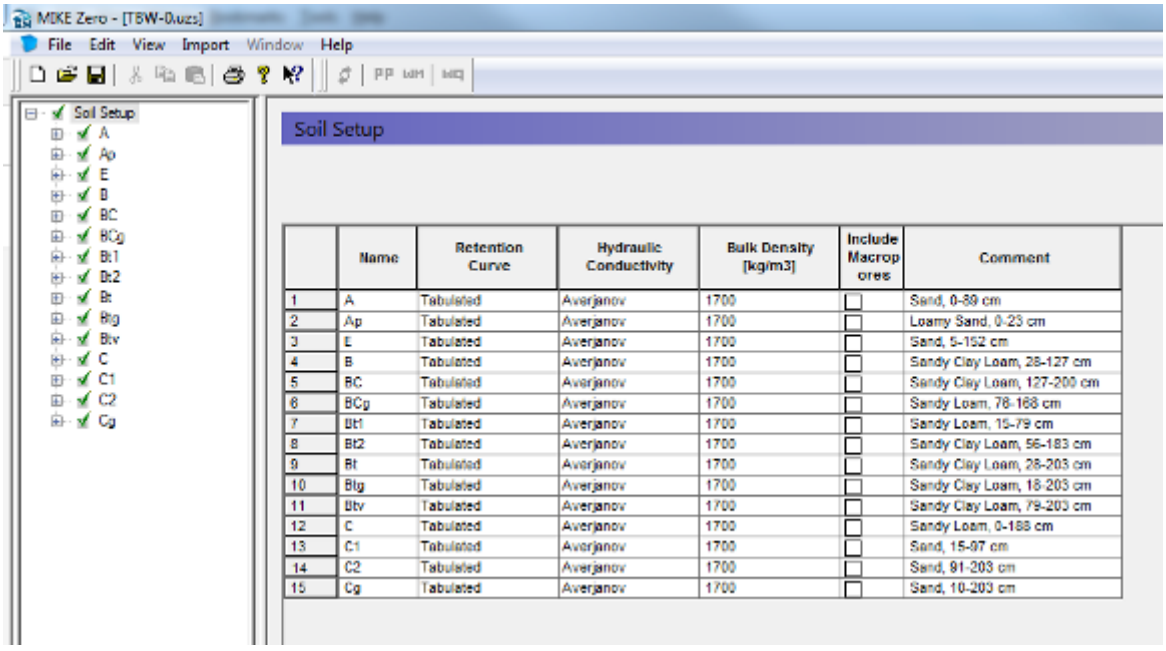

Figure 2-30. UZ file set up for soil horizons. Data was acquired from the USDA Web Soil Survey website for South Carolina.

- The spatial soil profile definition has been developed using both uniform and distributed methods. Currently, a uniform spatial distribution has been set up. Soil profile data was acquired and a report generated from the U.S. Department of Agriculture (USDA) Web Soil Survey website:

  (http://websoilsurvey.sc.egov.usda.gov/App/WebSoilSurvey.aspx).

- Each soil profile is comprised of several layers (horizons). The thickness of each layer varies from one soil type to another ranging from 0 – 80 in. Soil profiles consist of layers such as sand, sandy loam, loamy sand, and sandy clay loam. A report of the various soil profiles was created as MS Excel file.

- Vertical discretization has been defined according to soil layer thickness, and considering finer discretization closer to the ground surface and coarser discretization for deeper layers.

- In this model set up, the uniform soil profile is classified into 4 different uniform soil horizons. MIKE SHE unsaturated flow files (.uzs) for each soil horizon have been created. A total of 4 horizons were prepared. Default parameters have been used as preliminary setup for soil characterization. Vertical discretization is set to represent 8 cell layers with various heights. Table 2-26 shows details of the cell discretization.

Table 2-26. UZ Vertical Discretization (values in meters)

From depth	To depth	Cell height	No. of cells
0	0.076	0.076	1
0.076	0.584	0.254	2
0.584	0.762	0.178	1
0.762	1.762	0.2	5
1.762	2	0.238	1
2	4	1	2
4	20	2	8
20	50	3	10

- In SRS, the depth of unsaturated zone (also known as vadose zone) varies from 7 ft to 179 ft (Aadland et al., 1995; Hiergesell, 2004). In this model set up, 179 ft (~50 m) is assumed as the thickness of the unsaturated zone.

- Station-based timeseries data of groundwater table was acquired from 4 stations. Only one station was found inside the SRS boundary. Other remaining stations are within the neighboring counties (Aiken and Barnwell). Groundwater head timeseries data has been processed and converted to the format accepted by the MIKE SHE model.

- Uniform groundwater table depth is also being tested as an additional option for UZ set up.

- A progress report for modeling of surface water and sediment transport in the Tims Branch ecosystem was submitted on June 28, 2016 to relevant DOE HQ and SRS/SRNL

collaborators. This deliverable was reforecast from May 31, 2016 to June 30, 2016 to accommodate the extra time needed for the development of the report due to the leading researcher, Dr. Shimelis Setegn, taking an unexpected family leave. Dr. Reinaldo Garcia who joined the Applied Research Center on this project took over in assisting the project team in the development of this deliverable. The report describes research conducted over the past year related to the development of a surface water model of the Tims Branch watershed (TBW) at SRS and the extensive pre-processing that was carried out to prepare the data for input into the model. Efforts during 2015-2016 have been focused on revision of the preliminary model developed in 2014 to incorporate a study area that encompasses the full extent of the TBW as opposed to just the portion of the watershed lying within the SRS boundary, which was initially used. The report therefore builds upon the work carried out in 2014 and outlines the changes to the input configuration parameters that were required in order to incorporate the new model domain.

  - The model developed at this stage of the study is based on the MIKE SHE model that will be used as a tool to understand the dynamics of the different hydrological components of the TBW and to perform a comparative assessment of these processes using alternative models. Preliminary model development has included the simulation of overland flow, which is one of the main components of the MIKE SHE modeling system in hydrological analysis due to the fact that a significant amount of water flows as overland flow/surface runoff that joins streams and other water bodies. Knowledge of the temporal and spatial distribution of overland flow helps to understand flow as a function of climate and catchment characteristics in the land phase of the hydrological cycle.
  - Model simulations performed so far are preliminary as not all of the hydrological components have been incorporated. However, model results already provide a general understanding of the watershed response as a function of precipitation and other catchment characteristics. The developed surface water model will undergo a considerable calibration and validation process using measured streamflow/discharge data within the target watershed. The calibration of the model will refine the parameter values which will help to fully develop the integrated model for better representation of the watershed. Different statistical evaluation methods will be employed to ensure the accuracy of the calibration results. This calibration and validation exercise will help to improve the predictive capability and reliability of the model.

- This quarter FIU also began work on the input of the MIKE SHE model configuration parameters for simulation of saturated flow.
  - Preparation of the groundwater (GW) head data has included the download of GW head timeseries data from 4 nearby stations and conversion of the data to a binary file format that is readable by MIKE SHE.
  - Geologic layers have also been defined. For simplicity, both horizontal and vertical hydraulic conductivities have been applied as uniform values. The values are reported in various geologic reports online.

- FIU has also begun preliminary development of the Tims Branch stream network for the MIKE 11 model using a combination of ArcGIS and MIKE 11 tools. The following outlines the procedure used:
    - **<u>Pre-processing of MIKE 11 model configuration data using ArcGIS</u>**

      Prior to starting the model setup in MIKE 11, it was necessary to pre-process the required data using ArcGIS. In the existing stream network file, the streams were not accurately defined. The hydrology tool in ArcGIS was therefore used to define the streams as described below:

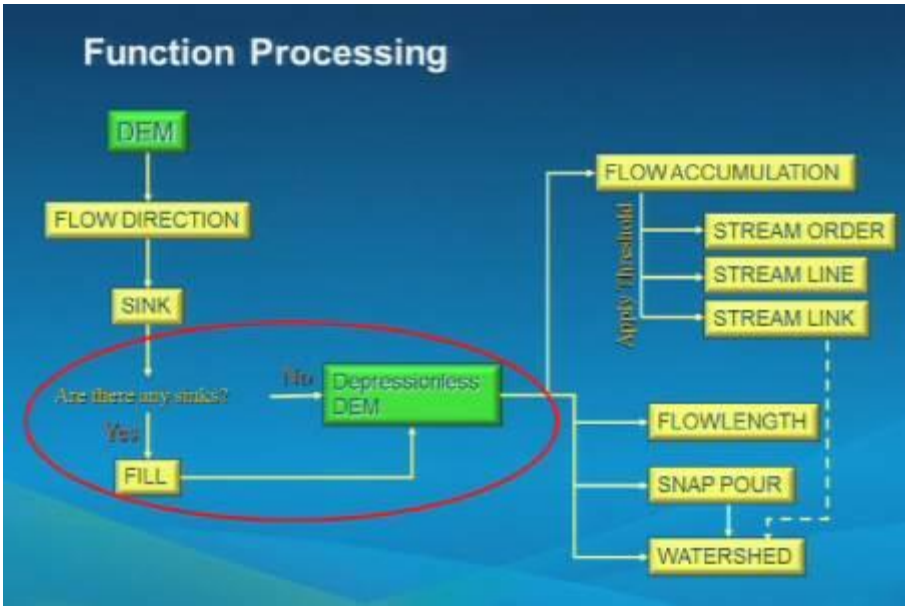

Figure 2-31. Stream/watershed delineation process in ArcGIS (Source: esri.com).

    - The Fill tool was used to fill low elevation cells that are surrounded by higher elevation cells; this avoids water being trapped.
    - The flow direction in each cell was computed. The values in the cells of the flow direction grid indicate the direction of the steepest descent from that cell.
    - The flow accumulation grid that contains the accumulated number of cells upstream of a cell was calculated for each cell in the input grid.
    - The symbology for the created flow accumulation file was selected and the number of classes changed to 2.

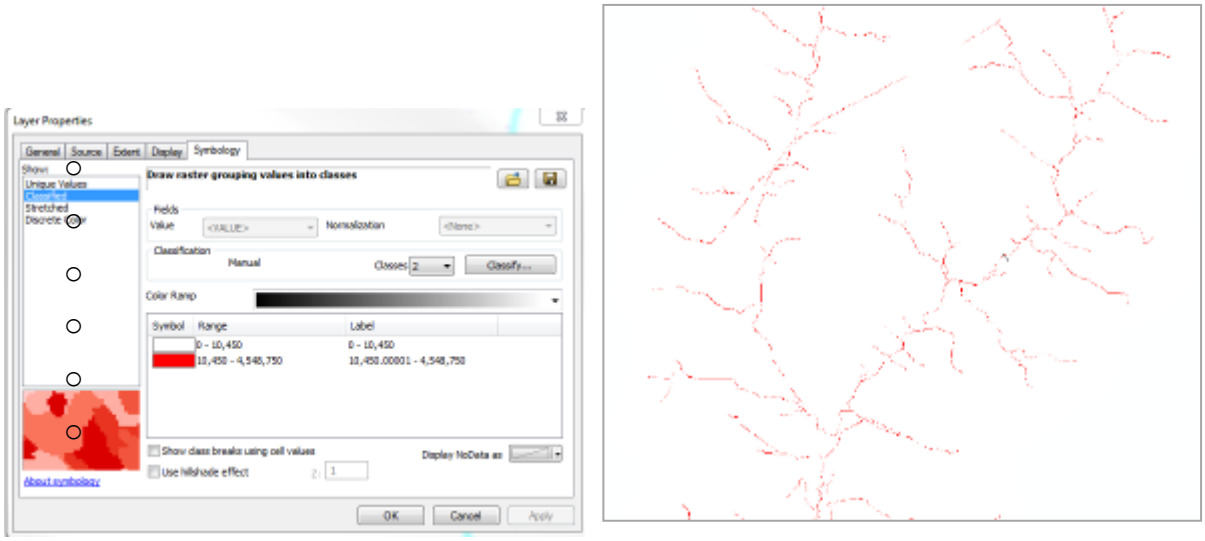

Figure 2-32. Symbol reclassification in Arc GIS for the flow accumulation.

- The Raster Calculator was used to create a raster file that has a value of 1 for any pixel >= 10450 and a value of 0 for any pixel below this value.

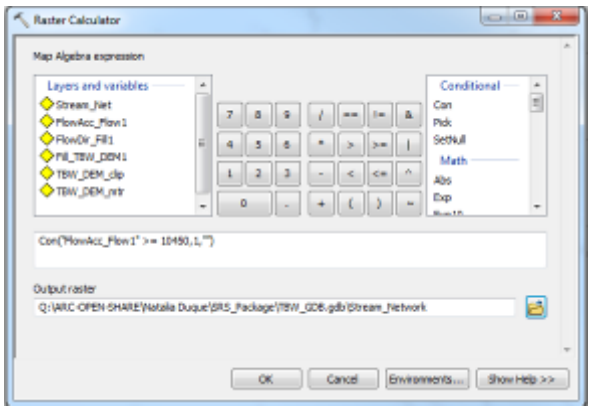

Figure 2-33. Raster calculator.

- The Raster to Polyline tool was used to convert the created file to a line shapefile.
- The resulting file contains all the streams in the network but Tims Branch is divided into small segments, so the Merge tool as used to make Tims Branch one continuous line.

- **<u>Preliminary set-up of the MIKE 11 model</u>**

  - After the data pre-processing was completed, the model setup was initiated in MIKE 11.
  - A folder was set up to contain all the model files: (TBW_Model).
  - A MIKE11 simulation file (.sim11) was then created.

- The MIKE 11 model requires a set of files that contain all the parameters necessary for the simulation, these include:
    - River Network file (.nwk11)
    - Cross Section file (.xns11)
    - Boundary file (.bnd11)
    - Hydrodynamic (HD) parameters (.hd11)

- ***River Network***
    - A River Network file (.nwk11) was created.
    - Workspace Area Coordinates were set up as described in table below.

Table 2-27. Workspace Area Coordinates

	X	Y	units
Lower Left Corner	428638	3682527	m
Upper Right Corner	439252	3697210	m

    - Map Projection: NAD_1983_UTM_Zone_17N
    - The shapefiles created using ArcGIS were imported to the River Network file as layers.

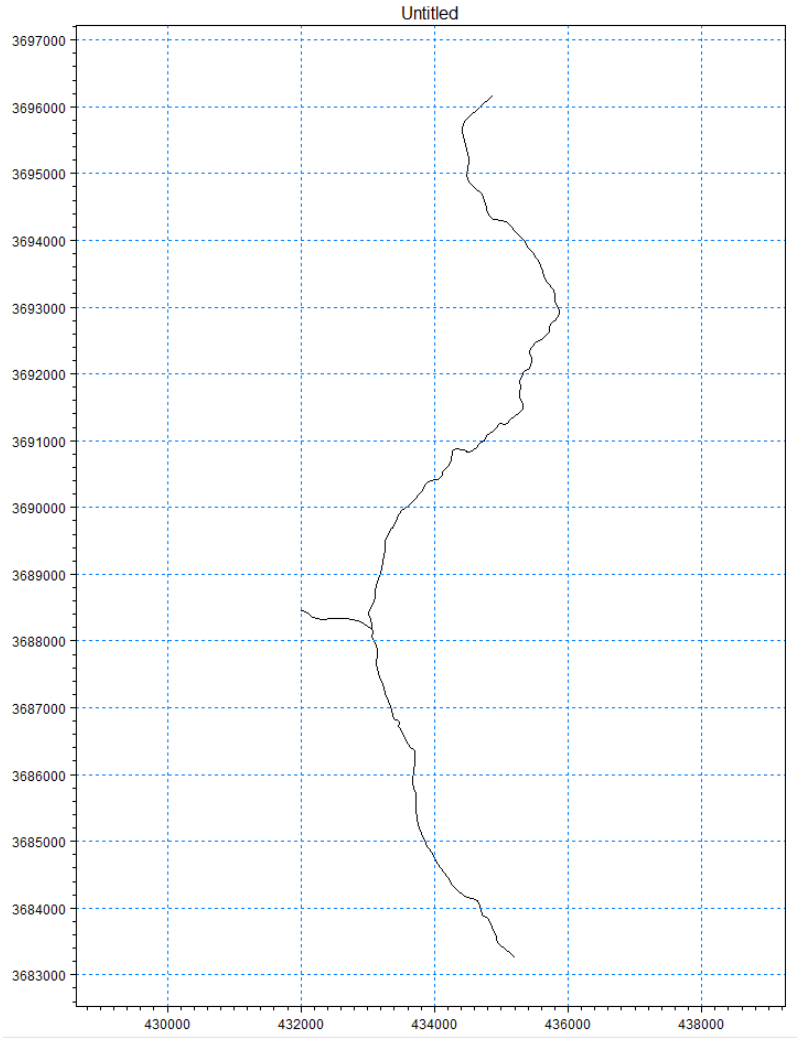

Figure 2-34. River network.

- The branches were then drawn in MIKE 11.
  - Points were created along the branches.
  - The points were then connected to define the branches.

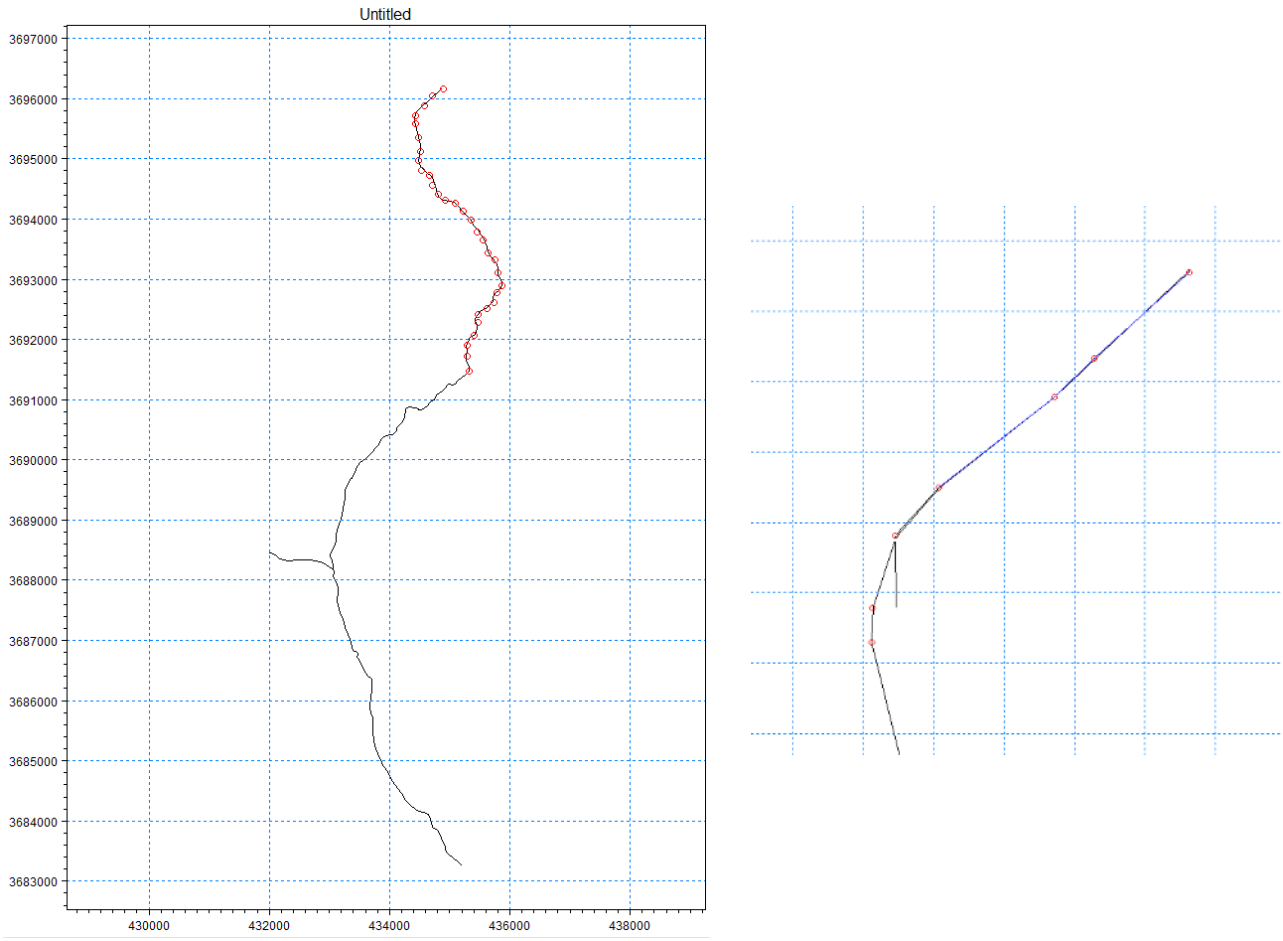

Figure 2-35. Stream branches.

- The two branches drawn were then connected.
- The network data created was then exported as a GIS shapefile.

- ***Cross-Sections***
  - A new cross-section file (.xns11) was created.
  - A cross-section was created at the beginning and end points of Tims Branch.
    - Parameters were set up as seen in tables below:

Table 2-28. MIKE 11 Cross-Section File Input Parameters

Parameters	
Transversal distribution	Uniform
Resistance type	Manning's M
Uniform value	25

Table 2-29. TB0

	X	Z	Resist.	Mark
1	0.000	140.000	25.000	1
2	30.000	130.000	25.000	2
3	70.000	130.000	25.000	
4	100.000	140.000	25.000	3

Table 2-30. TB1

	X	Z	Resist.	Mark
1	0.000	45.000	25.000	1
2	30.000	35.000	25.000	2
3	70.000	35.000	25.000	
4	100.000	45.000	25.000	3

- Interpolated cross-sections were then inserted every 1000 meters.

- ***Cross-sections from Digital Elevation Model (DEM)***
  - Using ArcGIS, the existing DEM of South Carolina seen below was converted to an ASCII file.

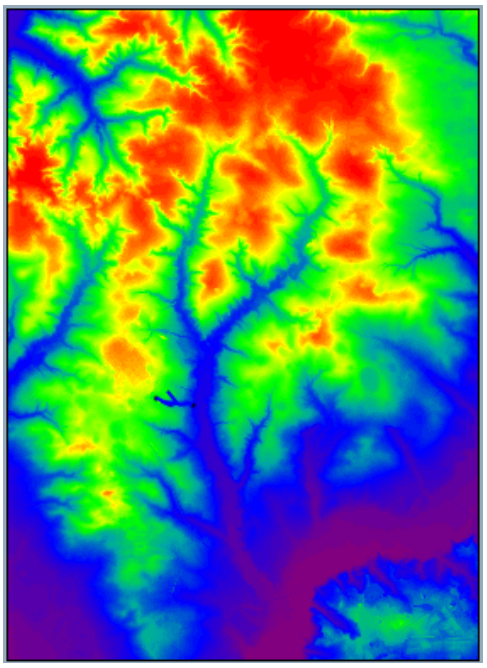

Figure 2-36. Existing DEM of South Carolina.

  - The MIKE Zero Toolbox was then used to convert the ASCII file to a dfs2 file, which is readable in MIKE SHE and MIKE 11.
  - In order to create a cross-section from the dfs2 grid file, a MIKE HYDRO file (.mhydro) was created.
  - The model type was then set up as 'River' and coordinate system was specified.

- The Stream Network shapefile was then imported into MIKE HYDRO.
- In MIKE HYDRO, the DEM and the cross-section file were then specified.
- With the tool 'Auto generate cross-sections', cross-sections were generated every 1000 meters along Tims Branch and every 200 meters along the Outfall A014 Branch. The cross-sections were each 100 meters wide.

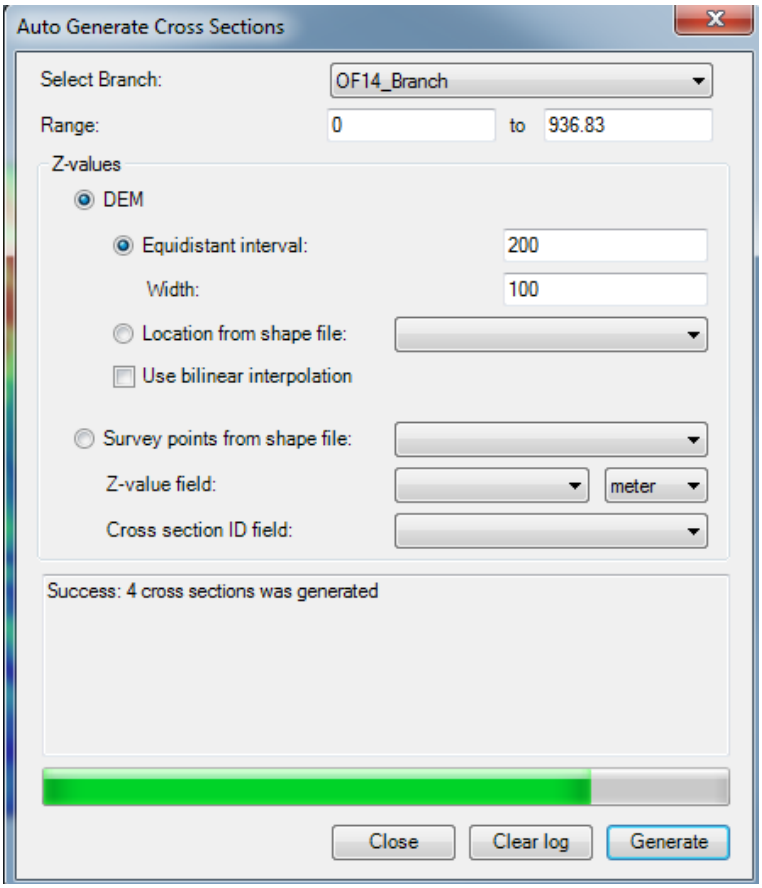

Figure 2-37. Auto generate cross sections tool.

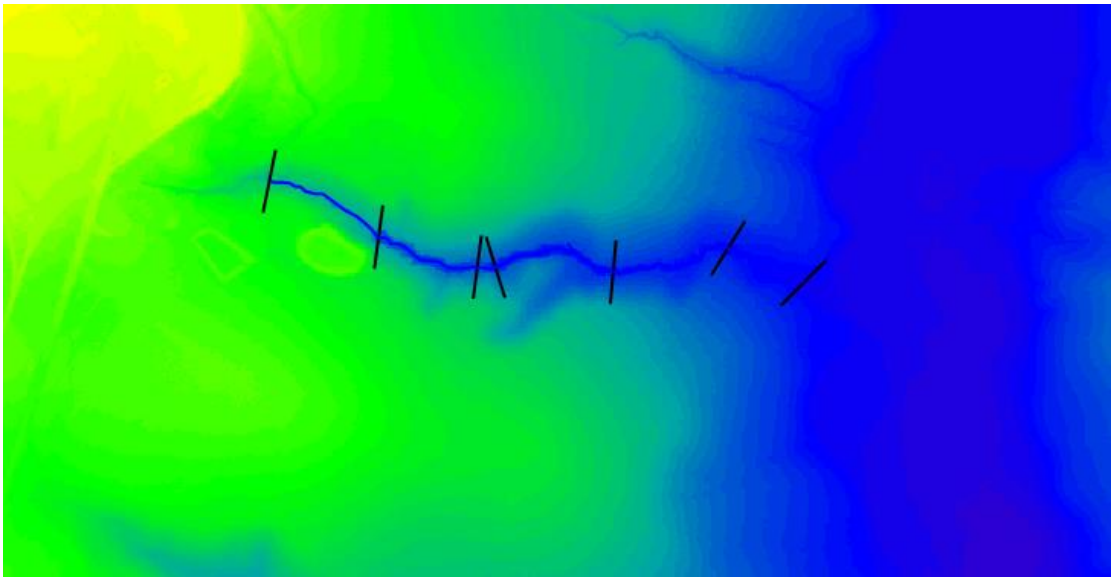

Figure 2-38. Cross-sections generated from DEM.

- The cross-sections appear as seen below when the cross-section file is opened in MIKE Zero:

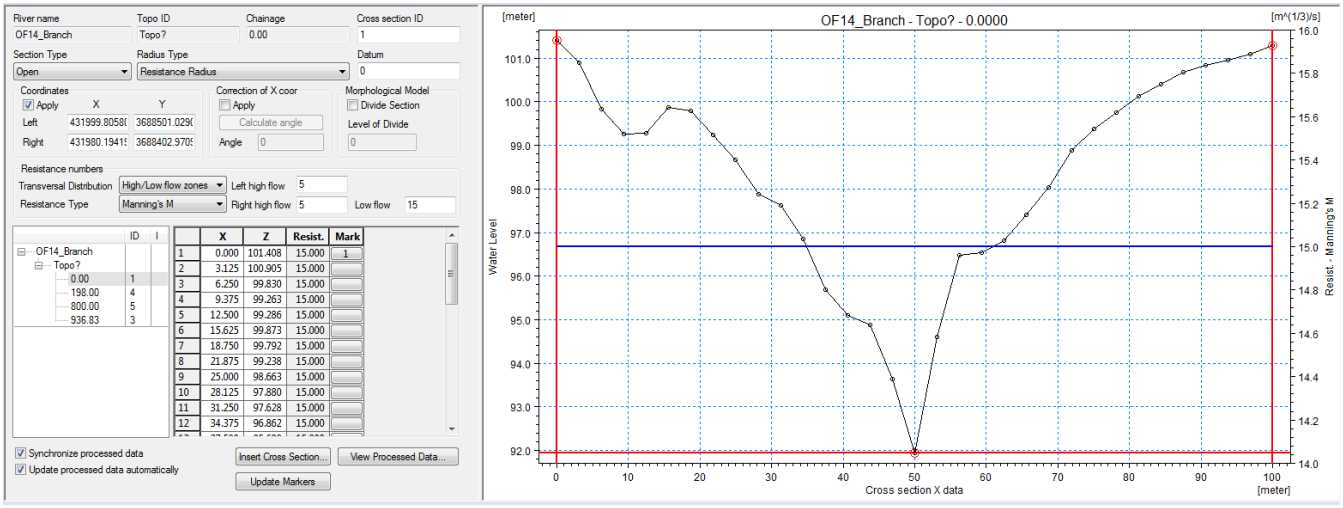

Figure 2-39. Cross section details and profile graph viewed in MIKE Zero.

- For all the cross-sections, the following parameters were entered:

Table 2-31. Cross-Section Input Parameters

Parameters	
Transversal distribution	High/Low flow zones
Resistance type	Manning's M
Left high flow	5
Right high flow	5
Low flow	15

- Markers 1, 2, and 3 were relocated to mark highest left point (1), lowest point (2), and highest right point (3).

- ***Boundary Conditions***
  - A new Boundary file (.bnd11) was created.
  - On the map view of the River Network file, a hydrodynamic boundary was created by right clicking at each of the unconnected end points.

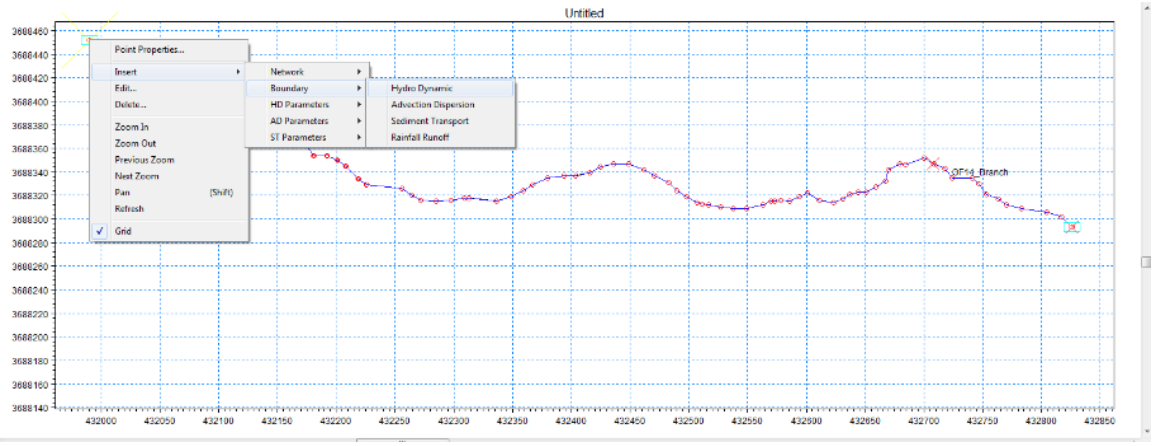

Figure 2-40. Setting boundary conditions.

  - A timeseries file containing water level depths to input as boundary condition was created:
    - A new dfs0 file was created.
    - Parameters were then specified as follows:

Table 2-32. Timeseries (dfs0) Input Parameters for Water Level Depths

Parameters	
Start time	1/1/2008
Time step	1 hour
Item name	Stage at OF0
Item type	Water Level
Item Unit	meter

    - The previously obtained water level data was then copied into the timeseries file.
  - In the Boundary file, parameters were specified for each of the created boundaries as Boundary Description "Open" and Boundary Type "Water Level" (seen in table below). The corresponding timeseries file was then inserted.

Table 2-33. Boundary Parameters

OF14.bnd11

	Boundary Description	Boundary Type	Branch Name	Chainage	Chainage	Gate ID	Boundary ID
1	Open	Water Level	OF14_Branc	0	0		
2	Open	Water Level	OF14_Branc	936.82	0		

- ***Hydrodynamic Conditions***
  - A new hydrodynamic file (.hd11) was created and specified in the MIKE 11 simulation file.
  - The global water level was set at 72 meters.

- ***Other Simulation Parameters***
  - In the MIKE 11 simulation file, the parameters were set as follows:

Table 2-34. MIKE 11 Simulation Parameters

Parameters	
Time step	1 day
Start date	1/1/2014
End date	1/1/2015
HD initial conditions	Steady State

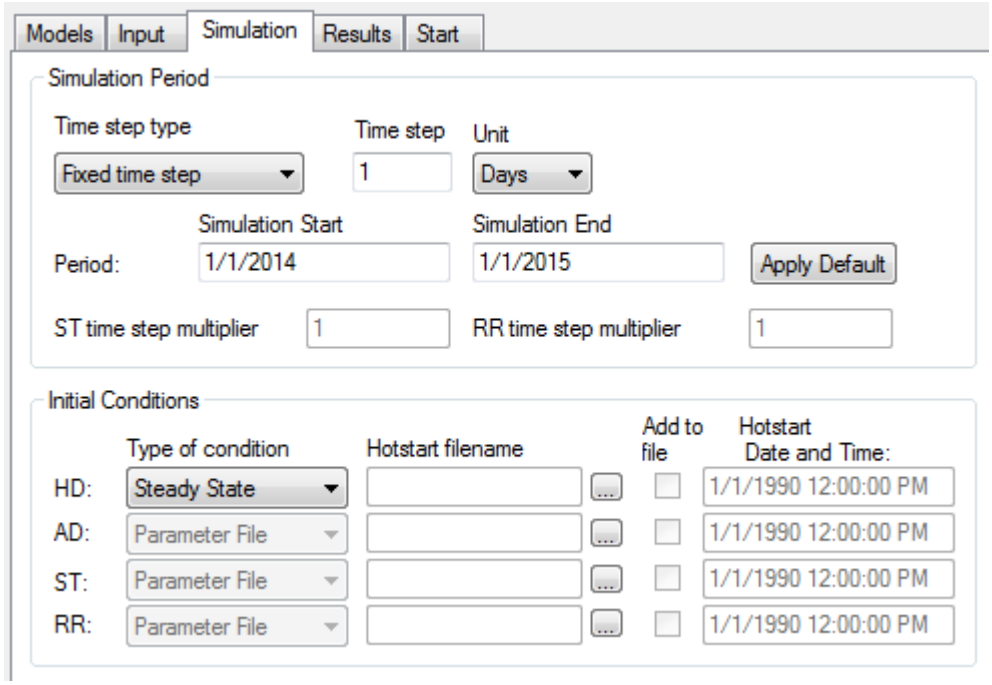

Figure 2-41. Setting MIKE 11 simulation parameters.

MIKE 11 Simulation Results

A preliminary simulation of the Outfall A014 Branch was conducted since this branch is of special interest in this research. The results are as follows:

- Network Setup

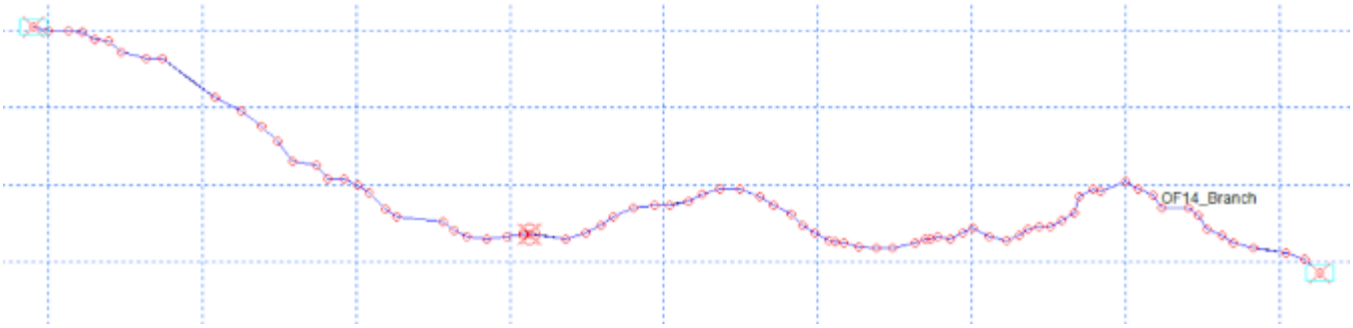

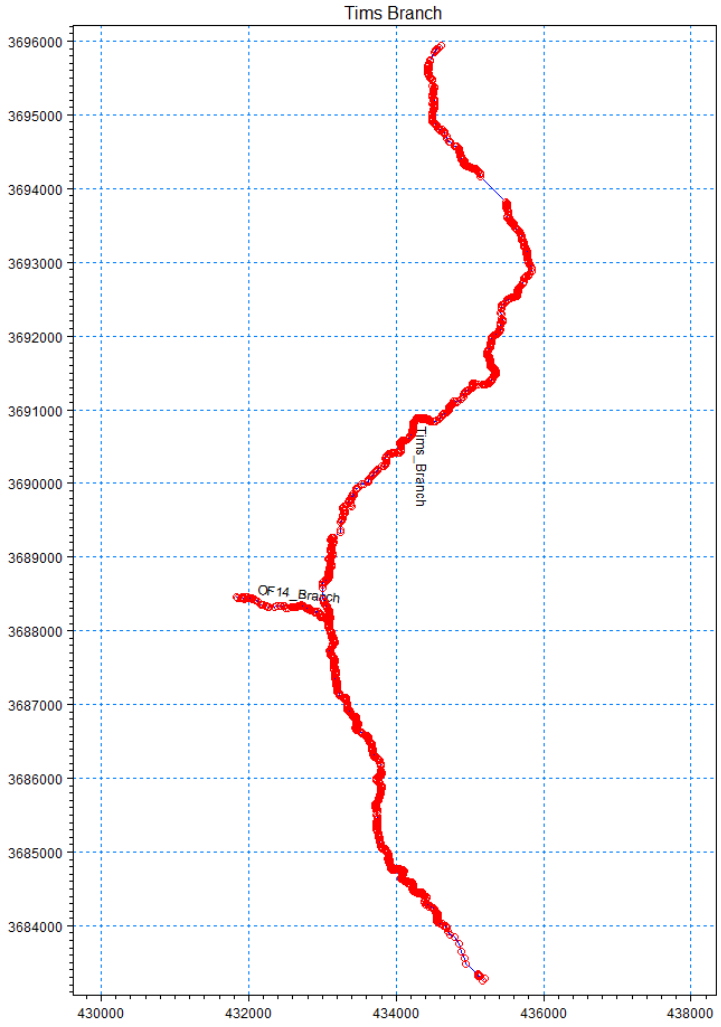

Figure 2-42. Network setup.

- Water Level Animation at Different Times

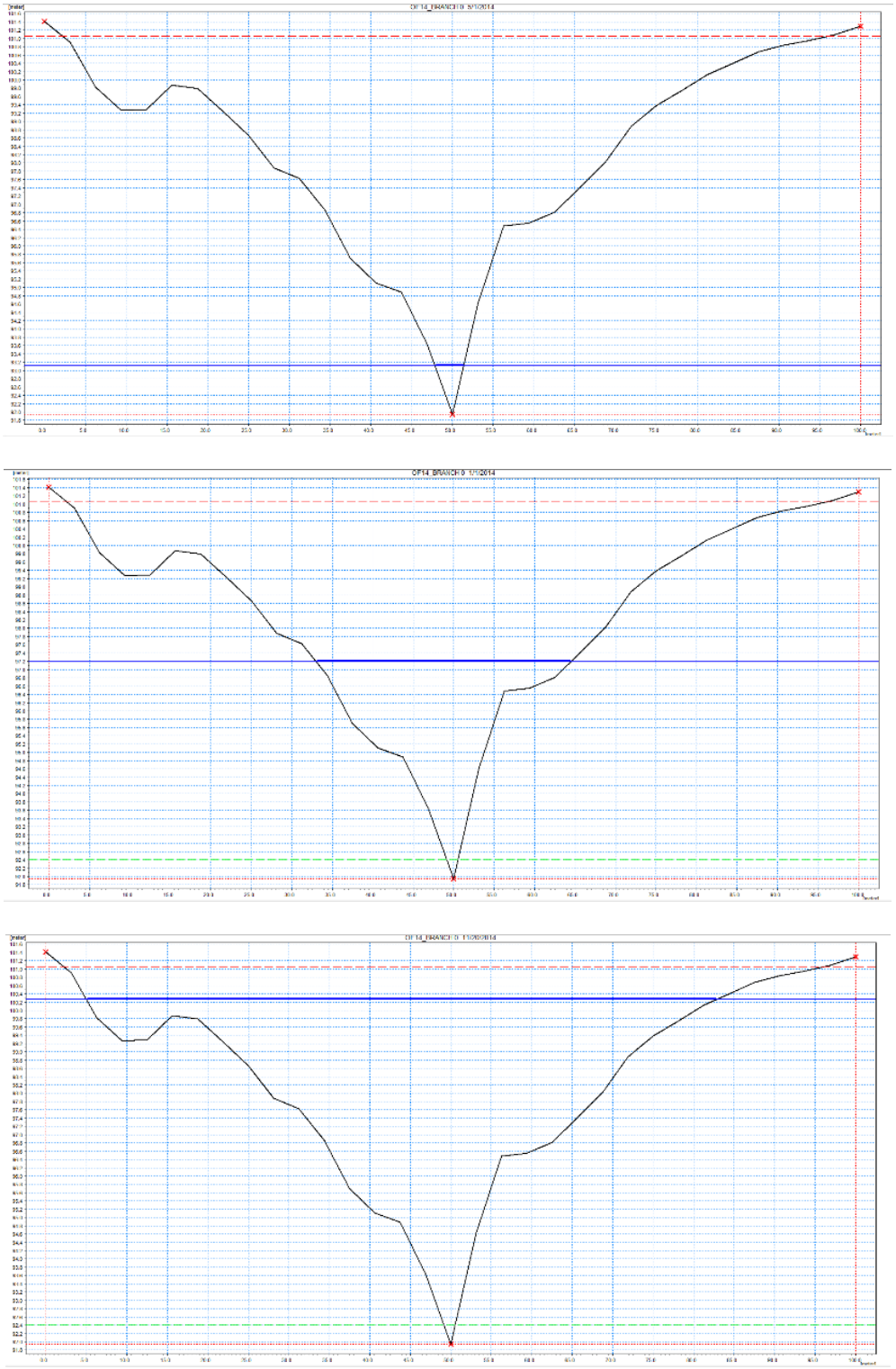

Figure 2-43. Water level animation.

- Average water level across Outfall A014 Branch

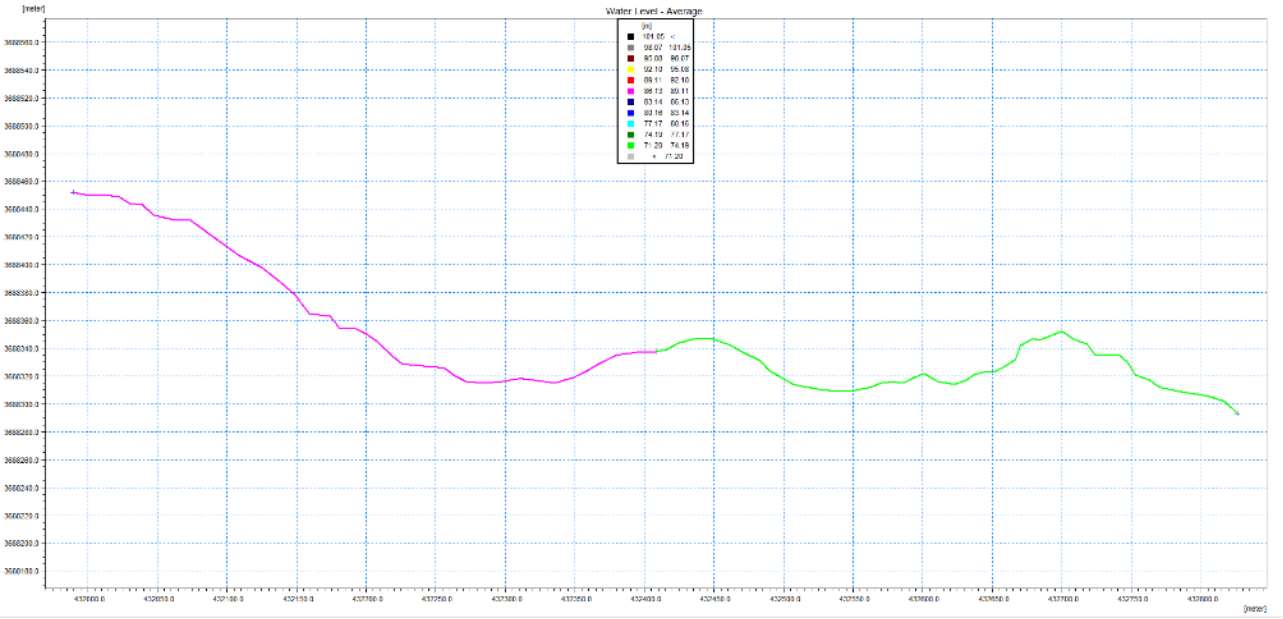

Figure 2-44. Average water level across Outfall A014 branch.

- Water level profile at the beginning of simulation

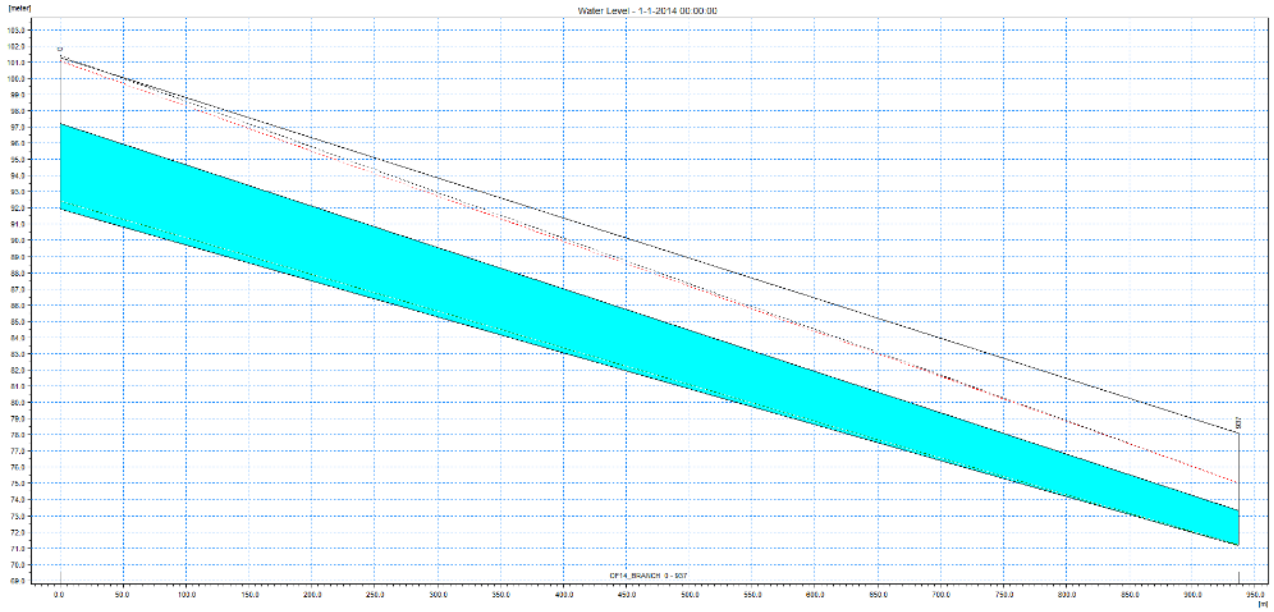

Figure 2-45. Water level profile at beginning of simulation.

- Water level time series at start and end points of branch

Figure 2-46. Water level time series at stand and end points of branch.

- Water volume balance summary

Table 2-35. Volume Balance Summary

A: Initial volume in model area					**42910.16**	**m^3**
B: Final volume in model area					**87650.62**	**m^3**
Lateral sources inflow	0.00	m^3				
Lateral correction	0.00	m^3				
Open boundaries inflow	19879803833.39	m^3				
C: Total inflow					**19879803833.39**	**m^3**
Lateral sinks outflow			0.00	m^3		
Open boundaries outflow			19879780217.73	m^3		
D: Total outflow					**19879780217.73**	**m^3**
E: Continuity balance = B-A-C+D =					**21124.81**	**m^3**
Relative deficit E/max(A,B,C,D) =					**0.00**	**()**

- ***Conclusions***
  - The preliminary MIKE 11 model was successfully set up.
  - The model is a preliminary, simplified, simulation of river flow. Future work is needed to include existing hydraulic structures such as the culvert and weir.

- After the model development is complete, calibration and validation processes are necessary.
- Results analysis is facilitated by a powerful visualization component.
- Important water flow parameters, such as Manning's coefficient, are crucial for accurate results.
- When coupled with MIKE SHE, the model will be able to simulate the complete water cycle hydrology.
- MIKE SHE is an integrated modeling system, which couples the surface water and the groundwater processes.
- MIKE SHE is able to successfully model rivers and channels (1D), overland flow (2D), unsaturated zone flow (1D), and groundwater flow (3D).

Subtask 3.2. Application of GIS Technologies for Hydrological Modeling Support

A combination of GIS and MIKE 11 tools are being used to support the development of the stream flow model which involves delineation of the stream network and generation of cross-sections and chainages for the major and minor tributaries of Tims Branch.

Hydrological model development has been fully supported by the use of GIS tools to store and manage spatial and timeseries model configuration parameters; pre- and post-process model-specific data and automate repetitive geoprocessing tasks; produce maps for visualization and reporting purposes; and conduct geospatial analyses that further support hydrological modeling results. Focus during this reporting period has been on refining the evapotranspiration module by attempting to create a spatially distributed rainfall grid. Precipitation is one of the critical variables in the integrated hydrological model, which determines the surface water flows in the watershed and the dynamics of the groundwater table. The aim is to refine the MIKE SHE model which currently includes data for a single rain gauge station (700-A, located in the A/M Area) to include data from several other monitoring stations located within SRS in order to generate spatially distributed rainfall and evapotranspiration timeseries grids. FIU has mapped several monitoring stations located within SRS using ArcGIS. A MS Excel spreadsheet containing location coordinates of the monitoring stations as well as time series rainfall data for a the period 1961-2016 was created from a text file provided by SRNL and used to generate a point shapefile using ArcToolbox geoprocessing tools within the ArcMap user interface. The point shapefile will be added to MIKE SHE and used to run simulations for various time periods based on the event or scenario being simulated.

DOE Fellow Awmna Rana began a preliminary geospatial analysis of land cover and land use change due to urbanization in the Tims Branch watershed using ArcGIS geoprocessing and statistical analysis tools, as this can have an impact on the watershed hydrology. The geospatial analysis conducted involved:

- Downloading land cover datasets for different years from the NLCD online database.
- Clipping the data to the Tims Branch watershed study domain.
- Converting the downloaded grid files from the NLCD database to GIS shapefiles.
- Extracting regions within Tims Branch watershed where land cover change occurred.
- Projecting the data to the appropriate coordinate system.

- Calculating the area of land cover change from 1992 to 2011 due to urbanization.

During the geospatial analysis, however, a discrepancy was noted when attempting to conduct the spatial join. The attribute table of the 1992 shapefile had one classification that was not present in the 2011 shapefile. For the purpose of this preliminary exercise, and in order to compare the 1992 and 2011 shapefiles, the classification type "Urban/ Recreational Grasses" in the 1992 shapefile was changed to "Developed Medium Intensity." It is noted on the NLCD website that "the NLCD 1992 is not recommended for direct comparisons with any subsequent NLCD data products (i.e. NLCD 2001, NLCD 2006, NLCD 2011). The typical result of direct comparison will result in a change map showing differences between legends and mapping methods rather than real changes on the ground." This study will therefore be repeated to compare data from the 2001, 2006 and 2011 NLCD datasets and the results reported in the final end of year report due in October 2016.

A technical progress report entitled "Application of GIS Technologies for Hydrological Modeling Support" was submitted on May 25, 2016, that details the accomplishments of the GIS-related component of the surface water modeling of Tims Branch.

Subtask 3.3. Biota, Biofilm, Water and Sediment Sampling in Tims Branch

FIU undergraduate student and DOE Fellow Awmna Rana departed for an internship opportunity on May 20, 2016, as part of the SREL REU in Radioecology during summer 2016 under the mentorship of Dr. John Seaman with whom FIU has been collaborating on this task.

The collection of samples and data required for the Tims Branch modeling effort by DOE Fellows during their summer internship participation at SRS may not be supportable, due to limited time. FIU is working on the identification and mapping of key points along the Tims Branch stream for data collection and will coordinate with Dr. Seaman from SREL with respect to the parameters required, the frequency of data collection and who will collect the data. FIU is investigating the possibility of undertaking the collection effort by FIU ARC researchers/staff. FIU is making inquiries with respect to the requirements/security clearance/training etc. necessary to gain on-site access to collect this data, and also whether site support will be available to provide escort to the sample locations by authorized DOE/SRNL/SREL personnel.

Below are the parameters necessary for development of a more accurate surface water model:

1. The Tims Branch stream and A-014 outfall tributary cross section survey/measurements.
2. Time series of discharge and suspended particle concentration in the water column in both A-014 and Tims Branch and further lab analyses.
3. Sediment core content (weight %) and core particle size (sieve) analyses.

Task 4: Sustainability Plan for the A/M Area Groundwater Remediation System

Task 4 Overview

The research and analysis performed under this task was being performed to support DOE EM-13 (Office of D&D and Facilities Engineering) under the direction of Mr. Albes Gaona, program lead for DOE's Sustainable Remediation Program. This task and associated research was completed and a technical report was submitted to SRNL and DOE on December 18, 2015.

Task 5: Remediation Research and Technical Support for WIPP

Task 5 Overview

This new task is in collaboration with research scientists Donald Reed and Timothy Dittrich in support of Los Alamos National Laboratory's field office in Carlsbad, New Mexico. This research center has been tasked with conducting experiments in the laboratory to better understand the science behind deep geologic repositories for the disposal of nuclear waste. The majority of their work is conducted in high ionic strength systems relevant to the Waste Isolation Pilot Plant (WIPP) located nearby. WIPP is currently the only licensed repository for the disposal of transuranic (TRU) defense waste in the world. However, the facility is not currently operating following an airborne release from a waste drum which failed to contain waste following an exothermic reaction of the waste. This was due to incompatibility of mixed waste received from LANL (organic adsorbent mixed with nitrate salt waste). The off-site releases of $^{239/240}$Pu and ^{241}Am detected were only slightly above background and were still below public exposure limits. However, FIU-ARC is now initiating a new task to support the basic research efforts requested to update risk assessments for the WIPP site as it moves towards restarting operations.

The objective of this task is to support LANL researchers in the basic science research required to address concerns in risk assessment models for the re-opening of the WIPP site for acceptance of defense waste.

Task 5 Quarterly Progress

The deployment of Hilary Emerson to CEMRC ended on April 9, 2016. Results are presented below for the kinetic batch experiments at 20 ppb Nd(III) and in the presence of a 3 mM $NaHCO_3$ buffer and 5 g/L dolomite for 0.01, 0.1 and 1.0 M total ionic strength (3 mM $NaHCO_3$ + NaCl). In addition, results are presented for 0.1 M ionic strength [0.003 M $NaHCO_3$ + 0.097 M NaCl] and 20 ppb Nd(III) for a long-term mini column experiment that is being continued by the LANL collaborators.

During the month of May, a student (Frances Zengotita, B.S. Chemistry and B.A. English, 2018) was hired as a DOE Fellow to work on the project. Mini column (5 M total ionic strength) and batch sorption (2 and 5 M total ionic strength at variable solids loading) are also in progress at FIU ARC.

Kinetic Batch Experiments

Batch kinetics experiments were completed at 0.01, 0.1 and 1.0 M total ionic strength (3 mM $NaHCO_3$ + NaCl), 5 g/L dolomite, and 20 ppb Nd (Figure 2-48) at LANL CEMRC. Additional experiments are ongoing at FIU ARC for 2 amd 5 M total ionic strength. Figure 2-47 represents sorption with respect to time in terms of a K_d in mL/g while Figure 2-48 is normalized to the measured surface area of the 355 – 500 µm size fraction of dolomite used in these experiments (1.6991 m^2/g as measured by BET method). Samples were collected for up to 3 days (4,320 minutes). However, preliminary data shows that sorption is strong and fast with equilibrium reached by 24 hours with sampling up to seven days without changes after the initial 24 hours. Equilibrium K_d's are measured between 500 – 900 mL/g for 0.01, 0.1 and 1.0 M ionic strengths.

Further, it should be noted that kinetics are similar for each of the different ionic strengths considered, although the highest ionic strength has not yet been considered (5.0 M).

Table 2-36 shows the equilibrium pH and pC_{H+} as determined using the corrections based on equation 1 as outlined previously (Borkowski, Lucchini et al., 2009). Borkowski has previously measured the K-value correction for 5 M NaCl as 0.82±0.03. These corrections are necessary because at high ionic strength, the pH (hydrogen ion activity) and pC_{H+} (hydrogen ion concentration) are not equivalent. The pH reading of a glass electrode is not the same due to (1) calibration with low ionic strength buffers and (2) lack of data for activity coefficients. However, a linear function has been shown to fit the data to predict pH and pC_{H+} and is in agreement with previous data (Rai, Felmy et al. 1995, Borkowski, Lucchini et al. 2009). The linear equation is shown in equation 2, where K=correction factor and IS is the total ionic strength in mol/L.

$$pC_{H+} = pH + K \qquad \text{Eqn. 1}$$

$$K = [IS \times -0.1868 \pm 0.0082] + 0.073 \qquad \text{Eqn. 2}$$

Table 2-36. Summary of pH and pCH+ Values for Batch Sample Sets

	pH	**pC_{H+}**
1.0 M	8.29±0.08	8.41±0.38
0.1 M	8.64±0.08	8.59±0.38
0.01 M	8.67±0.11	8.60±0.39

Note: pC_{H+} corrections based on Borkowski et al., 2009 with error propagated from their fit with a linear model

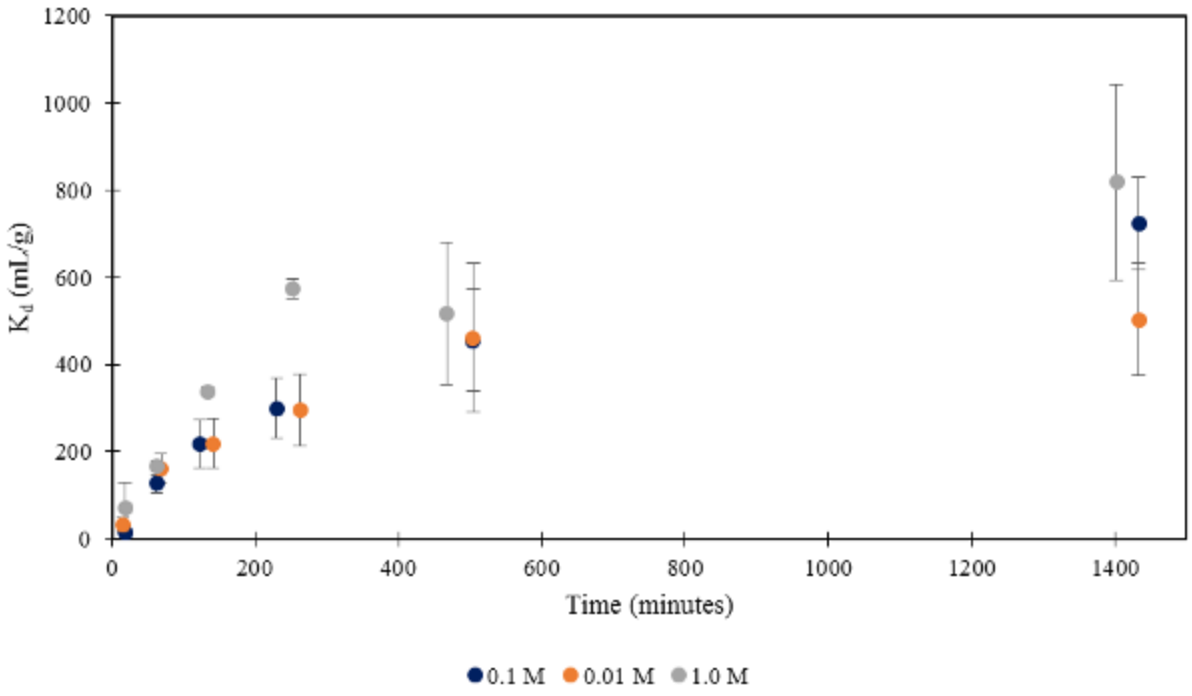

Figure 2-47. K_d (mL/g) partitioning of 20 ppb Nd(III) in the presence of 5 g/L dolomite with respect to time in 0.01, 0.1, and 1.0 M total ionic strength (NaCl + 0.003 M $NaHCO_3$).

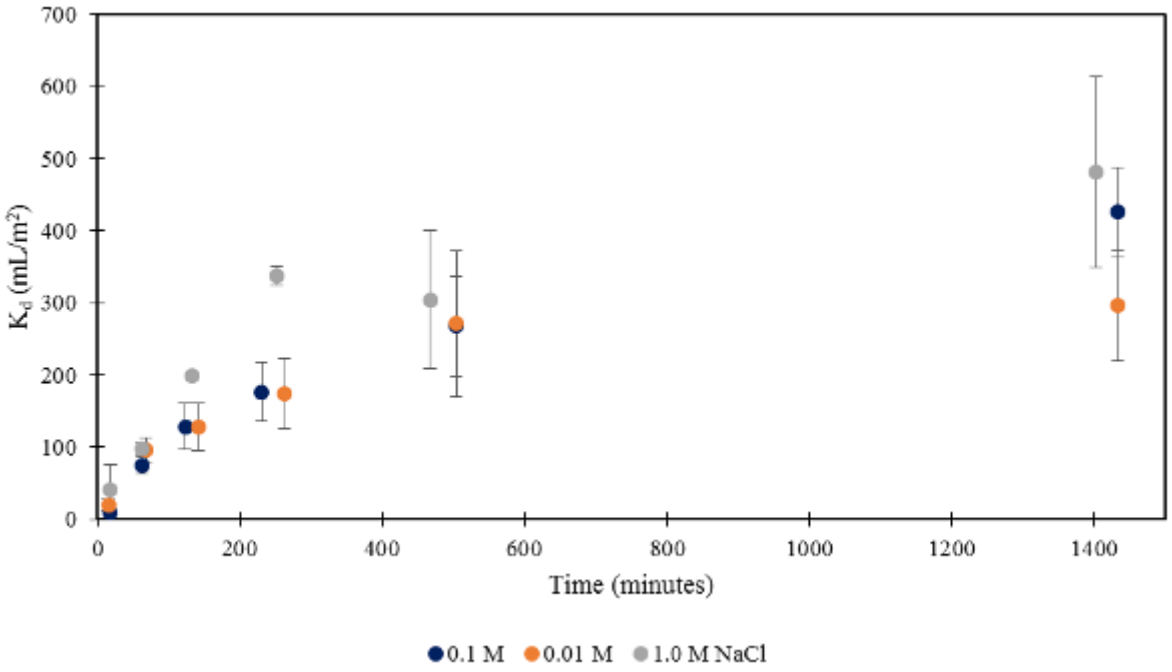

Figure 2-48. K_d (mL/m^2) partitioning of 20 ppb Nd(III) in the presence of 5 g/L dolomite with respect to time in 0.01, 0.1, and 1.0 M total ionic strength (NaCl + 0.003 M $NaHCO_3$).

Kinetic Sorption Models

Time dependent batch sorption data was fit with both first order and second order kinetic models as described in Table 2-37 below. The data was fit to 250 – 500 minutes as the reaction seemed to slow after this period and not follow either reaction model. However, the second order model appears to give the best fit for each of the datasets as shown by the R^2 correlation value in Table 2-37. Figures 2-49 to 2-54 show the model fits based on the plot of the linearized equation.

Table 2-37. Kinetic Model Equations and Fits for Batch Sorption Experiments

Kinetic model	General Equation	Linear Equation	Plot	R^2 Correlation		
				0.01 M	0.1 M	1.0 M
First-order	$C_t = C_o e^{-k_1 t}$	$ln[C_t] = ln[C_o] - k_1 t$	$ln[C_t]\ vs.\ t$	0.8471	0.8535	0.9761
Second-order	$C_t = \frac{C_0}{1 + C_0 k_2 t}$	$\frac{1}{C_t} = \frac{1}{C_0} + k_2 t$	$\frac{1}{C_t}\ vs.\ t$	0.9475	0.9141	0.9971

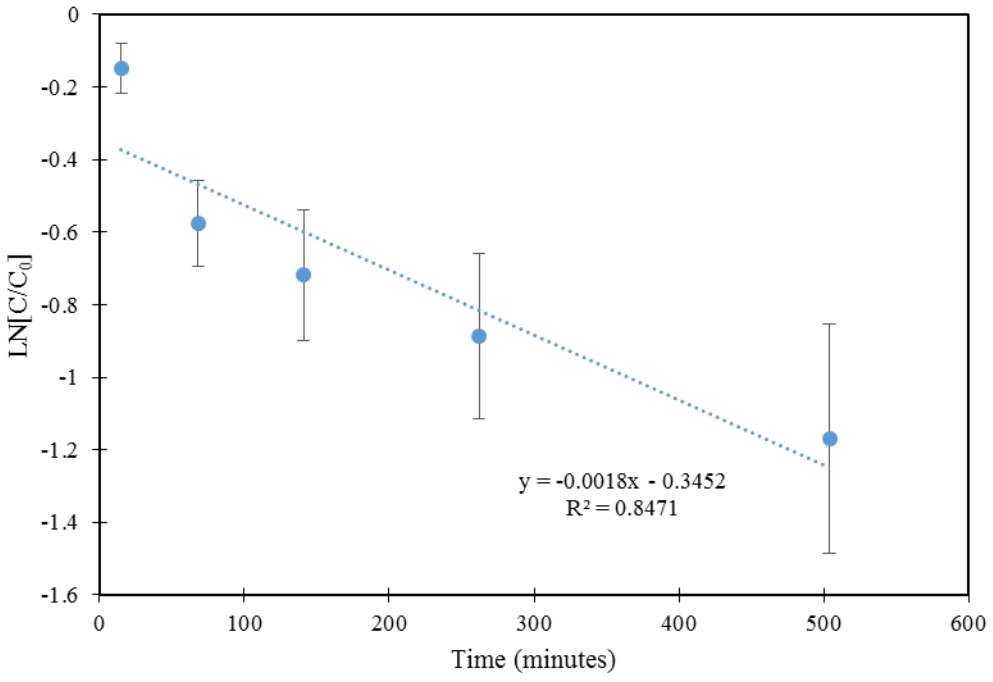

Figure 2-49. First order model fit for 0.01 M total ionic strength (3 mM $NaHCO_3$ + NaCl) for 20 ppb Nd(III) in the presence of 5 g/L dolomite.

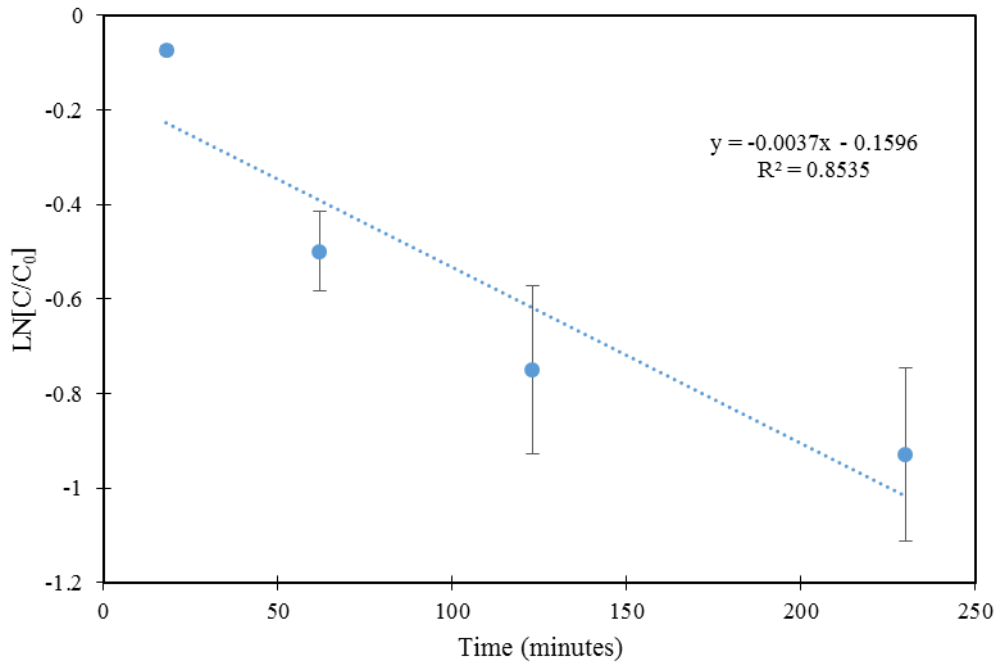

Figure 2-50. First order model fit for 0.1 M total ionic strength (3 mM $NaHCO_3$ + NaCl) for 20 ppb Nd(III) in the presence of 5 g/L dolomite.

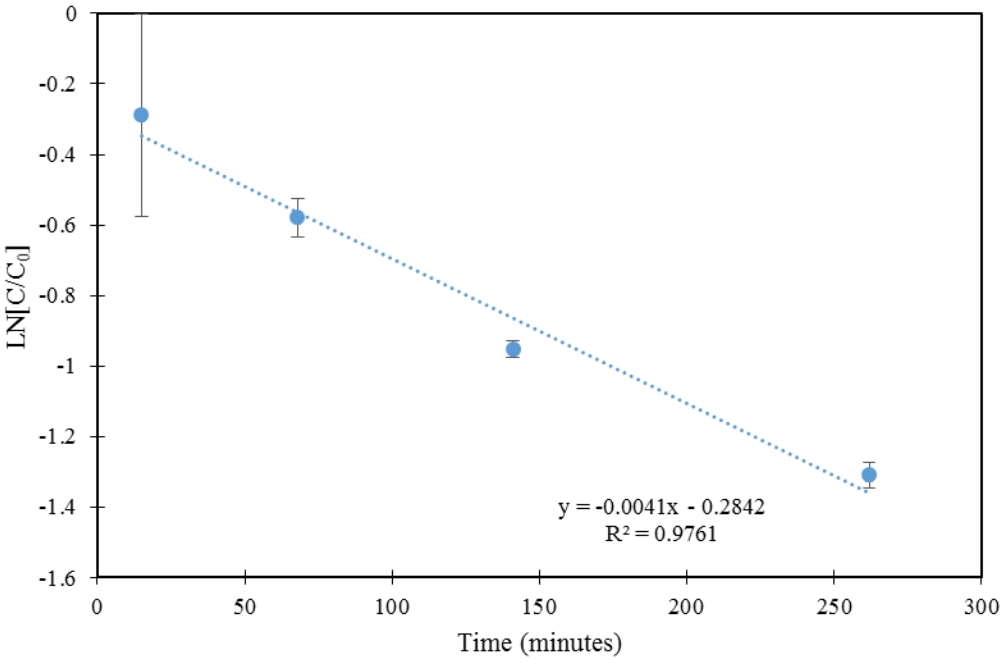

Figure 2-51. First order model fit for 1.0 M total ionic strength (3 mM $NaHCO_3$ + NaCl) for 20 ppb Nd(III) in the presence of 5 g/L dolomite.

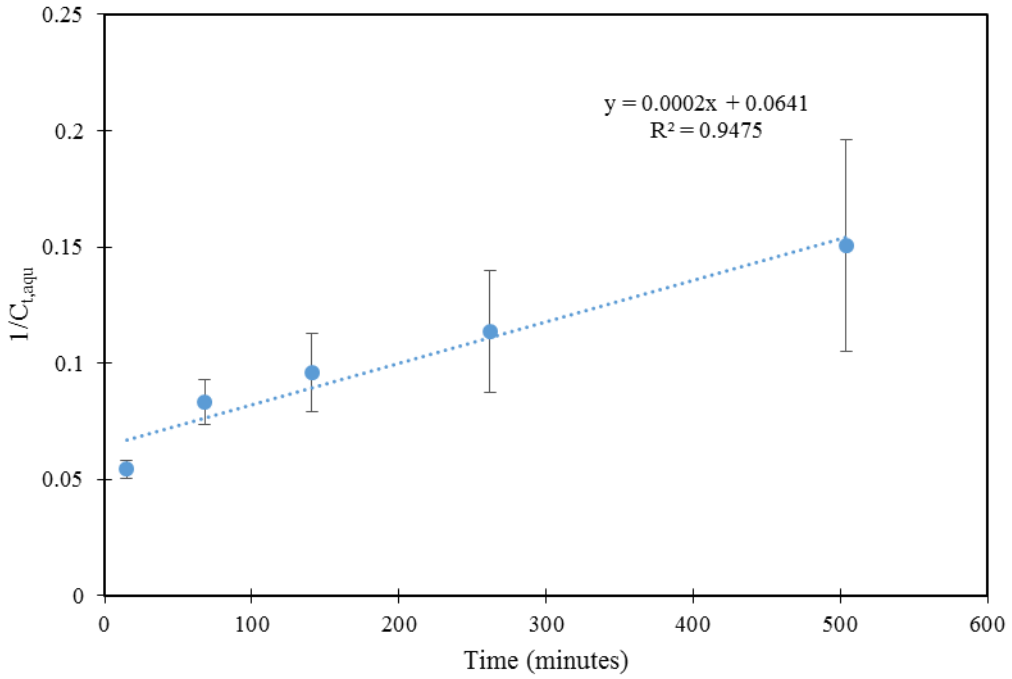

Figure 2-52. Second order model fit for 0.01 M total ionic strength (3 mM $NaHCO_3$ + NaCl) for 20 ppb Nd(III) in the presence of 5 g/L dolomite.

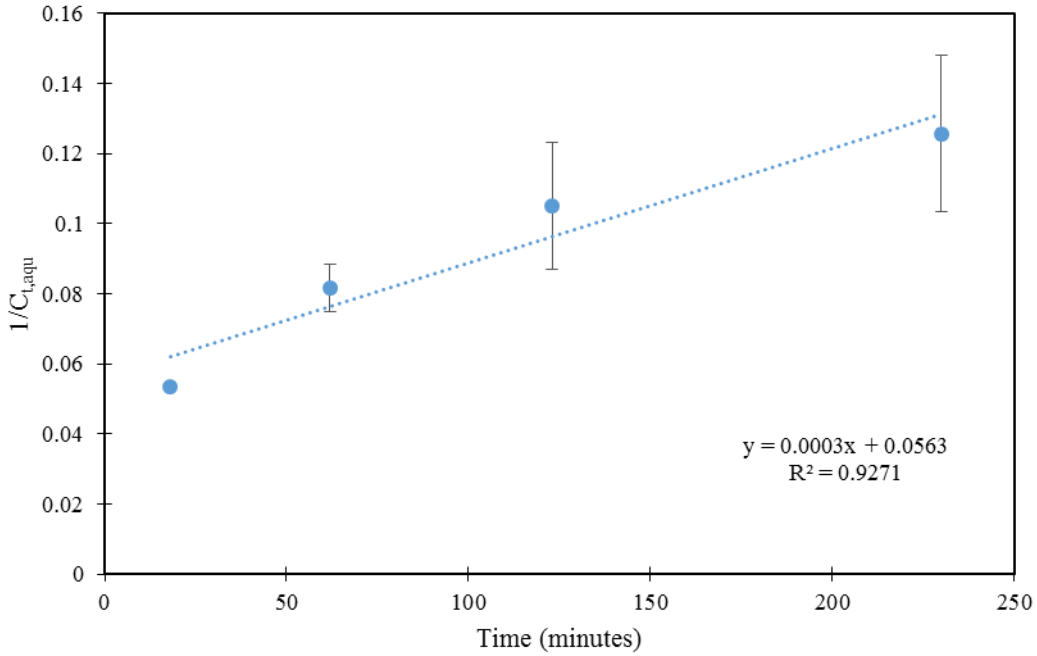

Figure 2-53. Second order model fit for 0.1 M total ionic strength (3 mM $NaHCO_3$ + NaCl) for 20 ppb Nd(III) in the presence of 5 g/L dolomite.

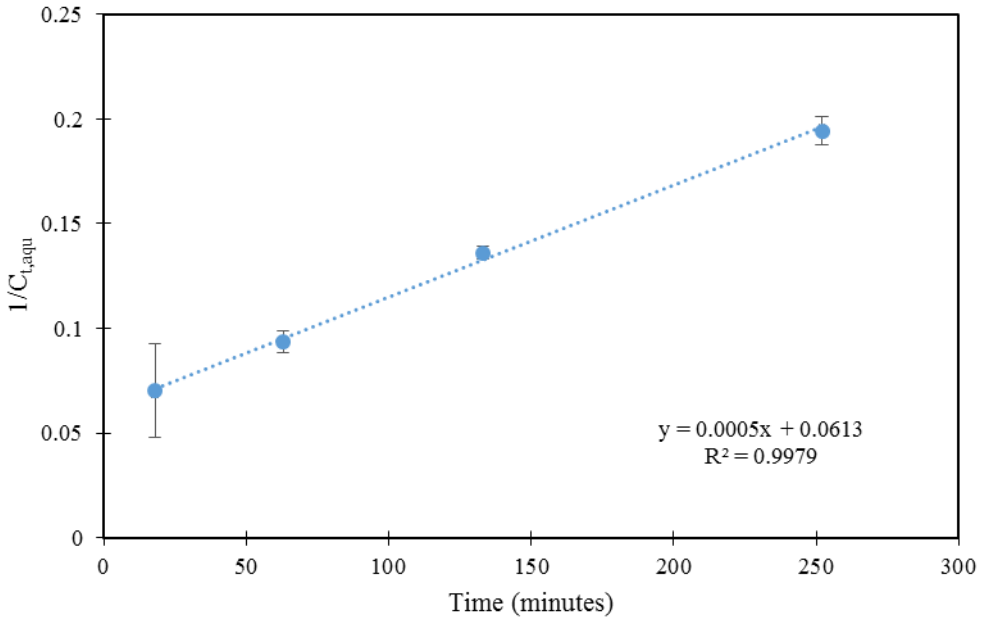

Figure 2-54. Second order model fit for 1.0 M total ionic strength (3 mM $NaHCO_3$ + NaCl) for 20 ppb Nd(III) in the presence of 5 g/L dolomite.

Filtration Comparison

One of the challenges with the preliminary experiments was the difficulty in generating reproducible data when comparing centrifugation versus filtration. In an attempt to differentiate between sorption of Nd(III) to filters versus precipitates being removed by the filters, three different variations of filtration were performed: (1) comparison of pre-conditioning of filters, (2) sequential filtration of stock solutions through the same filter, and (3) sequential filtration of stock solutions through new filters. The filters used for these experiments were 0.5 mL Amicon Ultra 30k MWCO centrifugal filters. Each sample was centrifuged for 40 minutes at 13.5k rpm to ensure that all of the aqueous phase passed through the filter.

Figure 2-55 represents the results from the first set of filtration where the effects of pre-conditioning of filters was considered. Filters were (1) not pre-conditioned (i.e. sample was immediately placed into filter and centrifuged), (2) pre-conditioned with 0.1 M NaCl (equivalent ionic strength to the stock solution), or (3) pre-conditioned with the 0.1 M NaCl + 100 ppb Nd(III) stock solution. The stock solution was at a pH near 7.5 with a theoretical solubility of 195 ppb in the presence of atmospheric carbon dioxide. While there were significant losses in comparison to the unfiltered sample, there was no statistical difference between the different pre-conditioning steps. The error on these measurements is based on triplicate measurement by ICP-MS and does not represent analysis of multiple samples. Based on the first set of experiments, pre-conditioning does not appear to be necessary for these types of filters. However, it is not clear whether Nd(III) was removed from the aqueous phase due to precipitation leading to size exclusion in the filter or sorption to filter materials.

Figure 2-56 shows sequential filtration through the same filter of either the 0.1 M NaCl + 100 ppb stock solution or an acidified Nd(III) stock solution (2% HNO_3) with the error based on

triplicate measurement by ICP-MS. The acidified stock solution remains near 100% with multiple filtrations through the same filter. The stock solution near pH 7.5 shows significant losses to the filter. However, it is not clear whether or not these losses are due to sorption to the filters or precipitation of Nd(III). The elevated pH could enhance both sorption and precipitation of the Nd(III) in the stock solution.

The final set of filtering experiments was designed based on the assumptions that a second filtration step through a clean filter should: (1) not remove Nd(III) if all precipitates were removed in the first step, and (2) remove Nd(III) if sorption is occurring to the filter material. The total concentration of Nd(III) was also lowered to 20 ppb and 3 mM $NaHCO_3$ was added (0.003 M $NaHCO_3$ + 0.097 M NaCl = 0.1 M total ionic strength) to decrease the risk of precipitation due to pH fluctuations within the solution. The theoretical solubility of Nd(III) at pH 8.5 is 21 ppb without carbonate and 54 ppb with 3 mM HCO_3. Figure 2-57 shows the results of duplicate samples with losses of ~30% of the Nd(III) with each filtration step. Therefore, it would appear the Nd(III) is sorbing to the filter materials.

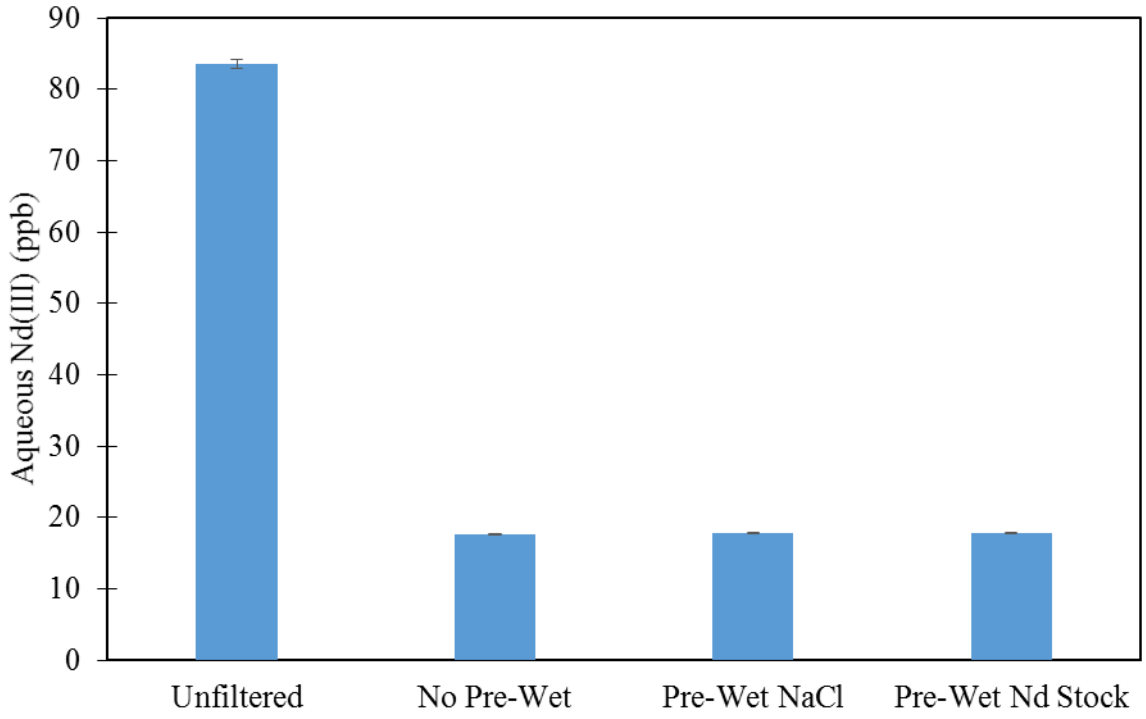

Figure 2-55. Filtration of 100 ppb Nd(III) stock in 0.1 M NaCl at pH ~ 7.5 following variable pre-treatment steps, error based on triplicate measurement by ICP-MS.

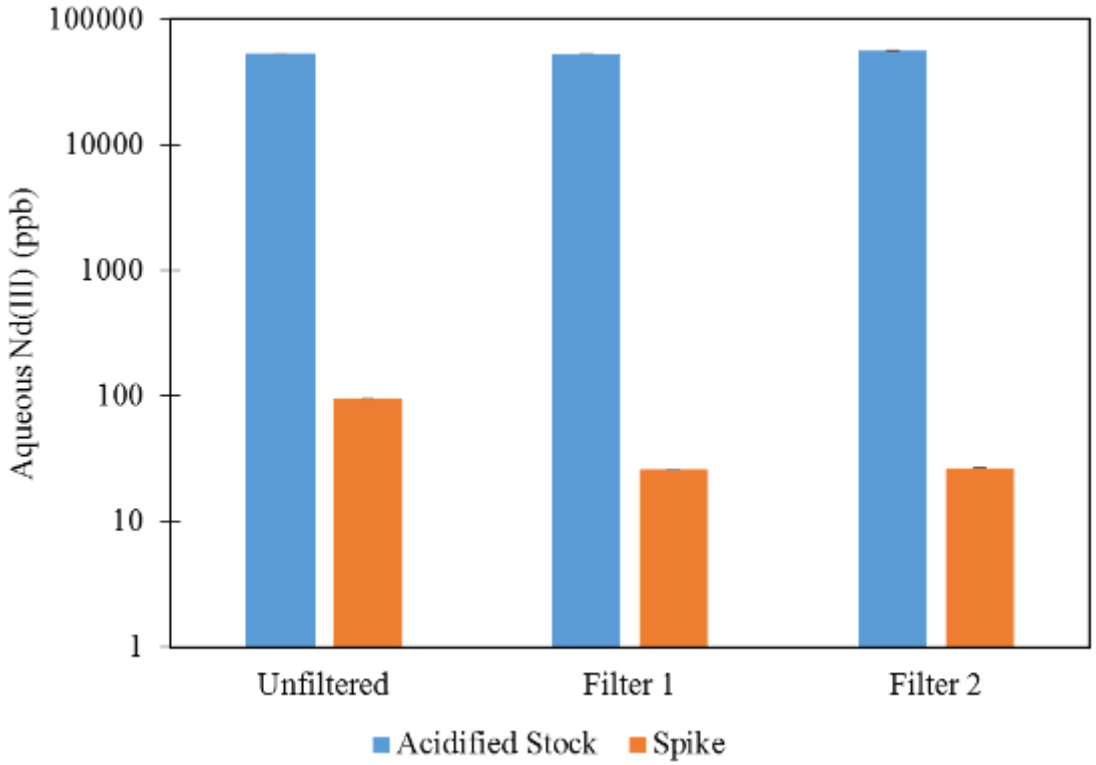

Figure 2-56. Sequential filtration of 100 ppb Nd(III) in 0.1 M NaCl or 50,000 ppb Nd(III) in 2% HNO_3 through the same 30k MWCO filter, error based on triplicate measurement by ICP-MS.

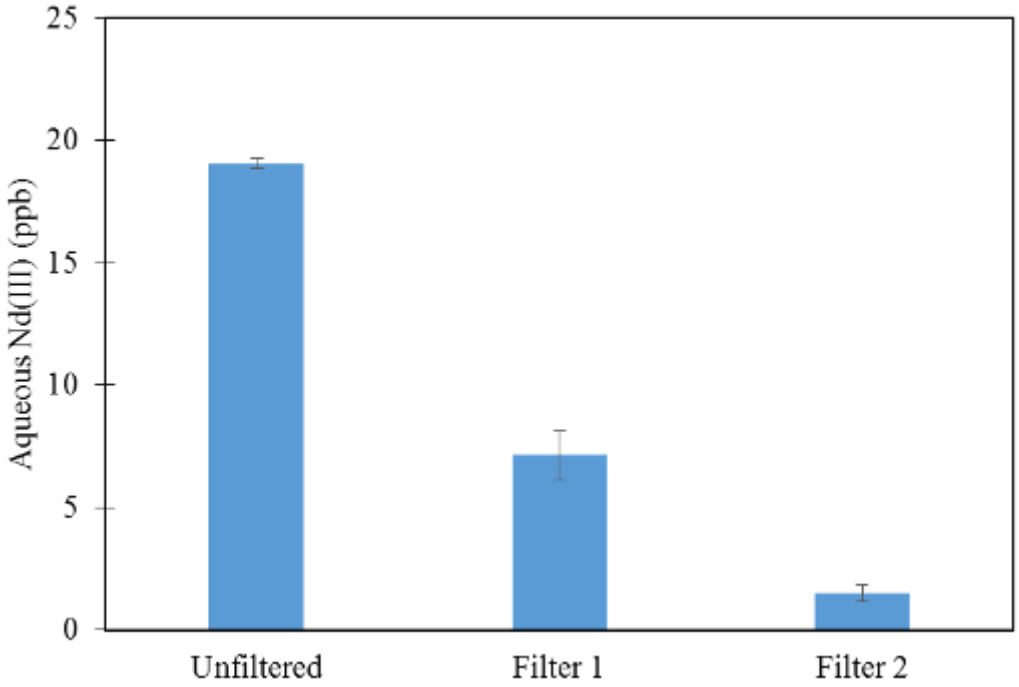

Figure 2-57. Sequential filtration of 20 ppb Nd(III) stock solution in 0.1 M total ionic strength (3 mM $NaHCO_3$ + NaCl) with the second filtration step through a new filter, error based on duplicate samples.

Mini Column Experiments

A long-term mini column with 0.1 M total ionic strength (3 mM $NaHCO_3$ + NaCl) and 20 ppb Nd(III) continuous injection at 1.5 mL/hr is currently in progress at LANL CEMRC (Figure 2-58) and a 5 M total ionic strength mini column has begun at FIU ARC. More than 19000 pore volumes have been pushed through the 0.1 M column without saturation of the column with Nd(III). The column is 1 cm in length and contains approximately one gram of dolomite with a porosity of ~0.32. Therefore, if breakthrough had occurred at 1900 pore volumes, the K_d for Nd(III) as calculated by the mini columns would be 200 mL/g. Therefore, based on the K_d's reported for the batch experiments (500 – 900 mL/g at equilibrium), the breakthrough point for the columns should not have been reached.

This is based on equation 1 below where θ=porosity, ρ=bulk density of dolomite and K_d=equilibrium partition coefficient for Nd. The retardation factor (R) is generally described as equivalent to the ratio of groundwater velocity to the contaminant velocity. Further, this ratio can be related to the number of pore volumes in the column in the same manner because a conservative tracer should move through the column with the flow of groundwater, or after one pore volume. Therefore, the retardation factor can also be considered equivalent to the number of pore volumes that must go through the column before breakthrough of the contaminant.

$$R = 1 + \frac{\rho_B}{\theta} K_d \qquad \text{Eqn. 1}$$

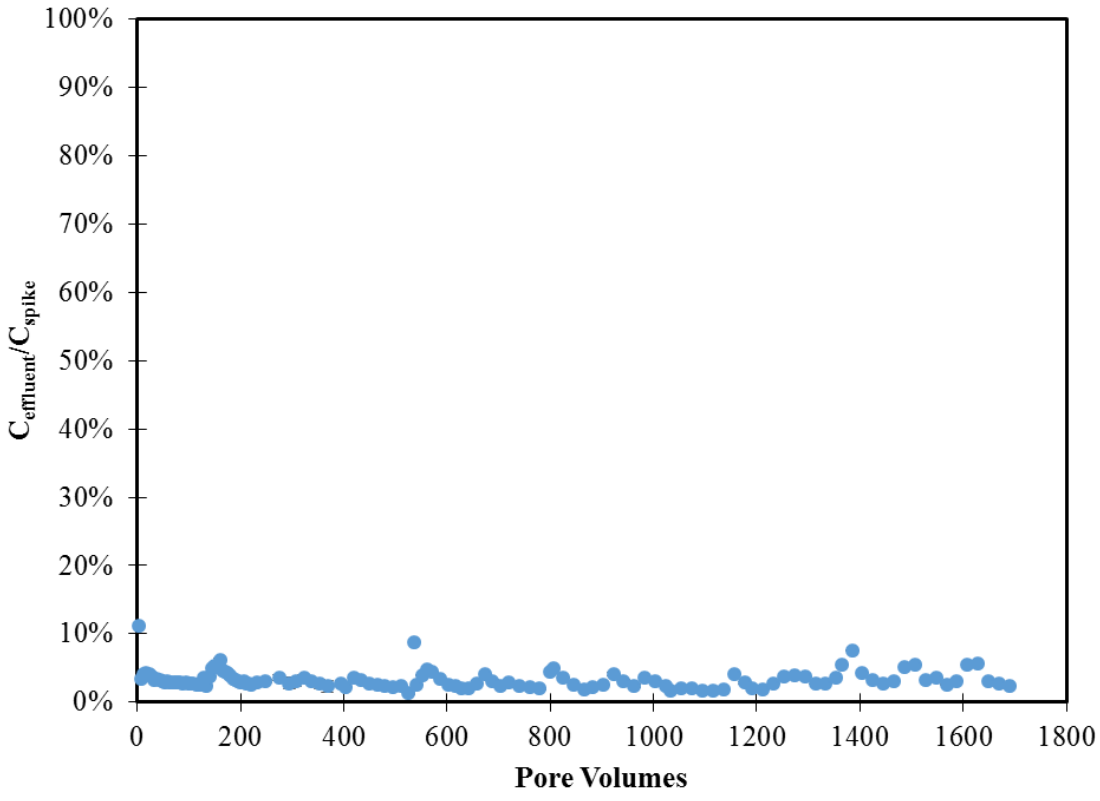

Figure 2-58. Continuous input of 20 ppb Nd + 0.097 M NaCl + 0.003 M $NaHCO_3$ into mini column packed with dolomite at 1.5 mL/hr flow rate.

At each time interval for the batch kinetic experiment, the tubes were allowed to settle for 15 minutes to ensure that the dolomite mineral was not present in the aqueous phase prior to sampling as solids could damage the ICP-MS during analysis. While the six mixtures (0.5g-dol-1,2,3; 1.0g-dol-1,2,3) were left to sit, the pH was measured and the time was recorded. Once the seventh batch kinetics data was collected, the final mass of each tube was taken to ensure that total volume losses throughout the experiment were minimal.

A mini column experiment was also begun for the 5 M electrolyte background [3 mM bicarbonate + NaCl] + 20 ppb Nd. A photograph and description is included below of the current experimental setup for comparison to the setup at LANL CEMRC. The mini column experiment also investigated the sorption processes of neodymium (Nd) to the dolomite mineral via Kloehn pump with the 2 and 5 M electrolyte background [3 mM bicarbonate + NaCl] + 20 ppb Nd. The columns have 2.2 cm length (1 cm length of dolomite + fittings) and have a 1.5 mL/hr flow rate. The effluent is collected every 4 hours into 13x100 mm polystyrene tubes in an Eldex fraction collector. The mini column experiment will be measured over at least three months until breakthrough (i.e., when the dolomite mineral is saturated with Nd).

The tubes that were collected from the column experiment were weighed and then placed into 2 mL vials for the ICP-MS analysis with a 1:5 dilution in 2% HNO_3. An additional dilution of at least 1:10 (for a total of 1:50) will be completed to further dilute the salts. Nitric acid was added in order to preserve the solution for ICP-MS analysis. The column has been running for approximately two weeks with continuous effluent collection and pH analysis of each effluent tube.

Future Work

Additional batch kinetics experiment are in progress at 2 and 5 M total ionic strength [3 mM $NaHCO_3$ + NaCl] with measurements up to two days and will be analyzed for fit with common kinetic sorption models for comparison with the 0.01 – 1.0 M ionic strength experiments. In addition, batch experiments will be conducted at variable concentrations of dolomite to investigate the saturation concentration for comparison with mini column results. The long-term mini column at 0.1 M total ionic strength will be continued by our LANL collaborators until breakthrough (i.e. saturation) has been reached. However, a 1 and 5 M total ionic strength column will be conducted at FIU. Finally, a model will be developed to interpret the column breakthrough data utilizing PHREEQC.

The 5 M ionic strength mini column experiment will continue until break through with a continuous collection of samples. Following completion of the 5 M ionic strength column, a 2 M ionic strength column will also be conducted. All samples collected at FIU ARC are currently awaiting analysis by ICP-MS as the instrument is not currently operational. However, samples will continue to be prepared and stored until the ICP-MS at FIU MMC is functioning. If the instrument is not fixed soon, the samples will be sent to LANL CEMRC facilities for analysis.

Mini Column Experimental Design @ FIU ARC

All equipment for the mini column experiments is contained within a plastic storage bin (Sterilite, 58 quart) with the exception of the laptop for programming commands for the Kloehn syringe pump. In addition, the fraction collector, syringe pump and laptop are hooked up to a

UPS battery backup. Within the storage bin, the mini column is taped to the wall. The 1-liter glass bottle contains the stock solution (5 M NaCl + 3 mM $NaHCO_3$ + 20 ppb Nd) and the Kloehn syringe is programmed to automatically refill from the bottle through PTFE tubing (Cole-Parmer, 1/32" ID, 1/16" OD) which is pulled through a spring-loaded fitting. A small hole is also drilled into the 1-liter bottle cap to keep the bottle from becoming pressurized with minimal evaporation. The storage bin remains closed unless samples are being pulled for analysis and has a 500 mL beaker filled with deionized H_2O (>18 MΩ*cm) to increase humidity and decrease evaporation within the box.

Figure 2-59. Mini-column set up.

References

Borkowski, M., J. F. Lucchini, M. Richmann and D. Reed (2009). Actinide (III) Solubility in WIPP Brine: Data Summary and Recommendations. L. A. N. Lab.

Rai, D., A. R. Felmy, S. P. Juracich and L. F. Rao (1995). Estimating the Hydrogen Ion Concentration in Concentrated NaCl and Na_2SO_4 Electrolytes. S. N. Laboratories. Albuquerque, NM, Sandia National Lab.

Milestones and Deliverables

The milestones and deliverables for Project 2 for FIU Performance Year 6 are shown on the following table. The deliverable for Task 2 (Subtask 2.1), progress report on batch experiments on sodium silicate application in multi-contaminant systems, was submitted to DOE and site contacts on April 4, 2016. The deliverable for Task 2 (Subtask 2.4), progress report on the synergy between colloidal Si and HA on the removal of U(VI), was submitted to DOE and site contacts on April 21, 2016. Milestone 2015-P2-M4, Complete input of MIKE SHE model configuration parameters for simulation of unsaturated flow (Subtask 3.1), was completed by April 29, 2016. The deliverable for Task 3 (Subtask 3.2), progress report on the application of GIS technologies for hydrological modeling support, was submitted to collaborators at SRNL, SREL and DOE HQ on May 25, 2016. The deliverable for Task 1 (Subtask 1.3.1), progress

report on the effect of ammonia on uranium partitioning and kaolinite mineral dissolution, was submitted to DOE and Hanford Site contacts on June 22, 2016. In addition, the deliverable for Task 2 (Subtask 2.5), a progress report on the column experiments to investigate uranium mobility in the presence of humic acid, was submitted to DOE and SRS contacts on June 30, 2016. Finally, the deliverable for Task 3 (Subtask 3.1), progress report for modeling of surface water and sediment transport in the Tims Branch ecosystem, was submitted to DOE and SRS contacts on June 28, 2016.

FIU Performance Year 6 Milestones and Deliverables for Project 2

Task	Milestone/ Deliverable	Description	Due Date	Status	OSTI
Project	2015-P2-M1	Submit draft papers to Waste Management 2016 Symposium	11/6/2015	Complete	
Task 1: Hanford Site	Deliverable	Progress report on the experimental results on autunite mineral biodissolution (Subtask 1.2)	2/15/2016	Complete	OSTI
	Deliverable	Progress report on batch experiments for ammonia injection task (Subtask 1.3.1)	6/22/2016	Complete	OSTI
	Deliverable	Literature Review of Geophysical Resistivity Measurements and Microbial Communities (Subtask 1.3.3)	3/18/2016	Complete	
Task 2: SRS	Deliverable	Progress report on batch experiments on sodium silicate application in multi-contaminant systems (Subtask 2.1)	4/11/2016	Complete	OSTI
	Deliverable	Progress report on the synergy between colloidal Si and HA on the removal of U(VI) (Subtask 2.4)	4/21/2016	Complete	OSTI
	Deliverable	Progress report on column experiments to investigate uranium mobility in the presence of HA (Subtask 2.5)	5/20/2016 Reforecast to 7/1/2016	Complete	OSTI
Task 3: Tims Branch	2015-P2-M2	Complete refinement of MIKE SHE model configuration parameters for the simulation of overland flow using revised model domain (Subtask 3.1)	12/30/2015	Complete	
	2015-P2-M3	Complete input of MIKE SHE model configuration parameters for simulation of evapotranspiration (Subtask 3.1)	2/29/2016 Reforecast to 3/31/16	Complete	
	2015-P2-M4	Complete input of MIKE SHE model configuration parameters for simulation of unsaturated flow (Subtask 3.1)	3/31/2016 Reforecast to 4/29/2016	Complete	

	Deliverable	Progress Report for Subtask 3.1: Modeling of surface water and sediment transport in the Tims Branch ecosystem	4/29/2016 Reforecast to 6/30/16	Complete	OSTI
	Deliverable	Progress Report for Subtask 3.2: Application of GIS technologies for hydrological modeling support	4/29/2016 Reforecast to 5/31/16	Complete	OSTI
	2015-P2-M5	Complete input of MIKE SHE model configuration parameters for simulation of flow in the saturated zone (Subtask 3.1)	6/30/2016	Reforecast to 7/29/16	
Task 4: Sustainability Plan	Deliverable	Draft sustainable remediation report for the M1 air stripper	12/18/2015	Complete	OSTI

Work Plan for Next Quarter

Project-wide:

- Draft the Year End Report (YER) for FIU Performance Year 6 (August 2015 to August 2016).
- Draft the Project Technical Plan (PTP) for FIU Performance Year 7 (August 2016 to August 2017).

Task 1: Remediation Research and Technical Support for the Hanford Site

Subtask 1.1 – Sequestering Uranium at the Hanford 200 Area Vadose Zone by in situ Subsurface pH Manipulation using NH_3 Gas

- Continue with isopiestic measurements of water adsorption/desorption on precipitates.
- Prepare new samples composed of Si, Al, HCO_3, U and Ca for sequential extraction experiments with uranium-bearing solids with various compositions.
- Obtain samples for ERMA analysis from PNNL.
- Conduct EMRA analysis at FIU.
- Digest sample precipitates followed by KPA and/or ICP-OES analysis.

Subtask 1.2. Investigation on Microbial-Meta-Autunite Interactions - Effect of Bicarbonate and Calcium Ions

- Sampling of sacrificial samples prepared with three different bicarbonate concentrations in mineral-free experiments for chemical and protein analysis.
- Completion of the experiment: chemical analysis, microbiological and protein analysis.

Subtask 1.3. Evaluation of Ammonia Fate and Biological Contributions During and After Ammonia Injection for Uranium Treatment

- Experimental results for kaolinite (batch and sequential extraction experiments) will be submitted for publication in JER

- Aqueous speciation modeling via GWB will be completed for comparison with the experimental results.
- Statistical analysis will be used to compare the samples that had pH adjusted by NaOH versus by NH_4OH (t-test).
- Mineral dissolution experiments begun at PNNL will continue at FIU following Silvina Di Pietro's summer internship.
- Saturated batch experiments for the suite of minerals relevant to Hanford begun in August 2016 will be completed.

Task 2: Remediation Research and Technical Support for Savannah River Site

Subtask 2.1. FIU's Support for Groundwater Remediation at SRS F/H –Area

- Initiate writing of a manuscript with the ultimate goal of publishing.

Subtask 2.2 – Monitoring of U(VI) Bioreduction after ARCADIS Demonstration at F-Area

- Continue with a summary of the results and write a final report.

Subtask 2.3.Sorption Properties of the Humate Injected into the Subsurface System

- Perform FTIR of SRS sediments + Huma-K but at concentrations higher than 50 ppm to investigate surface complexation.
- Perform kinetics of Huma-K sorption on SRS sediments at different times (less than 30 min) to complete the experiment.
- Study the effects of salts ($NaNO_3$) on desorption of Huma-K.
- Initiate experiments on uranium adsorption kinetics onto SRS sediments.

Subtask 2.4 – The synergetic effect of HA and Si on the removal of U(VI)

- Continue with experiments and sample analysis.

Subtask 2.5 – Investigation of the migration and distribution of natural organic matter injected into subsurface systems

- Submit draft progress report on column experiments detailing the results obtained.
- Continue column experiments to study the sorption/desorption of Huma-K and study the effect of sorbed Huma-K on uranium mobility.

Task 3: Surface Water Modeling of Tims Branch

Subtask 3.1. Modeling of Surface Water and Sediment Transport in the Tims Branch Ecosystem

- Complete input of MIKE SHE model configuration parameters for simulation of flow in the saturated zone.

Subtask 3.2. Application of GIS Technologies for Hydrological Modeling Support

- Geospatial distribution of ET over time including the creation of a raster data set for ET in SRS and Tims Branch.
- Preparation of timeseries datasets of Leaf Area Index and Root Depth to generate raster datasets.
- Preparation of a groundwater table GIS shapefile. This may require revisiting the available water table shapefiles and adding current data from various online sources.
- Continue with preliminary MIKE 11 model development which involves delineation of stream network, and generation of cross-sections and chainages for Tims Branch major and minor tributaries.

Subtask 3.3. Biota, Biofilm, Water and Sediment Sampling in Tims Branch

- Dr. Mahmoudi is working on the identification and mapping of key points along the Tims Branch stream for data and sample collection and analysis, and is coordinating with Dr. Seaman from SREL with respect to the parameters required and the standard field and laboratory procedures to be employed. Dr. Mahmoudi will be traveling to SRS in August 2016 to conduct this exercise and will be supported by 3 FIU students (DOE Fellows).

Task 4: Sustainability Plan for the A/M Area Groundwater Remediation System

- This task was completed and a technical report submitted to DOE and SRNL on Dec. 15, 2015 entitled, "A Sustainability Analysis for the M1 Air Stripper and Pumps of the M Area Groundwater Remediation System at the Savannah River Site." No additional effort is planned on this task.

Task 5: Remediation Research and Technical Support for WIPP

- Work in collaboration with LANL to continue parallel experiments including mini-columns and batch experiments with Nd(III) for 0.01 – 5 M NaCl.
- Begin model development for mini column experiments in PHREEQC.
- Investigate and apply kinetic models to fit batch sorption data.
- Develop a technical report based on worked performed at CEMRC Carlsbad facilities between February 15 to April 8, 2016.

Project 3
Waste and D&D Engineering & Technology Development

Project Manager: Dr. Leonel E. Lagos

Project Description

This project focuses on delivering solutions under the decontamination and decommissioning (D&D) and waste areas in support of DOE HQ (EM-13). This work is also relevant to D&D activities being carried out at other DOE sites such as Oak Ridge, Savannah River, Hanford, Idaho and Portsmouth. The following tasks are included in FIU Performance Year 6:

Task No	Task
Task 1: Waste Information Management System (WIMS)	
Subtask 1.1	Maintain WIMS – database management, application maintenance, and performance tuning
Subtask 1. 2	Incorporate new data files with existing sites into WIMS
Task 2: D&D Support to DOE EM for Technology Innovation, Development, Evaluation and Deployment	
Subtask 2.1	D&D Technology Demonstration & Development and Technical Support to SRS's 235-F Facility Decommissioning
Subtask 2.2	Technology Demonstration and Evaluation
Subtask 2.3	Support to DOE EM-13 and the D&D Community
Task 3: D&D Knowledge Management Information Tool	
Subtask 3.1	Web and Mobile Application for D&D Decision Model
Subtask 3.2	Mobile Applications/Platforms for DOE Sites
Subtask 3.3	Development & Integration of International KM-IT Pilot for UK Collaboration
Subtask 3.4	Outreach and Training (D&D Community Support)
Subtask 3.5	Data Mining and Content Management
Subtask 3.6	D&D KM-IT Administration and Support

Task 1: Waste Information Management System (WIMS)

Task 1 Overview

This task provides direct support to DOE EM for the management, development, and maintenance of a Waste Information Management System (WIMS). WIMS was developed to receive and organize the DOE waste forecast data from across the DOE complex and to automatically generate waste forecast data tables, disposition maps, GIS maps, transportation details, and other custom reports. WIMS is successfully deployed and can be accessed from the web address http://www.emwims.org. The waste forecast information is updated at least

annually. WIMS has been designed to be extremely flexible for future additions and is being enhanced on a regular basis.

Task 1 Quarterly Progress

The Waste Information Management System (WIMS) was developed to receive and organize the DOE waste forecast data from across the DOE complex and to automatically generate waste forecast data tables, disposition maps, GIS maps, transportation details, and other custom reports. WIMS is successfully deployed and can be accessed from the web address http://www.emwims.org. During this reporting period, FIU performed database management, application maintenance, and performance tuning to the online WIMS in order to ensure a consistent high level of database and website performance.

FIU received the new set of waste stream forecast and transportation forecast data from DOE on April 8, 2016. The revised waste forecast data was received as formatted data files and, to incorporate these new files, FIU built a data interface to allow the files to be received by the WIMS application and import it into SQL Server. SQL server is the database server where the actual WIMS data is maintained.

FIU completed the data import and deployed onto the test server for DOE testing and review on May 13, 2016 (completing milestone 2015-P3-M1.1). Figure 3-1 shows screenshots of the new dataset in WIMS. FIU received feedback from the DOE data review on June 13, 2016, incorporated the recommended revisions, and deployed the new data on the public server on June 14, 2016. The 2016 waste data replaces the previous waste data from 2015 and is now fully viewable and operational in WIMS.

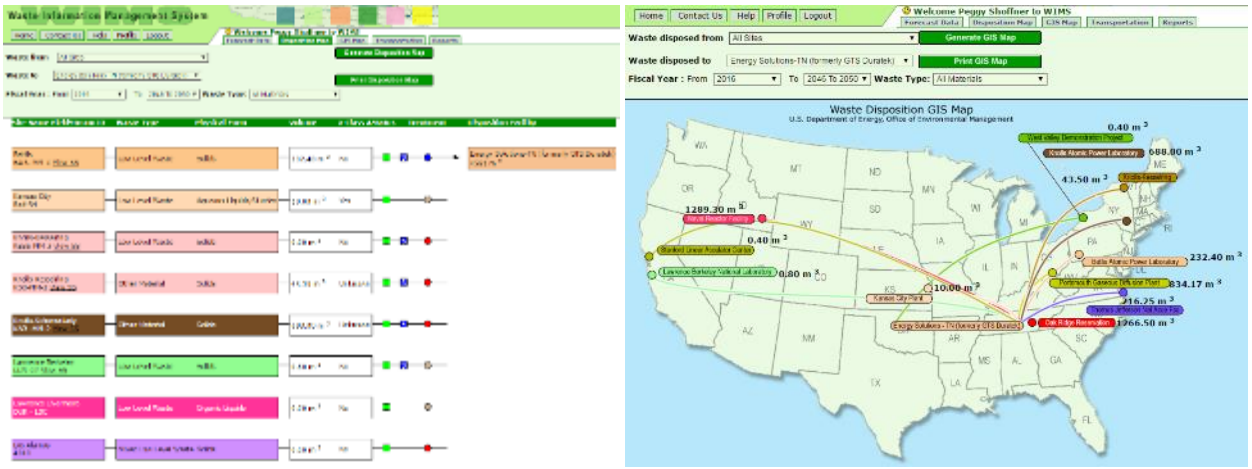

Figure 3-1. WIMS screenshots with 2016 dataset: Disposition Map (left) and GIS Map (right).

Task 2: D&D Support to DOE EM for Technology Innovation, Development, Evaluation and Deployment

Task 2 Overview

This task provides direct support to DOE EM for D&D technology innovation, development, evaluation and deployment. For FIU Performance Year 6, FIU will assist DOE EM-13 in meeting the D&D needs and technical challenges around the DOE complex. FIU will expand the research in technology demonstration and evaluation by developing a phased approach for the demonstration, evaluation, and deployment of D&D technologies. One area of focus will be working with the Savannah River Site to identify and demonstrate innovative technologies in support of the SRS 235-F project. FIU will further support the EM-1 International Program and the EM-13 D&D program by participating in D&D workshops, conferences, and serving as subject matter experts.

Task 2 Quarterly Progress

Task 2.1.1: Incombustible Fixatives

The objective of this research task is to improve the operational performance of fixatives by enhancing their fire resiliency. Most fixatives begin to see degradation between 200-400 degrees, at which time radioisotopes could potentially be released into the environment. The layering or combining of an intumescent coating with the fixative is being investigated as a way to mitigate the release of radioisotopes during fire and/or extreme heat conditions.

FIU continued discussions and coordination with SRNL and SRS 235-F site personnel concerning a potential demonstration of the intumescent coating concept on a contaminated entry hood at the SRS 235-F facility in the October/November 2016 timeframe. FIU is developing tailored testing protocols to demonstrate the following: 1) The designated intumescent coating maintains its fire resilient properties to the standards of, and as measured by, ASTM E119 or similar test when applied to dirty, roughed up surfaces without a primer; 2) Once applied under these conditions, the designated intumescent coating can continue to fix contaminants under impact factors outlined in DOE Standard 3010; and 3) The designated intumescent coating can prevent the release of contaminants when exposed to fire/extreme heat conditions.

Baselining of additional commercial-off-the-shelf (COTS) intumescent coatings (IC) also continued, with a particular emphasis on developing individual mass loss profiles (Figure 3-2). Developing the mass loss profiles for each intumescent coating is critical due to its expected correlation to enhancing a fixative's operational performance and fire resiliency under a layering configuration. These baseline experiments also have the potential of identifying an IC as a possible candidate to function as a standalone fixative. As depicted by the data points and associated graphs below, 2 of 3 of the additional ICs (Fire Dam and Interchar) performed exceptionally well, with one (Fire Dam) identifying itself as a possible candidate for a standalone fixative. Fire Dam exhibited the least amount of mass loss thus far with an average weighted profile of 36%. More importantly, as depicted in Figure 3-3, Fire Dam displayed the least observable damage when exposed to extreme temperatures for extended periods. It did not exhibit the same degree of discoloration, desiccation, or chemical breakdown, and demonstrated an improved overall adhesion to the substrate.

Though more testing is required, initial results associated with layering Fire Dam (FD) over fixatives and exposing to high temperatures (800ºF) for 15 minutes in the muffle furnace showed that the fixatives were significantly protected by the overlaying IC. Figure 3-4a shows a test coupon of stainless steel with fixative E (fixative only) after being exposed to 800ºF for 15 minutes in the muffle furnace. The fixative had significant mass loss, discoloration, desiccation, cracking, and significant flaking. Figure 3-4b shows a glass test coupon with an application of fixative E (white in color) and the intumescent coating FD applied over the fixative (red in color). FD was then also applied to the opposite side of the glass test coupon so that that fixative had the IC layered on both sides. Finally, Figure 3-4c shows the same glass test coupon after being exposed to 800ºF for 15 minutes in the muffle furnace, with the bottom layer of IC (dark red in color) scraped away to show the fixative layer. The fixative remained largely intact, with the outer edge showing some color change and bubbling.

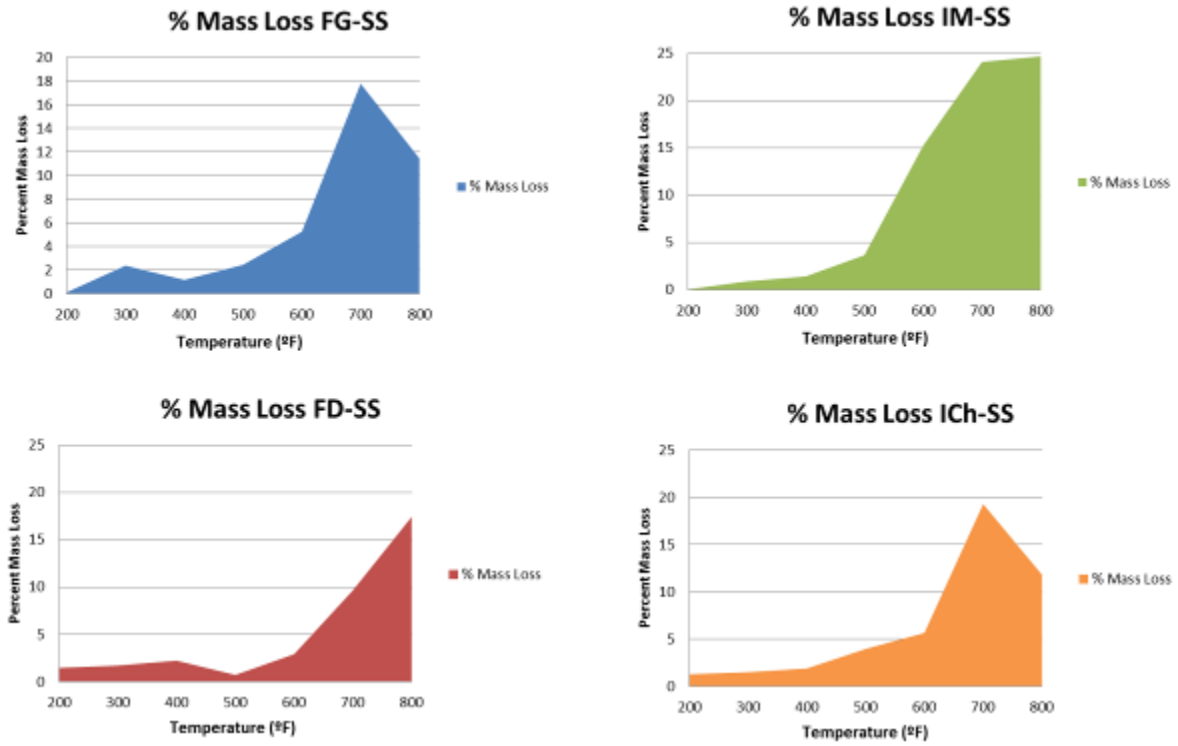

Figure 3-2. Mass loss profiles of intumescent coatings.

Figure 3-3. Fire Dam intumescent coating after exposure to 800º F.

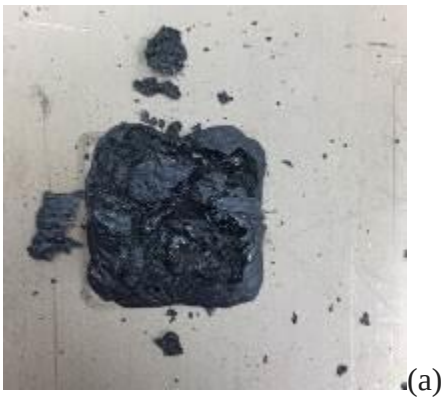
(a)

(b)

(c)

Figure 3-4. (a) Fixative E after exposure to high heat, (b) fixative E (white) layered with FD intumescent coating, and (c) fixative E layered with FD after exposure to 800ºF.

FIU provided a detailed briefing to Mr. Andrew Szilagyi and Mr. John De Gregory with DOE EM-13 on the efforts and results related to this task to date on May 11, 2016. The update was well received with additional guidance provided by EM-13 on the path forward. During this briefing, the proposed scope of work for FIU Performance Year 7 for the overall D&D task (Task 2) of Project 3 was also presented and discussed in support of the development of the Continuation Application.

Finally, FIU prepared additional test coupons of the new IC products and, along with liquid samples of the fixatives and ICs tested to date, shipped them to the SRNL collaborators to support their parallel research on the products under varying environmental and radioactive conditions.

Task 2.1.3: Robotic Technologies for SRS 235-F

The SRS 235-F facility has a need to identify a remote system that can make one-time entry to highly contaminated areas. The one-time-entry requirement indicates that the technology will not be retrieved at the end of the work but would remain inside the facility due to the high levels of contamination. FIU will perform research to identify robotic technology systems applicable to the challenges and needs of the SRS 235-F Facility. Research will include working with SRNL to define the requirements for the robotic technology and utilizing the Robotic Database in D&D KM-IT to search and identify potential technologies that meet the defined requirements. A deliverable for a summary report on robotic technologies applicable to the SRS 235-F Facility has been reforecast to August 12, 2016. The circumstances and end path forward, including the new reforecasted date for this deliverable, have been closely coordinated with the stakeholders at Savannah River and DOE HQ. FIU discussed the issue with the SRNL collaborators and confirmed the agreement the deliverable date with an email sent to SRS on May 24, 2016 and DOE HQ contacts on May 27, 2016.

Task 2.2: Technology Demonstration and Evaluation

The primary objective of this task is to standardize and implement proven processes to refine and better synchronize DOE-EM technology needs, requirements, testing, evaluation, and acquisition by implementing a three-phased technology test and evaluation model. The development of uniformly accepted testing protocols and performance metrics is an essential component for testing and evaluating D&D technologies.

FIU continues leading the standards development process for D&D technologies through the ASTM International E10.03 Subcommittee. A final agenda for the scheduled June Working Group on this initiative was approved, including:

1. Confirm / modify operational characteristics / requirements for fixatives used in support of D&D technologies. FIU will capture these and then begin a draft standard for D&D coatings similar to ASTM E-2731.

2. Begin initial standards development for testing protocols related to determining radiation resiliency of fixatives used for long-term D&D requirements.

3. Begin initial standards development for testing protocols related to determining the decontamination factor (DF) of fixatives/decon gels on contaminated concrete for D&D (and possibly other substrates).

4. Begin initial standards development for testing protocols related to fixative/decon gel/coating performance on contaminated steel for D&D.

A general approach was agreed upon as a starting point for the Working Group members. There are some testing protocols associated with various R&D efforts for D&D technologies that have gained informal acceptance. Identifying these, codifying them, then reformatting into the ASTM standard and staffing across community stakeholders for review will allow the formal process of standards development to occur. This will allow for the development of not only uniform testing protocols and performance metrics to justify test and evaluation methods, but also facilitate institutional objectives related to capturing, preserving, and sharing information.

During June, FIU participated in the ASTM International's Executive Steering Committee Meeting from June 27 to June 29, 2016, and led an ASTM International E10.03 Subcommittee meeting to develop standardized testing protocols and performance metrics for D&D technologies. Participating members of this subcommittee meeting included Joe Sinicrope (FIU ARC), Rick Demmer (INL), Steve Reese (INL), Aaron Washington (SRNL), Connor Nicholson (SRNL), Andy Jung (Areva), Edward Walter (consultant), Steve Halliwell (VJT Technologies), and Bob Walcheski (UESI). Accomplishments during the meeting and the next steps to be taken include:

- Completed the development of two (2) new draft standard specifications on fixative technologies: a) strippable/removal coatings, and b) permanent coatings and fixatives. The standard specifications outline the performance, mechanical, chemical, and physical requirements expected of the technology with the associated performance criteria.
- Connor Nicholson will forward those drafts to Ed Walker and Joe Sinicrope to refine before distribution to the entire working group for one final review/edit.
- Joe Sinicrope will engage the Staff Manager (Steve Mawn) and acquire official working document numbers for the 2 drafts so they can begin to be formally tracked.
- The working group's final drafts for the 2 standard specifications will be sent to the E10.03 Subcommittee members for a Subcommittee vote. Incorporation of any comments from the Subcommittee will be incorporated prior to submitted the specifications for a full E10 Committee vote.
- Bob Walcheski and Rick Demmer will forward the specified data to support drafting of a third standard specification for fixatives used in basin operations. The two existing drafts will be used as the foundation and the necessary requirements from Rick and Bob will be integrated.
- Will begin the initial development of a DF Testing Protocols using Rick Demmer's past work as the basis. This will be the priority development effort during the subcommittee's January 2017 meeting.
- A second priority development effort in January 2017 will be a testing protocol for an "immobilization factor" associated with both of the standard specifications.

Task 3: D&D Knowledge Management Information Tool (KM-IT)

Task 3 Overview

The D&D Knowledge Management Information Tool (KM-IT) is a web-based system developed to maintain and preserve the D&D knowledge base. The system was developed by Florida International University's Applied Research Center (FIU-ARC) with the support of the D&D community, including DOE-EM (EM-13 & EM-72), the former ALARA centers at Hanford and Savannah River, and with the active collaboration and support of the DOE's Energy Facility Contractors Group (EFCOG). The D&D KM-IT is a D&D community driven system tailored to serve the technical issues faced by the D&D workforce across the DOE Complex. D&D KM-IT can be accessed from web address http://www.dndkm.org.

Task 3 Quarterly Progress

D&D knowledge management through contributions in Wikipedia was a part of the outreach and training (D&D community support) subtask. FIU completed the related milestone, 2015-P3-M3.4, and sent a draft summary report to DOE on April 15, 2016. The general D&D knowledge which has been gained through this project offers an opportunity to expand access to a broad audience via Wikipedia, which has a significant presence on the web, thereby offering greater opportunities for collaboration on D&D knowledge. FIU researched and targeted D&D information on Wikipedia where D&D KM-IT could provide additional relevant information while citing the source of the original information on D&D KM-IT.

During the completion of this task, four Wikipedia articles were edited with information. For each of these articles, relevant and significant text was added to the body of the article and a reference to the information source on D&D KM-IT was included. The edited entries included the following Wikipedia articles with the displayed text:

1. **Nuclear Decommissioning – Cost Section** with information from the best practice titled, "SRS P and R Reactor Disassembly Basin *In Situ* Decommissioning."

   New methods for decommissioning have been developed in order to minimize the usual high decommissioning costs. One of these methods is *in situ* decommissioning (ISD), which was implemented at the U.S. Department of Energy Savannah River Site in South Carolina for the closures of the P and R Reactors. With this tactic, the cost of decommissioning both reactors was $73 million. In comparison, the decommissioning of each reactor using traditional methods would have been an estimated $250 million. This results in a 71% decrease in cost by using ISD.

2. **Occupational Safety and Health – Hazard Identification Section** with information from the following best practice: "Historical Hazard Identification Process for D&D." The reference linking back to the best practice document on D&D KM-IT was subsequently removed by another Wikipedia editor. It is important to note that the information available on wikis is continually evolving and may be further edited by other participants at any time. FIU has further edited the entry to add the title and link to the best practice under the Further Reading section of the Wikipedia entry.

   The information that needs to be gathered from sources should apply to the specific type of work from which the hazards can come from. As mentioned previously, examples of these sources include interviews with people who have worked in the field of the hazard, history and analysis of past incidents, and official reports of work and the hazards encountered. Of these, the personnel interviews may be the most critical in identifying undocumented practices, events, releases, hazards and other relevant information. Once the information is gathered from a collection of sources, it is recommended for these to be digitally archived (to allow for quick searching) and to have a physical set of the same information in order for it to be more accessible. One innovative way to display the complex historical hazard information is with a historical hazards identification map, which distills the hazard information into an easy to use graphical format.

3. **Robotics – Applications Section** with information about the use of robotics for D&D.

   Another application area for robotics that is receiving increased interest is in the effort to deactivate and decommission (D&D) unnecessary and/or unusable facilities across the U.S. Department of Energy (DOE) complex. Many of these facilities pose hazards which prevent the use of traditional industrial demolition techniques. Such hazards include radiological, chemical, and hazardous materials contamination and structural instability. Efficient and safe D&D of the facilities will almost certainly require the use of remotely operated technologies to protect personnel and the environment during potentially hazardous D&D activities and operations. One database, developed by DOE, contains information on almost 500 existing robotic technologies and can be found on the D&D Knowledge Management Information Tool.

4. **Radioactive Contamination – Decontamination** with information about fixatives and other contamination control products.

   Contamination control products have been used by the U.S. Department of Energy (DOE) and the commercial nuclear industry for decades to minimize contamination on radioactive equipment and surfaces and fix contamination in place. "Contamination control products" is a broad term that includes fixatives, strippable coatings, and decontamination gels. A fixative product functions as a permanent coating to stabilize residual loose/transferrable radioactive contamination by fixing it in place; this aids in preventing the spread of contamination and reduces the possibility of the contamination becoming airborne, reducing workforce exposure and facilitating future deactivation and decommissioning (D&D) activities. Strippable coating products are loosely adhered paint-like films and are used for their decontamination abilities. They are applied to surfaces with loose/transferrable radioactive contamination and then, once dried, are peeled off, which removes the loose/transferrable contamination along with the product. The residual radioactive contamination on the surface is significantly reduced once the strippable coating is removed. Modern strippable coatings show high decontamination efficiencies and can rival traditional mechanical and chemical decontamination methods. Decontamination gels work in much the same way as other strippable coatings. The results obtained through the use of contamination control products is variable and depends on the type of substrate, the selected contamination control product, the contaminants, and the environmental conditions (e.g., temperature, humidity, etc.).

FIU sent a link to the pilot web-based fixative module to a selected individuals at DOE sites and national laboratories for beta testing. Comments and input from the beta testers was received and FIU completed the incorporated of beta testing feedback to improve the tool before launching it on the public server. FIU also designed and developed a mobile application for this tool, which was sent to DOE for review and testing on May 20, 2016, completing milestone 2015-P3-M3.5. Where the beta testing feedback was relevant to the light version of the D&D Fixative Module for mobile devices, FIU also incorporated the feedback into the mobile version.

The D&D Fixative Module can assist in the selection of commercially available fixatives, strippable coatings, and decontamination gels for application during D&D activities. The module includes a comprehensive database of commercially available fixatives and other contamination

control products and is capable of filtering and sorting the available products according to the criteria entered by the user.

Both the web-based (https://www.dndkm.org/FixativeModule/) and mobile (https://m.dndkm.org/FixativeModule.aspx) versions of the D&D Fixative Module were deployed live on June 29, 2016. Figures 3-5 through 3-8 show screenshots of the web-based fixative module and Figures 3-9 through 3-12 show screenshots from the fixative mobile app.

Benefits of the D&D Fixative Module include:

1. Cuts down research time to identify contamination control products to use depending on site-specific conditions.
2. Provides an instant overview of the commercially available products filtered and sorted for the criteria entered.
3. Provides access to concise information on over 40 commercially available contamination control products.
4. Can be easily expanded to include more criteria or newly available products.

Figure 3-5. Fixative module home page.

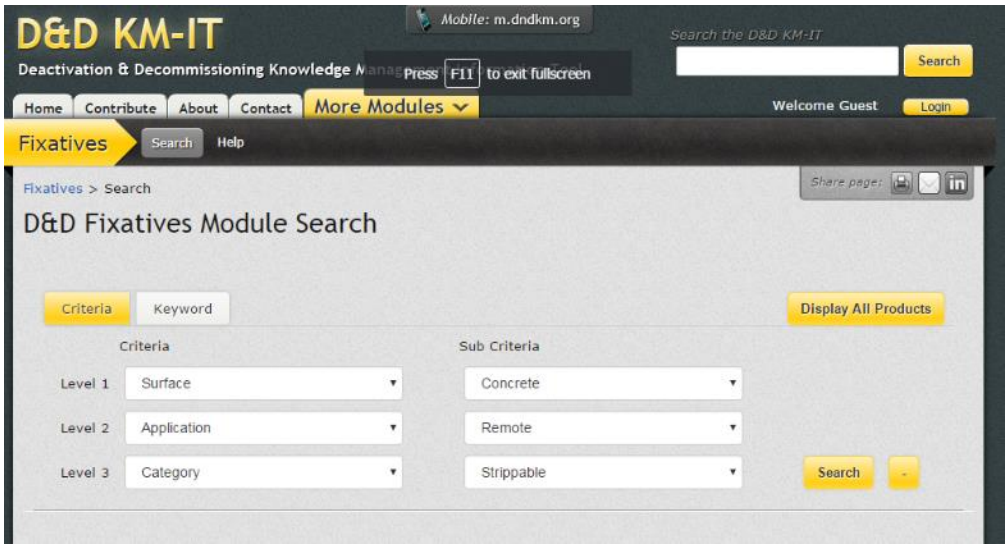

Figure 3-6. Fixative module search by product criteria.

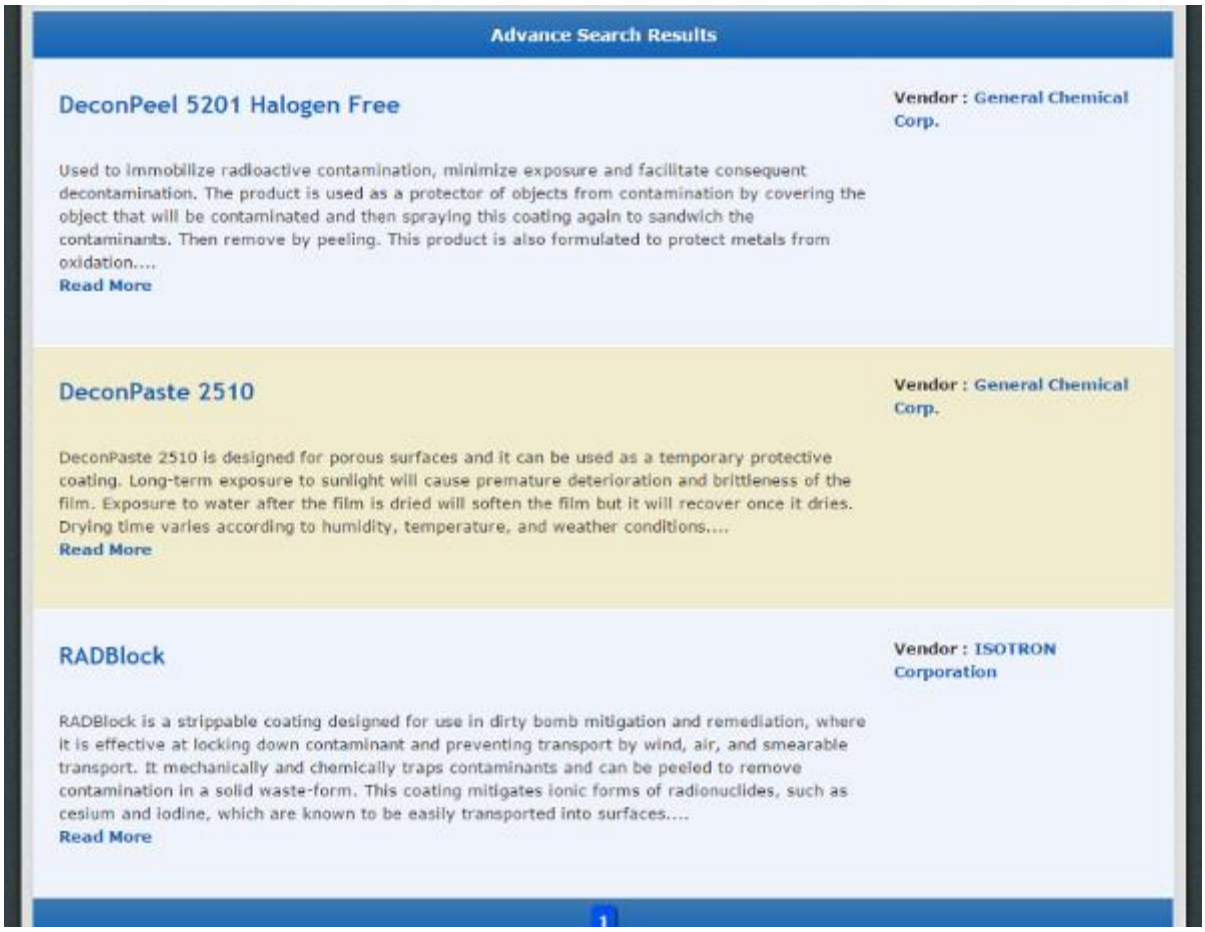

Figure 3-7. Fixative module sample search results.

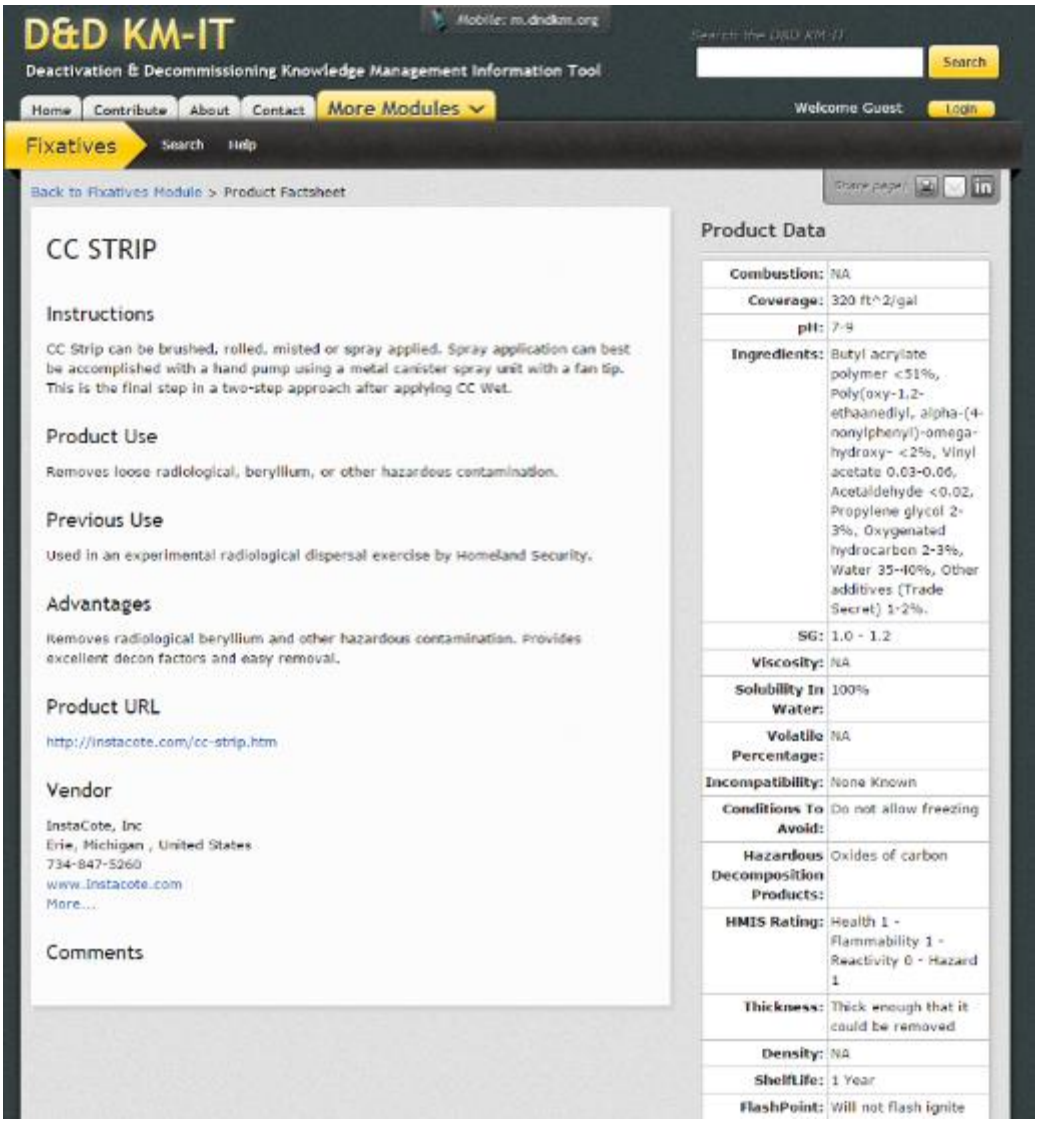

Figure 3-8. Fixative module sample product factsheet.

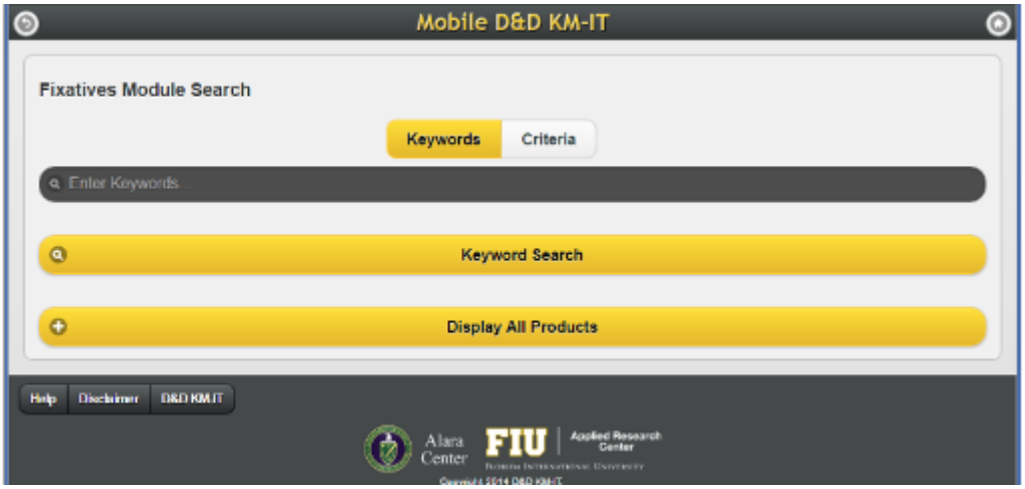

Figure 3-9. Fixative mobile app homepage.

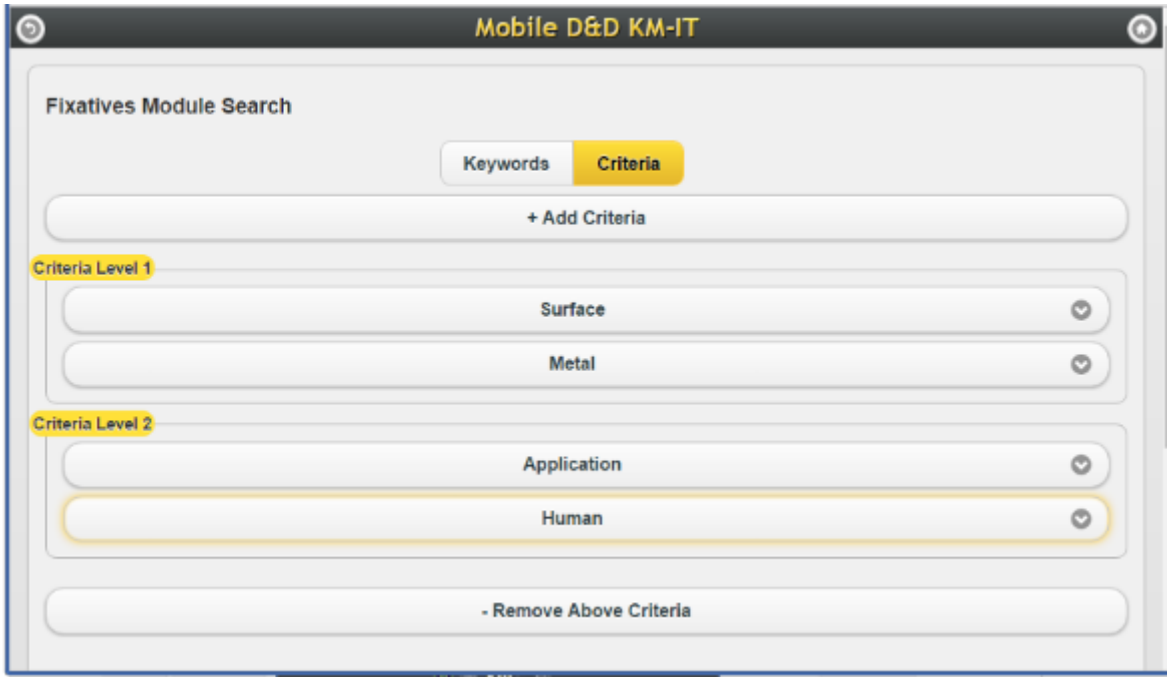

Figure 3-10. Fixative mobile app sample search criteria.

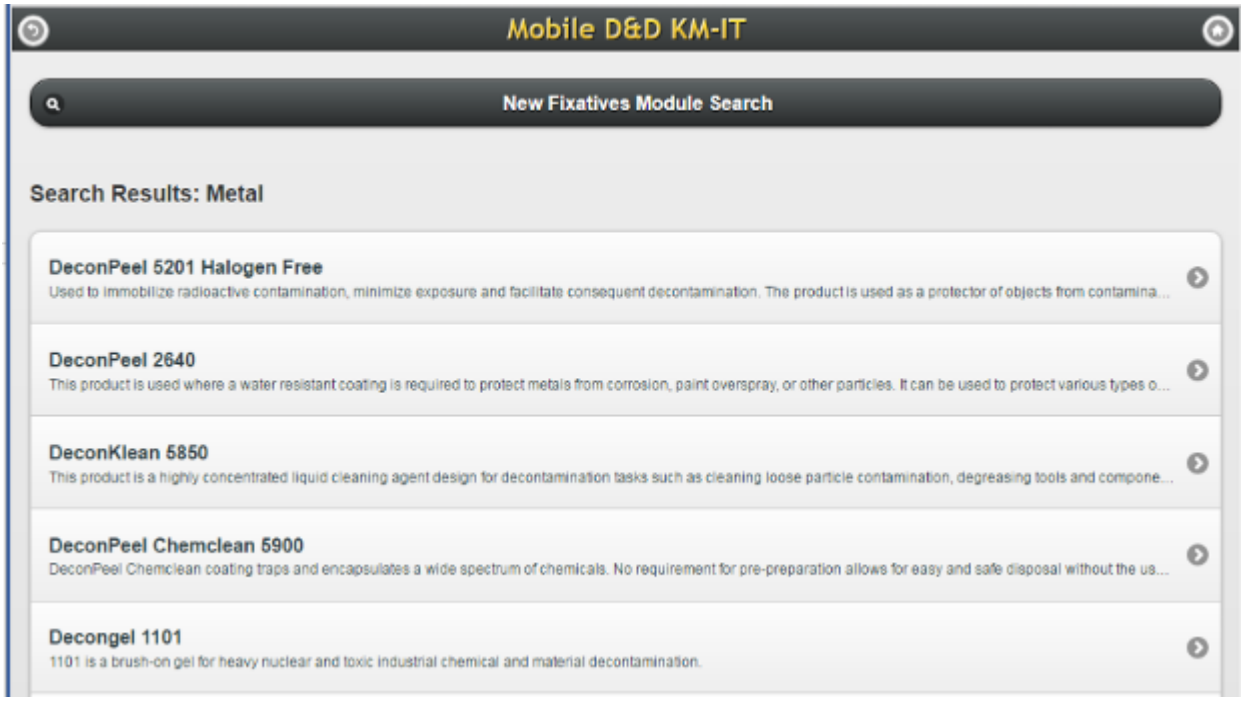

Figure 3-11. Fixative mobile app sample search results.

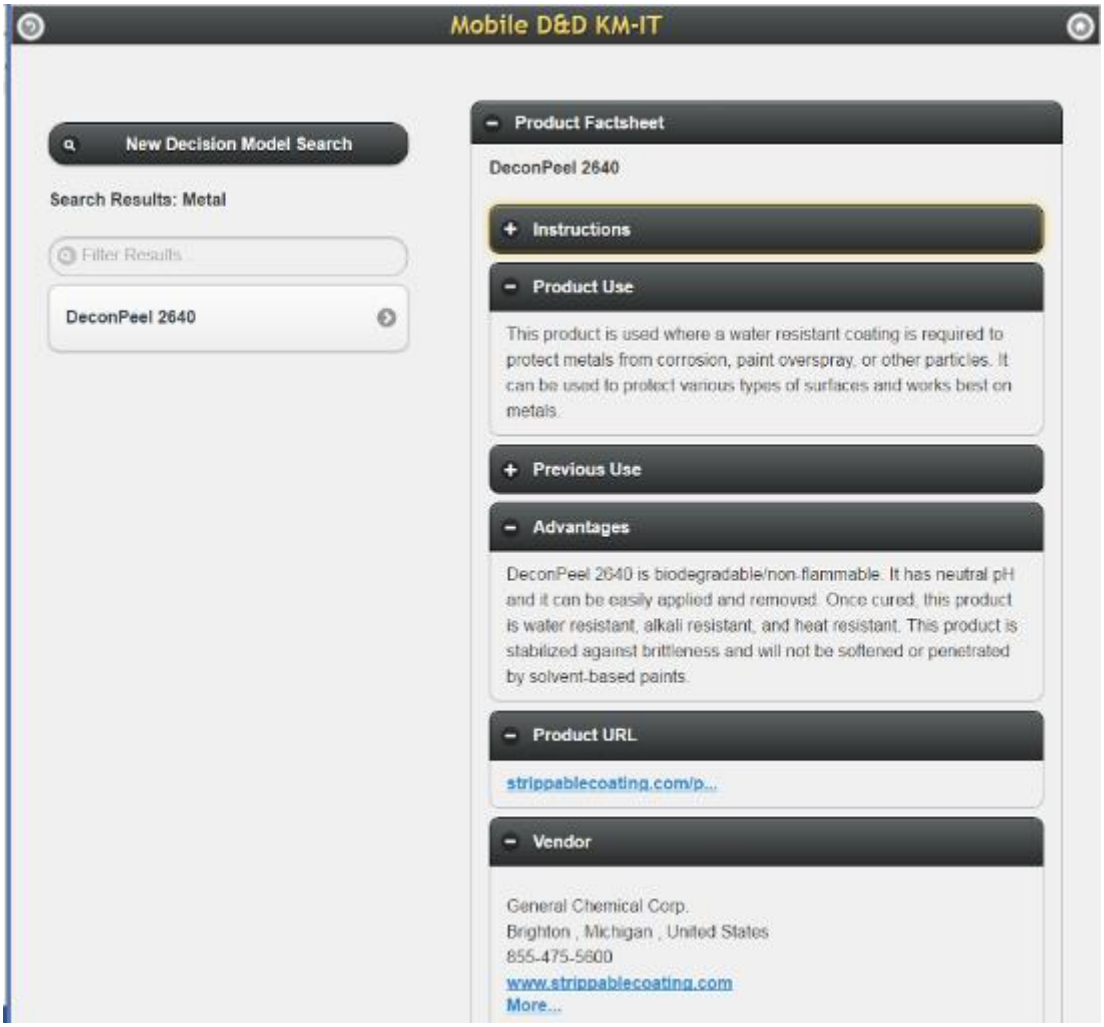

Figure 3-12. Fixative mobile app sample product factsheet.

FIU developed two draft newsletters during this reporting period. The first was based on an analysis performed to better understand the seasonal variations of photovoltaic (PV) power generation. This research work to better understand solar energy generation patterns and seasonal variations was performed during the summer of 2015 by DOE Fellow Natalia Duque during a summer internship at SRNL under the supervision and guidance of Mr. Ralph L. Nichols, Fellow Engineer at the Environmental Sciences & Biotechnology Directorate. The second draft newsletter was developed to announce the launch of a D&D Fixative Module on D&D KM-IT to assist in the selection of commercially available fixatives, strippable coatings, and decontamination gels for application during D&D activities. The draft newsletters were sent to DOE for review on June 15, 2016 and June 30, 2016, respectively, and will be subsequently revised before being distributed to D&D KM-IT users.

FIU developed a quarterly update document for the *D&D KM-IT Strategic Approach for the Long-Term Sustainability of Knowledge* document and sent it to DOE on June 29, 2016. The strategic plan for D&D KM-IT is a living document. The projected schedule and status evolve over time as the recommended strategic approaches are implemented. The update document,

developed on a quarterly basis, provides an update to the table of recommended actions contained in the original document.

FIU completed the development of a Google Web Analytic report for D&D KM-IT for the first quarter of 2016 (January to March) and submitted it to DOE on June 15, 2016. This report included information from Google Analytics (GA) and Google Web Master Tools (GWT) and a narrative to explain the results. Figure 3-13 shows an infographic of the web analytics for the first quarter of 2016. Some of the highlights of this report include:

- There were a total of 5,319 combined sessions (GA + GWT) by 2,155 users (GA) that generated 8,738 page views (GA).
- This quarter showed an improvement in web traffic in combined sessions, an increase of 13.5% over last quarter and 28.4% over the same quarter last year.
- Google Chrome is the browser used by almost half of the users who visit the site.
- Canada is no longer one of the top 5 countries that visit D&D KM-IT. A new country in the top 5 is South Korea.
- The top document accessed on the site is the "NITON XL-800 Series Multi-Element Spectrum Analyzer (Alloy Analyzer)" from the Innovative Technology Summary Reports (ITSRs) category. The ITSRs category holds 8 of the top 10 documents on the site.
- Wikipedia is one of the top ten domains linking to D&D KM-IT during this period.
- "Mobile Systems" continues to be the top query impression for D&D KM-IT.
- The most used modules during this quarter include Technology, Vendors and Training.
- Registered users increased by 64 while the number of subject matter specialists (SMS) increased by 7 during this period. The majority of the new users (51) were gained at the Waste Management Symposia 2016 (WM2016) which took place in Phoenix, AZ during the month of March. Conferences continue to prove to be the best platform to recruit new users and SMS to the system.

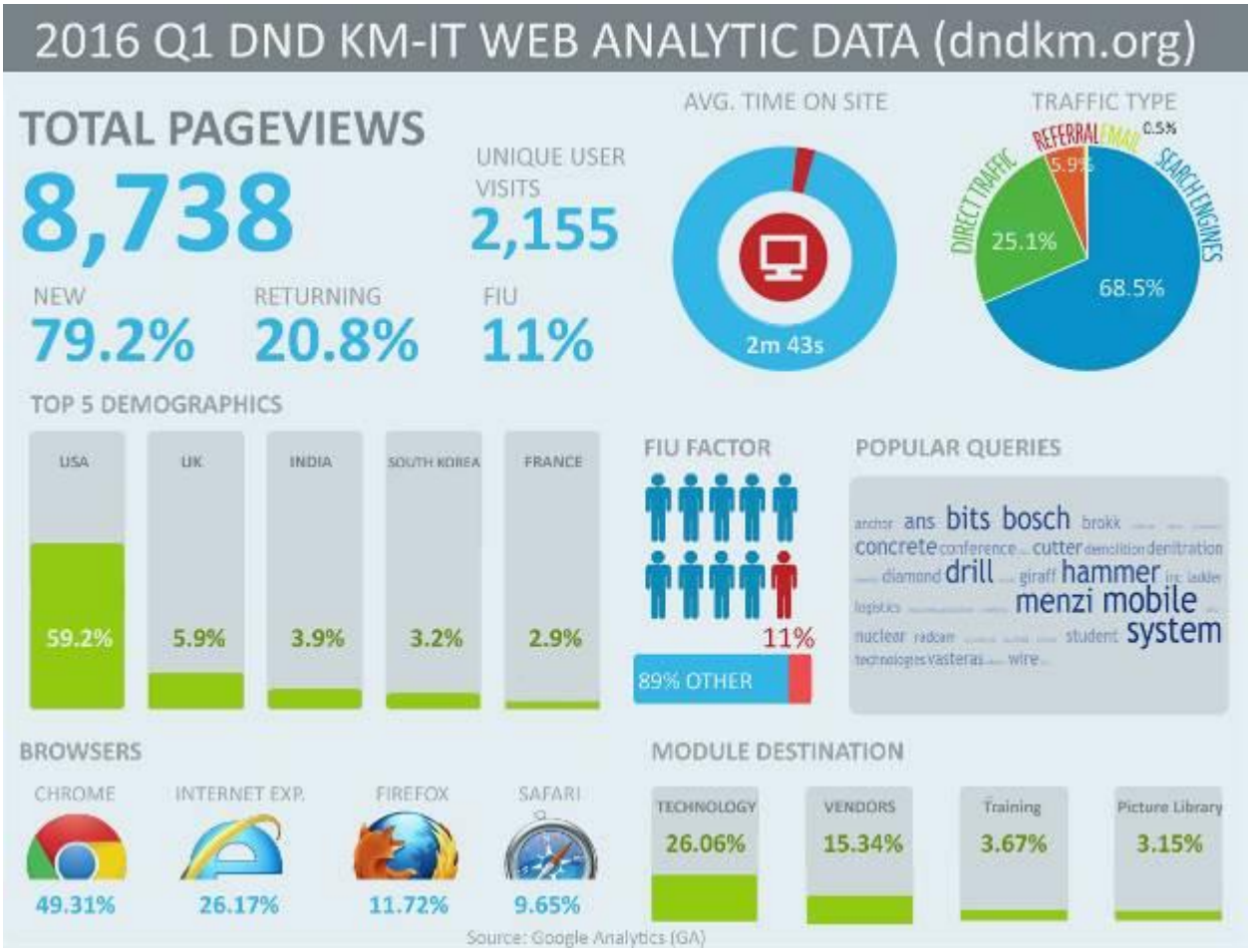

Figure 3-13. Web analytic infographic for 1st quarter of 2016.

FIU also provided information to DOE to enhance two entries on their internal Powerpedia system: Green and Sustainable Remediation and the D&D Knowledge Management Information Tool.

DOE Fellows and other FIU students are supporting D&D KM-IT by reviewing the information in the vendor and technology modules and updating contact information. As of June 24, the system included a total of 1279 technologies and 948 vendors.

Milestones and Deliverables

The milestones and deliverables for Project 3 for FIU Performance Year 6 are shown on the following table. FIU completed milestone 2015-P3-M3.4, the integration of D&D information into 4 Wikipedia articles, and sent a summary report sent to DOE on April 15, 2016. FIU completed milestone 2015-P3-M1.1, importing the 2016 data set for waste forecast and transportation data into WIMS, on May 13, 2016, and sent to DOE for review and testing. FIU also completed milestone 2015-P3-M3.5, deployment of a pilot mobile application for the D&D Fixative Module on D&D KM-IT on May 20, 2016, and sent to DOE for review and testing. FIU completed a deliverable for a decision brief to Andrew Szilagyi and John De Gregory with DOE EM-13 on recommended technologies to test for FIU Performance Year 7 on May 11, 2016, as part of a larger briefing on FIU's current and future D&D research activities. FIU completed

milestone 2015-P3-M2.3 by participating in the ASTM International's Executive Steering Committee Meeting from June 27 to June 29, 2016, and leading an ASTM International E10.03 Subcommittee meeting to develop standardized testing protocols and performance metrics for D&D technologies. FIU completed a deliverable for a technical progress report on the research to improve the operational effectiveness of fixative technologies in the critical area of fire resistance to better address the unique D&D challenges being faced by the SRS 235-F Project and other high priority efforts across the DOE complex.

A deliverable for a summary report on robotic technologies applicable to the SRS 235-F Facility has been reforecast to August 12, 2016. The circumstances and end path forward, including the new reforecasted date for this deliverable, have been closely coordinated with the stakeholders at Savannah River and DOE HQ. FIU discussed the issue with the SRNL collaborators and confirmed the agreement the deliverable date with an email sent to SRS on May 24, 2016 and DOE HQ contacts on May 27, 2016.

FIU Performance Year 6 Milestones and Deliverables for Project 3

Task	Milestone/ Deliverable	Description	Due Date	Status	OSTI
Task 1: WIMS	2015-P3-M1.1	Import 2016 data set for waste forecast and transportation data	Within 60 days of data receipt	Complete	
	2015-P3-M1.2	WM 2016 Paper for WIMS	11/6/2015	Complete	
Task 2: D&D	2015-P3-M2.1	Completion of Phase 1 testing of incombustible fixatives	12/31/2015	Complete	
	2015-P3-M2.2	Participate in ASTM E10 Committee Meeting to introduce a requirement for standardized D&D testing protocols & performance metrics	01/31/2016	Complete	
	Deliverable	Summary Report on Robotic Technologies for SRS 235-F Facility	Reforecast to 8/12/2016	Reforecast	OSTI
	Deliverable	Draft Progress Report for incombustible fixatives testing and evaluation	06/30/2016	Complete	OSTI
	2015-P3-M2.3	Participate in ASTM International's Executive Steering Committee Meeting to solicit final approval for development of standardized testing protocols and performance metrics for D&D technologies.	06/30/2016	Complete	
	Deliverable	Decision brief to DOE-EM 13 on recommended technologies to test for FY'17 using FIU's 3-Phased Technology Test and Evaluation Model.	07/29/2016	Complete	
	Deliverable	Draft technical reports for demonstrated technologies	30-days after demo	On Target	OSTI
	Deliverable	Draft Tech Fact Sheet for technology evaluations/ demonstrations	30-days after demo	On Target	
Task 3: D&D KM-IT	2015-P3-M3.1	Waste Management Symposium Paper for D&D KM-IT	11/06/2015	Complete	
	Deliverable	First D&D KM-IT Workshop to DOE EM staff at HQ	TBD**	Reforecast	
	2015-P3-M3.2	Deployment of pilot web-based D&D Decision Model application	01/16/2016	Complete	

	2015-P3-M3.3	Completion of development & integration of International KM-IT pilot for UK collaboration	03/04/2016	Complete	
	Deliverable	Preliminary Metrics Progress Report on Outreach and Training Activities	02/29/2016	Complete	
	Deliverable	First D&D KM-IT Workshop to D&D community	03/31/2016	Complete	
	2015-P3-M3.4	Four Wikipedia integration edits/articles	03/31/2016 Reforecasted to 04/15/16	Complete	
	2015-P3-M3.5	Deployment of pilot mobile application for D&D Fixative Module	05/20/2016	Complete	
	Deliverable	Second D&D KM-IT Workshop to DOE EM staff at HQ	TBD**	Reforecast	
	Deliverable	First infographic to DOE for review	07/25/2016	Complete	
	Deliverable	Second infographic to DOE for review	08/08/2016	On Target	
	Deliverable	Metrics Progress Report on Outreach and Training Activities	08/15/2016	On Target	
	Deliverable	Second D&D KM-IT Workshop to D&D community	08/25/2016	On Target	
	Deliverable	Draft Security Audit Report	30-days after audit	On Target	
	Deliverable	D&D KM-IT Web Analysis Report	Quarterly	On Target	
	Deliverable	Draft Tech Fact Sheet for new modules or capabilities of D&D KM-IT	30-days after deployment of new module	On Target	

***Completion of this deliverable depends on scheduling and availability of DOE EM staff*

Work Plan for Next Quarter

Project-wide:

- Draft the Year End Report (YER) for FIU Performance Year 6 (August 2015 to August 2016).
- Draft the Project Technical Plan (PTP) for FIU Performance Year 7 (August 2016 to August 2017).

Task 1: Waste Information Management System

- Perform database management, application maintenance, and performance tuning to WIMS.

Task 2: D&D Support

- Continue testing for evaluating additional intumescent coatings, selected by FIU and SRS.
- Participate in ASTM International's E10 Committee on Nuclear Technologies and Applications and Subcommittee E10.03 - Radiological Protection for Decontamination and Decommissioning of Nuclear Facilities and Components. Lead the working group to

support the initiative of developing and promulgating uniform testing protocols and performance metrics for D&D technologies across the stakeholder community.

- Collaborate with SRNL to research robotic technologies to support D&D activities at the SRS 235-F facility as well as across the DOE complex.

Task 3: D&D Knowledge Management Information Tool

- Draft a new infographic on a topic selected by FIU and DOE.
- Develop quarterly website analytics report and submit to DOE for review.
- Complete the D&D KM-IT Workshop to DOE EM staff at HQ, based on scheduling and availability of DOE EM staff.
- Perform outreach and training, community support, data mining and content management, and administration and support for the D&D KM-IT system, database, and network. Develop a metrics progress report on the outreach and training activities.

Project 4
DOE-FIU Science & Technology Workforce Development Initiative

Project Manager: Dr. Leonel E. Lagos

Project Description

The DOE-FIU Science and Technology Workforce Development Initiative has been designed to build upon the existing DOE/FIU relationship by creating a "pipeline" of minority engineers specifically trained and mentored to enter the Department of Energy workforce in technical areas of need. This innovative program was designed to help address DOE's future workforce needs by partnering with academic, government and DOE contractor organizations to mentor future minority scientists and engineers in the research, development, and deployment of new technologies, addressing DOE's environmental cleanup challenges.

Project Overview

The main objective of the program is to provide interested students with a unique opportunity to integrate course work, Department of Energy (DOE) field work, and applied research work at ARC into a well-structured academic program. Students completing this research program would complete the M.S. or Ph.D. degree and immediately be available for transitioning into the DOE EM's workforce via federal programs such as the Pathways Program or by getting directly hired by DOE contractors, other federal agencies, and/or STEM private industry.

Project Quarterly Progress

FIU STEM (Science, Technology, Engineering, and Math) students are actively supporting the research efforts under the DOE-FIU Cooperative Agreement during FIU Performance Year 6. The following DOE Fellows are supporting the research under Projects 1 – 3:

Project 1: Anthony Fernandez (undergraduate, mechanical engineering), Brian Castillo (undergraduate, biomedical engineering), Erim Gokce (undergraduate, mechanical engineering), Gene Yllanes (undergraduate, electrical engineering), Iti Mehta (undergraduate, mechanical engineering), John Conley (undergraduate, mechanical engineering), Max Edrei (graduate, M.S., mechanical engineering), Ryan Sheffield (undergraduate, mechanical engineering), Sebastian Zanlongo (graduate, Ph.D., computer science), Clarice Davila (undergraduate, mechanical engineering), and Michael DiBono (undergraduate, mechanical engineering).

Project 2: Alejandro Garcia (graduate, M.S. geoscience), Alejandro Hernandez (undergraduate, chemistry), Alexis Smoot (undergraduate, environmental engineering), Awmna Kalsoom Rana (undergraduate, chemistry), Christine Wipfli (undergraduate, environmental engineering), Christopher Strand (undergraduate, civil & environmental engineering), Claudia Cardona (graduate, PH.D., environmental engineering), Hansell Gonzalez (graduate, Ph.D., chemistry), Natalia Duque (graduate, M.S., environmental engineering), Robert Lapierre (graduate, M.S.,

chemistry), Sarah Bird (undergraduate, environmental engineering), Silvina Di Pierto (graduate, Ph.D., chemistry), Sarah Solomon (undergraduate, environmental engineering), Mohammed Albassam (graduate, M.S., environmental engineering), Frances Zongotita (undergraduate, chemistry and health), and Juan Morales (graduate, M.S., public health).

Project 3: Jesse Viera (undergraduate, mechanical engineering), Janesler Gonzalez (undergraduate, mechanical engineering), Meilyn Planas (undergraduate, electrical engineering), Orlando Gomez (graduate, physics), Yoel Rotterman (undergraduate, mechanical engineering), Jorge Deshon (undergraduate, computer engineering), Alexander Piedra (undergraduate, mechanical engineering).

Fellows continue their support to the DOE-FIU Cooperative Agreement by actively engaging in EM applied research and supporting ARC staff in the development and completion of the various tasks. The program director continues to work with DOE sites and HQ to fully engage DOE Fellows with research outside ARC where Fellows provide direct support to mentors at DOE sites, DOE-HQ, and DOE contractors. All Fellows also participated in a weekly meeting conducted by the program director, a conference line has been established to enable DOE Fellows conducting internship to join to weekly meeting and update the program director on their internship activities. During each of these meetings, DOE Fellows presents the work they perform during their summer internship and/or EM research work they are performing at ARC.

During the April 5 to April 7 program review conducted between DOE EM and FIU ARC as part of the DOE Cooperative Agreement, three (3) DOE Fellows presented during the workforce development presentations to highlight the applied research they are performing for DOE EM as part of this Cooperative Agreement.

Three DOE Fellows (Sarah Bird, Alexis Smoot, and Alejandro Fernandez) had the opportunity to present their DOE EM research at the 2016 Life Sciences South Florida STEM Symposium held at Broward State College in April. The Fellows presented posters showcasing their research conducted as part of Project 2 under the supervision and mentorship of Dr. Ravi Gudavalli, Dr. Yelena Katsenovich, and Dr. Vasileios Anagnostopoulos. Alejandro Fernandez obtained first place at the poster competition/exhibition, competing among 80 posters presented by STEM students representing state colleges and universities in the South Florida area. Mr. Fernandez's accomplishments were also reported on the FIU website: http://news.fiu.edu/2016/04/symposium-showcases-student-research/99080

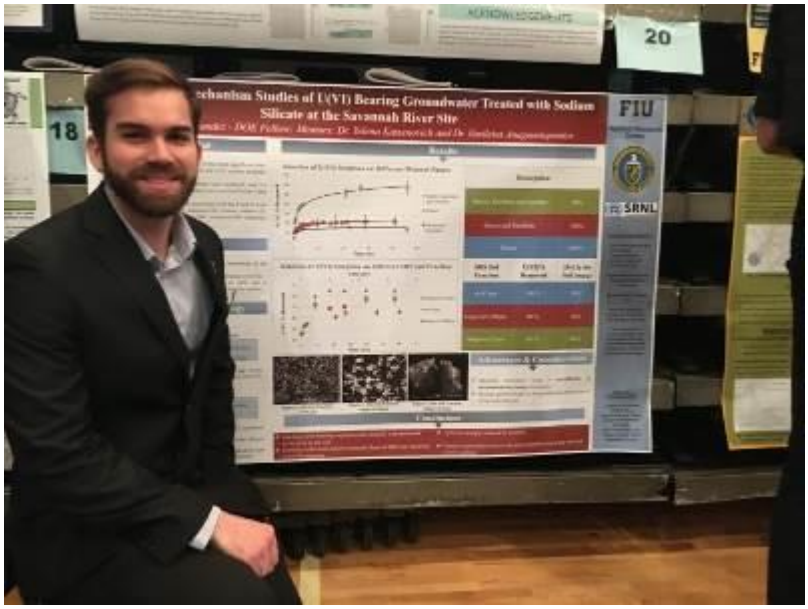

Figure 4-1. DOE Fellow Alejandro Hernandez presenting DOE EM research at the Life Sciences South Florida STEM Symposium.

Three DOE Fellows graduated from FIU and participated during FIU's spring 2016 graduation ceremony held during May 7-9, 2016:

- Iti Mehta (Class of 2015) - B.S., Mechanical Engineering
- Meilyn Planas (Class of 2014) - B.S., Electrical Engineering
- Jorge Deshon (Class of 2014) - B.S., Computer Engineering

DOE Fellows spring recruitment efforts were initiated on March 21 and ran through April 15. Recruitment campaigns were conducted by placing recruitment tables at the College of Engineering and at the main FIU campus in the Physics & Chemistry building and Computer Science building. Large group of students showed interest in the program and a signup sheet was used to collect student information. Emails were sent to interested students with information on requirements and components of the program along with the application procedure and application checklist. The deadline for FIU students to submit applications for the DOE Fellowship was April 15, 2016. Nineteen (19) FIU students applied for the DOE Fellows program. The DOE Fellows selection committee, comprised of ARC researchers and staff, recommended twelve (12) FIU students for formal interviews which were conducted from May 9 through May 11, 2016. Dr. Leonel Lagos (Program Director) subsequently asked for the committees input and recommendations to make the final selections and complete the recruitment process. Seven (7) students were selected to join the program as DOE Fellows Class of 2016 and subsequently joined the program and were assigned an ARC mentor based on their field of study (Table 4-1).

Table 4-1. New DOE Fellows and ARC Mentors

First Name	Last name	Major	Degree	ARC Mentor
Alexander	Piedra	Mechanical Engineering	BS	Joseph Sinicorpe
Clarice	Davila	Mechanical Engineering	BS	Aparna Aravalli
Frances	Zongotita	Chemistry and English	BS	Hilary Emerson
Juan	Morales	Public Health	MS	Angelique Lawrence / Reinaldo Garcia
Michael	DiBono	Mechanical Engineering	BS	Dwayne McDaniel
Mohammed	Albassam	Environmental Engineering	MS	Mehrnoosh Mahmoudi
Sarah	Solomon	Environmental Engineering	BS	Vasileios Anagnostopoulos

All seven (7) new DOE Fellows completed the required environmental health and safety trainings shown below prior to engaging in laboratory work. The Fellows also attended hands-on radiation safety training on June 2, provided by FIU's radiation safety officer, and successfully passed the training evaluation.

- Chemical Handling Safety
- Laboratory Hazard Awareness Training
- HazCom: In Sync with GHS
- Fire Safety
- Environmental Awareness Part II
- Small Spills and Leaks
- EPA Hazardous Waste Awareness and Handling
- Personal Protective Equipment
- Safe Use of Fume Hoods
- Radiation Safety

Dr. Leo Lagos and Dr. Ravi Gudavalli conducted orientation sessions for the new class of DOE Fellows on June 7, 2016, and discussed the expectations of the program, including program components such as hands-on research on DOE related challenges, summer internships, and potential future employment with DOE EM, national laboratories and DOE contractors.

The DOE Fellows program director finalized coordination with DOE-HQ, DOE sites, DOE national laboratories, and DOE contractors for placement of DOE Fellows for summer 2016 internships. A total of eleven (11) DOE Fellows started their summer internships in June. The 10-week internships will be conducted from June 6 to August 12, 2016. Table 4-2 lists the summer internship assignments. In addition, DOE Fellow Alejandro Garcia completed a 10-week spring 2016 internship at PNNL and returned to ARC.

Table 4-2. Summer 2016 Internships

DOE Fellow	Location	Internship Mentor	Comments
Erim Gokce	WRPS	Ruben Mendoza/ Dennis Washenfelder	High Level Waste
Gene Yllanes	SRS	Mike Serrato	Mechanical Systems & Custom Equipment Development and Imaging & Radiation Systems
Max Edrei	NETL	Chris Gunter	Investigating parameters affecting mixing times for a multiphase PJM process through CFD analysis
Sebastian Zanlongo	LANL	David Mascarenas	LANL Robotics Group
Alejandro Hernandez	SRNL	Ralph Nichols/ Miles Denham	Column experiments to study *in situ* precipitation of AgCl to treat I-129 contamination in groundwater
Alexis Smoot	DOE HQ	Skip Chamberlain	Sustainability analysis of the SRS F-Area treatment system, evaluating aspects of the pump and treat system relative to the funnel and gate base passive treatment system
Awmna Rana	REU/SREL	John Seaman (SREL)	MSIPP Internship or SRNL
Christopher Strand	LANL	Bill Foley	Soil & Groundwater
Hansel Gonzalez	SRNL	Miles Denham	Study of the sorption of silver (Ag+) and zinc (Zn2+) on Huma-K coated sediments
Sarah Bird	DOE HQ	Skip Chamberlain	Sustainability analysis of the SRS F-Area treatment system, evaluating aspects of the pump and treat system relative to the funnel and gate base passive treatment system
Silvina Di Pietro	PNNL	Jim Szecosdy/Nik Qafoku	Evaluation of the rate of pure minerals and Hanford sediments dissolving in synthetic porewater under anaerobic (oxygen free) conditions

Highlights from the internship assignments:

DOE FELLOW: **Silvina Di Pietro**
LOCATION: **Pacific Northwest National Laboratory**
MENTORS: **Jim Szecosdy and Nik Qafoku**

Ammonia gas injection is being considered as a potential field remediation technique for vadose zone contamination at the Hanford Site in Washington State. During her 10-week summer internship at PNNL, Ms. Silvina Di Pietro will be assisting with research on the dissolution rate of pure minerals and Hanford sediments in synthetic porewaters under anaerobic (oxygen-free) conditions. The experiments will be conducted using two different aqueous NH_3 concentrations (3.1 mol/L and 0.3 mol/L) as well as NaOH for comparison. Major cations and anions in the aqueous phase will be monitored to determine the rate of mineral dissolution. Investigating the rate of mineral dissolution will help to understand how different cations/anions affect ammonia gas treatment under anaerobic environment conditions.

Figure 4-2. DOE Fellow Silvina Di Pietro with PNNL summer intern mentor Jim Szecosdy.

DOE FELLOW: **Erim Gokce**
LOCATION: **Washington River Protection Solutions**
MENTORS: **Ruben Mendoza and Dennis Washenfelder**

Mr. Erim Gokce is spending his summer internship making improvements in the technical basis information to support the underpinning for the direct feed low-activity waste (DF LAW) and single-shell tank (SST) retrieval OR model and assessment initiatives. Specifically, Mr. Gokce is researching and compiling failure data and forecast recommendations for waste transfer lines, spare jumpers, and SST retrieval equipment. Tasks associated with these three efforts include:

- Update waste transfer line failure reliability, availability, and maintainability (RAM) data by researching previous waste transfer line failure events, determining the cause of failure, categorizing these failures and providing this information for incorporation into the RAM data.

- Develop recommendations for the spare jumpers by assessing the types and number of spare jumpers needed for WFD transfer efforts.

- Update SST retrieval RAM data based on investigation of previous equipment failures for both sluicing and mobile arm retrieval vacuum systems (MARS). Once the types of failures are determined, and categorized, this information can be incorporated into the existing SST Retrieval RAM data.

Figure 4-3. DOE Fellow Erim Gokce (far right) with WRPS staff during summer internship.

DOE FELLOW: Awmna Rana
LOCATION: Savannah River Ecology Laboratory
MENTOR: John Seaman

Ms. Awmna Rana's internship includes evaluating the dynamics of non-exchangeable organically-bound tritium and its accumulation properties by studying the tritium (3H) cycle in a variety of contaminated aquatic biodata from Fourmile Pond at the Savannah River Site. Specific internship tasks include:

- Design and perform experiments as an independent lab technician.
- Assist in assembling the Carbolite MTT Carbon-14 & Tritium Analyzer and performing an analytical technique to combust the freeze-dried aquatic biodata samples to completion, aided by a catalyst, and selectively trapping the chief combustion products (i.e., carbon dioxide and water).
- Assess the concentration of the carbon-14 and tritium (tritiated water) in the trapping agents using a liquid scintillation counting technique.

- Calculate the sample tritium and carbon-14 concentrations using the data collected.
- Understand why gaps exist in tritium environmental science in regards to the radionuclides properties of accumulation, and use data to support existing disagreement.
- Research more about non-existing OBT standard, which is needed to validate the combustion procedure.
- Use data to support claims of bio magnification in the environment as OBT has a much higher accumulation factor in marine species.

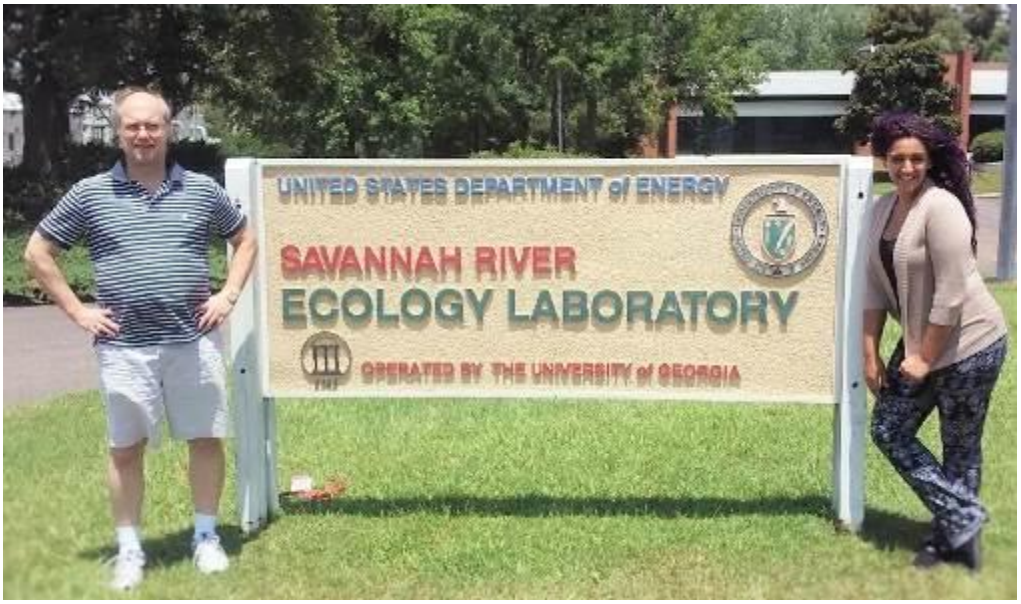

Figure 4-4. DOE Fellow Awmna Rana with SREL summer intern mentor John Seaman.

DOE Fellow Christine Wipfli continued a one year internship at the International Atomic Energy Agency (IAEA) in the Waste Technology Section, Division of Nuclear Fuel Cycle & Waste Technology at IAEA's Headquarters in Vienna, Austria. Christine recently had the opportunity to attend the International Conference on Advancing the Global Implementation of Decommissioning and Environmental Remediation Programmes in Madrid Spain. This week-long conference was organized by IAEA and hosted by the government of Spain. The following text and figures were taken from an article that Christine developed on her experience at the conference:

> Over the coming decades, all over the world, the number of existing nuclear facilities leaving operation will be drastically increasing, as well as the continued presence of a significant number of legacy sites. This emphasized the continued international effort required in the area commonly termed, "capacity building", which encompasses several concepts including the increased training of current industry personnel, as well as the vast efforts required to recruit and develop training opportunities for young professionals entering the field.
>
> The relationship between the Department of Energy's Office of Environmental Management and FIU's Applied Research Center is a great example of this cooperation between industry and academia, and exemplifies the yields of such mutually beneficial agreements.

Significant advancements have been made over the last decades in the areas of technology and innovation pertaining to [decommissioning and environmental remediation] D&ER. Particularly in the fields of virtual reality, sensors/monitoring equipment, 3D modelling, robotics, and drone technology have all made significant contributions to characterization and segmentation. When utilized at nuclear facilities and site, this technology can provide more accurate data which allows for more efficient solutions to be selected in the decision-making process.

However, with all of the technology and innovations currently existing, presenters during the conference noted that the current technology is not sufficient to manage the complexity of the different types of radioactive waste that exists today; therefore, the push for continued research and development, technological innovations, and international collaboration is paramount. It was highlighted by the conference president Mr. Zaballa, that fostering relationships with universities and research laboratories is a two-fold solution to this issue, the first being the advantage of developing solutions to complex challenges, the second that it will introduce scientists and engineers to the field of radioactive waste management. By expanding the pool of talent and support in the areas of D&ER we can ensure that qualified personnel are in place to stabilize the transition of the aging workforce.

Figure 4-5. Leo Lagos, Andy Szilagyi, Christine Wipfli (left) and Christine Wipfli, Monica Regalbuto, Leo Lagos (right) at the International D&ER Conference in Madrid, Spain.

FIU continues to aggressively identify federal entry-level career opportunities within DOE with a particular emphasis on federal positions within DOE EM, the national labs, or DOE tier-1 contractors. The following DOE Fellows accepted offers of employment during this reporting period: 1) Kiara Pazan with AECOM, 2) Aref Shehadeh with Nova Consulting Group, Inc., 3) Meilyn Planas with Florida Power & Light (FPL), and 4) Andrew De La Rosa with Lockheed Martin, 5) Brian Castillo with Stryker, 6) Janesler Gonzalez with Velossa Tech, and 7) Jorge Deshon with Lockheed Martin.

During this reporting period, the Fellows continued their research in the DOE EM applied research projects under the cooperative agreement and research topics identified as part of their summer internships at DOE sites, national labs, and/or DOE HQ. Each DOE Fellow is assigned to DOE EM research projects as well as ARC mentors. A list of the current Fellows, their classification, areas of study, ARC mentor, and assigned project task is provided below.

Table 4-4. Project Support by DOE Fellows

Name	Classification	Major	ARC Mentor	Project Support
Alejandro Garcia	Graduate - B.S.	Geoscience	Dr. Yelena Katsenovich	FIU's Support for Groundwater Remediation at PNNL
Alejandro Hernandez	Undergrad - B.S.	Chemistry	Dr. Vasileios Anagnostopoulos	Groundwater Remediation at SRS F/H -Area
Alexander Piedra	Undergrad - B.S.	Mechanical Eng.	Mr. Joseph Sinicrope	Database of Robotic Technologies for D&D Activities
Alexis Smoot	Undergrad - B.S.	Envr. Eng.	Dr. Ravi Gudavalli	Synergistic Effects of Silica and Humic Acid on U(VI) Removal
Anthony Fernandez	Undergrad - B.S	Mechanical Eng.	Mr. Amer Awwad	Evaluation of Nonmetallic Components in the Waste Transfer System
Awmna Kalsoom Rana	Undergrad - B.S.	Chemistry	Ms. Angelique Lawrence	Surface Water Modeling of Tims Branch
Brian Castillo	Undergrad - B.S.	Biomedical Eng.	Ms. Aparna Aravelli	Development of a Micromachined Ultrasonic Transducer System for Analysis of High Level Waste Pipes at Hanford
Christine Wipfli	Undergrad - B.S.	Envr. Eng.	Dr. Vasileios Anagnostopoulos	Groundwater Remediation at SRS F/H Area
Christopher Strand	Undergrad - B.S.	Civil & Env. Eng.	Dr. Noosha Mahmoudi	Surface Water Modeling of Tims Branch
Clarice Davila	Undergrad - B.S	Mechanical Eng.	Dr. Aparna Aravalli	Investigation Using an Infrared Temperature Sensor to Determine the Inside Wall Temperature of DSTs
Claudia Cardona	Graduate - Ph.D.	Envr. Eng.	Dr. Yelena Katsenovich	Sequestering Uranium at the Hanford 200 Area Vadose Zone
Erim Gokce	Undergrad - B.S.	Mechanical Eng.	Mr. Anthony Abrahao	Development of Inspection Tools for DST Primary Tanks
Frances Zongotita	Undergrad - B.S.	Chemistry & Health	Dr. Hilary Emerson	Absorption of Neodymium into the Dolomite Mineral
Gene Yllanes	Undergrad - B.S.	Electrical Eng.	Dr. David Roelant	Evaluation of FIU's SLIM for Estimating the Onset of Deep Sludge Gas Release Events
Hansell Gonzalez	Graduate - Ph.D.	Chemistry	Dr. Yelena Katsenovich	Sorption Properties of Humate Injected into the Subsurface System

Iti Mehta	Undergrad - B.S.	Mechanical Eng.	Dr. Aparna Aravalli	Investigation Using an Infrared Temperature Sensor to Determine the Inside Wall Temperature of DSTs
Janesler Gonzalez	Undergrad - B.S.	Mechanical Eng.	Mr. Joseph Sinicrope	Incombustible Fixatives
Jesse Viera	Undergrad - B.S.	Mechanical Eng.	Mr. Joseph Sinicrope	Incombustible Fixatives
John Conley	Undergrad - B.S.	Mechanical Eng	Mr. Amer Awwad	Evaluation of Nonmetallic Components in the Waste Transfer System
Jorge Deshon	Undergrad - B.S.	Computer Eng.	Dr. Himanshu Upadhyay	Information Technology for Environmental Management
Juan Morales	Graduate – M.S.	Public Health	Ms. Angelique Lawrence / Dr. Reinaldo Garcia	Development of Flow and Contaminant Transport Models for Savannah River Site
Maximiliano Edrei	Graduate – M.S.	Mechanical Eng.	Dr. Dwayne McDaniel	Computational Fluid Dynamics Modeling of HLW Processes in Waste Tanks
Meilyn Planas	Undergrad - B.S.	Electrical Eng.	Mr. Joseph Sinicrope	Incombustible Fixatives
Michael DiBono	Undergrad - B.S.	Mechanical Eng.	Dr. Dwayne McDaniel	Development of Inspection Tools for DST Primary Tanks
Mohammed Albassam	Graduate – M.S.	Envr. Eng.	Dr. Noosha Mahmoudi	Environmental Remediation and Surface Water Modeling of Tims Branch Watershed at SRS
Natalia Duque	Graduate – M.S.	Envr. Eng.	Dr. Noosha Mahmoudi	Surface Water Modeling of Tims Branch
Orlando Gomez	Graduate - Ph.D.	Physics	Mr. Joseph Sinicrope	Incombustible Fixatives
Robert Lapierre	Graduate – M.S.	Chemistry	Dr. Yelena Katsenovich	Sequestering Uranium at the Hanford 200 Area Vadose Zone
Ryan Sheffield	Undergrad - B.S.	Mechanical Eng.	Mr. Hadi Fekrmandi	Development of Inspection Tools for DST Primary Tanks
Sarah Bird	Undergrad - B.S.	Envr. Eng.	Dr. Ravi Gudavalli	Modeling of the Migration and Distribution of Natural Organic Matter Injected into Subsurface Systems
Sarah Solomon	Undergrad - B.S.	Envr. Eng.	Dr. Vasileios Anagnostopoulos	Investigation on Microbial-Meta-Autunite Interactions - Effect of Bicarbonate and Calcium Ions
Sebastian Zanlongo	Graduate – Ph.D.	Computer Science	Dr. Dwayne McDaniel	Cooperative Controls for Robotic Systems
Silvina Di Pietro	Graduate - Ph.D.	Chemistry	Dr. Hilary Emerson	Evaluation of Ammonia for Uranium Treatment
Yoel Rotterman	Undergrad - B.S.	Mechanical Eng.	Mr. Joseph Sinicrope	Incombustible Fixatives

Highlights of DOE EM Research Being Conducted at ARC by DOE Fellows:

DOE Fellow John Conley, working alongside FIU's Applied Research Center, has been tasked with conducting a post service examination of hose-in-hose transfer line (HIHTL) nonmetallic components to improve the existing technical basis for component service life. John is conducting multi-stressor testing on the typical nonmetallic materials used at the Hanford tank farms. Baseline tests have been performed on the nonmetallic materials, and material aging is currently ongoing. Once the materials have been aged, testing will be repeated to determine the long term effect of multiple stressors on the nonmetallic materials.

DOE Fellow Yoel Rotterman performed an analysis of the mechanical components of the A/M groundwater remediation system at the Savanna River Site (SRS) to recommend site modifications that would offer the potential for less electrical power consumption and lower groundwater pumping rates of the system. The three main recommendations made were: A solar photovoltaic system for powering the A/M Area groundwater remediation system, the determination and use of an optimal speed for the blower motor that is sufficient to run the countercurrent stripper and removes the volatile organic contaminants to below the required level, and a groundwater modeling analysis be completed to optimize the pumping rate for each recovery well and for the entire system that provides hydrologic containment and maximizes the concentration of contaminants pumped to the stripper.

DOE Fellow Orlando Gomez, a graduate student at FIU in physics with a specialization in nuclear physics, is supporting a research task under Project 3 to improving the fire resiliency of industry fixatives. Orlando is analyzing the potential of combining and/or layering of an intumescent coating to improve the fire resiliency of multiple fixative technologies. Orlando has recently been accepted for a highly competitive assistantship in the Nuclear Astrophysics Ph.D. Program at Notre Dame.

DOE Fellow Iti Mehta, an undergraduate student pursuing a Bachelor of Science degree in mechanical engineering and a professional certificate in robotics at FIU, is supporting research at ARC to investigate using an infrared temperature sensor to determine the inside wall temperature of double-shell tanks in support of the high level waste research area under FIU Project 1. Maintaining specified temperature limits is critical to ensure tank integrity at the Hanford tank farms. Iti's research will assist site engineers with obtaining additional temperature data within the tank and understanding the uniformity of the temperature near the tank walls. This information will aid in the evaluation of various theories of the cause of tank leaks and provide a means to ensure that tank temperatures stay within specified parameters.

Milestones and Deliverables

The milestones and deliverables for Project 4 for FIU Performance Year 6 are shown on the following table. No milestones or deliverables were due during this quarter.

FIU Performance Year 6 Milestones and Deliverables for Project 4

Milestone/ Deliverable	Description	Due Date	Status	OSTI
2015-P4-M1	Draft Summer Internships Reports	10/16/15	Complete	
Deliverable	Deliver Summer 2015 interns reports to DOE	10/30/15 Reforecast	Complete 11/30/15	OSTI
Deliverable	List of identified/recruited DOE Fellow (Class of 2015)	10/30/15	Complete	
2015-P4-M2	Selection of new DOE Fellows – Fall 2015	10/30/15	Complete	
2015-P4-M3	Conduct Induction Ceremony – Class of 2015	11/05/15	Complete	
2015-P4-M4	Submit student poster abstracts to Waste Management Symposium 2016	01/16/16	Complete	
Deliverable	Update Technical Fact Sheet	30 days after end of project	On Target	

Work Plan for Next Quarter

- Draft the Year End Report (YER) for FIU Performance Year 6 (August 2015 to August 2016).
- Draft the Project Technical Plan (PTP) for FIU Performance Year 7 (August 2016 to August 2017).
- Continue research by DOE Fellows in the four DOE-EM applied research projects under the cooperative agreement and research topics identified as part of their summer internships.
- Complete DOE Fellow internships for summer 2016 at DOE sites, national laboratories, DOE-HQ, and DOE contractors.
- Begin preparation of summer internship technical reports.
- Coordinate fall recruitment period and complete review submitted application packages.
- Begin preparation and coordination for the DOE Fellows Poster Exhibition & Competition (October 2016).
- Begin preparation and coordination for the DOE Fellows Induction Ceremony for the Class of 2016 (November 2016).